

Université de Montréal

**Visible-Light-Mediated Synthesis of Helicenes in  
Batch and Continuous Flow Systems**

par

Anna Vlassova

Département de Chimie

Faculté des Arts et Sciences

Mémoire présenté à la Faculté des études supérieures et postdoctorales  
en vue de l'obtention du grade de maître ès sciences (M. Sc.)  
en chimie

Juillet 2014

© Anna Vlassova, 2014

## RÉSUMÉ

Le présent mémoire décrit le développement d'une méthode de synthèse des hélicènes catalysée par la lumière visible. Les conditions pour la formation de [5]hélicène ont été établies par une optimisation du photocatalyseur, du solvant, du système d'oxydation et du temps réactionnel. Suite aux études mécanistiques préliminaires, un mécanisme oxydatif est proposé. Les conditions optimisées ont été appliquées à la synthèse de [6]hélicènes pour laquelle la régiosélectivité a été améliorée en ajoutant des substituants sur la colonne hélicale. La synthèse de thiohélicènes a aussi été testée en utilisant les mêmes conditions sous irradiation par la lumière visible. La méthode a été inefficace pour la formation de benzodithiophènes et de naphthothiophènes, par contre elle permet la formation du phenanthro[3,4-b]thiophène avec un rendement acceptable. En prolongeant la surface- $\pi$  de la colonne hélicale, le pyrène a été fusionné aux motifs de [4]- et [5]hélicène. Trois dérivés de pyrène-hélicène ont été synthétisés en utilisant les conditions optimisées pour la photocyclisation et leurs caractéristiques physiques ont été étudiées.

La méthode de cyclisation sous l'action de la lumière visible a aussi été étudiée en flux continu. Une optimisation du montage expérimental ainsi que de la source lumineuse a été effectuée et les meilleures conditions ont été appliquées à la formation de [5]hélicène et des trois dérivés du pyrène-hélicène. Une amélioration ou conservation des rendements a été observée pour la plupart des produits formés en flux continu comparativement à la synthèse en batch. La concentration de la réaction a aussi été conservée et le temps réactionnel a été réduit par un facteur de dix toujours en comparaison avec la synthèse en batch.

**Mots Clés:** lumière visible; [4]-, [5]-, [6]hélicène; thiohélicène; pyrène-hélicène; flux continu.

## ABSTRACT

The present work describes the development of a visible-light-mediated method for the synthesis of helicenes. The conditions for the formation of [5]helicene were established in a batch process as a result of an extensive optimization of the photosensitizer, solvent, oxidant system and reaction time. Following preliminary mechanistic studies, an oxidative reaction mechanism was proposed. The optimized conditions were applied to the synthesis of [6]helicenes and the regioselectivity of the reaction was improved through substitution along the helicene backbone. Synthesis of thiohelicenes was also explored under the same conditions and although ineffective for the formation of benzodithiophenes and naphthothiophene, it did provide phenanthro[3,4-b]thiophene in a moderate yield. In an effort to extend the  $\pi$ -surface of the helical backbone, a pyrene moiety was fused to the [4]- and [5]helicene core. Three pyrene-helicene hybrid derivatives were synthesized under the visible-light-mediated cyclization conditions and their physical properties investigated.

The visible-light-mediated method for the formation of helicenes was also explored using the continuous flow method. An optimization of the reaction set up, the reaction medium as well as the light source was conducted with the [5]helicene model system. The optimal conditions were applied to the formation of various pyrene-helicene derivatives. In most cases the reaction yields were maintained or significantly improved when compared with the batch process. Also, the reaction concentration was conserved while the reaction time was decreased tenfold from the batch method to the continuous flow process.

**Key words:** visible-light; [4]-, [5]-, [6]helicene; thiohelicene; pyrene-helicene; continuous flow process.

## TABLE OF CONTENTS

RÉSUMÉ .....	i
ABSTRACT.....	ii
LIST OF ABBREVIATIONS.....	v
LIST OF FIGURES .....	vii
LIST OF SCHEMES.....	ix
LIST OF TABLES .....	xi
ACKNOWLEDGEMENTS / REMERCIEMENTS .....	xii
CHAPTER 1: INTRODUCTION.....	1
1.1 Description and Nomenclature of Helicenes.....	1
1.2 Synthesis of Helicenes .....	3
1.3 Applications of Helicenes .....	13
1.4 Introduction to Pyrene.....	19
1.5 Chemical Modifications of Pyrene.....	19
1.6 Applications of Pyrene.....	31
1.7 Research Goals.....	34
CHAPTER 2: DISCUSSION OF VISIBLE-LIGHT-MEDIATED SYNTHESIS OF HELICAL POLYCYCLIC AROMATIC COMPOUNDS .....	36
2.1 Introduction to Visible-Light-Mediated Photoredox Reactions.....	36
2.2 Visible-Light-Mediated Synthesis of [5]Helicenes.....	43
2.2.1 Optimization of first-generation visible-light-mediated conditions for photocyclization .....	43
2.2.2 Preliminary mechanistic studies .....	52
2.3 Visible-Light-Mediated Formation of [6]Helicenes .....	54
2.4 Visible-Light-Mediated Photocyclization of Thiohelicenes .....	58
2.5 Visible-Light-Mediated Formation of Pyrene-Helicene Derivatives.....	61
CHAPTER 3: DISCUSSION OF VISIBLE-LIGHT-MEDIATED SYNTHESIS OF HELICENES IN A CONTINUOUS FLOW PROCESS .....	72
3.1 Introduction to the Continuous Flow Processes.....	72
3.2 Development of Visible-Light-Mediated Photocyclization Conditions in a Continuous Flow Process .....	77



3.3 Application of the Optimized Visible-Light-Mediated Conditions in Flow to the Synthesis of Pyrene-Helicene Derivatives .....	83
CHAPTER 4: CONCLUSION AND FUTURE WORK .....	86
CHAPTER 5: EXPERIMENTAL SECTION.....	91
ANNEX 1 - SPECTRAL DATA .....	xiii

## LIST OF ABBREVIATIONS

aq	aqueous
Bu	butyl
<i>t</i> -Bu	<i>tert</i> -butyl
cat.	catalytic
°C	degree Celsius
$\delta$	chemical displacement
°	degree
d	doublet (NMR)
DCM	dichloromethane
dd	doublet of doublet (NMR)
DDQ	2,3-dichloro-5,6-dicyano-1,4-benzoquinone
DMF	<i>N,N'</i> -dimethyl formamide
DMSO	dimethylsulfoxide
dt	doublet of triplet (NMR)
<i>ee</i>	enantiomeric excess
eq	equivalent
g	gram
h	hour
HRMS	high resolution mass spectrometry
Hz	hertz
<i>i</i> -Pr	isopropyl
<i>J</i>	coupling constant
M	molarity
m	multiplet (NMR)
<i>m</i>	meta
Me	methyl
MeOH	methanol
mg	milligram
MHz	megahertz
min	minute
mL	milliliter
mm	millimeter
mM	millimolar
mmol	millimole

mol	mole
mol %	molar percentage
MS	mass spectrometry
NMR	nuclear magnetic resonance
<i>o</i>	ortho
<i>p</i>	para
q	quadruplet (NMR)
quint	quintuplet (NMR)
R	general group
RCM	ring closing metathesis
rt	room temperature
s	singlet (NMR)
t	triplet (NMR)
V	volume

## LIST OF FIGURES

<b>Figure 1:</b> Left-handed and right-handed heptahelicenes.....	1
<b>Figure 2:</b> Various classes of helicenes.....	2
<b>Figure 3:</b> The first helicenes made in 1903.....	3
<b>Figure 4:</b> UV-light mediated photocyclization of stilbenes by Martin and co-workers.....	4
<b>Figure 5:</b> Cyclization possibilities for the photocyclization reaction between C1 and C2 with further oxidation.....	5
<b>Figure 6:</b> Examples of helicenes used in self-assembly.....	15
<b>Figure 7:</b> Some organic D- $\pi$ -A dyes developed by Harima and co-workers.....	16
<b>Figure 8:</b> Enantiopure helicene moiety used in the formation of Langmuir-Blodgett films by Yamaguchi <i>et al.</i> ....	16
<b>Figure 9:</b> Schematic representation of columnar aggregation formed by helicenes as observed by Katz and co-workers.....	17
<b>Figure 10:</b> Three different types of helicenes used as dopants to induce chirality in achiral liquid crystals by Spada <i>et al.</i> .....	17
<b>Figure 11:</b> A schematic representation of the chiral phase and helical pitch induced by enantiopure helicenes in the presence of achiral liquid crystals.....	18
<b>Figure 12:</b> Various helicenes employed in organic electronics.....	18
<b>Figure 13:</b> Numbering of the pyrene molecule.....	20
<b>Figure 14:</b> Hexapyrenylbenzene derivative.....	26
<b>Figure 15:</b> Chemical structures of phenylethynylpyrenes synthesized by Yamato <i>et al.</i> ....	27
<b>Figure 16:</b> Indirect substitution of pyrene <i>via</i> reduction, electrophilic aromatic substitution and re-aromatization.....	28
<b>Figure 17:</b> Synthesis of 4,10-disubstituted pyrenes <i>via</i> photocyclization of divinylbiphenyls. ..	30
<b>Figure 18:</b> Formation of benzo[ <i>ghi</i> ]perylene and [2+2] intermolecular cycloaddition product during the UV-light-mediated photocyclodehydrogenation of <b>12</b> .....	36
<b>Figure 19:</b> Photoexcitation of Ru(bpy) <sub>3</sub> <sup>+2</sup> photosensitizer, a common catalyst in photoredox reactions. <sup>118</sup> .....	38
<b>Figure 20:</b> Ir-based sensitizers employed in photocatalysis by MacMillan <i>et al.</i> .....	39
<b>Figure 21:</b> MacMillan's visible-light-mediated asymmetric intermolecular $\alpha$ -alkylation of aldehydes.....	40
<b>Figure 22:</b> Stephenson's visible-light-mediated dehalogenation reaction.....	42
<b>Figure 23:</b> The optimized Cu-based sensitizer.....	50
<b>Figure 24:</b> The proposed mechanism for the formation of [5]helicene.....	54
<b>Figure 25:</b> Possible extensions of the helicene backbone.....	61
<b>Figure 26:</b> Pyrene numbering.....	62
<b>Figure 27:</b> Proposed retrosynthesis for the formation of stilbene precursors for compounds <b>230</b> and <b>232</b> .....	63
<b>Figure 28:</b> X-Ray crystallographic analysis of the molecular packing of [5]helicene <b>3</b> (a) side view, b) top view) and pyrene[5]helicene <b>245</b> (c) side view, b) top view).....	70
<b>Figure 29:</b> Various examples of commercially available continuous flow systems.....	72

<b>Figure 30:</b> a) The Uniqsis FlowSyn Multi-X continuous flow system and b) borosilicate glass mixing block. ....	78
<b>Figure 31:</b> Calculation examples for volume and residence time. ....	78
<b>Figure 32:</b> Fluorinated ethylene propylene tubing. ....	80
<b>Figure 33:</b> a) Vapourtec R-Series continuous flow system, b) standard PFA coiled tube reactor and c) the irradiation setup. ....	84
<b>Figure 34:</b> The proposed oxidative mechanism for the formation of [5]helicene. ....	87

## LIST OF SCHEMES

<b>Scheme 1:</b> Poor regioselectivity observed with UV-light photocyclization of unsubstituted stilbene-type precursors. ....	6
<b>Scheme 2:</b> Improved regioselectivity observed with UV-light photocyclization of bromo-substituted stilbene-type precursors. ....	6
<b>Scheme 3:</b> Diels-Alder conditions by Liu and Katz for the formation of helicenes. ....	7
<b>Scheme 4:</b> Newman's Friedel-Crafts acylation approach for the synthesis of [6]helicene. ....	7
<b>Scheme 5:</b> The Ichikawa Friedel-Crafts-type synthesis of a disubstituted [6]helicene. ....	8
<b>Scheme 6:</b> Pd-catalyzed C-H arylation for the synthesis of disubstituted [5]- and [6]helicenes. ..	8
<b>Scheme 7:</b> Double Stille coupling by Scott and Xue for the synthesis of benzo[5]helicene. ....	9
<b>Scheme 8:</b> Double Suzuki-Miyaura coupling by Shimizu <i>et al.</i> to form diphenyl-substituted [5]helicene. ....	9
<b>Scheme 9:</b> RCM synthesis of [5]helicene developed by Collins <i>et al.</i> ....	10
<b>Scheme 10:</b> Starý, Starà <i>et al.</i> 's Co-catalyzed [2+2+2] intramolecular cycloisomerization for the synthesis of tetrahydrohelicenes. ....	10
<b>Scheme 11:</b> Platinum-catalyzed double [2+2+2] cycloisomerization developed by Storch <i>et al.</i> for the synthesis of substituted [6]helicenes. ....	11
<b>Scheme 12:</b> Gingras and Dubois' synthesis of substituted [5]- and [7]helicenes <i>via</i> a carbenoid coupling. ....	12
<b>Scheme 13:</b> Gingras' conditions for the formation of helicene <b>49</b> . ....	12
<b>Scheme 14:</b> Harrowven <i>et al.</i> developed a radical cyclization route for the synthesis of variously substituted helicenes. ....	12
<b>Scheme 15:</b> Bromination provides 1,3,6,8-tetrabromopyrene. ....	21
<b>Scheme 16:</b> Suzuki couplings between tetrabromopyrene and various boronic acids. ....	21
<b>Scheme 17:</b> Sonogashira coupling with tetrasubstituted pyrene. ....	22
<b>Scheme 18:</b> Diels–Alder cycloaddition to form a monomer for future dendrimers. ....	22
<b>Scheme 19:</b> Müllen's <i>et al.</i> strategy for the synthesis of a 1,3-substituted pyrene derivative. ....	24
<b>Scheme 20:</b> A novel and facile synthesis for the formation of 2- and 2,7-substituted pyrenes ...	25
<b>Scheme 21:</b> One-step synthesis of pyrene-4,5-dione and pyrene-4,5,9,10-tetraone. ....	27
<b>Scheme 22:</b> Synthesis of pyrene twistacene. ....	27
<b>Scheme 23:</b> Various conditions for translannular ring closure. ....	29
<b>Scheme 24:</b> Müllen's synthesis of multisubstituted pyrenes by thermal annulation of tetrathiones. ....	30
<b>Scheme 25:</b> Synthesis of pyrene <i>via</i> cyclization of bis-alkynylbiphenyls. ....	31
<b>Scheme 26:</b> First generation conditions for photocyclization of stilbene-type precursors. ....	34
<b>Scheme 27:</b> Yoon's formal [2+2] intramolecular visible-light-mediated cycloaddition. ....	41
<b>Scheme 28:</b> Stephenson's photoredox-catalyzed reductive radical cyclization. ....	43
<b>Scheme 29:</b> Synthesis of (+)-gliocladin C by Stephenson <i>et al.</i> using photoredox chemistry. ....	43
<b>Scheme 30:</b> Formation of the stilbene-type precursor for the cyclization of [5]helicene. ....	44
<b>Scheme 31:</b> Use of Cu-based sensitizer <b>128</b> for the formation of [5]helicene. ....	46
<b>Scheme 32:</b> Optimized conditions for the visible-light-mediated synthesis of [5]helicenes. ....	51
<b>Scheme 33:</b> Formation of the electron-rich stilbene-type precursor <b>183</b> . ....	52

<b>Scheme 34:</b> Formation of the electron-poor stilbene-type precursor <b>186</b> .	52
<b>Scheme 35:</b> Cyclization of an electron-rich and an electron-poor stilbene-type precursor.	52
<b>Scheme 36:</b> Formation of the stilbene-type cyclization precursor for [6]helicene.	55
<b>Scheme 37:</b> Visible-light-mediated cyclization of <b>202</b> .	55
<b>Scheme 38:</b> Preparation of the 3-(2-(6-methoxynaphthalen-2-yl)vinyl)phenanthrene substrate.	56
<b>Scheme 39:</b> Visible-light-mediated photocyclization of <b>208</b> .	57
<b>Scheme 40:</b> Preparation of 3-(2-(3-methoxynaphthalen-2-yl)vinyl)phenanthrene substrate <b>214</b> .	57
<b>Scheme 41:</b> Visible-light-mediated cyclization of <b>214</b> .	58
<b>Scheme 42:</b> Synthesis of the dithiophene-stilbene-type precursors.	59
<b>Scheme 43:</b> The formation of 3-styrylthiophene.	59
<b>Scheme 44:</b> Attempted photocyclization for the formation of benzodithiophenes <b>225</b> and <b>226</b> and naphthothiophene <b>227</b> .	60
<b>Scheme 45:</b> Visible-light-mediated formation of thio[4]helicene.	61
<b>Scheme 46:</b> Ir-catalyzed borylation of pyrene with bis(pinacolate)diboron.	64
<b>Scheme 47:</b> Friedel-Crafts alkylation of pyrene.	64
<b>Scheme 48:</b> Ir-catalyzed borylation followed by bromination of the 2- <i>t</i> -Bu-pyrene.	65
<b>Scheme 49:</b> Synthesis of aldehyde <b>243</b> .	65
<b>Scheme 50:</b> Wittig reaction for the formation of stilbene precursor <b>244</b> .	65
<b>Scheme 51:</b> Visible-light-mediated photocyclization of pyrene-[5]helicene <b>245</b> .	66
<b>Scheme 52:</b> Formation of the stilbene-type precursor <b>248</b> .	67
<b>Scheme 53:</b> Visible-light-mediated formation of trimethoxy pyrene-[4]helicene.	67
<b>Scheme 54:</b> Formation of the 5-substituted aldehyde <b>252</b> .	68
<b>Scheme 55:</b> Synthesis of the stilbene-type precursor <b>253</b> and visible-light-mediated photocyclization of pyrene-helicene <b>254</b> .	69
<b>Scheme 56:</b> Jamison's UV-mediated ene-yne coupling in a continuous flow process.	75
<b>Scheme 57:</b> Visible-light-mediated reduction of aromatic azides.	76
<b>Scheme 58:</b> UV-mediated photocatalytic synthesis of L-pipecolinic acid using the continuous flow system.	77
<b>Scheme 59:</b> Optimized conditions for the batch visible-light-mediated synthesis of [5]helicenes.	77
<b>Scheme 60:</b> Optimized conditions for the formation of [5]helicene in a continuous flow system.	83
<b>Scheme 61:</b> Formation of various pyrene-helicenes in a continuous flow process.	85
<b>Scheme 62:</b> Visible-light-mediated synthesis of [5]helicenes in a batch process with <i>in situ</i> formation of the Cu-based sensitizer.	86
<b>Scheme 63:</b> Visible-light-mediated synthesis of [6]helicene and its methoxy derivatives.	88
<b>Scheme 64:</b> Optimized conditions for the formation of [5]helicene in a continuous flow system.	89

## LIST OF TABLES

<b>Table 1:</b> Photosensitizers tested for visible-light-mediated synthesis of [5]helicene. ....	45
<b>Table 2:</b> Solvent optimization for the visible-light-mediated synthesis of [5]helicene. ....	47
<b>Table 3:</b> Oxidant optimization for the visible-light-mediated synthesis of [5]helicene.....	48
<b>Table 4:</b> <i>In-situ</i> formation of the Cu-sensitizer for the photosynthesis of [5]helicene. ....	49
<b>Table 5:</b> Optimization of reaction parameters for the formation of [5]helicene using a borosilicate glass mixing block and various sources of light in a continuous flow process. ....	79
<b>Table 6:</b> Optimization of the reaction parameters for the formation of [5]helicene using FEP-Teflon tubing and a compact fluorescent energy-saving light bulb (30 W). ....	81



## ACKNOWLEDGEMENTS / REMERCIEMENTS

It is hard to believe that after two years of writing, I am finally here and ready to submit my M. Sc. thesis...pause for effect. I would first like to thank God for giving me the strength to persevere and keep away all temptation of giving up at every hard turn, and there were plenty. Immediately after, I would like to thank Prof. Shawn Collins for not only encouraging and supporting me, but also not giving up on me and always providing insightful mechanistic details and excellent pulled pork sandwiches. Without his help, I truly would not have been able to submit anything coherent.

I would also like to thank my wonderful family. Большое спасибо Папе, Маме, Петьке и моим дорогим Бабушкам и Дедушке, которые наверняка сейчас по локти в чернилах. I also want to send some love to Rob, who always put up with me at my best and at my worst in the writing process and was always available for helpful scientific and technological discussions, because of him, all my schemes are mostly identical.

J'aimerais aussi remercier le groupe entier de Collins. J'ai eu le plaisir de travailler avec plusieurs personnes vraiment magnifiques qui ont ajouté beaucoup de rires, de blagues et de la lumière pendant mes études graduées. Particulièrement j'aimerais dire un grand merci à Anne-Catherine Bédard. Sans elle, ce mémoire sera beaucoup plus court et ma vie sera ben plus plate. A-4, merci, merci pour tout. Muchas gracias a Augusto Hernandez-Perez por les noches de la canción con Juanes y por muchos fiestas con su familia y por la comida de Mama. Malheureusement, je ne connais pas assez d'espagnol pour te remercier pour tout ce que tu as fait pour moi pendant les dernières quatre ans, Tito. Un grand merci à Mike, for the bacon and beer; Tats, pour les sessions de karaoke et un français impeccable; Marie-Eve et Simon, pour les lifts, le camping et Gaston; et tous les autres membres du groupe Collins qui j'ai eu la chance de connaître et eu le plaisir de travailler avec à travers les années.

Finally, I would to thank all the people working in the analytical department at the University of Montréal, I apologize that our molecules never did ionize properly, thank you for always taking extra care to make the silver complexes!

Thank you!

## CHAPTER 1: INTRODUCTION

### 1.1 Description and Nomenclature of Helicenes

Helicenes are three-dimensional polycyclic aromatic compounds composed of *ortho*-fused benzene or heteroaromatic rings. Although helicenes contain no asymmetric carbon atoms or other chiral centres, they possess an inherent helical chirality which stems from the steric hindrance of the terminal rings which wind in opposite directions along a  $C_2$ -symmetric axis, perpendicular to the helical axis.<sup>1</sup> In 1966, Cahn, Ingold and Prelog proposed the nomenclature for compounds with helical chirality where *M* (*Minus*) describes a left-handed helix, while *P* (*Plus*) is reserved for the right-handed helix.<sup>2</sup> The prefix to the name denotes the number of aromatic rings present in the molecule and can be written in words or simply as a bracketed number, for example (*M*)-heptahelicene or (*M*)-[7]helicene is a left-handed helix made up of 7 *ortho*-fused aromatic rings (Figure 1).

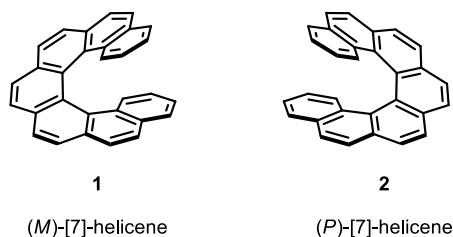


**Figure 1:** Left-handed and right-handed heptahelicenes.

If the helical molecule is made up of strictly benzene rings, the compound is referred to as carbohelicene. With the presence of a heteroaromatic ring, the nomenclature changes to heterohelicene (with sulfur as the main heteroatom – thiohelicene, with nitrogen – azahelicene and with oxygen – oxahelicene). Helicene-like compounds are another class of helicene derivatives, they are not always fully aromatic but possess a similar molecular shape (Figure 2).<sup>3</sup>

<sup>1</sup> Shen, Y.; Chen, C.-F. *Chem. Rev.* **2012**, *112*, 1463.

<sup>2</sup> Cahn, R. S.; Ingold, C.; Prelog, V. *Angew. Chem., Int. Ed.* **1966**, *5*, 385.

<sup>3</sup> Smith, P.J.; Liebman, J.F.; Hopf, H.; Sary, I.; Stara, I., G.; Halton, B. Strained Aromatic Molecules, in *Strained Hydrocarbons: Beyond the van-t Hoff and Le Bel Hypothesis*; Dodziuk, H., Ed.; Wiley-VCH Verlag GmbH & Co: Weinheim, 2009; pp. 166-203.

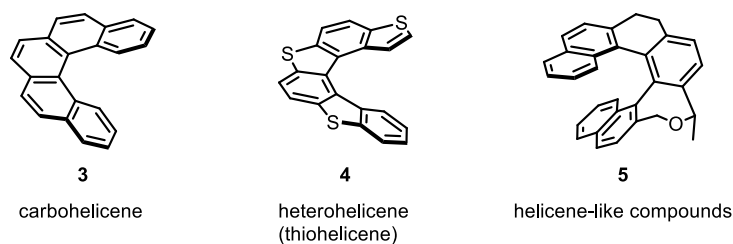


**Figure 2:** Various classes of helicenes.

Helicenes can be resolved into their *M* and *P* enantiomers if the interconversion barrier between the two enantiomers, which increases with the number of rings in the structure, is sufficiently high. Therefore, [3]-, [4]- and [5]helicenes racemize readily at room temperature and [6]helicenes or higher are found to be more configurationally stable and thus resolvable. The addition of bulky substituents on the terminal rings may add to the enantiomeric stability of the molecule making it possible to resolve lower helicenes at room temperature.<sup>4</sup>

Helicenes display increased solubility when compared to acenes, their planar aromatic counterparts. The solubility can be further improved by adding various substituents to the helical molecule, such as alkoxy or alkyl groups.<sup>5</sup> Helicenes are good  $\pi$ -donors and can form charge-transfer complexes with many  $\pi$ -acceptors, a trait that has been exploited in the past for the optical resolution of helicenes with chiral  $\pi$ -acceptors following a process driven by enthalpy.<sup>6</sup> Also, the

<sup>4</sup> Carreño, M. C.; Enriquez, A.; Garcìa-Cerrada, S.; Sanz-Cuesta, M. J.; Urbano, A.; Maseras, F.; Nonell-Canals, A. *Chem.-Eur. J.* **2008**, *14*, 603.

<sup>5</sup> a) Katz, T. J.; Liu, L. B.; Willmore, N. D.; Fox, J. M.; Rheingold, A. L.; Shi, S. H.; Nuckolls, C.; Rickman, B. H. *J. Am. Chem. Soc.* **1997**, *119*, 10054. b) Paruch, K.; Vyklický, L.; Wang, D. Z.; Katz, T. J.; Incarvito, C.; Zakharov, L.; Rheingold, A. L. *J. Org. Chem.* **2003**, *68*, 8539.

<sup>6</sup> a) TAPA  $\pi$ -acceptor: Newman, M. S.; Lutz, W. B.; Lednicer, D. *J. Am. Chem. Soc.* **1955**, *77*, 3420.; Brown, J. M.; Field, I. P.; Sidebottom, P. J. *Tetrahedron Lett.* **1981**, *22*, 4867. b) TCNQ  $\pi$ -acceptor: Tanaka, H.; Nakagawa, H.; Yamada, K.; Kawazura, H. *Bull. Chem. Soc. Jpn.* **1981**, *54*, 3665. c) TAPM  $\pi$ -acceptor.: Balan, A.; Gottlieb, H. E. *J. Chem. Soc., Perkin Trans. 2* **1981**, 350. d) TAPA, TABA  $\pi$ -acceptor: Mikeš, F.; Boshart, G.; Gilav, E. *J. Chem. Soc., Chem. Commun.* **1976**, 99. e) Electron-deficient helicene as  $\pi$ -acceptor: Okubo, H.; Nakano, D.; Yamaguchi, M.; Kabuto, C. *Chem. Lett.* **2000**, 1316.; Okubo, H.; Nakano, D.; Anzai, S.; Yamaguchi, M. *J. Org. Chem.* **2001**, *66*, 557. f) TAPA as a  $\pi$ -acceptor: Nakagawa, H.; Ogashiwa, S.; Tanaka, H.; Yamada, K.; Kawazura, H. *Bull. Chem. Soc. Jpn.* **1981**, *54*, 1903; Yamada, K.; Kobori, Y.; Nakagawa, H. *Chem. Commun.* **2000**, 97.; Eskildsen, J.; Krebs, F. C.; Faldt, A.; Sommer-Larsen, P.; Bechgaard, K. *J. Org. Chem.* **2001**, *66*, 200. g) TNB, DNBA, TCNQ, NIPA  $\pi$ -acceptor: Ermer, O.; Neudorfl, J. *Helv. Chim. Acta.* **2001**, *84*, 1268.

$\pi$ - $\pi$  donor-acceptor interactions influence the properties<sup>7</sup> as well as the self-assembly behaviour of helicenes in solid-state or in solution.<sup>8</sup>

## 1.2 Synthesis of Helicenes



**Figure 3:** The first helicenes made in 1903.

The first helicenes were synthesized in 1903 by Meisenheimer and Witte (Figure 3).<sup>9</sup> Although further exploration continued, no significant advancements were made until Martin and co-workers developed the photodehydrocyclization of stilbene-type precursors for the synthesis of carbohelicenes.<sup>10</sup> The method was based on UV-light-induced *cis/trans* isomerization of starting material **8** followed by conrotatory electrocyclization of *cis* isomer **9** providing dihydroaromatic compound **10** which was then oxidized to desired product **11**. The oxidant was air and catalytic amounts of iodine (Figure 4). The method was very efficient for the formation of helicenes because of the facile preparation of the stilbene-type starting materials *via* the Wittig olefination reaction.<sup>11</sup>

<sup>7</sup> a) Busson, B.; Kauranen, M.; Nuckolls, C.; Katz, T. J.; Persoons, A. *Phys. Rev. Lett.* **2000**, *84*, 79. b) Verbiest, T.; Van Elshocht, S.; Kauranen, M.; Hellemans, K.; Snauwaert, J.; Nuckolls, C.; Katz, T. J.; Persoons, A. *Science* **1998**, *282*, 913.

<sup>8</sup> a) Amemiya, R.; Yamaguchi, M. *Chem. Rec.* **2008**, *8*, 116. b) Amemiya, R.; Yamaguchi, M. *Org. Biomol. Chem.* **2008**, *6*, 26.

<sup>9</sup> Meisenheimer, J.; Witte, K. *Chem. Ber.* **1903**, *36*, 4153.

<sup>10</sup> a) Martin, R. H.; *Angew. Chem., Int. Ed.* **1974**, *13*, 649. b) Floyd, A. J.; Dyke, S. F.; Ward, S. E. *Chem. Rev.* **1976**, *76*, 509. c) Mallory, F. B.; Mallory, C. W. *Organic Reactions*; Wiley & Sons: New York, 1984; Vol. 30, pp. 1. d) Laarhoven, W. H. In *Organic Photochemistry*; Padwa, A., Ed; Marcel Dekker: New York, 1989; Vol. 10, pp. 163. e) Flammang-Barbieux, M.; Nasielski, J.; Martin, R. H. *Tetrahedron Lett.* **1967**, *8*, 743.

<sup>11</sup> a) Wynberg, H. *Acc. Chem. Res.* **1971**, *4*, 65. b) Laarhoven, W. H.; Prinsen, W. J. C. *Top. Curr. Chem.* **1984**, *125*, 63. c) Meurer, K. P.; Vogtle, F. *Top. Curr. Chem.* **1985**, *127*, 1.

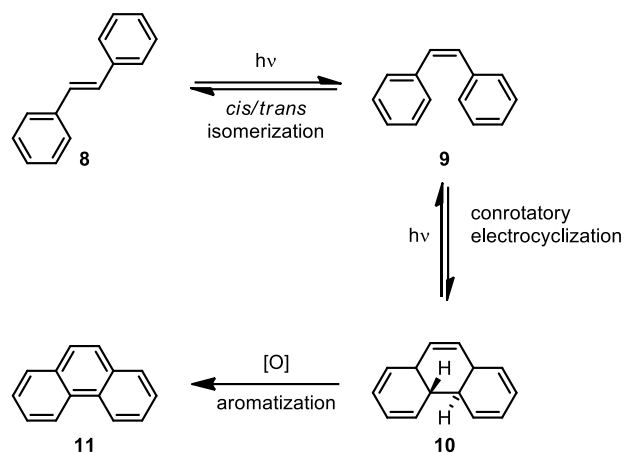


**Figure 4:** UV-light mediated photocyclization of stilbenes by Martin and co-workers.

Although the strategy was atomically efficient and provided moderate to good yields, several problems were observed with the photocyclization route. Firstly, the cyclization of an unsubstituted stilbene was not regioselective and oftentimes resulted in the formation of regioisomers which were difficult to separate by flash column chromatography (Scheme 1). Additionally, hydrogen iodide (HI) generated as a by-product of the oxidation sometimes led to further reduction of the double bond, if no HI scavenger was added.<sup>12</sup> Also, during the formation of [5]helicene, overoxidation of desired product **3** was observed to form undesired benzo[*ghi*]perylene **13** (Figure 5).<sup>13</sup>

<sup>12</sup> a) Laarhoven, W. H. *Recl. Trav. Chim. Pays-Bas.* **1983**, *102*, 185. b) Mallory, F. B.; Mallory, C. W. *Photocyclization of Stilbenes and Related Molecules*. Organic Reactions. 2005; Vol. 30, pp. 1 – 456.

<sup>13</sup> Mallory, F. B.; Mallory, C. W. *J. Org. Chem.* **1983**, *48*, 526.

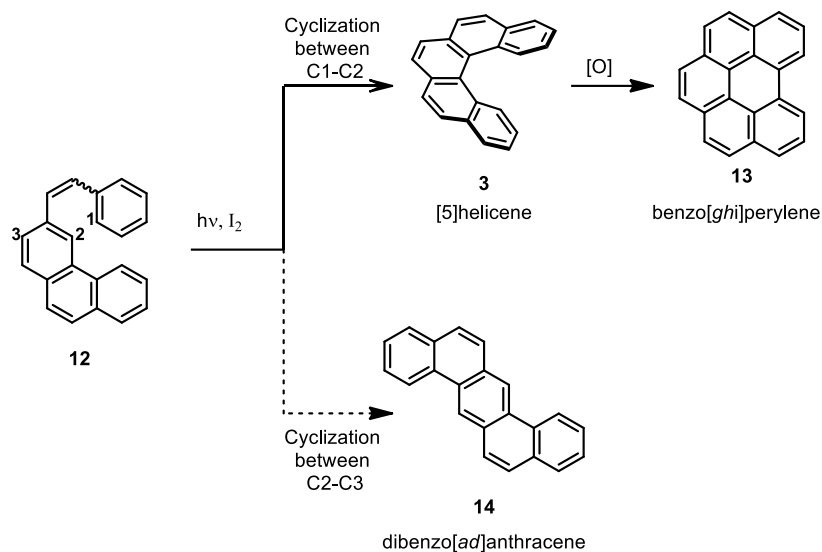
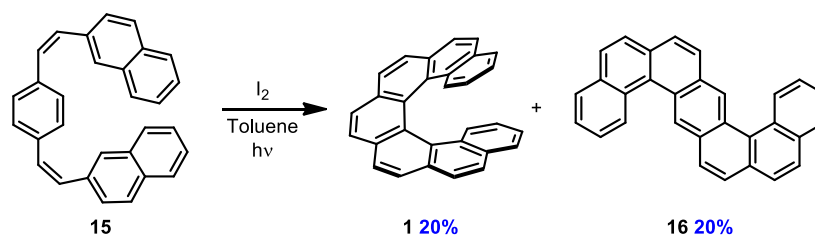


**Figure 5:** Cyclization possibilities for the photocyclization reaction between C1 and C2 with further oxidation.

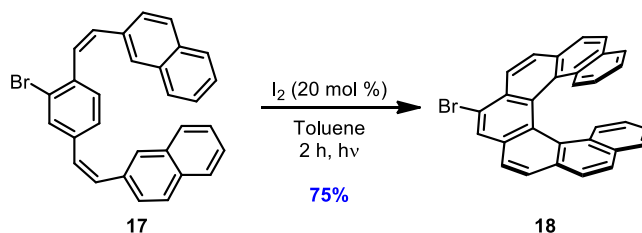
To resolve these issues, Katz and co-workers proposed incorporating a bromine substituent on the stilbene precursor to block two potential cyclization positions, the site of halogen substitution and the position *ortho* to the halogen atom, thus providing good regioselective control of the reaction (Scheme 2). The halogen was easily removed to give an unsubstituted helicene or further modified to afford a variety of compounds.<sup>14</sup> The same group also developed conditions using stoichiometric iodine and an excess of propylene oxide, which trapped HI, the by-product of  $I_2$  reduction. The synthetic strategy increased the overall yield and minimized the photoreduction of products, done by HI in the presence of light, as well as overoxidation of the desired helicene, observed when  $O_2$  was the oxidant.<sup>15</sup>

<sup>14</sup> a) Sudhakar, A.; Katz, T. J. *Tetrahedron Lett.* **1986**, 27, 2231. b) Liu, L. B.; Katz, T. J. *Tetrahedron Lett.* **1991**, 32, 6831.

<sup>15</sup> Liu, L. B.; Yang, B. W.; Katz, T. J.; Poindexter, M. K. *J. Org. Chem.* **1991**, 56, 3769.



**Scheme 1:** Poor regioselectivity observed with UV-light photocyclization of unsubstituted stilbene-type precursors.



**Scheme 2:** Improved regioselectivity observed with UV-light photocyclization of bromo-substituted stilbene-type precursors.

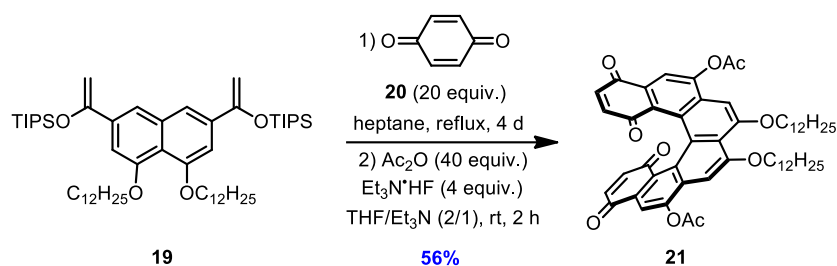
Although Katz's method had become the standard for the synthesis of helicenes of various lengths, from [5]- to [14]helicene,<sup>14b,16</sup> it suffered from several disadvantages. In order to prevent the formation of [2+2] intermolecular cycloaddition products the reaction was performed at a high dilution, thus limiting any significant scale-up. The method also did not tolerate certain functional groups such as acetyl, dimethylamino and nitro groups as they were known to disrupt or depopulate the reactive excited state of the substrate.<sup>17</sup> Finally, there was no enantiocontrol of the reaction, thus limiting the formation of enantiopure higher helicenes.

To overcome the disadvantages of the photocyclization reaction, various non-photochemical approaches have been developed. In the early 1990's, Katz and Liu made a significant contribution by establishing effective Diels-Alder conditions for the synthesis of

<sup>16</sup> a) Martin, R. H.; Marchant, M.-J.; Baes, M. *Helv. Chim. Acta* **1971**, *54*, 358. b) Moradpour, A.; Nicoud, J. F.; Balavoise, G.; Kagan, H.; Tsoucaris, G. *J. Am. Chem. Soc.* **1971**, *93*, 2353. c) Moradpour, A.; Kagan, H.; Baes, M.; Morren, G.; Martin, R. H. *Tetrahedron* **1975**, *31*, 2139. d) Martin, R. H.; Flammang-Barbieux, M.; Cosyn, J. P.; Gelbcke, M. *Tetrahedron* **1968**, *9*, 3507. e) Martin, R. H.; Schurter, J. J. *Tetrahedron* **1972**, *28*, 1749. f) Martin, R. H.; Libert, V. *J. Chem. Res. Miniprint* **1980**, *4*, 1940. g) Martin, R. H.; Baes, M. *Tetrahedron* **1975**, *31*, 2135. h) Martin, R. H.; Morren G.; Schurter, J. J. *Tetrahedron Lett.* **1969**, *10*, 3683.

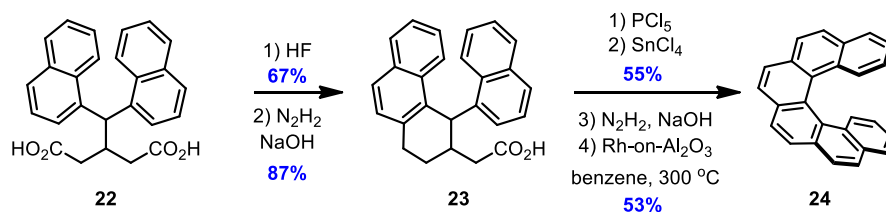
<sup>17</sup> a) Kaupp, G. *Methoden der Organischen Chemie (Houben-Weyl)*; Müller, E., Ed; Thieme Verlag, Stuttgart, 1975. b) Willmore, N. D.; Liu, L. B.; Katz, T. J. *Angew., Chem., Int. Ed.* **1992**, *31*, 1093. c) Blackburn, E. V.; Timmons, C. J. *Quart. Rev. Chem. Soc.* **1969**, *23*, 482.

helicenes (Scheme 3).<sup>18</sup> The method allowed for the facile formation of functionalized [5]-, [6]- and [7]helicenes on a multigram scale and has been extensively employed by several groups.<sup>18a,19</sup>



**Scheme 3:** Diels-Alder conditions by Liu and Katz for the formation of helicenes.

Another non-photochemical synthetic strategy was developed by Newman and co-workers, who used a double Friedel-Crafts acylation for the synthesis of [6]helicene **24** (Scheme 4).<sup>20</sup> Yamaguchi *et al.* reported a similar method for the synthesis of [4]helicenes, where substituents were used to direct the acylation and decrease the rate of racemization.<sup>21</sup>



**Scheme 4:** Newman's Friedel-Crafts acylation approach for the synthesis of [6]helicene.

<sup>18</sup> a) Willmore, N. D.; Liu, L. B.; Katz, T. J. *Angew. Chem., Int. Ed.* **1992**, *31*, 1093. b) Nuckolls, C.; Katz, T. J.; Katz, G.; Collins, P. J.; Castellanos, L. *J. Am. Chem. Soc.* **1999**, *121*, 79.

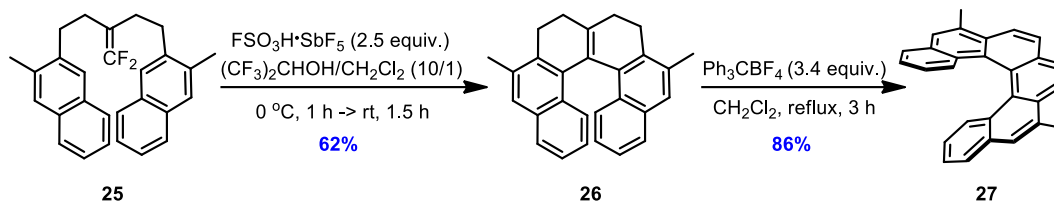
<sup>19</sup> a) Willmore, N. D.; Liu, L. B.; Katz, T. J. *Angew. Chem., Int. Ed.* **1992**, *31*, 1093. b) Minuti, L.; Taticchi, A.; Marrochi, A.; Gacs-Baitz, E.; Galeazzi, R. *Eur. J. Org. Chem.* **1999**, 3155. c) Carreño, M. C.; Garcia-Cerrada, S.; Urbano, A. *J. Am. Chem. Soc.* **2001**, *123*, 7929. d) Dreher, S. D.; Katz, T. J.; Lam, K. C.; Rheingold, A. L. *Org. Chem.* **2000**, *65*, 806. e) Katz, T. J.; Liu, L. B.; Willmore, N. D.; Fox, J. M.; Rheingold, A. L.; Shi, S. H.; Nuckolls, C.; Rickman, B. H. *J. Am. Chem. Soc.* **1997**, *119*, 10054. f) Fox, J. M.; Goldberg, N. R.; Katz, T. J. *J. Org. Chem.* **1998**, *63*, 7456. g) Paruch, K.; Katz, T. J.; Incarvito, C.; Lam, K. C.; Rhatigan, B.; Rheingold, A. L. *J. Org. Chem.* **2000**, *65*, 7602. h) Dreher, S. D.; Weix, D. J.; Katz, T. J. *J. Org. Chem.* **1999**, *64*, 3671.

<sup>20</sup> a) Newman, M. S.; Lednicer, D. *J. Am. Chem. Soc.* **1956**, *78*, 4765. b) Newman, M. S.; Wolf, M. *J. Am. Chem. Soc.* **1952**, *74*, 3225.

<sup>21</sup> Yamaguchi, M.; Okubo, H.; Hiram, M. *Chem. Commun.* **1996**, 1771.



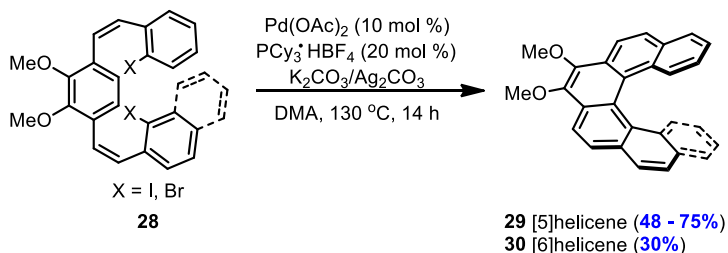
Ichikawa and co-workers also developed a Friedel-Crafts-type reaction for the synthesis of [6]helicene. The presence of two methyl groups on substrate **25** facilitated the domino cyclization by increasing the nucleophilicity of the aromatic moiety and directing the cyclization to form helicene **27** (Scheme 5).<sup>22</sup>



**Scheme 5:** The Ichikawa Friedel-Crafts-type synthesis of a disubstituted [6]helicene.

The various Friedel-Crafts-type methods for the synthesis of helicenes have several common features such as the need for functional blocking groups to direct the cyclization and groups containing polar unsaturated bonds, such as carboxyl, carbonyl and cyano groups incorporated in the precursors. Unfortunately, the lengthy syntheses of the starting materials rendered this synthetic strategy impractical for preparing helicenes on multigram scale.

Recently, numerous metal-catalyzed cyclization methods have been developed for the synthesis of helicenes. Several Pd-catalyzed couplings were reported where double C-H arylation was successful in synthesizing [5]- and [6]helicenes **29** and **30** (Scheme 6). The approach required a methoxy substituent at the 3- and 12-positions as a blocking group to control the regioselectivity of the cyclization.<sup>23</sup>

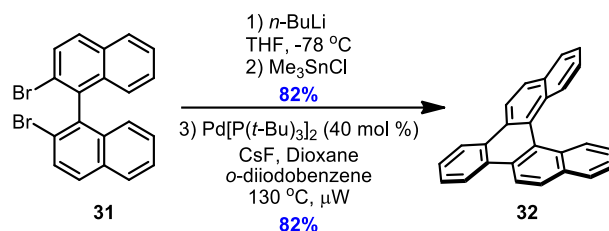


**Scheme 6:** Pd-catalyzed C-H arylation for the synthesis of disubstituted [5]- and [6]helicenes.

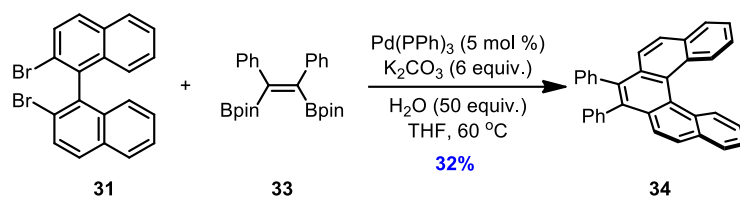
<sup>22</sup> Ichikawa, J.; Yokota, M.; Kudo, T.; Umezaki, S. *Angew., Chem., Int. Ed.* **2008**, *47*, 4870.

<sup>23</sup> Kamikawa, K.; Takemoto, I.; Takemoto, S.; Matsuzaka, H. *J. Org. Chem.* **2007**, *72*, 7406.

Other examples of Pd-catalyzed couplings for the synthesis of helicenes were reported by Scott and Xue, who developed a double Stille coupling for the preparation of benzo[5]helicene **32** (Scheme 7),<sup>24</sup> and Shimizu *et al.*, who established a double Suzuki-Miyaura reaction for the synthesis of diphenyl-substituted [5]helicene **34** (Scheme 8).<sup>25</sup> Unfortunately, further functionalization of the products was difficult and this route proved effective only for the synthesis of [5]- and [6]helicenes.



**Scheme 7:** Double Stille coupling by Scott and Xue for the synthesis of benzo[5]helicene.



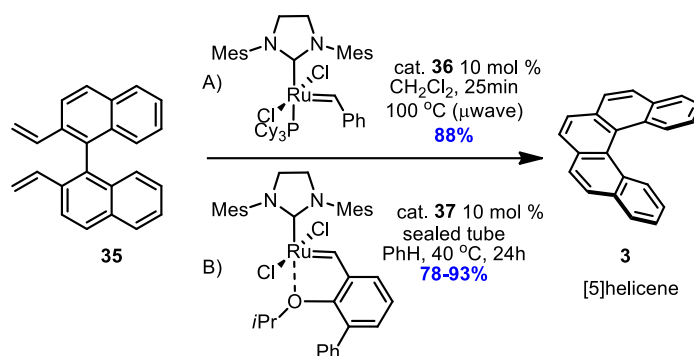
**Scheme 8:** Double Suzuki-Miyaura coupling by Shimizu *et al.* to form diphenyl-substituted [5]helicene.

In 2006, Collins and co-workers developed an efficient ring-closing metathesis (RCM) based synthesis of [5]-, [6]- and [7]helicenes. Two routes were proposed where route A was rapid, but required high temperatures (100 °C, 25 min), while route B took longer (40 °C, 24 h), but employed milder conditions and was tolerant of sensitive functional groups (Scheme 9).<sup>26</sup> The main drawback of the strategy was the complex multistep preparation of the starting materials which limited the possibilities of a large-scale synthesis of higher helicenes.

<sup>24</sup> Xue, X.; Scott, L. T. *Org. Lett.* **2007**, *9*, 3937.

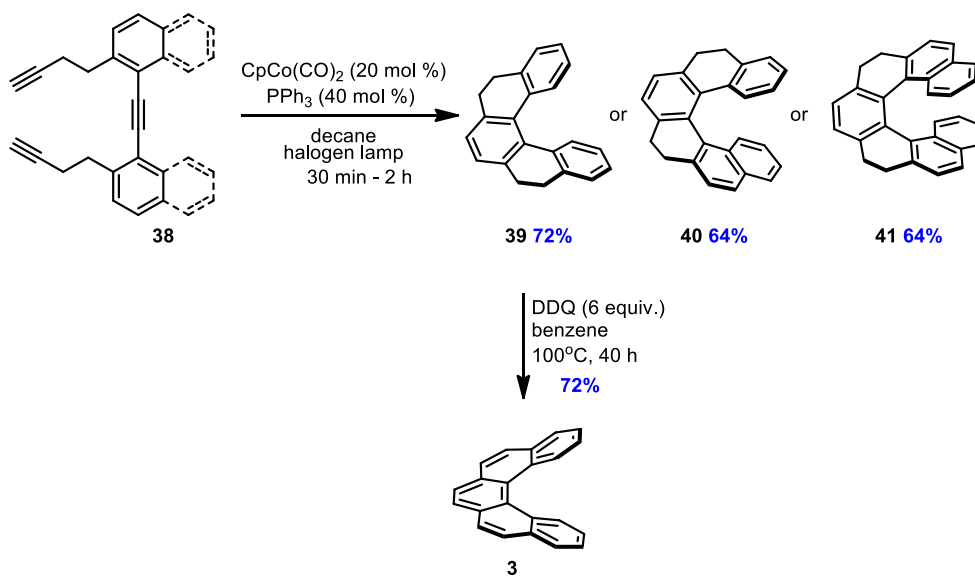
<sup>25</sup> Shimizu, M.; Nagao, I.; Tomioka, Y.; Hiyama, T. *Angew. Chem., Int. Ed.* **2008**, *47*, 8096.

<sup>26</sup> Collins, S. K.; Grandbois, A.; Vachon, M. P.; Côté, J. *Angew. Chem., Int. Ed.* **2006**, *45*, 2923.



**Scheme 9:** RCM synthesis of [5]helicene developed by Collins *et al.*

Further exploration of transition-metal catalysis for the synthesis of helicenes led to the development of a novel Co/Ni-catalyzed intramolecular [2+2+2] cycloisomerization by Starý, Starà *et al.*<sup>27</sup> Tetrahydrohelicenes **39**, **40** and **41** were synthesized using a Co-based catalyst and then dehydrogenated with DDQ or  $\text{Ph}_3\text{CBF}_4$  to achieve the parent helical compounds (Scheme 10). If  $\text{Ni}(\text{cod})_2/\text{PPh}_3$  was employed instead of  $\text{CpCo}(\text{CO})_2/\text{PPh}_3$ , a similar yield was achieved at ambient temperature without supplementary irradiation.<sup>28</sup>



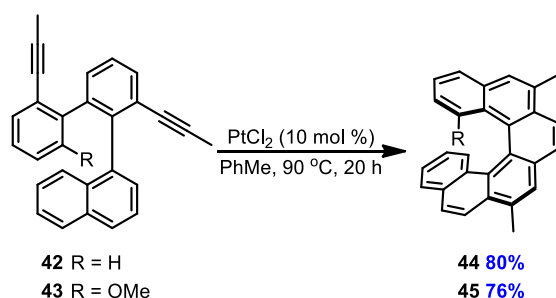
**Scheme 10:** Starý, Starà *et al.*'s Co-catalyzed [2+2+2] intramolecular cycloisomerization for the synthesis of tetrahydrohelicenes.

<sup>27</sup> Sehnal, P.; Stará, I. G.; Šaman, D.; Tichý, M.; Míšek, J.; Cvačka, J.; Rulišek, L.; Chocholousova, J.; Vacek, J.; Goryl, G.; Szymonski, M.; Císařová, I.; Starý, I. *Proc. Natl. Acad. Sci. U.S.A.* **2009**, *106*, 13169.

<sup>28</sup> Stará, I. G.; Starý, I.; Kollárovič, A.; Teplý, F.; Vyskočil, Š.; Šaman, D. *Tetrahedron Lett.* **1999**, *40*, 1993.

The [2+2+2] cycloisomerization method is very efficient because of the 100% atom economy in the reaction. Also, it provides the possibility of installing a plethora of functional groups on the aromatic or the alkyl moiety to afford various non-symmetric and multisubstituted helicenes. A wide range of complex helicenes and helicene-like structures have been synthesized using the strategy.<sup>29</sup>

Storch *et al.* developed a Pt-catalyzed double [2+2+2] cycloisomerization of biphenyl-naphthalenes **42** and **43** which led to the synthesis of hexahelicenes **44** and **45** by a convergent and modular assembly method (Scheme 11). The building blocks allowed the introduction of substituents at a more sterically hindered position of the helicene.<sup>30</sup>



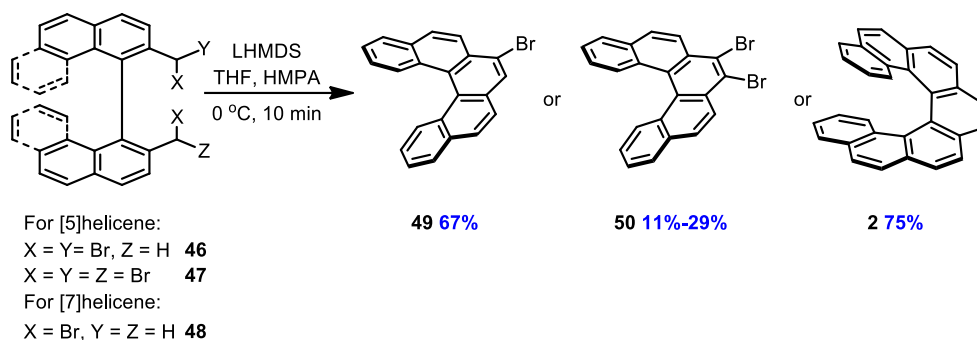
**Scheme 11:** Platinum-catalyzed double [2+2+2] cycloisomerization developed by Storch *et al.* for the synthesis of substituted [6]helicenes.

Dubois and Gingras synthesized substituted [5]- and [7]helicenes *via* a carbenoid coupling where bromo-substituted 2,2'-dimethyl-1,1'-binaphthyls **46**, **47** and **48** were treated with LiHMDS or PhLi to produce desired products **49**, **50** and **2** (Scheme 12).<sup>31</sup>

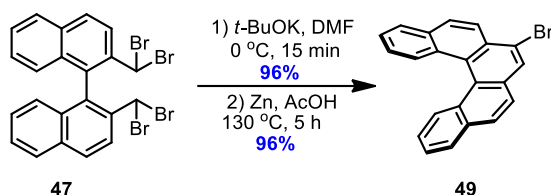
<sup>29</sup> a) Krausová, Z.; Sehnal, P.; Teplý, F.; Stará, I. G.; Starý, I.; Šaman, D.; Cvačka, J.; Fiedler, P. *Collect. Czech Chem. Commun.* **2007**, *72*, 1499. b) Songis, O.; Mísek, J.; Schmid, M. B.; Kollárovič, A.; Stará, I. G.; Šaman, D.; Císařová, I.; Starý, I. *J. Org. Chem.* **2010**, *75*, 6889. c) Rybáček, J.; Huerta-Angeles, G.; Kollárovič, A.; Stará, I. G.; Starý, I.; Rahe, P.; Nimmrich, M.; Kühnle, A. *Eur. J. Org. Chem.* **2011**, 853. d) Teplý, F.; Stará, I. G.; Starý, I.; Kollárovič, A.; Luštinec, D.; Krausová, Z.; Šaman, D.; Fiedler, P. *Eur. J. Org. Chem.* **2007**, 4244. e) Tanaka, K.; Fukawa, N.; Suda, T.; Noguchi, K. *Angew. Chem., Int. Ed.* **2009**, *48*, 5470. f) Adriaenssens, L.; Severa, L.; Šálová, T.; Císařová, I.; Pohl, R.; Šaman, D.; Rocha, S. V.; Finney, N. S.; Pospíšil, L.; Slaviček, P.; Teplý, F. *Chem. – Eur. J.* **2009**, *15*, 1072. g) Carbery, D. R.; Crittall, M. R.; Rzepa, H. S. *Org. Lett.* **2011**, *13*, 1250.

<sup>30</sup> Storch, J.; Sýkora, J.; Čermák, J.; Karban, J.; Císařová, I.; Ružička, A. *J. Org. Chem.* **2009**, *74*, 3090.

<sup>31</sup> a) Dubois, F.; Gingras, M. *Tetrahedron Lett.* **1998**, *39*, 5039. b) Gingras, M.; Dubois, F. *Tetrahedron Lett.* **1999**, *40*, 1309.

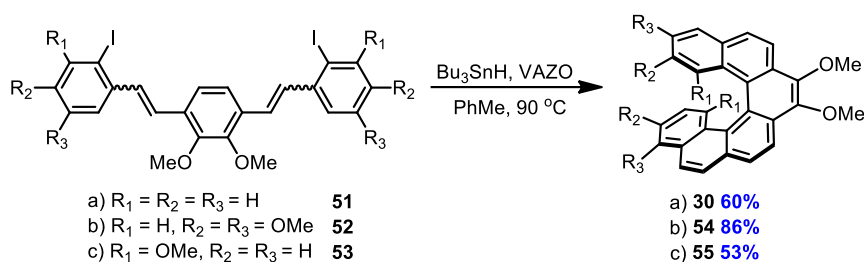


**Scheme 12:** Gingras and Dubois' synthesis of substituted [5]- and [7]helicenes *via* a carbenoid coupling.



**Scheme 13:** Gingras' conditions for the formation of helicene **49**.

Gingras further improved the synthesis of **49** by using *t*-BuOK and DMF for the benzylic(dibromo)methane coupling which provided the desired product in 96% yield (Scheme 13).<sup>32</sup> The high-yielding carbenoid-coupling methods were a practical way to prepare helicenes because the reagents involved are inexpensive and the reaction rates of the coupling are extremely rapid.



**Scheme 14:** Harrowven *et al.*'s radical cyclization route for the synthesis of variously substituted helicenes.

<sup>32</sup> Goretta, S.; Tasciotti, C.; Mathieu, S.; Smet, M.; Maes, W.; Chabre, Y. M.; Dehaen, W.; Giasson, R.; Raimundo, J. M.; Henry, C. R.; Barth, C.; Gingras, M. *Org. Lett.* **2009**, *11*, 3846.

Another method for synthesizing helicenes is through radical cyclization. Harrowven *et al.* reported an intramolecular aryl radical addition reaction where the stilbene-type cyclization precursor underwent a radical cyclization after treatment with tributyltin hydride.<sup>33</sup> The group later developed an efficient tandem radical cyclization reaction with tributyltin hydride where the two *ortho*-methoxy groups controlled the diastereoselectivity and directed the cyclization to provide helicenes **30**, **54** and **55** (Scheme 14).<sup>34</sup> Although the radical cyclization route was a useful approach for the synthesis of helicenes due to the facile preparation of the stilbene-type starting material and the fair to good yields, this method is not widely used because of its narrow functional group tolerance.

### 1.3 Applications of Helicenes

Helicenes have found an application in a wide variety of fields. In asymmetric catalysis, [7]helicenes have been used as chiral auxiliaries, chiral reagents, chiral additives<sup>35, 36</sup> and chiral ligands<sup>1</sup> in various diastereoselective reactions such as hydroxyaminations,<sup>37</sup> epoxidations of olefins,<sup>38</sup> reductions of  $\alpha$ -keto esters,<sup>39</sup> syntheses of atrolactic esters<sup>40</sup> as well as ene reactions.<sup>41</sup> The helicene motif has also been applied to molecular recognition,<sup>42</sup> as a part of molecular machinery<sup>43</sup> as well as in supramolecular<sup>44</sup> and polymer chemistry in the synthesis of ladder

<sup>33</sup> a) Harrowven, D. C.; Guy, I. L.; Nanson, L. *Angew. Chem., Int. Ed.* **2006**, *45*, 2242. b) Harrowven, D. C.; Nunn, M. I. T.; Fenwick, D. R. *Tetrahedron Lett.* **2002**, *43*, 3189.

<sup>34</sup> Harrowven, D. C.; Nunn, M. I. T.; Fenwick, D. R. *Tetrahedron Lett.* **2002**, *43*, 7345.

<sup>35</sup> Sato, I.; Yamashima, R.; Kadowaki, K.; Yamamoto, J.; Shibata, T.; Soai, K. *Angew. Chem., Int. Ed.* **2001**, *40*, 1096.

<sup>36</sup> Kawasaki, T.; Suzuki, K.; Licandro, E.; Bossi, A.; Maiorana, S.; Soai, K. *Tetrahedron : Asymmetry* **2006**, *17*, 2050.

<sup>37</sup> Hassine, B.B.; Gorsane, M.; Pecher, J.; Martin, R. H. *Bull. Soc. Chim. Belg.* **1985**, *94*, 759.

<sup>38</sup> Hassine, B.B.; Gorsane, M.; Geerts-Evrard, F.; Pecher, J.; Martin, R. H.; Castelet, D. *Bull. Soc. Chim. Belg.* **1986**, *95*, 547.

<sup>39</sup> Hassine, B.B.; Gorsane, M.; Pecher, J.; Martin, R. H. *Bull. Soc. Chim. Belg.* **1985**, *94*, 597.

<sup>40</sup> Hassine, B.B.; Gorsane, M.; Pecher, J.; Martin, R. H. *Bull. Soc. Chim. Belg.* **1986**, *95*, 557.

<sup>41</sup> Hassine, B.B.; Gorsane, M.; Pecher, J.; Martin, R. H. *Bull. Soc. Chim. Belg.* **1987**, *96*, 801.

<sup>42</sup> a) Yamamoto, K.; Ikeda, T.; Kitsuki, T.; Okamoto, Y.; Chikamatsu, H.; Nakazaki, M. *J. Chem. Soc., Perkin Trans. I* **1990**, 271. b) Nakazaki, M.; Yamamoto, K.; Ikeda, T.; Kitsuki, T.; Okamoto, Y. *J. Chem. Soc., Chem. Commun.* **1983**, 787. c) Newcomb, M.; Toner, J. L.; Helgeson, R. C.; Cram, D. J. *J. Am. Chem. Soc.* **1979**, *101*, 4941.

<sup>43</sup> a) Kelly, T. R. *Acc. Chem. Res.* **2001**, *34*, 514. b) Kelly, T. R.; Tellitu, I.; Sestelo, J. P. *Angew. Chem., Int. Ed. Engl.* **1997**, *36*, 1866. c) Kelly, T. R.; Sestelo, J. P.; Tellitu, I. *J. Org. Chem.* **1998**, *63*, 3655.

<sup>44</sup> a) Deshayes, K.; Broene, R. D.; Chao, I.; Knobler, C. B.; Diederich, F. *J. Org. Chem.* **1991**, *56*, 6787. b) Owens, L.; Thilgen, C.; Diederich, F.; Knobler, C. B. *Helv. Chim. Acta.* **1993**, *76*, 2757.

polymers.<sup>45,46,47</sup> Helicenes have also been introduced into macromolecules *via* direct synthesis or through polymerization of helicene monomers.<sup>1</sup> Some helical compounds and their cyclization precursors display photochromism, a phenomena that has been studied extensively due to its application in devices such as switches and optical memories.<sup>48,49,50</sup> The observed photochromism lead to the application of helicenes in redox,<sup>51</sup> electrochiroptical<sup>52</sup> and multi-input/multi-output molecular switches.<sup>53</sup> The main focus of this section will be on the aggregation of helicenes in solution as well as their application in electronic devices and on Langmuir-Blodgett (LB) films.

Enantiopure helicenes have demonstrated spontaneous aggregation in solution. Katz and co-workers were the first to report the self-assembly of optically active helicenebisquinones in 1996 (Figure 6).<sup>54</sup> Enantiopure thiohelicenes assembled into columnar structures in the presence or absence of solvent. The aggregation exhibited good nonlinear optical properties.<sup>55</sup>

---

<sup>45</sup> a) Dai, Y. J.; Katz, T. J. *J. Org. Chem.* **1997**, *62*, 1274. b) Dai, Y. J.; Katz, T. J.; Nichols, D. A. *Angew. Chem., Int. Ed. Engl.* **1996**, *35*, 2109.

<sup>46</sup> a) Iwasaki, T.; Katayose, K.; Kohinata, Y.; Nishide, H. *Polym. J.* **2005**, *37*, 592. b) Iwasaki, T.; Kohinata, Y.; Nishide, H. *Org. Lett.* **2005**, *7*, 755. c) Iwasaki, T.; Nishide, H. *Curr. Org. Chem.* **2005**, *9*, 1665. d) Takemura, I.; Sone, R.; Nishide, H. *Polym. Adv. Technol.* **2008**, *19*, 1092.

<sup>47</sup> Tagami, K.; Tsukada, M.; Wada, Y.; Iwasaki, T.; Nishide, H. *J. Chem. Phys.* **2003**, *119*, 7491.

<sup>48</sup> a) Parthenopoulos, D. A.; Rentzepis, P. M. *Science*, **1989**, *245*, 843. b) Irie, M. *Chem. Rev.* **2000**, *100*, 1685.

<sup>49</sup> Norsten, T. B.; Peters, A.; McDonald, R.; Wang, M. T.; Branda, N. R. *J. Am. Chem. Soc.* **2001**, *123*, 7447.

<sup>50</sup> a) Wigglesworth, T. J.; Sud, D.; Norsten, T. B.; Lekhi, V. S.; Branda, N. R. *J. Am. Chem. Soc.* **2005**, *127*, 7272. b) Tani, Y.; Ubukata, T.; Yokoyama, Y.; Yokoyama, Y. *J. Org. Chem.* **2007**, *72*, 1639. c) Okuyama, T.; Tani, Y.; Miyake, K.; Yokoyama, Y. *J. Org. Chem.* **2007**, *72*, 1634.

<sup>51</sup> Nishida, J.; Suzuki, T.; Ohkita, M.; Tsuji, T. *Angew. Chem., Int. Ed.* **2001**, *40*, 3251.

<sup>52</sup> Ohta, E.; Higuchi, H.; Kawai, H.; Fujiwara, K.; Suzuki, T. *Org. Biomol. Chem.* **2005**, *3*, 3024.

<sup>53</sup> Suzuki, T.; Ishigaki, Y.; Iwai, T.; Kawai, H.; Fujiwara, K.; Ikeda, H.; Kano, Y.; Mizuno, K. *Chem. – Eur. J.* **2009**, *15*, 9434.

<sup>54</sup> Nuckolls, C.; Katz, T. J.; Castellanos, L. *J. Am. Chem. Soc.* **1996**, *118*, 3767.

<sup>55</sup> Phillips, K. E. S.; Katz, T. J.; Jockusch, S.; Lovinger, A. J.; Turro, N. J. *J. Am. Chem. Soc.* **2001**, *123*, 11899.

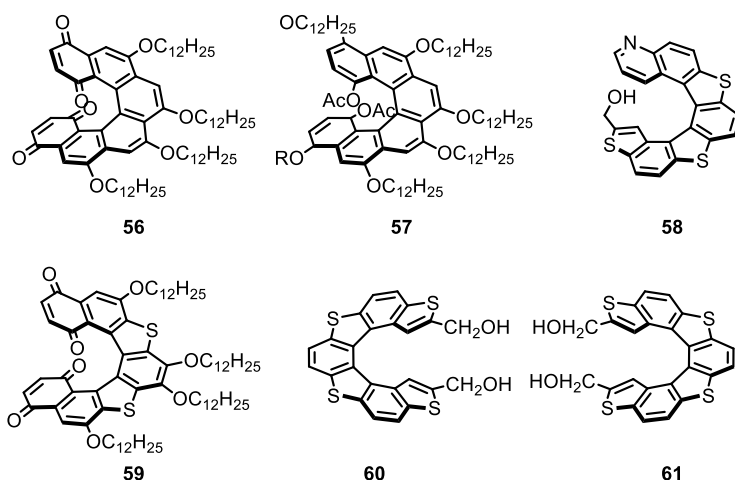


**Figure 6:** Examples of helicenes used in self-assembly.

Helicenes may self-assemble through nonplanar  $\pi$ - $\pi$  interactions, as well as *via* hydrogen bonding. Tanaka's group demonstrated that thiohelicene **60** with carboxylic acid substitutions on its periphery, readily crystallized from ethanol forming a 1:1 host-guest clathrate by hydrogen bonding.<sup>56</sup> The same group reported that enantiopure (*P*)-thiohelicene **61** aggregated into a four-leaf clover motif in a left-handed manner.<sup>57</sup> Tanaka *et al.* also described the formation of a homochiral dimer of **58** *via* intermolecular hydrogen bonding.<sup>58</sup>

Heterohelicenes have been used as building blocks for the preparation of organic donor-acceptor  $\pi$ -conjugated (D- $\pi$ -A) dyes, an environmentally-friendly alternative to the expensive ruthenium-based dyes traditionally used in dye-sensitized solar cells (DSSCs).<sup>59</sup> These cells were seen as the next generation of solar cells because of their low-cost, high performance and ease of production.<sup>60</sup> Harima and co-workers developed a series of heterohelicene-containing D- $\pi$ -A dyes which take advantage of the conjugation framework and the helical backbone (Figure 7).<sup>61</sup>

<sup>56</sup> Tanaka, K.; Shogase, Y.; Osuga, H.; Suzuki, H.; Nakanishi, W.; Nakamura, K.; Kawai, Y. *J. Chem. Soc., Chem. Commun.* **1995**, 1873.

<sup>57</sup> Tanaka, K.; Kithara, Y. *Chem. Commun.* **1998**, 1141.

<sup>58</sup> Tanaka, K.; Kithara, Y.; Suzuki, H.; Osuga, H.; Kawai, Y. *Tetrahedron Lett.* **1996**, 37, 5925.

<sup>59</sup> Mishra, A.; Fischer, M. K. R.; Bauerle, P. *Angew. Chem., Int. Ed.* **2009**, 48, 2474.

<sup>60</sup> Grätzel, M. *Nature* **2001**, 414, 338.

<sup>61</sup> a) Ooyama, Y.; Ito, G.; Fukuoka, H.; Nagano, T.; Kagawa, Y.; Imae, I.; Komaguchi, K.; Harima, Y. *Tetrahedron* **2010**, 66, 7268. b) Ooyama, Y.; Ishii, A.; Kagawa, Y.; Imae, I.; Harima, Y. *New J. Chem.* **2007**, 31, 2076. c) Ooyama, Y.; Shimada, Y.; Kagawa, Y.; Imae, I.; Harima, Y. *Org. Biomol. Chem.* **2007**, 5, 2046. d) Ooyama, Y.; Shimada, Y.; Kagawa, Y.; Yamada, Y.; Imae, I.; Komaguchi, K.; Harima, Y. *Tetrahedron Lett.* **2007**, 48, 9167. e) Ooyama, Y.; Harima, Y. *Eur. J. Org. Chem.* **2009**, 2903. f) Ooyama, Y.; Shimada, Y.; Ishii, A.; Ito, G.; Kagawa, Y.; Imae, I.;



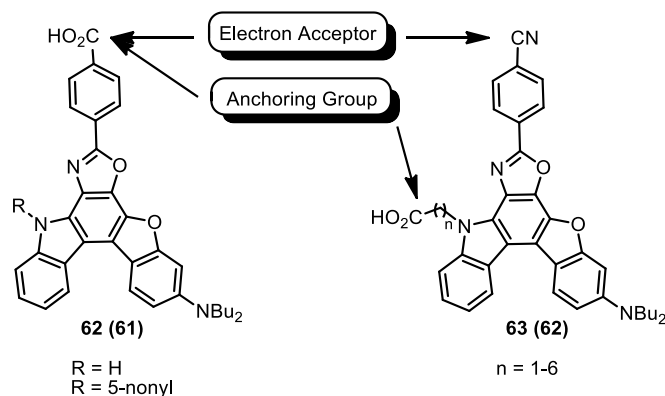


**Figure 7:** Some organic D- $\pi$ -A dyes developed by Harima and co-workers.

The use of helicenes also extends into the formation of Langmuir-Blodgett (LB) films. Yamaguchi *et al.* reported the first chiral LB film bearing enantiopure helicene moieties (Figure 8).<sup>62</sup> Core **64** was essential to the production of stable LB films and the properties could be improved by N-alkylation, thus affording a variety of optically active films.<sup>8a, 63</sup>

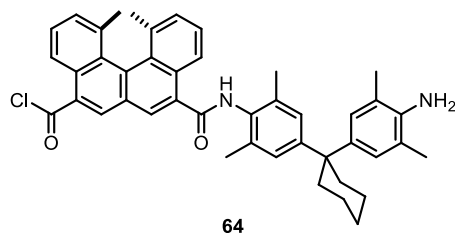


**Figure 8:** Enantiopure helicene moiety used in the formation of Langmuir-Blodgett films by Yamaguchi *et al.*

Katz *et al.* developed another novel class of Langmuir-Blodgett films using enantiopure helicene **56** (Figure 6).<sup>64</sup> Self-assembly of the helicene resulted in the formation of long fibers in solution and in liquid crystalline material (Figure 9).<sup>65</sup> The liquid crystalline fibers comprised long

Komaguchi, K.; Harima, Y. *J. Photochem. Photobiol. A* **2009**, *203*, 177. g) Ooyama, Y.; Inoue, S.; Asada, R.; Ito, G.; Kushimoto, K.; Komaguchi, K.; Imae, I.; Harima, Y. *Eur. J. Org. Chem.* **2010**, 92. h) Ooyama, Y.; Ito, G.; Kushimoto, K.; Komaguchi, K.; Imae, I.; Harima, Y. *Org. Biomol. Chem.* **2010**, *8*, 2756.

<sup>62</sup> Feng, P.; Miyashita, T.; Okubo, H.; Yamaguchi, M. *J. Am. Chem. Soc.* **1998**, *120*, 10166.

<sup>63</sup> Okubo, H.; Feng, F.; Nakano, D.; Hirata, T.; Yamaguchi, M.; Miyashita, T. *Tetrahedron* **1999**, *55*, 14855.

<sup>64</sup> Nuckolls, C.; Katz, T. J.; Verbiest, T.; Van Elshocht, S.; Kuball, H. G.; Kiesewalter, S.; Lovinger, A. J.; Persoons, A. *J. Am. Chem. Soc.* **1998**, *120*, 8656.

<sup>65</sup> Lovinger, A. J.; Nuckolls, C.; Katz, T. J. *J. Am. Chem. Soc.* **1998**, *120*, 264.

parallel columns that were stacked into lamellae, which were visible under an optical microscope.<sup>65, 66</sup>

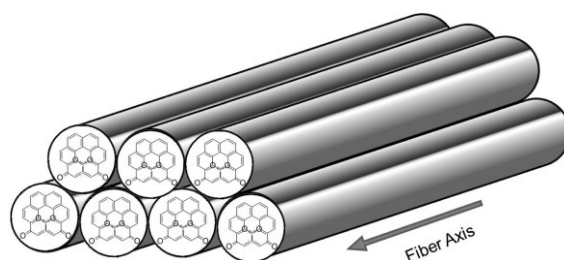


**Figure 9:** Schematic representation of columnar aggregation formed by helicenes as observed by Katz and co-workers.

It has been observed that helicenes dissolved in achiral liquid crystals could act as chiral dopants and transfer their molecular chirality to the whole phase.<sup>67</sup> Spada *et al.* used three different types of helicenes as dopants (Figure 10) and observed that rigid chiral probes **65**, **66** and **24** provided a left-handed cholesteric structure with helical twists (Figure 11).<sup>68</sup>

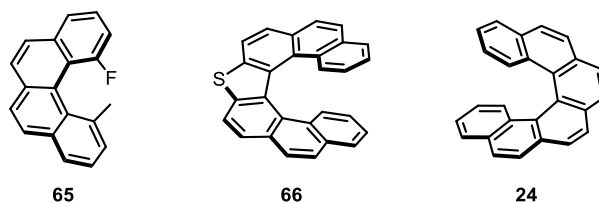


**Figure 10:** Three different types of helicenes used as dopants to induce chirality in achiral liquid crystals by Spada *et al.*

<sup>66</sup> Lovinger, A. J.; Nuckolls, C.; Katz, T. J. *J. Am. Chem. Soc.* **1998**, *120*, 1944.

<sup>67</sup> a) Lemieux, R.P. *Acc. Chem. Res.* **2001**, *34*, 845. b) Gottarelli, G.; Osipov, M. A.; Spada, G. P. *J. Phys. Chem.* **1991**, *95*, 3879.

<sup>68</sup> Gottarelli, G.; Proni, G.; Spada, G. P.; Fabbri, D.; Gladiali, S.; Rosini, C. *J. Org. Chem.* **1996**, *61*, 2013.

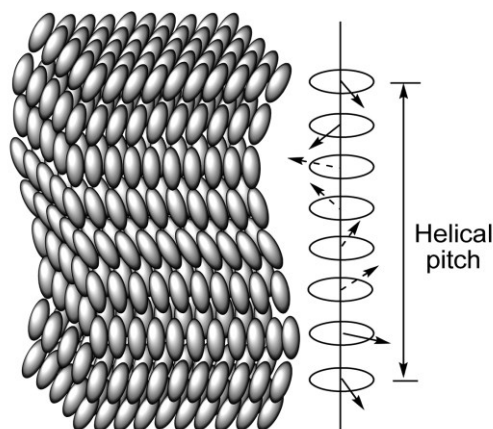


**Figure 11:** A schematic representation of the chiral phase and helical pitch induced by enantiopure helicenes in the presence of achiral liquid crystals.

Barnes *et al.* observed a chiroptical response of a single molecule of **67** which may have potential applications in polarized organic light-emitting diodes (POLEDs).<sup>69</sup> Also, Soosksimuang *et al.* used helicene **68** (DDH) as a novel organic emissive material where the pull and push structure resulted in absorption and fluorescence at longer wavelengths.<sup>70</sup> OLEDs were also fabricated using a similar DDH moiety.

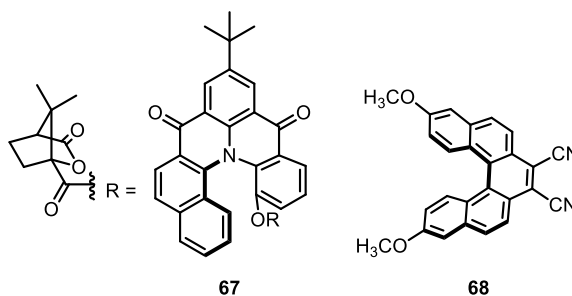


**Figure 12:** Various helicenes employed in organic electronics.

Other interesting polycyclic aromatic hydrocarbon cores which possess extended conjugated systems and enhanced optical and electronic properties include pyrene and its

<sup>69</sup> a) Hassey, R.; Swain, E. J.; Hammer, N. I.; Venkataraman, D.; Barnes, M. D. *Science* **2006**, *314*, 1437. b) Hassey, R.; McCarthy, K. D.; Basak, E. S. D.; Venkataraman, D.; Barnes, M. D. *Chirality* **2008**, *20*, 1039. c) Tang, Y. Q.; Cook, T. A.; Cohen, A. E. *J. Phys. Chem. A* **2009**, *113*, 6213. d) Cohen, A.; Tang, Y. Q. *J. Phys. Chem. A* **2009**, *113*, 9759.

<sup>70</sup> Sahasithiwat, S.; Mophuang, T.; Menbangpung, L.; Komatonwong, S.; Soosksimuang, T. *Synth. Met.* **2010**, *160*, 1148.

derivatives. These compounds have recently been studied more profoundly due to their potential applications in many areas of chemistry. The next section will focus on pyrene and its discovery and applications as well as recent developments in the chemical modifications of pyrene.

## 1.4 Introduction to Pyrene

Pyrene, meaning “fire” in Greek, was first isolated as a by-product of the destructive distillation of coal tar.<sup>71</sup> Initially, pyrene derivatives were employed in the synthetic dye industry,<sup>72</sup> however their prominence increased after 1954, the year Förster and Kasper observed intermolecular excimers in a pyrene solution.<sup>73</sup> Aside from excimer formation, pyrene molecules are known to possess long-lived excited states, high fluorescence quantum yield<sup>74</sup> and an exceptional distinction of the fluorescence bands between the monomer and the excimer. Notably, the excitation spectra of these molecules possess a sensitivity to microenvironmental changes,<sup>75</sup> which makes them an excellent molecular probe of microenvironments. The combination of these characteristics make pyrene one of the most studied organic molecules in terms of its photophysical properties.

## 1.5 Chemical Modifications of Pyrene

Weitzenböck was the first to synthesize pyrene in 1913.<sup>76</sup> Other routes were developed in the 1950s.<sup>77</sup> Because considerable quantities were extracted through distillation of coal tar and

---

<sup>71</sup> Figueira-Duarte, T. M.; Müllen, K. *Chem. Rev.* **2011**, *111*, 7260.

<sup>72</sup> Welham, R. D. *J. Soc. Dyers Color* **1963**, *79*, 98.

<sup>73</sup> Förster, T.; Kasper, K. *Z. Elektrochem.* **1955**, *59*, 976.

<sup>74</sup> Birks, J. B. *Photophysics of Aromatic Molecules*; Wiley-Interscience: London, 1970.

<sup>75</sup> Kalyanasundaram, K.; Thomas, J. K. *J. Am. Chem. Soc.* **1977**, *99*, 2039.

<sup>76</sup> Weitzenböck, R. *Mh. Chem.* **1913**, *34*, 193.

<sup>77</sup> a) Chatterjee, N. N.; Bose, A.; Roy, H., B. *J. Indian. Chem. Soc.* **1947**, *24*, 169. b) Freund, M.; Fleischer, K. *Liebigs Ann.* **1914**, *402*, 77. c) Fleischer, K.; Retze, E. *Chem. Ber.* **1922**, *55*, 3280. d) Von Braun, J.; Rath, E. *Chem. Ber.* **1928**, *61*, 956. e) Cook, J. W. *J. Chem. Soc.* **1934**, 366. f) Baker, W.; McOmie, J. F. W.; Norman, J. M. *Chem. Ind.* **1950**, 77. g) Baker, W.; McOmie, J. F. W.; Norman, J. M. *J. Chem. Soc.* **1951**, 1114. h) Baker, W.; McOmie, J. F. W.; Warburton, W. K. *J. Chem. Soc.* **1952**, 2991. i) Pelchowicz, Z.; Bergmann, E. D. *Bull. Res. Council Israel* **1953**, *3*, 91. j) Bacon, R. G. R.; Lindsay, W. S. *J. Chem. Soc.* **1958**, 1375.

destructive hydrogenation of hard coal, the need for a facile synthesis decreased as pyrene was commercially accessible and relatively inexpensive.

The chemistry of pyrene has been extensively studied, however regioselectivity of substitution and purification still remains a challenge. Experimentally, functionalization *via* electrophilic substitution occurs preferentially at the 1-, 3-, 6- and 8-positions<sup>78</sup> (Figure 13).<sup>79</sup> The exception is *tert*-butylation of the molecule, where steric hindrance favours the substitution at positions 2 and 7 (Figure 13).<sup>80</sup>

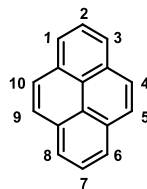


**Figure 13:** Numbering of the pyrene molecule

Metal-catalyzed cross-coupling reactions, such as the Suzuki, Stille, Sonogashira, Ullmann and Heck couplings, have been extensively used to functionalize pyrenes at position 1, as the method allows the formation of larger  $\pi$ -systems by coupling several pyrenes to each other.<sup>71,78a,81</sup> The Wittig olefination is also useful for the coupling of a triphenylphosphonium ylide and a pyrene aldehyde.<sup>82</sup>

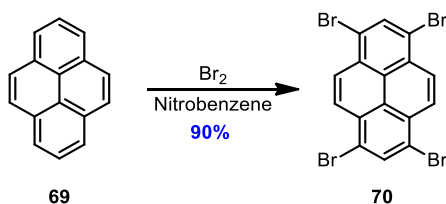
<sup>78</sup> a) Vollmann, H.; Becker, H.; Corell, M.; Streeck, H. *Liebigs Ann.* **1937**, *531*, 1. b) Altschuler, L.; Berliner, E. *J. Am. Chem. Soc.* **1966**, *88*, 5837.

<sup>79</sup> a) Dewar, M. J. S.; Dennington, R. D. *J. Am. Chem. Soc.* **1989**, *111*, 3804. b) Hites, R. A. *Calculated Molecular Properties of Polycyclic Aromatic Hydrocarbons*; Elsevier: New York, **1987**.

<sup>80</sup> Miyazawa, A.; Yamato, T.; Tashiro, M. *Chem. Express.* **1990**, *5*, 381.

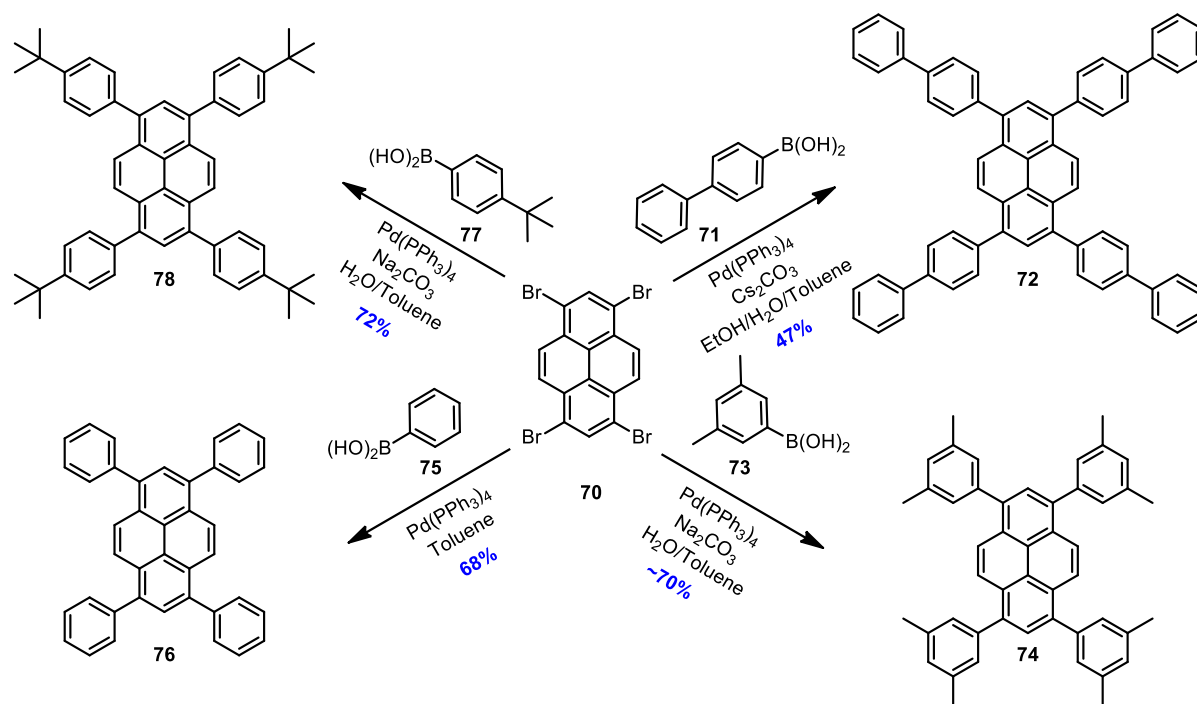
<sup>81</sup> a) Maeda, H.; Maeda, T.; Mizuno, K.; Fujimoto, K.; Shimizu, H.; Inouye, M. *Chem. – Eur. J.* **2006**, *12*, 824. b) Yang, C. H.; Guo, T. F.; Sun, I. W. *J. Luminesc.* **2007**, *124*, 93. c) Amann, N.; Pandurski, E.; Fiebig, T.; Wagenknecht, H. A. *Angew. Chem., Int. Ed.* **2002**, *41*, 2978. d) Amann, N.; Pandurski, E.; Fiebig, T.; Wagenknecht, H. A. *Chem. – Eur. J.* **2002**, *8*, 4877. e) Suzuki, K.; Seno, A.; Tanabe, H.; Ueno, K. *Synth. Met.* **2004**, *143*, 89. f) Wu, K. C.; Ku, P. J.; Lin, C. S.; Shih, H. T.; Wu, F. I.; Huang, M. J.; Lin, J. J.; Chen, I. C.; Cheng, C. H. *Adv. Funct. Mater.* **2008**, *18*, 67. g) Mikroyannidis, J. A.; Fenenko, L.; Adachi, C. *J. Phys. Chem. B* **2006**, *110*, 20317. h) Liu, F.; Tang, C.; Chen, Q. Q.; Li, S. Z.; Wu, H. B.; Xie, L. H.; Peng, B.; Wei, W.; Cao, Y.; Huang, W. *Org. Electron.* **2009**, *10*, 256. i) Suzuki, H.; Kondo, A.; Inouye, M.; Ogawa, T. *Synthesis* **1986**, 121. j) Radner, F. *Acta Chem. Scand.* **1989**, *43*, 481.

<sup>82</sup> a) Okamoto, H.; Arai, T.; Sakuragi, H.; Tokumaru, K. *Bull. Chem. Soc. Jpn.* **1990**, *63*, 2881. b) Moggia, F.; Vidélot – Ackermann, C.; Ackermann, J.; Raynal, P.; Brisset, H.; Fages, F. *J. Mater. Chem.* **2006**, *16*, 2380.



**Scheme 15:** Bromination provides 1,3,6,8-tetrabromopyrene.

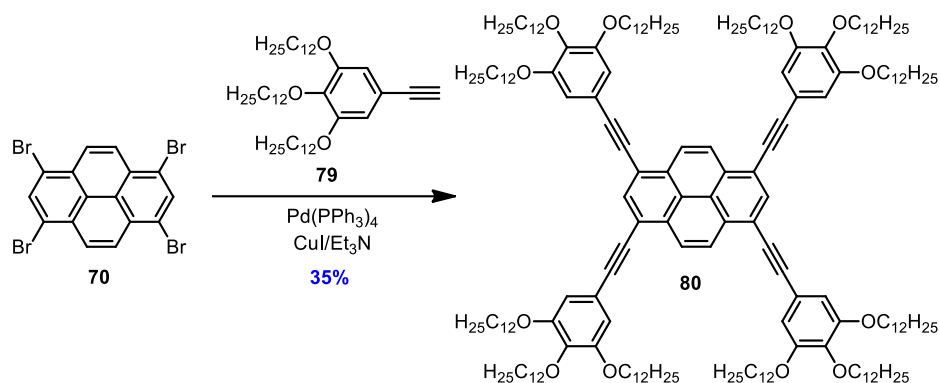
The bromination of pyrene provides access to tetrabromopyrene **70**, a valuable precursor for the synthesis of tetrasubstituted pyrenes (Scheme 15), which could undergo further functionalization *via* the Suzuki (Scheme 16)<sup>83</sup> or the Sonogashira coupling (Scheme 17).<sup>84</sup> Tetrasubstitution provides a particular conformation of pyrene which prevents aggregation in the system thus permitting the use of pyrene-derived compounds in light-emitting devices.



**Scheme 16:** Suzuki couplings between tetrabromopyrene and various boronic acids.

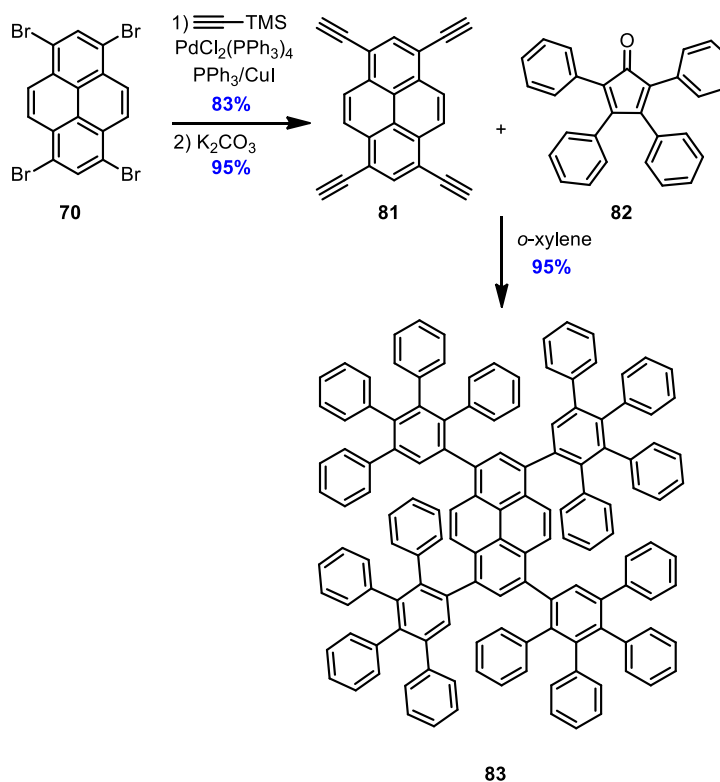
<sup>83</sup> a) Sotoyama, W.; Sato, H.; Kinoshita, M.; Takahashi, T. *SID 03 Dig.* **2003**, 1294. b) Kyoto University; Nippon Telegraph and Telephone Corporation; Pioneer Corporation; Hitachi, Ltd.; Mitsubishi Chemical Corporation; Rohm Co., Ltd. WO2006/57326, A1, 2006. c) Zoephel, L.; Berger, R.; Gao, P.; Enkelmann, V.; Baumgarten, M.; Wagner, M.; Muellen, K. *Chemistry – A European Journal* **2013**, *19*, 17821. d) Oyamada, T.; Akiyama, S.; Yahiro, M.; Saigou, M.; Shiro, M.; Sasabe, H.; Adachi, C. *Chem. Phys. Lett.* **2006**, *421*, 295.

<sup>84</sup> Hayer, A.; de Halleux, V.; Kohler, A.; El-Garouhy, A.; Meijer, E. W.; Barbera, J.; Tant, J.; Levin, J.; Lehmann, M.; Gierschner, J.; Cornil, J.; Geerts, Y. H. *J. Phys. Chem. B* **2006**, *110*, 7653.



**Scheme 17:** Sonogashira coupling with tetrasubstituted pyrene.

The Diels Alder cycloaddition is also a useful reaction for multifunctionalization of a tetrabromopyrene molecule which provided derivative **83** that could be implemented as active monomers of dendrimers (Scheme 18).<sup>71</sup>



**Scheme 18:** Diels–Alder cycloaddition to form a monomer for future dendrimers.

Bromination has also been used to prepare mixtures of 1,6- and 1,8-disubstituted pyrenes (Figure 13), which are separable by fractional crystallization.<sup>85</sup> Direct oxidation of pyrene was also found to be a useful method for synthesizing disubstituted derivatives, but the desired products were often difficult to separate from the resulting crude mixture of oxidation products.<sup>78a</sup>

1,3,6,8-Tetrasubstituted pyrenes have found many applications in the materials field. The linear structures of these multisubstituted compounds were strong blue light emitters in both the solid state and in solution with a high quantum yield.<sup>83a</sup> These compounds have also been employed as blue fluorescent dyes in white organic light-emitting diodes in conjunction with tris(1-phenylisoquinoline)iridium(III) as a red phosphorescent dye.<sup>86</sup> Tetrasubstituted pyrene molecules have also been studied as mesogens for discotic liquid crystals because they can be easily functionalized with flexible alkyl chains on the periphery of the molecule. Chemical modification allows for a better control of the interactions between the subunits and thus influences the self-aggregation which in turn affects the solubility, thermal properties and the charge injection/collection at the interfaces as well as the charge transport within the bulk material.<sup>71</sup> Due to their excellent fluorescent properties and supramolecular organization in columnar liquid crystal phases, tetrasubstituted pyrene derivatives have significant potential for OLEDs. A series of luminescent pyrene-based liquid crystalline aromatic esters was reported by Bock *et al.* The molecules combine the excellent charge transport and film-forming properties of columnar liquid crystals with the ability to emit light.<sup>87</sup>

Previously, positions 1 and 3 of pyrene (Figure 13) were not easily accessible since the substitution preferentially occurred at the 1,6 and 1,8-positions. However, a novel approach was developed by Müllen *et al.*, who employed a *t*-Bu blocking group at position 2 before effecting a bromination at -78 °C to obtain the desired 1,3-dibromo-7-*t*-Bu pyrene **85** (Scheme 19).<sup>88</sup> Compound **85** was further polymerized to a blue-light-emitting polymer for use in single-layer OLEDs.

---

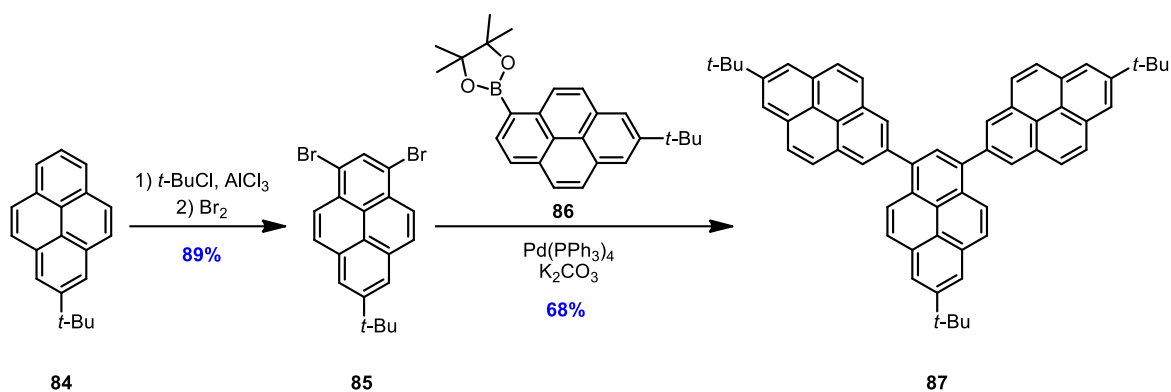
<sup>85</sup> Grimshaw, J.; Trocha-Grimshaw, J. *J. Chem. Soc. Perkin Trans. 1* **1972**, 1622.

<sup>86</sup> Qin, D. S.; Tao, Y. *Appl. Phys. Lett.* **2005**, *86*, 113507.

<sup>87</sup> Hassheider, T.; Benning, S. A.; Kitzerow, H. S.; Achard, M. F.; Bock, H. *Angew. Chem., Int. Ed.* **2001**, *40*, 2060.

<sup>88</sup> Figueira-Duarte, T. M.; Simon, S. C.; Wagner, M.; Drtzezhinin, S. I.; Zachariasse, K. A.; Müllen, K. *Angew. Chem., Int. Ed.* **2008**, *47*, 10175.



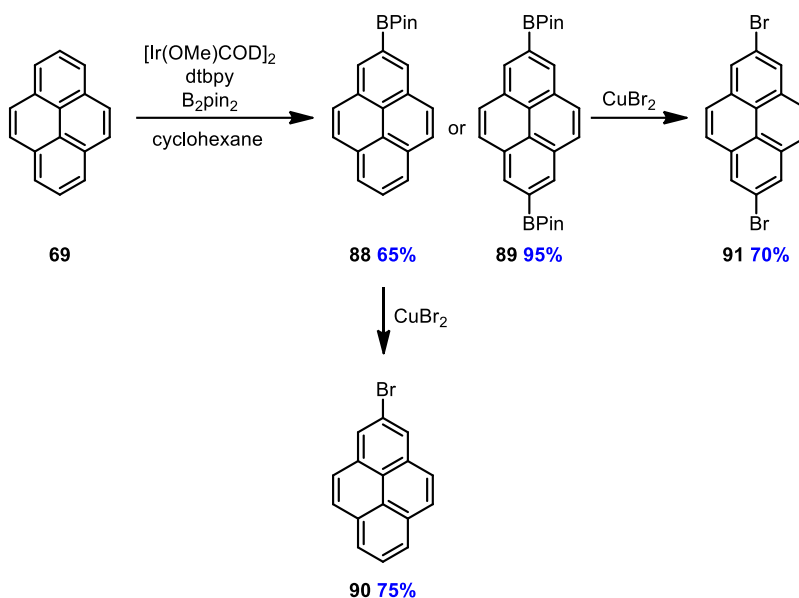


**Scheme 19:** Müllen's *et al.* strategy for the synthesis of a 1,3-substituted pyrene derivative.

Given that substitution of pyrene at positions 2 and 7 (Figure 13) was not accessible by electrophilic substitution, another route was required to accomplish the desired functionalization. The first attempts were based on the work of Vollmann *et al.* and involved the formation of pyrene carboxylic acids substituted at the 2-position, which were prepared from 1,2-phthaoylpyrene in the presence of molten potassium.<sup>78a</sup> Unfortunately, it was difficult to control the regioselectivity of the substitution which led to the formation of complex mixtures of nearly inseparable isomers.

A one-step synthesis was recently developed for the formation of pyrene-2,7-bis(boronate)esters using an Ir-based catalyst.<sup>89</sup> The products **88** and **89** could be used directly in a Suzuki coupling or be further transformed to bromo-substituted compounds **90** and **91** using  $\text{CuBr}_2$ , thus providing important 2- or 2,7-substituted building blocks (Scheme 20).

<sup>89</sup> Coventry, D. N.; Batsanov, A. S.; Goeta, A. E.; Howard, J. A. K.; Marder, T. B.; Perutz, R. N. *Chem. Commun.* **2005**, 2172.



**Scheme 20:** A novel and facile synthesis for the formation of 2- and 2,7-substituted pyrenes

Oligopyrenes linked at the 2,7-positions possess electronically decoupled pyrene subunits due to the nodal properties of their frontier orbitals.<sup>90</sup> Such polymers should act as both blue light emitters and as probes for local polarity. Also, highly symmetrical hexaarylbenzenes have already attracted interest in the materials field for applications as light-emitting charge-transport layers in OLEDs, precursors for photoconductive polycyclic aromatic hydrocarbons and discotic liquid crystals. A hexapyrenylbenzene counterpart **92** could be interesting as a replacement to traditionally used benzene derivatives (Figure 14).<sup>91</sup>

<sup>90</sup> Kreyenschmidt, M.; Baumgarten, M.; Tyutyulkov, M.; Müllen, K. *Angew. Chem., Int. Ed.* **1994**, *33*, 1957.

<sup>91</sup> Rausch, D.; Lambert, C. *Org. Lett.* **2006**, *8*, 5037.

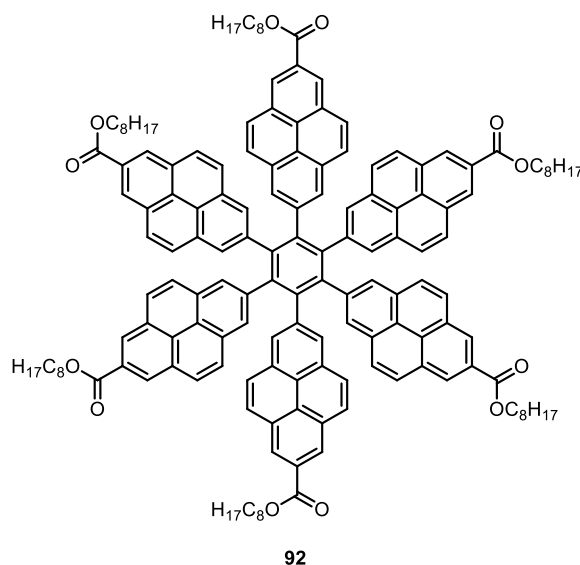


**Figure 14:** Hexapyrenylbenzene derivative.

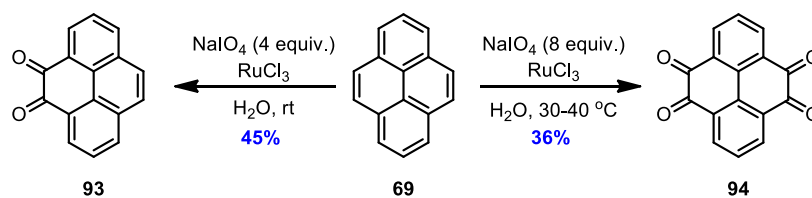
Other interesting but not easily accessible positions on the pyrene ring are the 4-, 5-, 9- and 10-positions (Figure 13) as these sites are particularly important for the formation of extended aromatic systems. Although such functionalized derivatives tend to aggregate spontaneously in solution, they can be controlled by introducing bulky *t*-Bu substituents, which distort the planarity of the aromatic framework, greatly increasing the solubility of the compounds.<sup>92</sup>

Further exploration of regioselective pyrene substitution led to the development of several multistep syntheses which provided pyrene-4,5-dione and pyrene-4,5,9,10-tetraone. In order to avoid such lengthy routes, an oxidation was developed which provided pyrene-4,5-dione **93** or pyrene-4,5,9,10-tetraone **94** selectively, depending on the reaction conditions (Scheme 21).<sup>93</sup> Intermediates **93** and **94** could be further functionalized to a variety of compounds. For example, condensation reactions extended the aromatic system<sup>94</sup> to yield an electroluminescent pyrene – twistacene **97**, which, when combined with a host polymer, acted as an emitter in single-layer white OLEDs (Scheme 22).

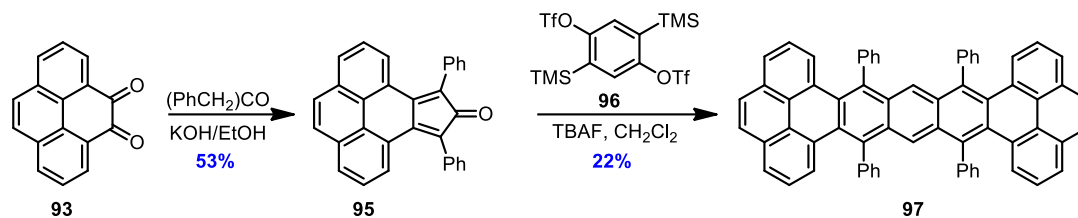
<sup>92</sup> Wasserfallen, D.; Kastler, M.; Pisula, W.; Hofer, W. A.; Fogel, Y.; Wang, Z. H.; Müllen, K. *J. Am. Chem. Soc.* **2006**, *128*, 1334.

<sup>93</sup> Hu, J.; Zhang, D.; Harris, F. W. *J. Org. Chem.* **2005**, *70*, 707.

<sup>94</sup> Mateo-Alonso, A.; Kulisic, N.; Valenti, G.; Marcaccio, M.; Paolucci, F.; Prato, M. *Chem. Asian J.* **2010**, *5*, 482.



**Scheme 21:** One-step synthesis of pyrene-4,5-dione and pyrene-4,5,9,10-tetraone.



**Scheme 22:** Synthesis of pyrene twistacene.

Another way to access the 4-, 5-, 9- and 10-positions of pyrene is through installation of blocking *t*-Bu groups at the 2- and 7-sites of the ring. Bromination of 2,7-di-*t*-Bu-pyrene in the presence of iron powder resulted in an acid-catalyzed rearrangement of the incorporated bromine atoms and provided 4,5,9,10-tetrabromo-2,7-di-*t*-Bu-pyrene. Further extension of the aromatic framework *via* palladium-coupling reactions provided phenylethynylpyrene **98** (Figure 15),<sup>95</sup> with *t*-Bu groups cleavable under acidic conditions.

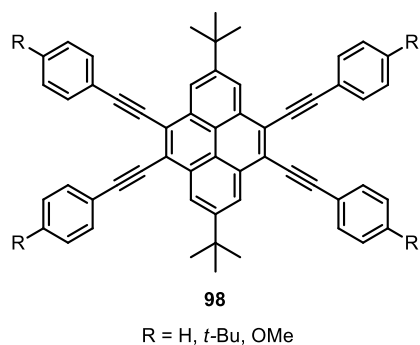


**Figure 15:** Chemical structures of phenylethynylpyrenes synthesized by Yamato *et al.*

<sup>95</sup> Hu, J. Y.; Era, M.; Elsegood, M. R. J.; Yamato, T. *Eur. J. Org. Chem.* **2010**, 72.

Several indirect methods for the formation of multisubstituted pyrenes have also been developed to overcome the challenges of regioselective substitution associated with direct functionalization of pyrene. Hydrogenation of pyrene afforded two products: tetrahydropyrene (THPy) **99** and hexahydropyrene (HHPy) **100**. The ratio of the compounds was dependent on the reaction conditions. Electrophilic aromatic substitution of **99** provided 2- or 2,7-substituted tetrahydropyrene **101** which could be re-aromatized to the desired product **102**. Electrophilic aromatic substitution of **100** provided 4-substituted hexahydropyrene **103** which could be re-aromatized to product **104** (Figure 16). The indirect substitution strategy allowed for predictable and reproducible regiocontrol for functionalization of reduced pyrene molecules.<sup>96</sup>

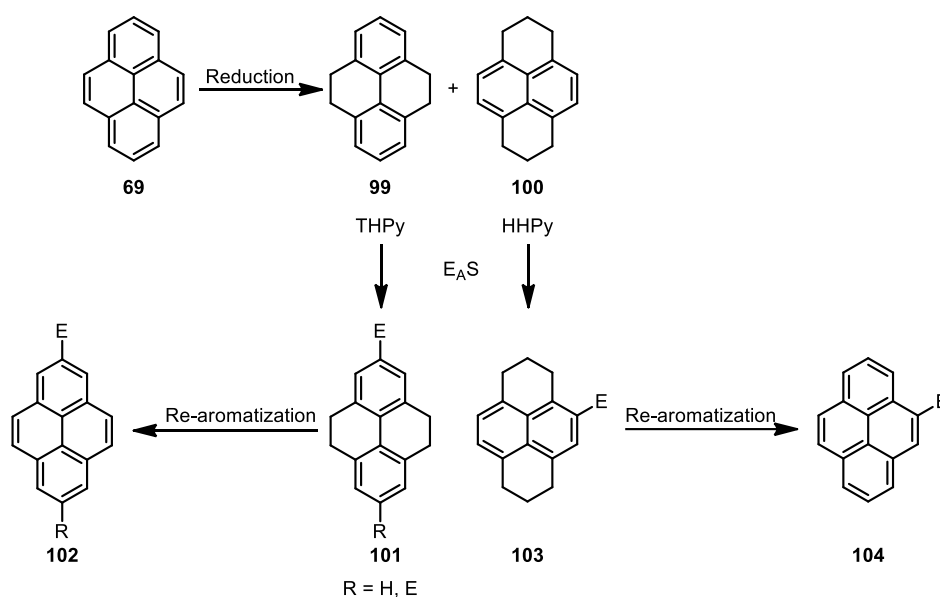
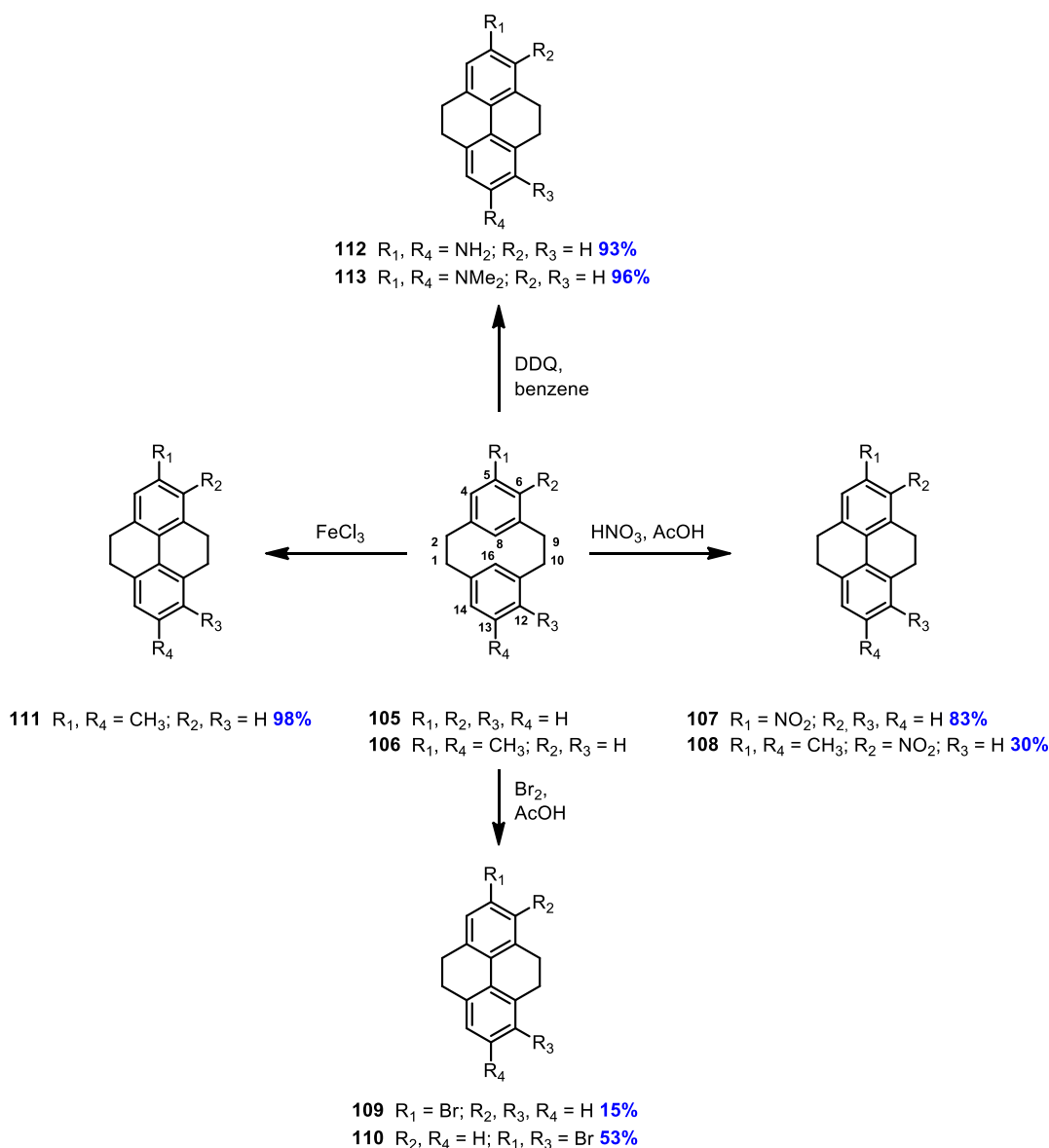


**Figure 16:** Indirect substitution of pyrene *via* reduction, electrophilic aromatic substitution and re-aromatization.

Another method for the formation of substituted pyrene-derivatives involved transannular ring closure of [2,2]metacyclophanes which led to the formation of tetrahydropyrene products **107** - **113**, which could then be re-aromatized to the desired pyrene compounds.<sup>97</sup>

<sup>96</sup> For further readings about indirect pyrene substitution *via* the tetrahydropyrene and the hexahydropyrene intermediates see the review by Casas-Solvas, J. M.; Howgego, J. D.; Davis, A. P. *Org. Biomol. Chem.* **2014**, *12*, 212.

<sup>97</sup> Vögtle, F.; Neumann, P. *Angew. Chem., Int. Ed. Engl.* **1972**, *11*, 73 – 158. For further readings about transannular ring closure of [2,2]metacyclophanes see ref 96.



**Scheme 23:** Various conditions for transannular ring closure.

A wide array of conditions was developed for transannular ring closures (Scheme 23) and it was observed that the substitution pattern on the [2,2]metacyclophane precursor influenced its functionalization. An unsubstituted [2,2]metacyclophane precursor **105** incorporated the electrophile at the 5- and/or 13-position, however a 5,13-disubstituted [2,2]metacyclophane, such as compound **106**, afforded products with additional substitutions at positions 6- and/or 12. The main limitation of the synthetic strategy was the formation of the macrocyclic cyclization precursors, which significantly limits the use of this method for large scale synthesis.

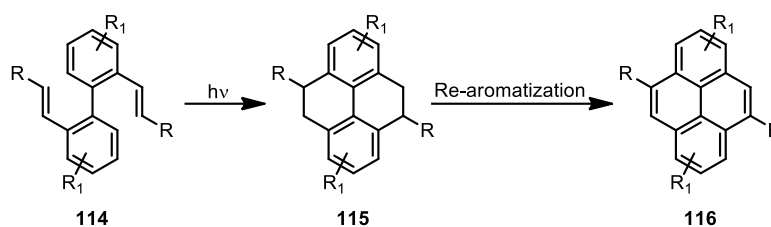
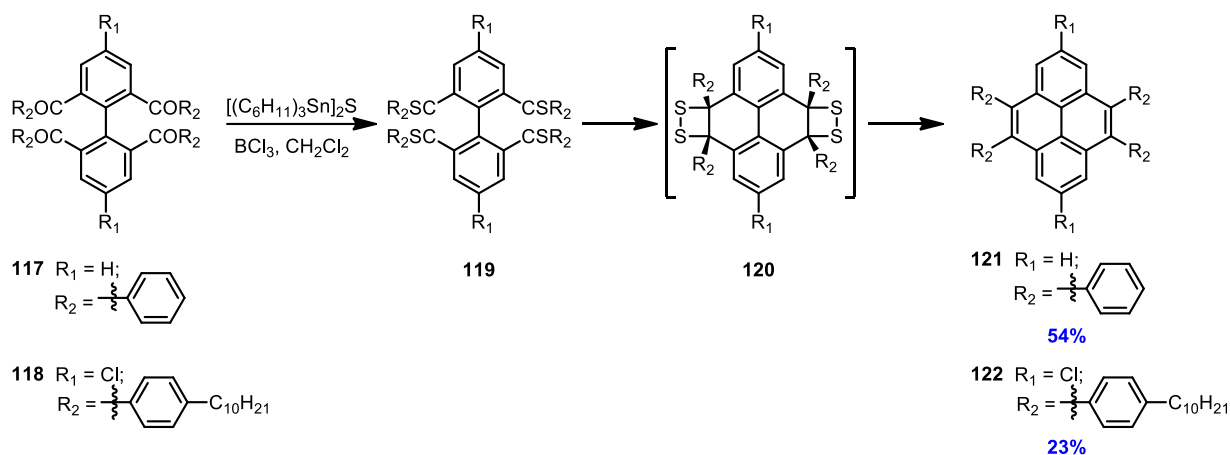


**Figure 17:** Synthesis of 4,10-disubstituted pyrenes *via* photocyclization of divinylbiphenyls.

Biphenyl annulation is another useful indirect synthetic strategy for the formation of substituted pyrene derivatives. The starting material **114** was prepared using well-established Pd-coupling methods, cyclized and re-aromatized to the desired product. Three different methods were described for the cyclization of the re-aromatization precursor. The first cyclization method was the UV-light-mediated photocyclization of 2,2'-divinyl biphenyls, such as **114** (Figure 17).<sup>98</sup>



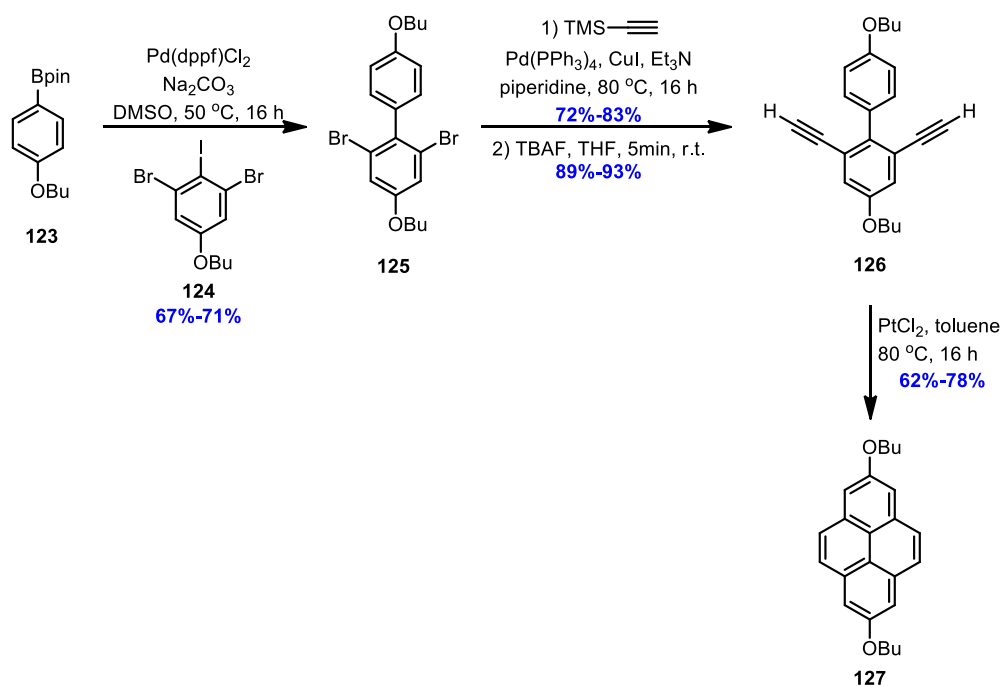
**Scheme 24:** Müllen's synthesis of multisubstituted pyrenes by thermal annulation of tetrathiones.

The second cyclization method involved the elimination of sulphur from *ortho*-thiocarbonyl substituents like **119** which afforded the desired cyclized pyrene product. Müllen *et*

<sup>98</sup> a) Laarhoven, W. H.; Cuppen, Th. J. H. M. *J. Chem. Soc., Perkin Trans. 1*, **1972**, 2074. b) Op Het Veld, P. H. G.; Laarhoven, W. H. *J. Chem. Soc., Perkin Trans. 2*, **1977**, 269. c) Padwa, A.; Doubleday, C.; Mazzu, A. *J. Org. Chem.* **1977**, *42*, 3271. d) Kreyenschmidt, M.; Baumgarten, M.; Tyutyulkov, N.; Müllen, K. *Angew. Chem., Int. Ed. Engl.* **1994**, *33*, 1957. e) Kreyenschmidt, M.; Uckert, F.; Müllen, K. *Macromolecules* **1995**, *28*, 4577.

al. used the strategy in the synthesis of multisubstituted pyrenes **121** and **122** which could be further polymerized (Scheme 24).<sup>99</sup>

The third cyclization approach reported was the Friedel-Crafts-like cyclization of alkynyl substituents such as **126** (Scheme 25).<sup>100</sup> The synthetic strategy has been extensively used to create a wide array of substituted pyrenes.<sup>101</sup>



**Scheme 25:** Synthesis of pyrene *via* cyclization of bis-alkynylbiphenyls.

## 1.6 Applications of Pyrene

Pyrene's electronic and optical properties can be fine-tuned through the introduction of electron-donating or accepting groups or *via* modification of the molecular architecture of the ring. So far fabrication of light-emitting field effect transistors with pyrene derivatives has been

<sup>99</sup> a) Wang, Z. Y.; Zhang, C. *Macromolecules* **1992**, *25*, 5851. b) Kawano, S.; Yang, C.; Ribas, M.; Balushev, S.; Baumgarten, M.; Müllen, K. *Macromolecules* **2008**, *41*, 7933.

<sup>100</sup> a) Barluenga, J.; Gonzalez, J. M.; Campos, P. J.; Asensio, G. *Angew. Chem., Int. Ed. Engl.* **1988**, *27*, 1546. b) Goldfinger, M. B.; Crawford, K. B.; Swager, T. M. *J. Am. Chem. Soc.* **1997**, *119*, 4578. c) Yao, T. L.; Campo, M. A.; Larock, R. C. *J. Org. Chem.* **2005**, *70*, 3511. d) Mamane, V.; Hannen, P.; Fürstner, A. *Chem. Eur. J.* **2004**, *10*, 4556.

<sup>101</sup> a) Walker, D. B.; Howgego, J.; Davis, A. P. *Synthesis* **2010**, 3686. b) Matsuda, T.; Moriya, T.; Goya, T.; Murakami, M. *Chem. Lett.* **2011**, *40*, 40. c) Machuy, M. M.; Würtele, C.; Schreiner, P. R. *Synthesis* **2012**, 1405.



extremely successful.<sup>71</sup> Also, bulk heterojunction (BHJ) solar cells with a pyrene-perylene acceptor have shown the highest reported values of power conversion efficiency for BHJ solar cells with perylene as the acceptor material.<sup>71</sup> Recent synthetic developments to access the 2,7-positions of the pyrene ring opened many further possibilities for the formation of new pyrene-based semi-conductors with enhanced opto-electronic properties. The devices have been used in flat-panel displays, lighting, radio frequency identification tags (RFID), electronic skin and solar modules.<sup>71</sup>

Due to its fluorescence properties, pyrene has been extensively used as a dye for fluorescence-labeled polymers allowing for the development of water-soluble polymers.<sup>102</sup> The chromophore of pyrene often serves as a probe to measure the properties of surfactant micelles, phospholipid vesicles and surfactant/polymer aggregates. The excimer of pyrene has been useful in supramolecular design and for probing structural properties in macromolecular systems. Pyrene labels have also been used in structural studies of proteins and peptides<sup>103</sup> as well as in DNA recognition<sup>104</sup> and studies of lipid membranes.<sup>105</sup> The excimer fluorescence of pyrene and its derivatives has been used to sense environmental parameters like temperature,<sup>106</sup> pressure<sup>107</sup> or

---

<sup>102</sup> a) Winnik, M. A.; Winnik, F. M. *Adv. Chem. Ser.* **1993**, 485. b) Winnik, F. M. *Chem. Rev.* **1993**, 93, 587.

<sup>103</sup> a) Goedeweck, R.; Vanderauweraer, M.; Deschryver, F. C. *J. Am. Chem. Soc.* **1985**, 107, 2334. b) Hammarstrom, P.; Kalman, B.; Jonsson, B. H.; Carlsson, U. *FEBS Lett.* **1997**, 420, 63. c) Sahoo, D.; Narayanaswami, V. *J. Mol. Bio.* **2002**, 39, 6594. d) Sahoo, D.; Narayanaswami, V.; Kay, C. M.; Ryan, R. O. *Biochemistry* **2000**, 39, 6594.

<sup>104</sup> a) Paris, P. L.; Langenhan, J. M.; Kool, E. T. *Nucleic Acids Res.* **1998**, 26, 3789. b) Lewis, F. D.; Zhang, Y. F.; Letsinger, R. L. *J. Am. Chem. Soc.* **1997**, 119, 5451. c) Yamana, K.; Iwai, T.; Ohtani, Y.; Sato, S.; Nakamura, M.; Nakano, H. *Bioconjugate Chem.* **2002**, 13, 1266. d) Yamana, K.; Takei, M.; Nakano, H. *Tetrahedron Lett.* **1997**, 38, 6051. e) Tong, G.; Lawlor, J. M.; Tregear, G. W.; Haralambidis, J. *J. Am. Chem. Soc.* **1995**, 117, 12151.

<sup>105</sup> a) Ollmann, M.; Schwarzmann, G.; Sandhoff, K.; Galla, H. J. *Biochemistry* **1987**, 26, 5943. b) Pap, E. H. W.; Hanicak, A.; Vanhoek, A.; Writz, K. W. A.; Visser, A. J. W. G. *Biochemistry* **1995**, 43, 9118. c) Kurzchalia, T. V.; Parton, R. G. *Curr. Opin. Cell. Biol.* **1999**, 11, 424. d) Song, X. D.; Swanson, B. I. *Langmuir* **1999**, 15, 4710. e) Smit, J. M.; Bittman, R.; Wilschut, J. *J. Virol.* **1999**, 73, 8476. f) Irurzun, A.; Nieva, J. L.; Carrasco, L. *Virology* **1997**, 227, 488. g) Pillot, T.; Goethals, M.; Vanloo, B.; Talussot, C.; Brasseur, R.; Vanderkerckhove, J.; Rosseneu, M.; Lins, L. *J. Biol. Chem.* **1996**, 271, 28757. h) Somerharju, P. *Chem. Phys. Lipids* **2002**, 116, 57.

<sup>106</sup> Birks, J. B.; Munro, I. H.; Lumb, M. D. *Proc. R. Soc. London A: Math. Phys. Sci.* **1964**, 280, 289.

<sup>107</sup> Templer, R. H.; Castle, S. J.; Curran, A. R.; Rumbles, G.; Klug, D. R. *Faraday Discuss.* **1998**, 41.

pH.<sup>108</sup> The same property has also been useful in the detection of guest molecules such as gases (O<sub>2</sub> or NH<sub>3</sub>),<sup>109</sup> organic molecules,<sup>110</sup> metals,<sup>111</sup> and other analytes.<sup>112</sup>

Pyrene's unique optical and electronic properties hold significant potential for applications in organic light-emitting diodes (OLEDs), organic field-effect transistors (OFETs), organic light-emitting field-effect transistors (OLEFETs) and in certain photovoltaic devices such as bulk heterojunction solar cells (BHJ) and dye-sensitized solar cells (DSCs).<sup>71</sup> Pyrene-based compounds could replace traditional inorganic semiconductors and consequently decrease manufacturing costs, increase the flexibility of fine tuning substrate properties and facilitate the fabrication of devices over large areas on lightweight and flexible substrates.

Based on the current and potential applications for the pyrene molecule and its substituted derivatives, it is evident that pyrene is a useful and promising motif in many areas of organic and bioorganic chemistry. It is therefore important to further explore, develop and facilitate the functionalization, transformation and application of pyrene.

---

<sup>108</sup> Pokhrel, M. R.; Bossmann, S. H. *J. Phys. Chem. B* **2000**, *104*, 2215.

<sup>109</sup> a) Fujiwara, Y.; Amao, Y. *Sens. Actuators B: Chem.* **2003**, *89*, 58. b) Lee, E. D.; Werner, T. C.; Seitz, W. R. *Anal. Chem.* **1987**, *59*, 279. c) Nagel, C. C.; Bensten, J. G.; Yafuso, M; *et al.* US Patent 5,498,549, 1996. d) Nagel, C. C.; Bensten, J. G.; Dektar, J. L.; *et al.* US Patent 5,409,666, 1995.

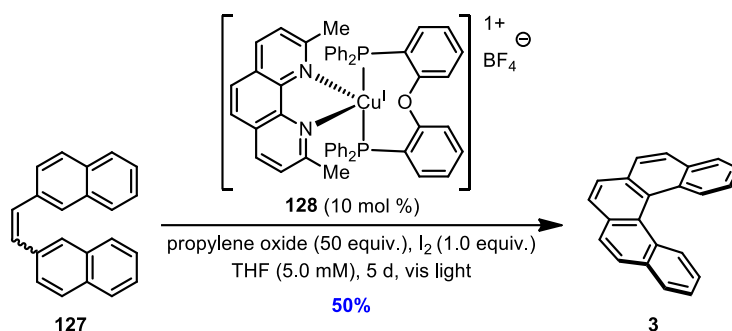
<sup>110</sup> a) Ikeda, H.; Nakamura, M.; Ise, N.; Oguma, N.; Nakamura, A.; Ikeda, T.; Toda, F.; Ueno, A. *J. Am. Chem. Soc.* **1996**, *118*, 10980. b) Aoyagi, T.; Ikeda, H.; Ueno, A. *Bull. Chem. Soc. Jpn.* **2001**, *74*, 157. c) Ueno, A.; Suzuki, I.; Osa, T. *Anal. Chem.* **1990**, *62*, 2461.

<sup>111</sup> a) Valeur, B.; Leray, I. *Coord. Chem. Rev.* **2000**, *205*, 3. b) Yang, R. H.; Chan, W. H.; Lee, A. W. M.; Xia, P. F.; Zhang, H. K.; Li, K. A. *J. Am. Chem. Soc.* **2003**, *125*, 2884. c) Strauss, J.; Daub, J. *Org. Lett.* **2002**, *4*, 683. d) Bodenant, B.; Fages, F.; Delville, M. H. *J. Am. Chem. Soc.* **1998**, *120*, 7511. e) Yang, J. S.; Lin, C. S.; Hwang, C. Y. *Org. Lett.* **2001**, *3*, 889. f) Ludwig, R.; Dzung, N. T. K. *Sensors* **2002**, *2*, 397. g) Bodenant, B.; Weil, T.; Businelli-Pourcel, M.; Fages, F.; Barbe, B.; Pianet, I.; Laguerre, M. *J. Org. Chem.* **1999**, *64*, 7034. h) Suzuki, Y.; Morozumi, T.; Nakamura, H.; Shimomura, M.; Hayashita, T.; Bartsh, R. A. *J. Phys. Chem. B* **1998**, *102*, 7910.

<sup>112</sup> Monaham, C.; Bien, J. T.; Smith, B. D. *Chem. Commun.* **1998**, 431.

## 1.7 Research Goals

Despite the development of a variety of non-photochemical synthetic strategies for the formation of helicenes, the UV-light-promoted photocyclodehydrogenation remains the most widely used method. Unfortunately, the UV-mediated synthetic route suffers from the formation of undesired side-products, including unwanted regioisomers and products of competitive intermolecular cycloadditions of the stilbene starting materials, necessitates high dilutions and requires quartz glassware. These combined factors significantly increase the overall cost of the reaction and render it impractical for large scale synthesis.



**Scheme 26:** First generation conditions for photocyclization of stilbene-type precursors.

Inspired by the recent work of MacMillan,<sup>113</sup> Yoon<sup>114</sup> and Stephenson,<sup>115</sup> who demonstrated the use of sensitizer metal complexes to promote various photoredox reactions in the presence of visible-light, research in the Collins group aimed at developing a visible-light-promoted alternative to the popular UV-light-mediated photocyclodehydrogenation. Conceptually, the approach would result in a different reaction mechanism than the UV-mediated

<sup>113</sup> a) Nicewicz, D. A.; MacMillan, D.W. C. *Science* **2008**, *322*, 77. b) Nagib, A.; Scott, M. E.; MacMillan, D.W. C. *J. Am. Chem. Soc.* **2009**, *131*, 10875. c) Shih, H.-W.; Vander Wal, M. N.; Grange, R. L.; MacMillan, D. W. C. *J. Am. Chem. Soc.* **2010**, *132*, 13600.

<sup>114</sup> a) Yoon, T. P.; Ischay, M. A.; Du, J. *Nat. Chem.* **2010**, *2*, 527. b) Ischay, M. A.; Lu, Z.; Yoon, T. P. *J. Am. Chem. Soc.* **2010**, *132*, 8572. c) Du, J.; Yoon, T. P. *J. Am. Chem. Soc.* **2009**, *131*, 14604. d) Ischay, M. A.; Anzovino, M. E.; Du, J.; Yoon, T. P. *J. Am. Chem. Soc.* **2008**, *130*, 12886. e) Lu, Z.; Shen, M.; Yoon, T. P. *J. Am. Chem. Soc.* **2011**, *133*, 1162.

<sup>115</sup> a) Condie, A. G.; González-Gómez, J.; Stephenson, C. R. J. *J. Am. Chem. Soc.* **2010**, *132*, 1464. b) Narayanam, J. M. R.; Tucker, J. W.; Stephenson, C. R. J. *J. Am. Chem. Soc.* **2009**, *131*, 8756. c) Dai, C.; Narayanam, J. M. R.; Stephenson, C. R. J. *Nat. Chem.* **2011**, *3*, 140. d) Nguyen, J. D.; Tucker, J. W.; Konieczynska, M. D.; Stephenson, C. R. J. *J. Am. Chem. Soc.* **2011**, *133*, 4160. e) Narayanam, J. M. R.; Stephenson, C. R. J. *Chem. Soc. Rev.* **2011**, *40*, 102.

approach and consequently benefit from the same simple preparation of stilbene-type precursors while avoiding the disadvantages of expensive glassware, special protective equipment and high dilutions. Preliminary visible-light-mediated cyclization conditions were already established by Augusto C. Hernandez-Perez (Scheme 26). When employing a Cu-based sensitizer, propylene oxide and iodine as the oxidant system, a 50% yield of [5]helicene **3** was obtained after 5 d at room temperature. The initial goal of the research project was to complete a thorough optimization of the reaction conditions. In collaboration with Augusto Hernandez-Perez, a survey of the various Cu-based sensitizers, concentrations, reaction times and oxidants was to be conducted and applied to the gram scale synthesis of [5]helicene. Once optimized conditions have been established, the research goals were to investigate the application of the new method towards the synthesis of higher, substituted carbohelicenes and various thiohelicenes. Also, a synthesis of novel pyrene-helicene materials using the visible-light-mediated protocol was to be developed (Figure 18). Finally, a separate goal was to further optimize the reaction time and yield by investigating the use of continuous flow conditions for the visible-light-mediated photocyclization of **127** and apply the developed method to the formation of [5]helicene and various pyrene-helicene derivatives (Figure 18).

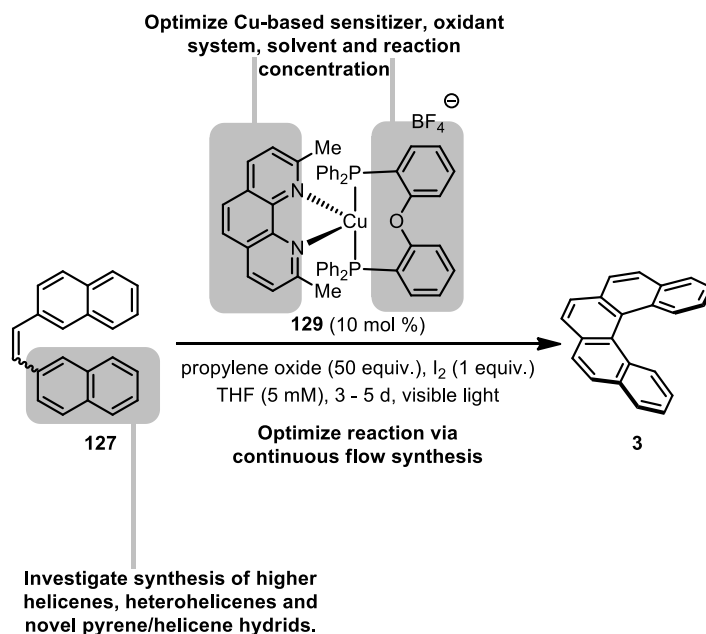


**Figure 18:** Research goals.

## CHAPTER 2: DISCUSSION OF VISIBLE-LIGHT-MEDIATED SYNTHESIS OF HELICAL POLYCYCLIC AROMATIC COMPOUNDS

### 2.1 Introduction to Visible-Light-Mediated Photoredox Reactions

Since the first reported synthesis of helicenes by Meisenheimer and Witte in 1903,<sup>9</sup> many synthetic strategies for the formation of helicenes have been developed. These include Diels-Alder cycloadditions,<sup>18,19</sup> the Friedel-Crafts alkylations,<sup>20,21,22</sup> transition-metal catalyzed couplings,<sup>23,24,25</sup> [2+2+2] cycloisomerizations,<sup>27,28,29,30</sup> ring closing metathesis<sup>26</sup> and radical cyclizations.<sup>33,34</sup> Despite these efforts, UV-light-promoted photocyclodehydrogenation, a method initially developed by Martin and co-workers.<sup>10,11,12</sup> and further optimized by Katz and co-workers,<sup>14,15,16</sup> remains the most widely used strategy for the preparation of various helicenes and heterohelicenes. Unfortunately, the synthetic strategy suffers from serious drawbacks such as the formation of undesired [2+2] intermolecular cycloaddition products, for example **130**. To address this problem reactions are run at high dilutions, which limits the potential for scale-up. Also, during the formation of [5]helicene, overoxidation was observed to benzo[*ghi*]perylene compound **13** (Figure 19).<sup>13</sup> The UV-mediated cyclization method also requires quartz glassware in addition to UV-protective equipment, which significantly increases the overall cost of the reaction. Due to the many challenges associated with the traditional methods, a facile, practical and inexpensive synthesis of helical aromatic compounds is highly desirable.

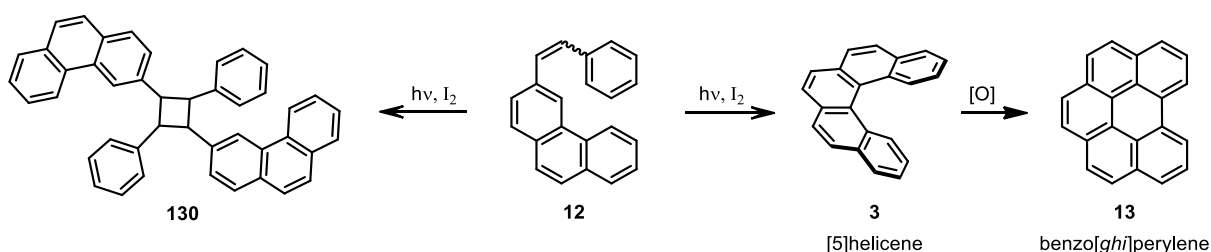


**Figure 19:** Formation of benzo[*ghi*]perylene and [2+2] intermolecular cycloaddition product during the UV-light-mediated photocyclodehydrogenation of **12**.

Recently, there has been a significant increase in the use of transition-metal complexes as photosensitizers to promote various visible-light-mediated photoredox reactions.<sup>116</sup> The photoredox catalysis is based on the ability of various transition-metal complexes to undergo single-electron transfer (SET) processes upon photoexcitation with visible-light. One of the most common visible-light photocatalysis is the Ru-based polypyridyl sensitizer **131** (Figure 20). Complex **131** absorbs light in the visible region of the electromagnetic spectrum and provides stable, long-lived photoexcited states.<sup>117</sup> Photoexcitation of Ru(bpy)<sub>3</sub><sup>2+</sup> generates a higher-energy electron, which can be expelled from the  $\pi^*$  orbital when the catalyst acts as a reducing agent. Photoexcitation simultaneously provides a lower-energy hole in the t<sub>2g</sub> orbital which may accept an electron when the photocatalyst acts as an oxidant (Figure 20). Therefore, Ru-based sensitizers can act as both reductants and oxidants when activated by visible-light.

---

<sup>116</sup> For an in-depth review for the use of transition-metal complexes in photoredox reactions see refs 113, 114, 115, 117, 118, 119, 120, 121, 122.

<sup>117</sup> a) Kalyanasundaram, K. *Coord. Chem. Rev.* **1982**, *46*, 159. b) Juris, A.; Balzani, V.; Barigelletti, F.; Campagna, S.; Belser, P.; Von Zelewsky, A. *Coord. Chem. Rev.* **1988**, *84*, 85.

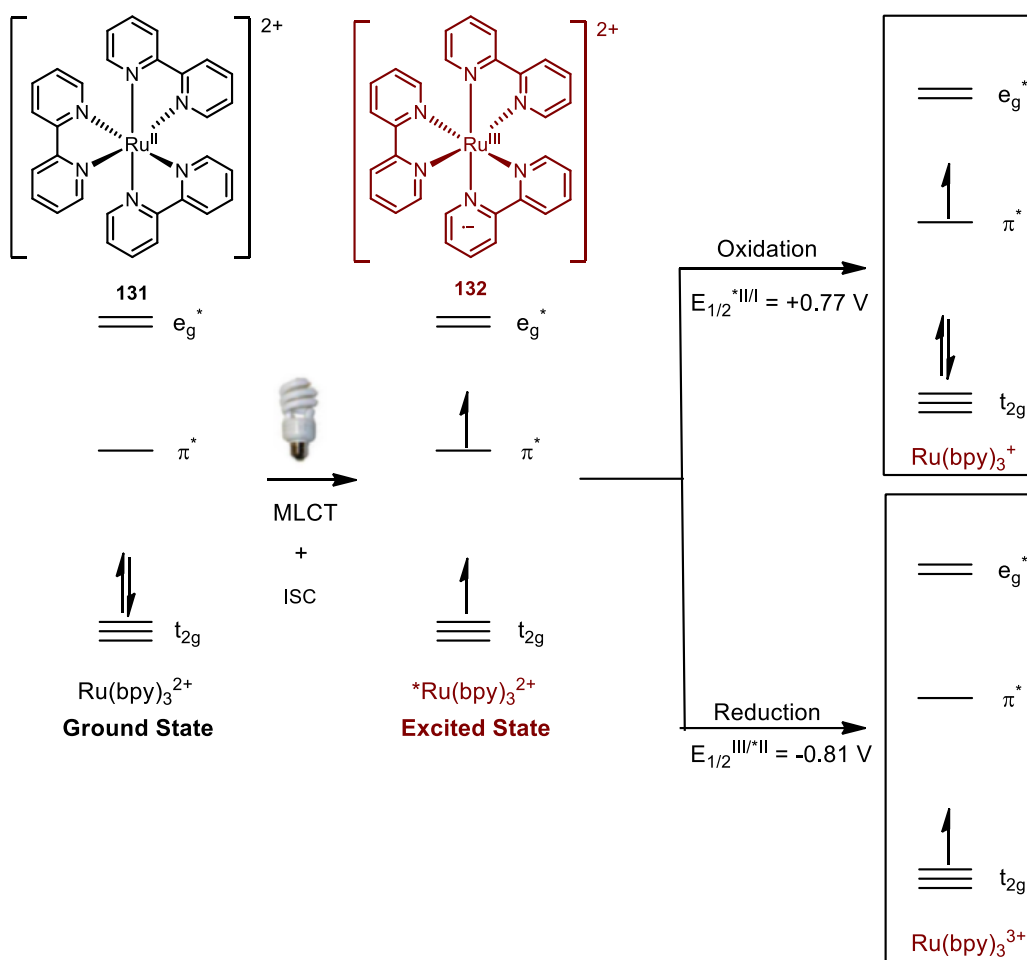


**Figure 20:** Photoexcitation of Ru(bpy)<sub>3</sub><sup>2+</sup> photosensitizer, a common catalyst in photoredox reactions.<sup>118</sup>

Photoexcitation of Ru-sensitizer **131** provides a very potent single-electron-transfer (SET) reagent. The SET processes allow access to radical ion intermediates, otherwise inaccessible through previously-developed activation methods, with a reactivity pattern that differs from the ground electronic or excited states. The photoredox reactions occur under mild conditions without the use of highly reactive radical initiators.<sup>118</sup> Photosensitizer **131** has also been extensively used for energy storage, hydrogen and oxygen evolution from water, and methane production for CO<sub>2</sub>.<sup>117</sup>

<sup>118</sup> Prier, C. K.; Rankic, D. A.; MacMillan, D. W. C. *Chem. Rev.* **2013**, *113*, 5322.

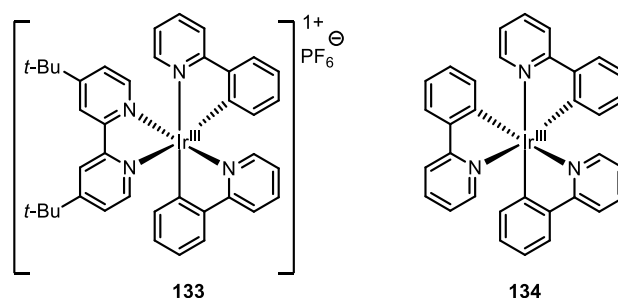


**Figure 21:** Ir-based sensitizers employed in photocatalysis by MacMillan *et al.*

In 2008, MacMillan reported a direct asymmetric intermolecular  $\alpha$ -alkylation of aldehydes using organocatalyst **137** and a  $\text{Ru}(\text{bpy})_3\text{Cl}_2$  sensitizer (Figure 22).<sup>113</sup> The proposed mechanism for the alkylation involves photoexcitation of  $\text{Ru}(\text{bpy})_3^{2+}$  to  $^*\text{Ru}(\text{bpy})_3^{2+}$  in the presence of visible-light *via* metal to ligand charge transfer (MLCT) pathway. The excited species oxidizes the enamine radical complex **141** producing  $\text{Ru}(\text{bpy})_3^{3+}$ , which reduces the alkyl halide species **145** and becomes  $\text{Ru}(\text{bpy})_3^{2+}$  in the process thus completing the photoredox catalytic cycle. The electron-deficient radical **140** adds to enamine **139**, generated from the addition of the organocatalyst **143** to the aldehyde **135**, to form radical asymmetric species **141**. Radical enamine **141** is oxidized to compound **142** and desired  $\alpha$ -alkylated product **144** is released from the organocatalytic cycle (Figure 22). The same group also established an enantioselective  $\alpha$ -trifluoromethylation<sup>119</sup> using Ir-based photosensitizer **133** (Figure 21) as well as an enantioselective  $\alpha$ -benzylation<sup>113c</sup> with another Ir-based sensitizer **134** (Figure 21), both of which followed a mechanism similar to the one depicted in Figure 22.

<sup>119</sup> Nagib, D. A.; Scott, M. E.; MacMillan, D. W. C. *J. Am. Chem. Soc.* **2009**, *131*, 10875.



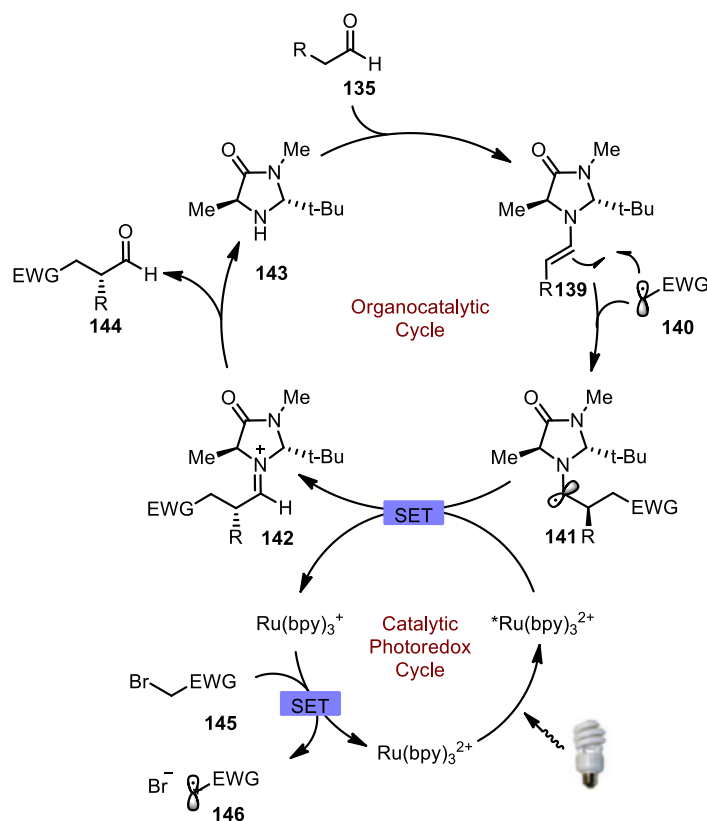
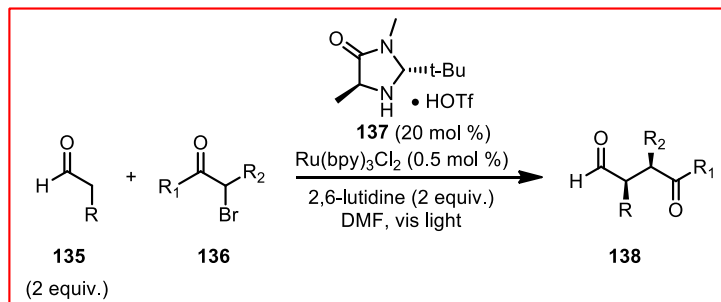
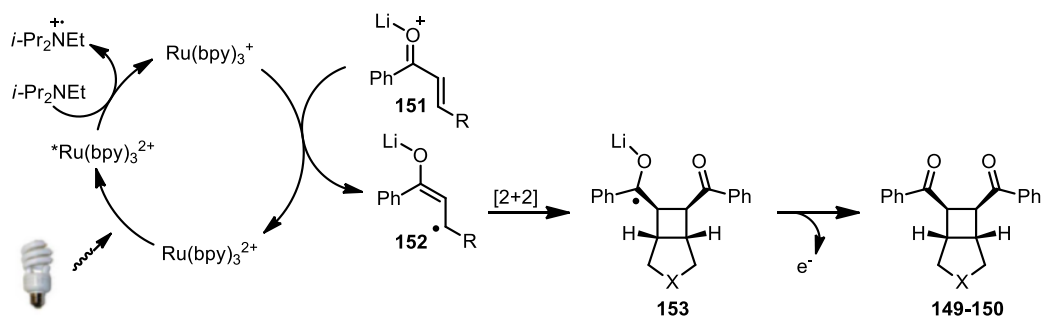
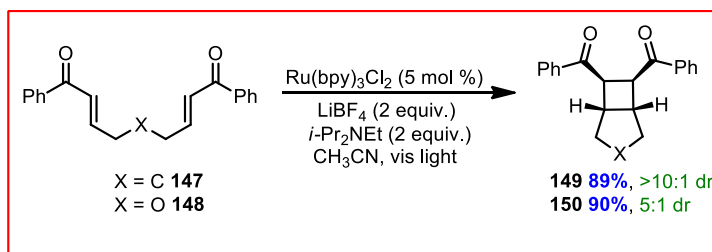


**Figure 22:** MacMillan's visible-light-mediated asymmetric intermolecular  $\alpha$ -alkylation of aldehydes.

Using the same  $\text{Ru(bpy)}_3\text{Cl}_2$  sensitizer, Yoon and co-workers developed a visible-light-mediated [2+2] cycloaddition of bis(enone)s like **147** and **148** to form cyclobutane derivatives like **149** and **150** in good yield and diastereoselectivity (Scheme 27). Hünig's base was necessary for reactivity, suggesting that the first step in the photocatalytic cycle is the reductive quenching of  $^*\text{Ru(bpy)}_3^{2+}$  by the base. The lithium ion likely acts as a Lewis acid and activates enone **151** for a one-electron reduction by  $\text{Ru(bpy)}_3^+$  which provides product **152**. Radical anion **152**, undergoes a [2+2] cycloaddition which provides ketyl radical **153**, which is subsequently oxidized to the

desired cyclobutanes like **149** and **150**.<sup>120</sup> Various substituted aryl and heteroaryl bis(enone) substrates cyclized well, however symmetrical aliphatic enones and enoates were unreactive, likely because they did not undergo reduction. However, with one aryl group present, cyclization was successful. Intramolecular cycloadditions provided mostly *meso cis*-dione products, while intermolecular cycloadditions yielded the *trans*-diones. Yoon further extended the synthetic method to include [4+2], [2+2+2] and [3+2] cycloadditions.<sup>118</sup>



**Scheme 27:** Yoon's formal [2+2] intramolecular visible-light-mediated cycloaddition.

Stephenson *et al.* explored a photoredox reductive dehalogenation reaction.<sup>115b</sup> In this synthetic route, Hünig's base acts as the stoichiometric reductant together with formic acid (**159e**) or the Hantzsch ester (**159c**). Single electron oxidation of the amine by  $*\text{Ru}(\text{bpy})_3^{2+}$  generates the aminium radical cation **159** and  $\text{Ru}(\text{bpy})_3^+$ , which likely reduces  $\alpha$ -chloroester **156** to  $\alpha$ -carbonyl radical **157**. Radical **157** could abstract a hydrogen atom from the  $\alpha$ -position of **159**, thus providing desired dehalogenated product **158** and iminium **160** (Figure 23). The developed conditions could be applied to the reduction of alkyl bromides, chlorides and are selective for the dehalogenation of benzylic and  $\alpha$ -carbonyl halides over aryl and vinyl halides.

<sup>120</sup> Ischay, M. A.; Anzovino, M. E.; Du, J.; Yoon, T. P. *J. Am. Chem. Soc.* **2008**, *130*, 12886.

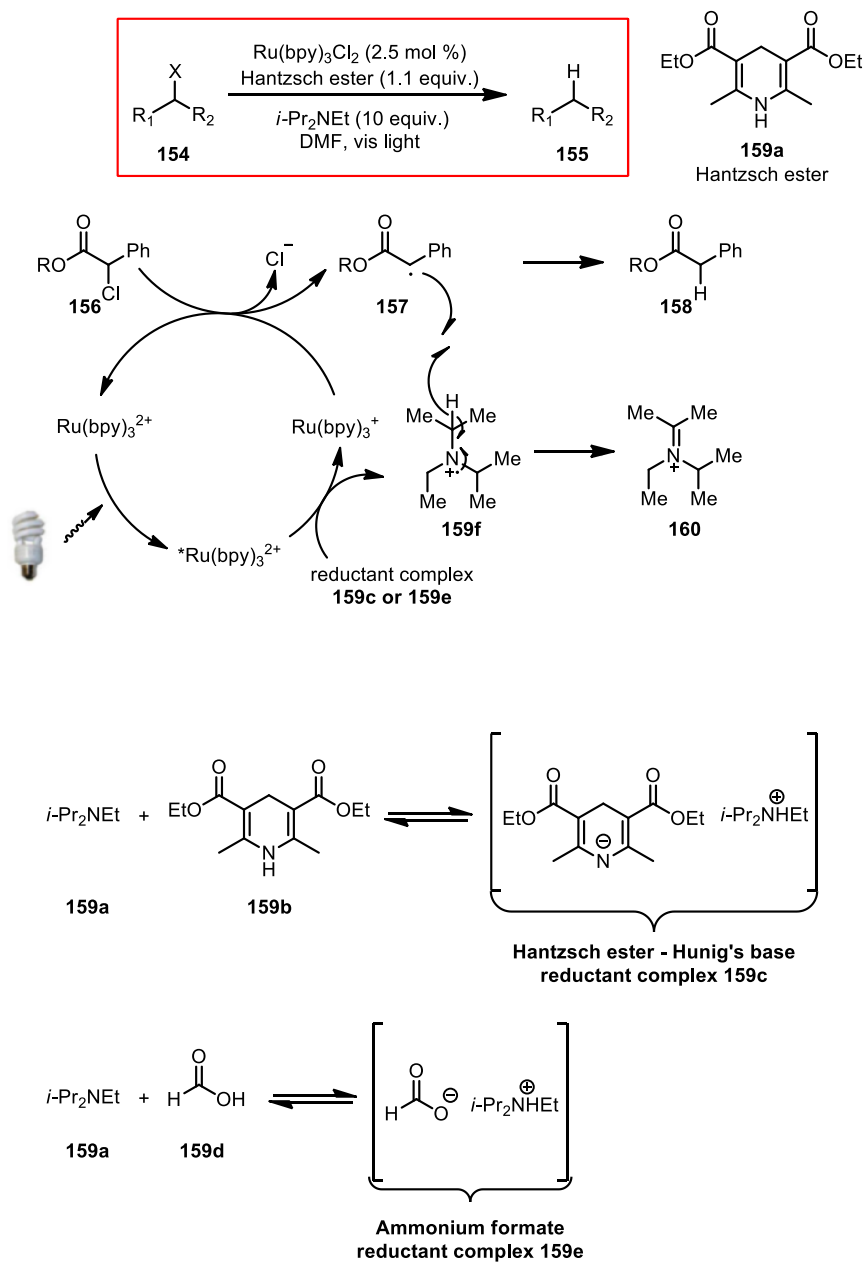
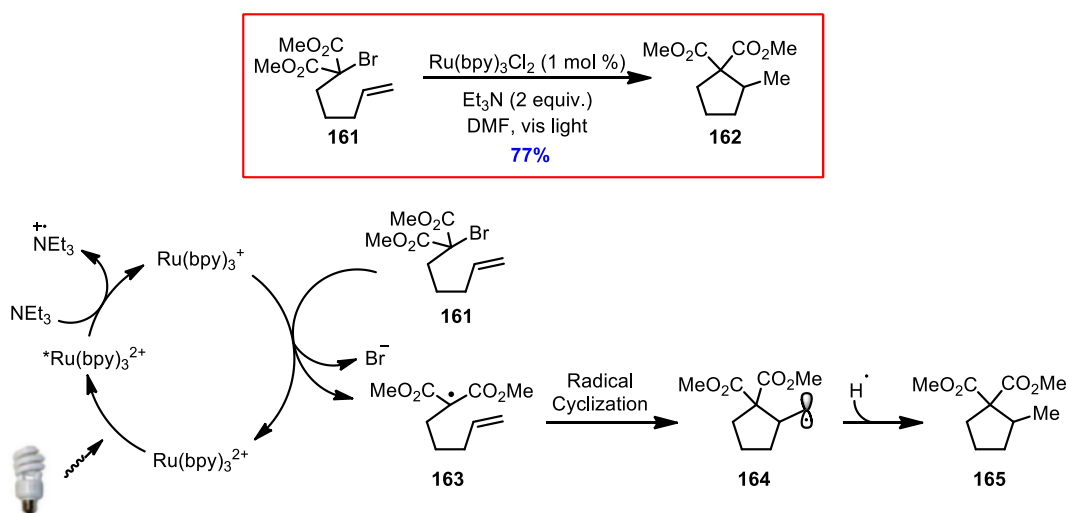


**Figure 23:** Stephenson's visible-light-mediated dehalogenation reaction.

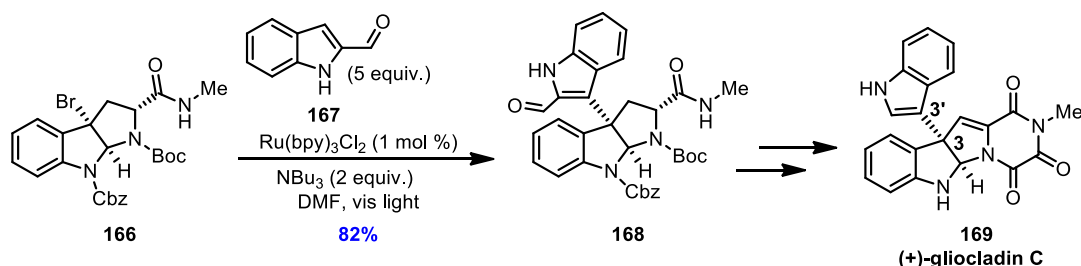
Stephenson and co-workers also established conditions for reductive radical cyclization reactions (Scheme 28).<sup>121</sup> The cyclization reaction pathway follows a mechanism similar to the dehalogenation reaction, however once radical **163** is generated, it reacts with the terminal alkene

<sup>121</sup> Tucker, J. W.; Nguyen, J. D.; Narayanam, J. M. R.; Krabbe, S. W.; Stephenson, C. R. J. *Chem. Commun.* **2010**, 46, 4985.

or alkyne to provide cyclized adduct **164**, which transforms to desired product **165** post a hydrogen atom abstraction. An intermolecular variation of the strategy was used by Stephenson *et al.* for the synthesis of (+)-gliocladin C, a natural product with a C3-C3' linked indole-pyrrolidine core<sup>122</sup> (Scheme 29).



**Scheme 28:** Stephenson's photoredox-catalyzed reductive radical cyclization.



**Scheme 29:** Synthesis of (+)-gliocladin C by Stephenson *et al.* using photoredox chemistry.

## 2.2 Visible-Light-Mediated Synthesis of [5]Helicenes

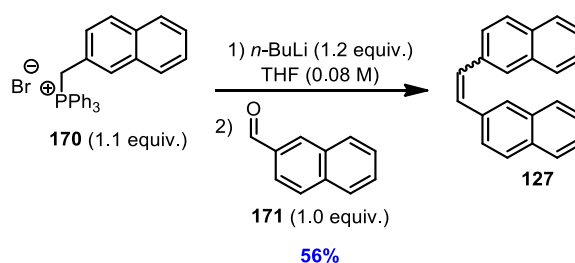
### 2.2.1 Optimization of first-generation visible-light-mediated conditions for photocyclization

Inspired by the recent advancements in photoredox chemistry with transition-metal-based catalysts, Ru- and Ir-based photosensitizers were applied in the development of a visible-light-

<sup>122</sup> Furst, L.; Narayanam, J. M. R.; Stephenson, C. R. J. *Angew. Chem., Int. Ed.* **2001**, *12*, 3104.

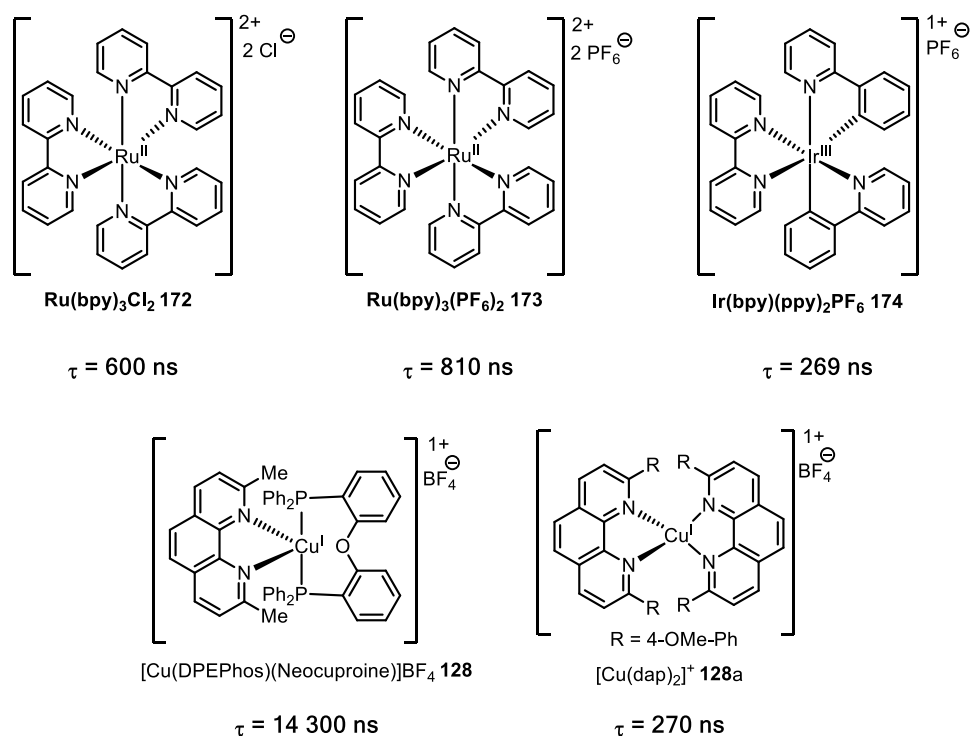
mediated synthesis of helicenes. Once established, the novel approach would benefit from the simple preparation of stilbene-type precursors, while avoiding the use of expensive glassware and special protective equipment during the reaction set-up. Also, since the photoredox reaction mechanism differs from that of the UV-light-mediated cyclization, formation of undesired [2+2] products could be avoided and thus a more practical reaction concentration could be achieved.

In collaboration with Augusto Hernandez-Perez, investigations began with efforts to cyclize stilbene precursor **127** under the standard photocyclodehydrogenation conditions in the presence of a photosensitizer. The starting material **127** was synthesized *via* Wittig olefination in 56% yield (Scheme 30), using 2-naphthylmethyltriphenylphosphonium bromide **170** and 2-naphthaldehyde **171**. It is important to note that although the *cis* and *trans* isomers are somewhat separable by flash column chromatography, the pure *cis* material slowly isomerizes to the *trans* when left on the bench. Both isomers are reactive following the proposed mechanism (Figure 25), and thus were often kept as mixtures.



**Scheme 30:** Formation of the stilbene-type precursor for the cyclization of [5]helicene.

Some of the common transition-metal sensitizers were explored as potential photocatalysis for the visible-light-mediated synthesis of helicenes including [Ru(bpy)<sub>3</sub>]Cl<sub>2</sub> **172**, [Ru(bpy)<sub>3</sub>](PF<sub>6</sub>)<sub>2</sub> **173** and [Ir(bpy)(ppy)<sub>2</sub>]PF<sub>6</sub> **174** (Table 1). Unfortunately, the Ru-based catalysts **172** and **173** afforded less than 10% conversion to the desired [5]helicene after three days of irradiation in THF. Ir-based sensitizer **174** afforded product **3** in a slightly higher 22% yield after three days of irradiation in acetonitrile. The preliminary yields obtained with Ru- and Ir-based photosensitizers were disappointing but led to further exploration of other transition-metal-based sensitizers.

**Table 1:** Photosensitizers tested for visible-light-mediated synthesis of [5]helicene.

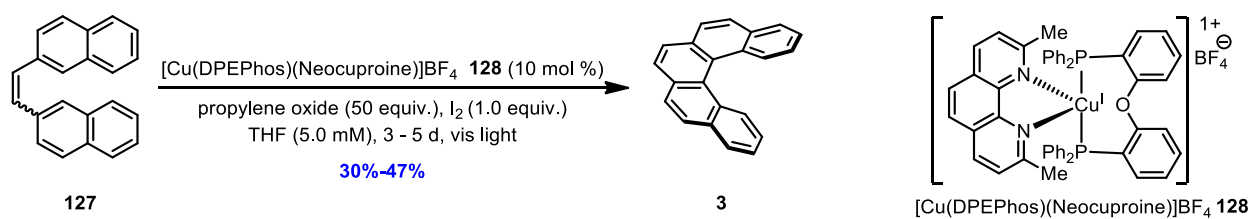
Entry	Sensitizer	Solvent	Yield
1	Ru(bpy) <sub>3</sub> Cl <sub>2</sub>	THF	<10%
2	Ru(bpy) <sub>3</sub> (PF <sub>6</sub> )	THF	<10%
3	Ir(bpy)(ppy) <sub>2</sub> PF <sub>6</sub>	CH <sub>3</sub> CN	22%
4	Cu(DPEPhos)(Neocuproine)]BF <sub>4</sub>	THF	30%

In an effort to improve the efficiency of the visible-light-mediated photocyclodehydrogenation reaction, a Cu-based sensitizer **128** reported by McMillin *et al.*, was tested.<sup>123, 124</sup> [Cu(DPEPhos)(Neocuproine)]BF<sub>4</sub> complex **128** was chosen due to its low cost and ease of preparation along with its tunable electronic properties, modifiable through ligand substitution. Cu-based complex **128** also possessed a longer excited state lifetime when compared with the Ru- and Ir-based sensitizers tested, 14 300 ns vs 269 – 810 ns. Sensitizer **128** provided

<sup>123</sup> a) Slinker, J. D.; Rivnay, J.; Moskowicz, J. S.; Parker, J. B.; Bernhard, S.; Abruña, H. D.; Malliaras, G. G. *J. Mater. Chem.* **2007**, *17*, 2976. b) Cuttell, D. G.; Kuang, S.-M.; Fanwick, P. E.; McMillin, D. R.; Walton, R. A. *J. Am. Chem. Soc.* **2002**, *124*, 6.

<sup>124</sup> For a review of photoactive Cu complexes see : a) McMillin, D. R.; McNett, K. M. *Chem. Rev.* **1998**, *98*, 1201. For recent examples of novel photoactive Cu complexes see : b) Harkins, S. B.; Peters, J. C. *J. Am. Chem. Soc.* **2005**, *127*, 2030. c) Hashimoto, M.; Igawa, S.; Yashima, M.; Kawata, I.; Hoshino, M.; Osawa, M. *J. Am. Chem. Soc.* **2011**, *133*, 10348.

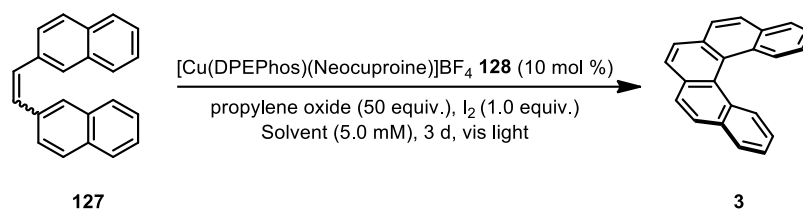
the desired product **3** in a yield of 30% after 3 days of irradiation (Table 1, Entry 4) and 30% – 47% after 5 days of irradiation in THF (Scheme 31). It is important to note that similar Cu(I)-complexes, such as [Cu(dap)<sub>2</sub>] **128a**, possessed a higher reduction potential (-1.43 V) than several Ir- and Ru-based complexes (-0.81 – 0.96 V)<sup>125</sup>, which could explain why a higher yield conversion was observed with the Cu-based photocatalyst for the photocyclization of [5]helicene. To the best of our knowledge, the redox potential of **128** in its excited state has not been reported. No further oxidation to the undesired benzo[*ghi*]perylene **13** was observed. Also, previously persistent side-product **130** of the UV light-mediated photocyclization, resulting from [2+2] intermolecular cycloaddition of the stilbene-type precursors, was not detected, thus allowing the reaction concentration to be raised from the UV-standard of 0.2 mM to 5.0 mM, a 25-fold increase in the reaction concentration. A control reaction was performed with Cu-based sensitizer **128** in the absence of light and no formation of product **3** was observed thus proving the necessity of visible-light for the transformation.



**Scheme 31:** Use of Cu-based sensitizer **128** for the formation of [5]helicene.

Encouraged by the preliminary results, an extensive optimization of the visible-light-mediated photocyclization of [5]helicene was conducted in collaboration with Augusto Hernandez-Perez. Firstly, various solvents were tested by Augusto (Table 2). THF provided a yield of 30% (Entry 1); hexanes, MeOH and DMF afforded poor yields of <5% – 14% (Entries 2 – 4); and DCM, dioxane and toluene gave fair yields of 27% – 35% (Entries 5 – 7). The optimization was continued with THF as the solvent of choice since it afforded the best yield of **3**, 47%, when the reaction time was extended to 5 days of irradiation.

<sup>125</sup> Paria, S.; Reiser, O. *ChemCatChem*, **2014**, *ASAP* (doi: 10.1002/cctc.201402237)

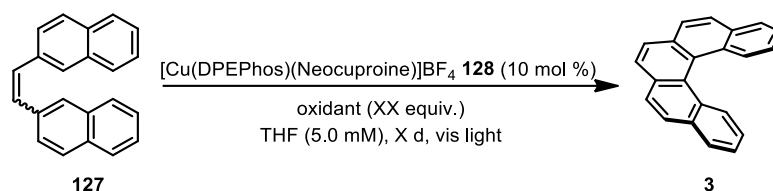
**Table 2:** Solvent optimization for the visible-light-mediated synthesis of [5]helicene.

Entry	Solvent	Yield <sup>a</sup>
1	THF	30%
2	hexanes	<5%
3	DMF	7%
4	MeOH	14%
5	DCM	27%
6	dioxane	32%
7	toluene	35%

<sup>a</sup> Isolated yields following flash chromatography.

The effect of the oxidant system on the visible-light-mediated formation of **3** from **127** was investigated next (Table 3). Stoichiometric iodine and propylene oxide as the oxidant system afforded moderate yields of 30% – 47% when the reaction was conducted for 3 – 5 days (Entries 1 and 2). DDQ and *t*-BuOOH provided acceptable yields of 21% and 29% respectively (Entries 3 and 4). Catalytic I<sub>2</sub> with molecular oxygen gave a yield of 42% and 38% after a reaction time of 3 and 5 days, respectively (Entries 5 and 6), a result comparable to that of the stoichiometric I<sub>2</sub> and propylene oxide oxidant system after 5 days (Entry 2). As the yields were higher with the combination of stoichiometric I<sub>2</sub> and propylene oxide, it was chosen as the optimal oxidant system.

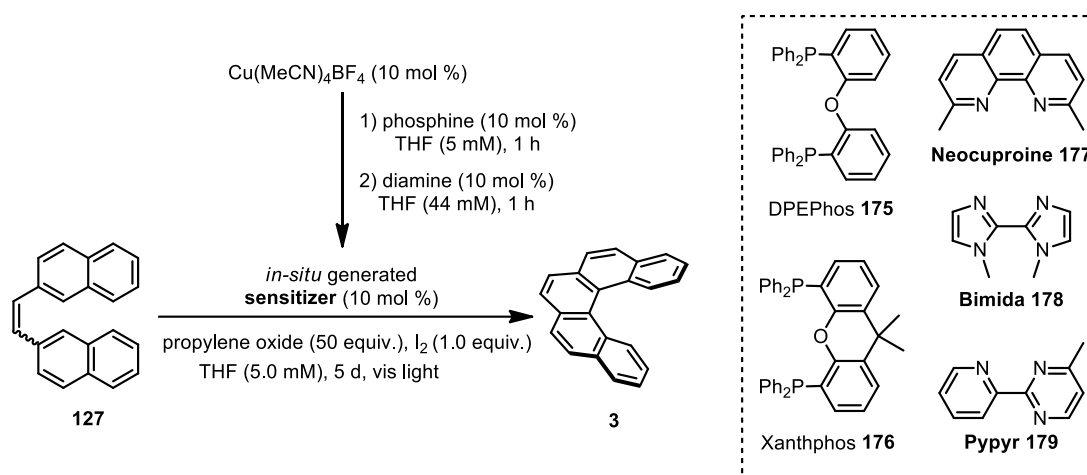


**Table 3:** Oxidant optimization for the visible-light-mediated synthesis of [5]helicene.

Entry	Oxidant System	Days	Yield <sup>a</sup>
1	I <sub>2</sub> (1 equiv.), propylene oxide (50 equiv.)	3	30%
2	I <sub>2</sub> (1 equiv.), propylene oxide (50 equiv.)	5	30 - 47%
3	DDQ (2 equiv.)	3	21%
4	<i>t</i> -BuOOH (4 equiv.), Δ	3	29%
5	I <sub>2</sub> (0.1 equiv.), O <sub>2</sub> (1 atm)	3	42%
6	I <sub>2</sub> (0.1 equiv.), O <sub>2</sub> (1 atm)	5	38%

<sup>a</sup> Isolated yields following flash chromatography.

In a continued effort to further improve the reaction yield, an in-depth optimization of the photosensitizer based on the promising catalyst **128** was performed. To simplify and expedite the screening process, an *in situ* protocol of the Cu-based photoredox catalyst was developed, where the desired Cu-complex was formed in THF *via* the sequential addition of DPEPhos and Neocuproine. The catalyst was used directly, without further purification, for the visible-light-mediated synthesis of [5]helicene with the addition of the remaining required reagents and the starting material (Table 4).

**Table 4:** *In-situ* formation of the Cu-sensitizer for the photosynthesis of [5]helicene.

Entry	Phosphine	Diamine	mol %	Yield <sup>a</sup>
1	DPEPhos	Neocuproine	10	32%
2	-	-	-	0% <sup>b</sup>
3	DPEPhos	Neocuproine	10	0% <sup>c</sup>
4	DPEPhos	Neocuproine	50	56%
5	DPEPhos	Bimida	10	40%
6	DPEPhos	Bimida	25	39%
7	DPEPhos	Pypyr	10	39%
8	Xanthphos	Neocuproine	10	50%
9	Xanthphos	Neocuproine	25	57%
10	Xanthphos	Bimida	10	36%
11	Xanthphos	Bimida	25	49%

<sup>a</sup> Isolated yields after chromatography. <sup>b</sup> Reaction performed in the absence of ligands. <sup>c</sup> Reaction performed in the absence of Cu(MeCN)<sub>4</sub>BF<sub>4</sub>.

The newly developed *in-situ* protocol was applied to the synthesis of the [Cu(DPEPhos)(Neocuproine)]BF<sub>4</sub> complex previously tested in the visible-light-mediated photocyclization reaction to prepare [5]helicene. A yield of 32% (Entry 1) was obtained, which is comparable to the 30% – 47% yields observed with pre-formed catalyst **128**. Using the *in-situ* procedure, two important control experiments were conducted. The first experiment was performed in the absence of ligands (Entry 2) and yielded none of [5]helicene **3**, only *cis* and *trans* isomers of the starting material were recovered. The second control was done without the Cu(MeCN)BF<sub>4</sub> complex and also led to no formation of product **3** with recovered *cis* and *trans* isomers of the starting material (Entry 3). The results obtained from the control experiments

demonstrated that the Cu-based sensitizer, in combination with a phosphine and an amine ligand was necessary to form the desired [5]helicene.

The effect of the catalyst loading was also investigated and it was observed that by increasing the catalyst loading from 10 to 50 mol %, the reaction yield increased to 56% (Entry 4). Substituting Neocuproine ligand **177** with *N,N'*-dimethyl bisimidazole (Bimida **178**) provided a yield of 39% – 40%, regardless of whether the catalyst loading was 10 or 25 mol % (Entries 5 and 6). Substituting the Neocuproine ligand **177** with the pyrimidine-derived ligand (Pypyr **179**) led to a yield of 39% (Entry 7). Both of the substitutions resulted in yields within the same range as the Cu[DPEPhos][Neocuproine] complex.

The photoredox catalyst optimization continued with an exploration of the substitution of the phosphine ligand. Using Xanthphos as the phosphine moiety provided yields of 50% and 57% at 10 mol % and 25 mol % catalyst loading respectively (Entries 8 and 9). Substituting the amine ligand with *N,N'*-dimethyl bisimidazole (Bimida **178**) provided a yield of 36% – 49%, with a catalyst loading of 10 or 25 mol % respectively (Entries 10 and 11). Overall, the best result obtained from the sensitizer optimization was the combination of the Xanthphos-Neocuproine ligands which consistently provided a yield above 50% (Figure 24).

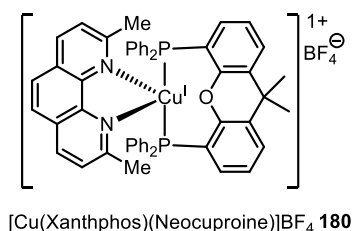
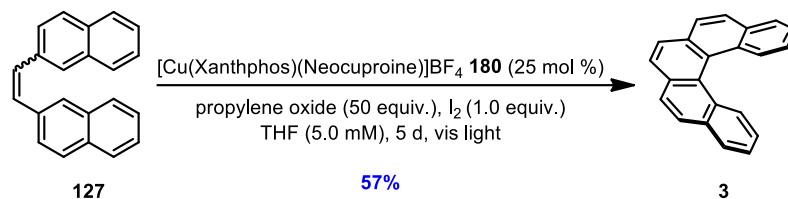


**Figure 24:** The optimized Cu-based sensitizer.

Photoredox complex **180** was used in the final optimization effort, where the reaction was irradiated for 14 days in an attempt to increase the isolated yield. A similar yield of 57% was observed with recovered *cis* and *trans* isomers of the starting material. A control experiment was conducted where a 1:1 ratio of the starting material **127** and [5]helicene **3** was submitted to the optimized reaction conditions. After 5 days, no change in the ratio of the starting material to product was observed, suggesting that the product may be inhibiting further conversion of stilbene-type precursor **127** to desired product **3**. Further studies are required to confirm this hypothesis.

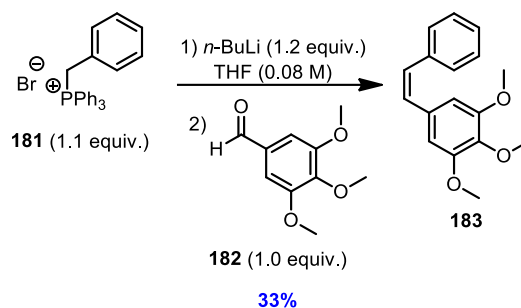
After extensive optimization efforts, the best reaction conditions obtained for the visible-light-mediated formation of [5]helicene included a 25 mol % loading of the Cu[DPEPhos][Neocuproine] photoredox catalyst **180**, stoichiometric I<sub>2</sub> as the oxidant, an excess of propylene oxide as the HI scavenger and THF as the reaction solvent. After irradiation for 5 days under a typical household light bulb (30 W), the desired [5]helicene **3** was obtained in a yield of 57% (Scheme 32).



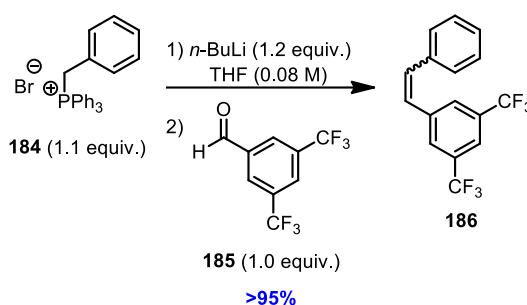
**Scheme 32:** Optimized conditions for the visible-light-mediated synthesis of [5]helicenes.

As previously mentioned, scaling-up the synthesis of [5]helicene using the traditional UV-light-mediated conditions would be very challenging because of the high dilution required to avoid the formation of side-products stemming from [2+2] intermolecular cycloaddition and overoxidation of [5]helicene to **13**. With the newly developed visible-light-mediated conditions in hand, a gram-scale synthesis of [5]helicene was attempted in collaboration with Augusto Hernandez-Perez. Approximately 225 mg of the Cu-based sensitizer **180** was formed *in-situ* and 1.68 g of the stilbene precursor **127** was added along with 1.6 g of I<sub>2</sub> and 22 mL of propylene oxide. The reaction was setup in a 3 L round bottom flask and irradiated with several compact fluorescent light bulbs (30 W) for 5 days. Overall, 1.2 L of solvent was used, a significant decrease from the 30 L that would have been required under UV-light-mediated conditions. After 5 days, 0.7 g of [5]helicene **3** was obtained in 42% yield.

## 2.2.2 Preliminary mechanistic studies

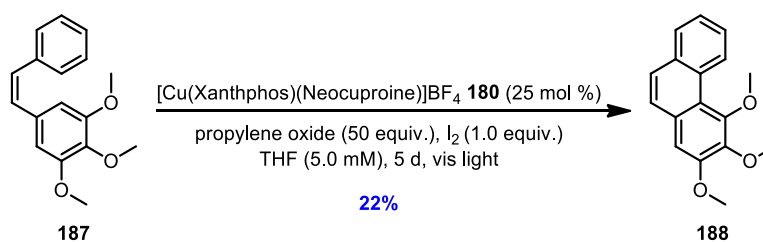


**Scheme 33:** Formation of the electron-rich stilbene-type precursor **183**.



**Scheme 34:** Formation of the electron-poor stilbene-type precursor **186**.

Preliminary studies were performed in an attempt to decipher the reaction mechanism. An electron-rich stilbene **183** (Scheme 33) and an electron-poor stilbene **186** (Scheme 34) were synthesized *via* Wittig olefination in yields of 33% and >95% respectively. The two substrates were submitted to the optimized conditions (Scheme 35) for visible-light-mediated photocyclization. Only electron-rich trimethoxy-substituted substrate **183** underwent the cyclization to desired product **188** in 22% yield, while the electron-poor ditrifluoromethyl-substituted stilbene **186** did not react.



**Scheme 35:** Cyclization of an electron-rich and an electron-poor stilbene-type precursor.

Based upon existing mechanistic data for Ru-based sensitizers<sup>114, 115a,b, 126</sup> an oxidative pathway for the formation of [5]helicene was proposed (Figure 25). Upon excitation with visible-light, the Cu-based sensitizer could reduce I<sub>2</sub> *via* a single electron transfer (SET) process to afford a Cu(II) species. The Cu(II) complex would then oxidize stilbene-type precursor **127** to radical cation **189**, effectively regenerating the initial Cu(I) catalyst in the process. Radical cation **189** would then cyclize to pentacycle **191**. Further oxidation of cyclic radical cation **191** to desired [5]helicene **3** could take place *via* iodide-mediated deprotonation and subsequent oxidation by iodine radical formed from the initial photoactivation of the Cu-based sensitizer. Any HI generated during the reaction is trapped by propylene oxide to provide product **194**. It is important to note that although the initial electron abstraction could occur at either the olefin or aromatic moiety, both intermediates, **189** and **190**, will lead to the same cyclic radical cation **191**. Further mechanistic studies are still required to fully confirm the proposed mechanism.

---

<sup>126</sup> a) Rueping, M.; Vial, C.; Koenigs, R. M.; Poscharny, K.; Fabry, D. C. *Chem. Commun.* **2011**, *47*, 2360. b) Xuan, J.; Cheng, Y.; An, J.; Lu, L.-Q.; Zhang, X.-X.; Xiao, W.-J. *Chem. Commun.* **2011**, *47*, 8337. c) Rueping, M.; Zhu, S.; Koenigs, R. M. *Chem. Commun.* **2011**, *47*, 8679. d) Zou, Y.-Q.; Lu, L.-Q.; Fu, L.; Chang, N.-J.; Rong, J.; Chen, J.-R.; Xiao, W.-J. *Angew. Chem., Int. Ed.* **2011**, *50*, 7171. e) Rueping, M.; Leonori, D.; Poisson, T. *Chem. Commun.* **2011**, *47*, 9615. f) Freeman, D. B.; Furst, L.; Condie, A. G.; Stephenson, C. R. J. *Org. Lett.* **2012**, *14*, 94. g) Oxidative generation of oxocarbenium intermediates: Tucker, J. W.; Narayanam, J. M. R.; Shah, P. S.; Stephenson, C. R. J. *Chem. Commun.* **2011**, *47*, 5040. h) McNally, A.; Prier, C. K.; MacMillan, D. W. C. *Science* **2011**, *334*, 1114. i) Fragmentation and annulation reactions of cyclopropyl ammoniumyl radical cations: Maity, S.; Zhu, M.; Shinabery, R. S.; Zheng, N. *Angew. Chem., Int. Ed.* **2012**, *51*, 222. j) Lin, S.; Ischay, M. A.; Fry, C. G.; Yoon, T. P. *J. Am. Chem. Soc.* **2011**, *133*, 19350.

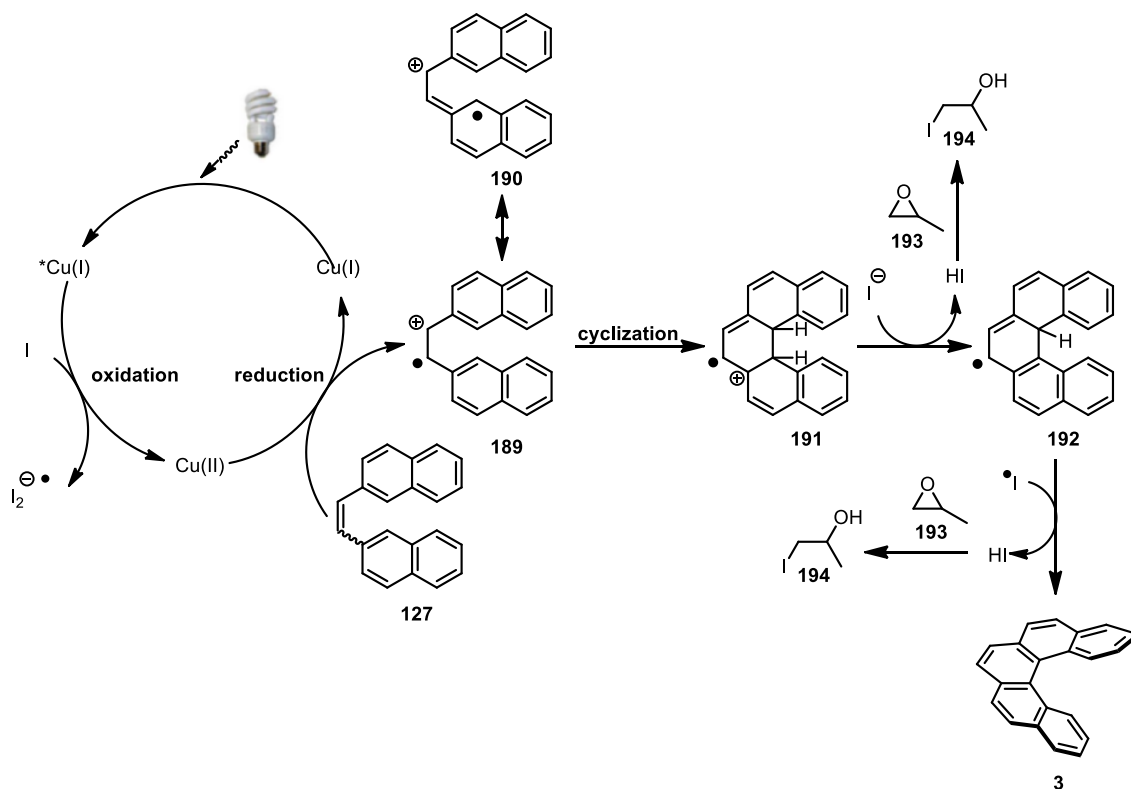
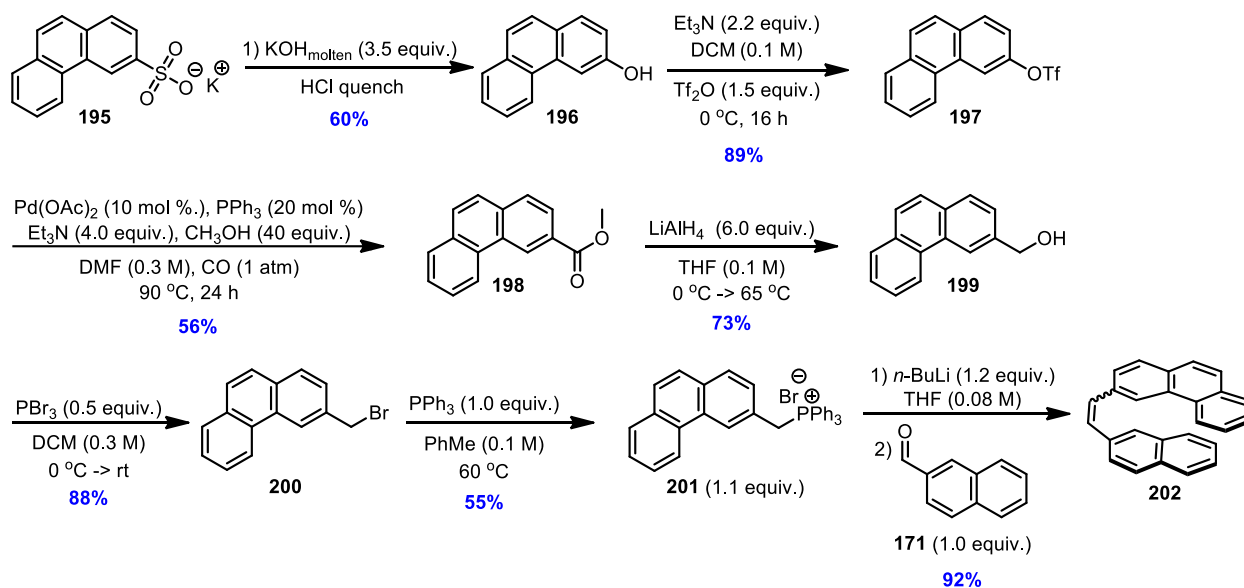


**Figure 25:** The proposed mechanism for the formation of [5]helicene.

### 2.3 Visible-Light-Mediated Formation of [6]Helicenes

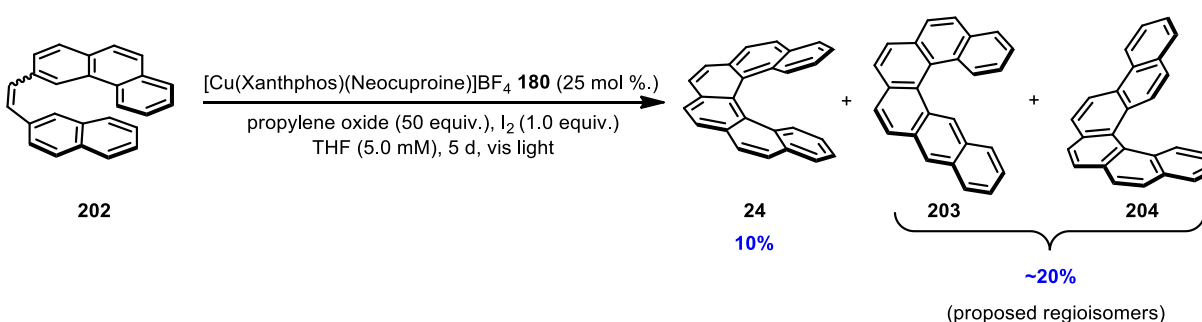
An investigation of the formation of [6]helicene **24**, as well as its methoxy-substituted derivatives, was conducted using the developed synthetic conditions for the visible-light-mediated photocyclization. The multistep synthesis of stilbene-type compound **202** (Scheme 36) began with desulphonylation of sulphonate **195**, a transformation achieved with molten potassium hydroxide followed by a quench with concentrated hydrochloric acid to afford the desired 3-phenanthrol **196** in 60% yield. The alcohol underwent triflation in the presence of  $\text{Et}_3\text{N}$ , to provide phenanthryl triflate **197** in 89% yield. Triflate **197** was submitted to Pd-catalyzed carboxymethylation conditions to afford the desired methyl ester **198** in 56% yield, which was subsequently reduced with lithium aluminium hydride to furnish primary alcohol **199** in 73% yield. Intermediate **199** underwent a bromination with phosphorous tribromide to provide alkyl bromide **200** in 88% yield which was converted to triphenylphosphonium bromide salt **201** with triphenylphosphine in toluene in 55% yield. The phosphonium salt **201** underwent a Wittig olefination with the

commercially available 2-naphthaldehyde **171** which afforded the stilbene-type precursor **202** for the photocyclization of [6]helicene in 92% yield.



**Scheme 36:** Formation of the stilbene-type cyclization precursor for [6]helicene.

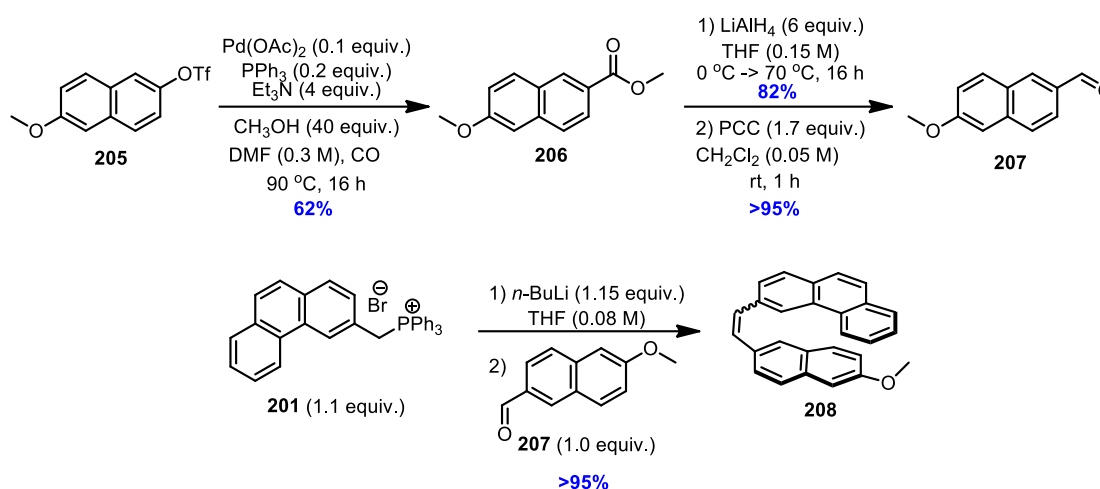
The photocyclization of stilbene precursor **202** resulted in a mixture of several products (Scheme 37) along with recovered *cis* and *trans* isomers of the starting material, which were inseparable from the products. Comparison with  $^1\text{H}$  NMR data from the literature suggested that desired [6]helicene **24** was obtained in approximately 10% yield (by NMR). A number of other inseparable regioisomers was also observed in the reaction mixture resulting in an overall yield of 30% with respect to the cyclized products.



**Scheme 37:** Visible-light-mediated cyclization of **202**.

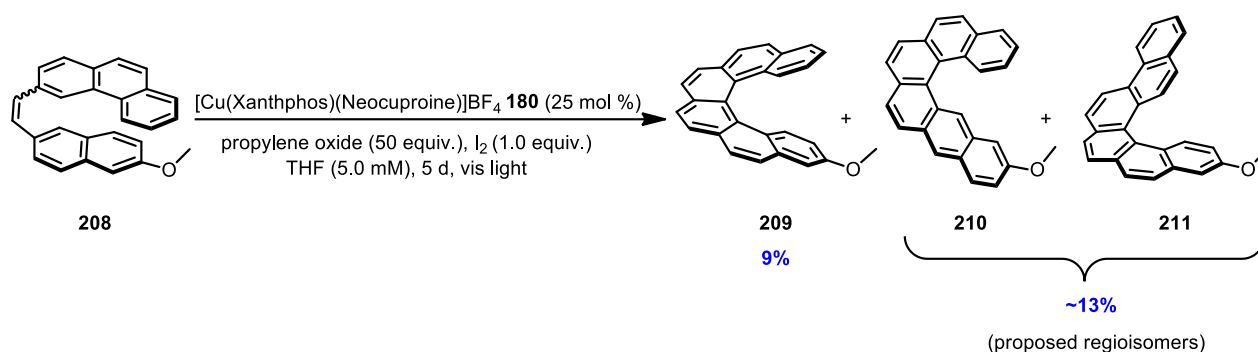


In an effort to improve the yield of the photocyclization reaction, methoxy substituents were added along the polyaromatic skeleton, since electron-rich stilbene-type precursors like **187** proved to cyclize more readily than electron-poor precursors. The preparation of stilbene-type precursor **208** (Scheme 38) began with Pd-catalyzed carboxymethylation of 6-methoxy-2-trifluoromethylsulfonylnaphthalene, which provided desired methyl ester **206** in 62% yield. Methyl 6-methoxy-2-naphthoate **206** was reduced to a primary alcohol with lithium aluminium hydride in 82% yield and subsequently oxidized to desired aldehyde **207** with pyridinium chlorochromate (PCC) in quantitative yield. Phosphonium salt **201** and methoxy-substituted aldehyde **207** were coupled *via* a Wittig olefination reaction to provide substituted stilbene substrate **208** in quantitative yield.



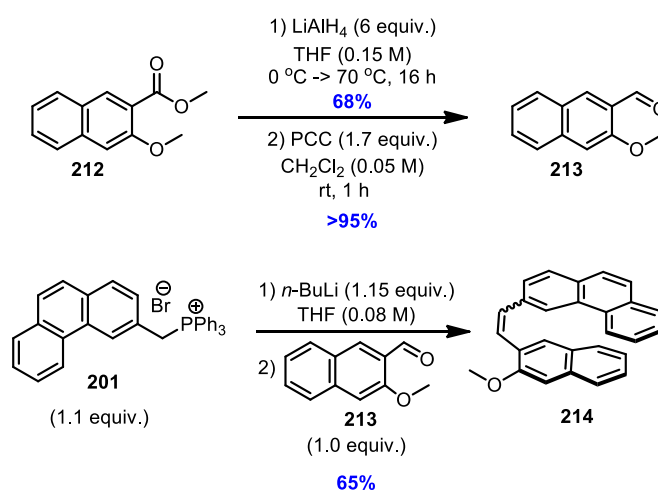
**Scheme 38:** Preparation of the 3-(2-(6-methoxynaphthalen-2-yl)vinyl)phenanthrene substrate.

Following photocyclization of precursor **208**, desired 10-methoxy-[6]helicene **208** was observed in a yield of about 9% (by NMR) as a product in a mixture with several other regioisomers, such as **210** and **211**, as well as *cis* and *trans* isomers of stilbene starting material **208** (Scheme 39). Unfortunately, the products within the complex mixture were inseparable by flash chromatography. It was concluded that incorporation of the methoxy group at the 6-position of the naphthyl moiety did not significantly increase the reaction yield nor diminish the formation of undesired regioisomers.



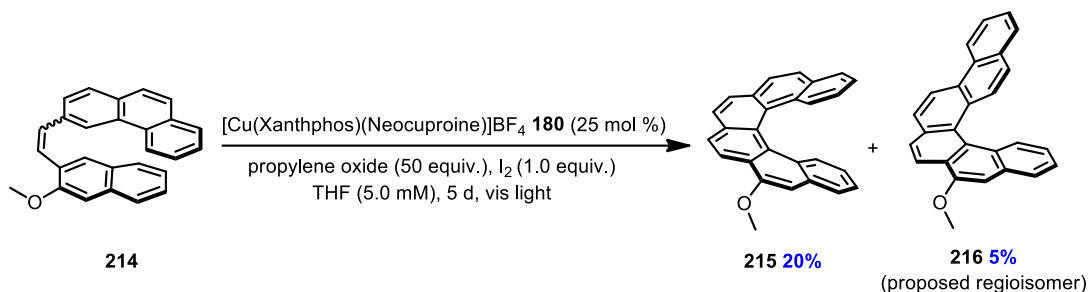
**Scheme 39:** Visible-light-mediated photocyclization of **208**.

One possible way to prevent or decrease the formation of various regioisomers involves placing a blocking group at the cyclization sites which lead to undesired products. Using a methoxy substituent as a blocking group would achieve two goals at once as it could hinder the formation of undesired regioisomers and enrich the electronic density of the stilbene precursor which should improve the reaction yield. 3-(2-(3-Methoxynaphthalen-2-yl)vinyl)phenanthrene **214** was synthesized in several steps starting from commercially available methyl ester **212**, which underwent a reduction with lithium aluminium hydride to the alcohol in 68% yield and was subsequently oxidized by pyridinium chlorochromate to provide desired aldehyde **213** in quantitative yield. The aldehyde was coupled with phosphonium salt **201** *via* Wittig olefination which afforded desired stilbene precursor **214** in a yield of 65% (Scheme 40).



**Scheme 40:** Preparation of 3-(2-(3-methoxynaphthalen-2-yl)vinyl)phenanthrene substrate **214**.

Cyclization of stilbene precursor **214** under the optimized photocyclization conditions led to the formation of the desired 2-methoxy-[6]helicene in 20% yield (by NMR) with only traces of another regioisomer and *cis* and *trans* isomers of the starting material, which were inseparable from the product. The blocking strategy was successful as the incorporation of the methoxy blocking group at position 3 of the stilbene precursor eliminated the formation of one potential regioisomer thus increasing the regioselective formation of desired [6]helicene **215** (Scheme 41).



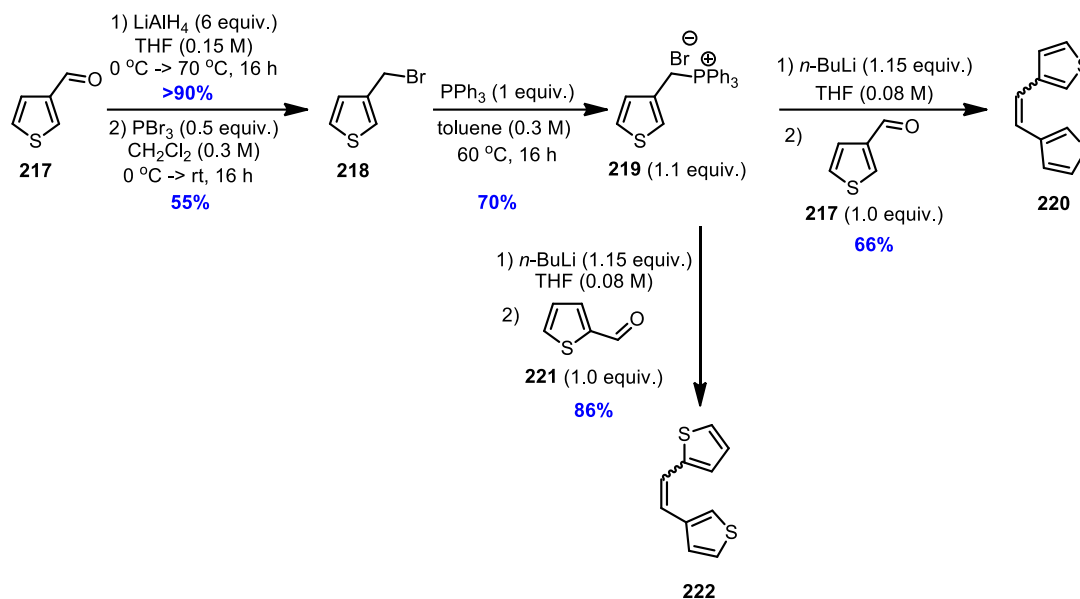
**Scheme 41:** Visible-light-mediated cyclization of **214**.

## 2.4 Visible-Light-Mediated Photocyclization of Thiohelicenes

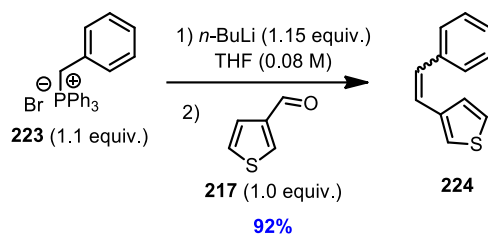
The formation of various thiohelicenes using the optimized visible-light-mediated photocyclization conditions was also investigated. Thiohelicenes have recently found applications in high-performance organic field-effect transistors as well as in organic thin-film transistors (OTFTs).<sup>127</sup> These heteroaromatics also exhibit interesting aggregation patterns with good nonlinear optical properties making them an interesting heterohelicene to investigate.<sup>55,57</sup> The exploration began with an attempt to synthesize three thio[3]helicenes that were unobtainable using the traditional UV-cyclization methods as described by Mallory.<sup>128</sup>

<sup>127</sup> a) Zhou, Y.; Lei, T.; Wang, L.; Pei, J.; Cao, Y.; Wang, J. *Adv. Mater.* **2010**, *22*, 1484. b) Kim, C.; Marks, T. J.; Facchetti, A.; Schiavo, M.; Bossi, A.; Maiorana, S.; Licandro, E.; Todescato, F.; Toffanin, S.; Muccini, M.; Graiff, C.; Tiripicchio, A. *Org. Electron.* **2009**, *10*, 1511.

<sup>128</sup> Mallory, F. B.; Mallory, C. W. *Org. React.* **1984**, *30*, 1.



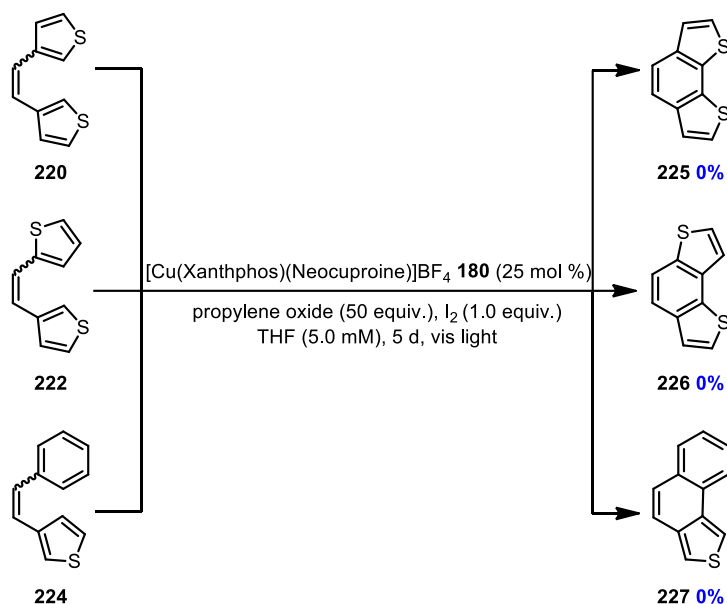
**Scheme 42:** Synthesis of the dithiophene-stilbene-type precursors.



**Scheme 43:** The formation of 3-styrylthiophene.

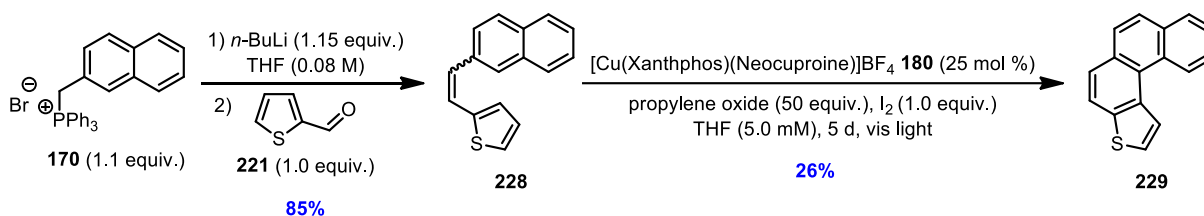
The multistep synthesis of two thiophene-based stilbene-type precursors **220** and **222** began with the formation of common intermediate **219** (Scheme 42). Firstly, commercially available thiophene-3-carbaldehyde **217** was reduced with lithium aluminium hydride to provide the desired alcohol in >90% yield. The intermediate was then brominated with phosphorous tribromide to obtain product **218** in 55% yield which was subsequently converted to triphenylphosphonium bromide salt **219** with triphenylphosphine in toluene in 70% yield. Salt **219** underwent a Wittig olefination with commercially available thiophene-3-carbaldehyde **217** to obtain stilbene-type precursor **220** in 66% yield. Salt **219** was also coupled with the commercially available thiophene-2-aldehyde **221** via the same olefination conditions providing stilbene-precursor **222** in 86% yield. 3-styrylthiophene cyclization precursor **224** was synthesized from two commercially available materials, benzyltriphenylphosphonium bromide **223** and the thiophene-3-carbaldehyde **217** via the Wittig olefination, in an excellent yield of 92% (Scheme 43). The

stilbene-type precursors were subjected to the optimized visible-light-mediated cyclization conditions. Unfortunately, the results were the same as Mallory had observed under the UV-light mediated conditions. All of the cyclizations were unsuccessful and only the *cis* and *trans* stilbene-type precursors **220**, **222** and **224** were recovered (Scheme 44). It may be that the cyclization was unsuccessful because the excited Cu-based sensitizer oxidized the sulfur atom, which was subsequently quenched *in situ*, as opposed to the stilbene unit. Further studies are required to confirm the hypothesis.



**Scheme 44:** Attempted photocyclization for the formation of benzodithiophenes **225** and **226** and naphthothiophene **227**.

Following the unsuccessful photocyclizations of naphtho- and benzodithiophenes stilbene-type precursors **220**, **222** and **224**, further investigation of the formation of thiohelicenes under visible-light-mediated conditions continued. In particular, the synthesis of phenanthro[3,4-b]thiophene **229** was studied as the naphthyl moiety on the cyclization precursor should be preferentially oxidized over the sulfur atom, due to their electronic character, thus providing the desired product more readily.



**Scheme 45:** Visible-light-mediated formation of thio[4]helicene.

Naphtha-thiophene stilbene-type precursor **228** was formed in 85% yield *via* the Wittig olefination between naphthyl triphenylphosphonium bromide **170** and thiophene-2-aldehyde **221**. Stilbene **228** was submitted to the optimized photocyclization conditions and desired phenanthro[3,4-*b*]thiophene **229** was obtained in 26% yield (by NMR) as a product in an inseparable mixture with recovered *cis* and *trans* isomers of the starting material (Scheme 45). It was encouraging to see the formation of the desired thio[4]helicene, although in modest yield, since it proved the theory of preferential oxidation of the naphthyl moiety over the sulfur.

## 2.5 Visible-Light-Mediated Formation of Pyrene-Helicene Derivatives

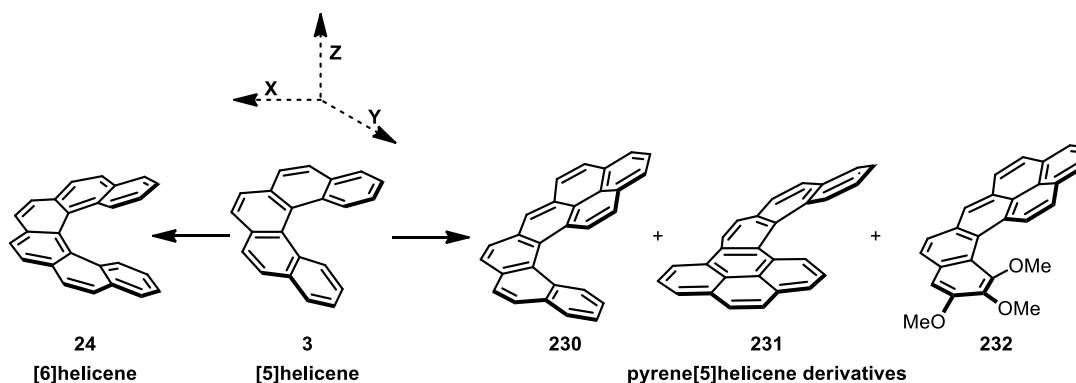


**Figure 26:** Possible extensions of the helicene backbone.

Recent developments regarding the synthesis of helicenes have focused on extending the helical backbone along the *Z*-axis (Figure 26). Unfortunately, very little chemistry has been

established to expand the  $\pi$  surface of the helicene along the X- and Y-axis.<sup>129</sup> A number of extended helical polycyclic aromatic compounds have been reported including helicene-triphenylene hybrids, synthesized *via* Rh-catalyzed asymmetric [2+2+2]-cyclotrimerization,<sup>129a</sup> helicene-perylene hybrids, prepared by UV-mediated photocyclization,<sup>130</sup> and recently, contorted octabenzocircumbiphenyls synthesised using the Scholl reaction.<sup>129b</sup> The lack of pyrene-helicene hybrid compounds is surprising since these novel structures could demonstrate interesting physical properties, crystallinity and enhanced solubility relative to other traditional planar aromatics.<sup>131</sup>

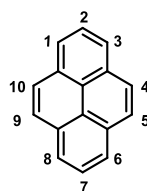


**Figure 27:** Pyrene numbering.

Pyrene-helicene derivatives **230**, **231** and **232** (Figure 26) were identified as synthetic targets that could be prepared using the previously established photoredox methodology. Structures **230** and **231** resemble the [5]helicene model substrate with a  $\pi$  surface extension along the Y-axis (Compound **230**, Figure 26) and the X-axis (Compound **231**, Figure 26) and structure **232** contains a [4]helicene motif that is electronically enriched with three methoxy substituents. The main synthetic challenge in the synthesis of structures **230** and **232** is the formation of the pyrene moiety in the desired compound as it requires functionalization at the 2- and 7-positions (Figure 27), not accessible by traditional aromatic substitution methods.<sup>132</sup> The commonly employed electrophilic aromatic substitution strategy provides products with functionalization at

<sup>129</sup> a) Sawada, Y.; Furumi, S.; Takai, A.; Takeuchi, M.; Noguchi, K.; Tanaka, K. *J. Am. Chem. Soc.* **2012**, *134*, 4080. b) Xiao, S.; Kang, S. J.; Wu, Y.; Ahn, S.; Kim, J. B.; Loo, Y.-L.; Siegrist, T.; Steigerwald, M. L.; Li, H.; Nuckolls, C. *Chem. Sci.* **2013**, *4*, 2018.

<sup>130</sup> Kelber, J.; Achard, M.-F.; Durola, F.; Bock, H. *Angew. Chem., Int. Ed.* **2012**, *51*, 5200.

<sup>131</sup> a) Bendikov, M.; Wudl, F.; Perepichka, D. F. *Chem. Rev.* **2004**, *104*, 4981. b) Duong, H. M.; Bendikov, M.; Steiger, D.; Zhang, Q.; Sonmez, G.; Yamada, J.; Wudl, F. *Org. Lett.* **2003**, *5*, 4433. c) Payne, M. M.; Parkin, S. R.; Anthony, J. E. *J. Am. Chem. Soc.* **2005**, *127*, 8028.

<sup>132</sup> a) Liu, Z.; Wang, Y.; Chen, Y.; Liu, J.; Fang, Q.; Kleeberg, C.; Marder, T. B. *J. Org. Chem.* **2012**, *77*, 7124. b) Batsanov, A. S.; Howard, J. A. K.; Albesa-Jove, D.; Collings, J. C.; Liu, Z.; Mkhaliid, I. A. I.; Thibault, M.-H.; Marder, T. B. *Cryst. Growth. Des.* **2012**, *12*, 2794.

the 1-, 3-, 6- and 8-positions only (Figure 27), therefore a novel method had to be investigated to establish the desired substitution pattern.

The proposed synthetic route to prepare compounds **230** and **232**, involved the formation of the desired stilbene-type precursor *via* a Wittig olefination of the appropriate aryl triphenylphosphonium salt **234** with 2-pyrene aldehyde **235**. The aldehyde would be the product of consecutive reduction and oxidation of methyl ester **236**, which would stem from 2-bromopyrene **90** (Figure 28).

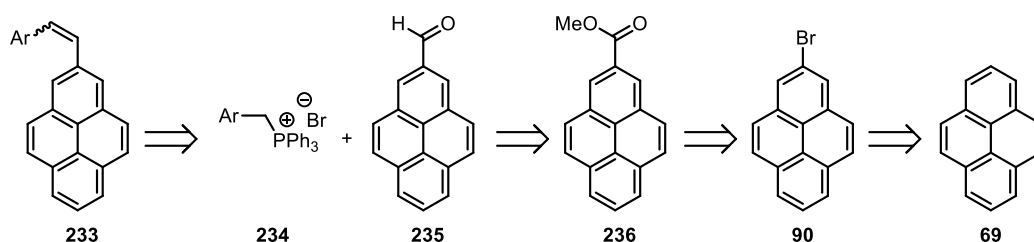
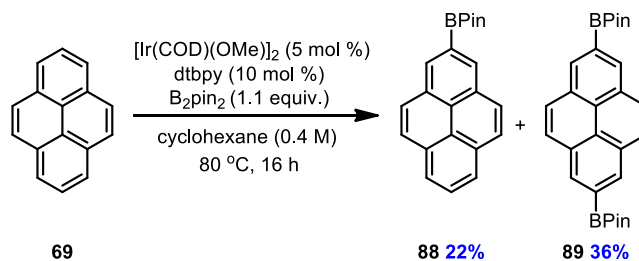


**Figure 28:** Proposed retrosynthesis for the formation of stilbene precursors for compounds **230** and **232**.

The principal synthetic challenge was to establish a procedure for the successful bromination of pyrene at the 2-position. Since direct bromination *via* electrophilic aromatic substitution would provide exclusively 1-, 3-, 6- and 8-position functionalization (Figure 27), another method reported by Coventry *et al.* was investigated. The group reported an Ir-catalyzed substitution of pyrene at the 2-position using the sterically bulky pinacol borane which could then be easily converted to the desired bromo-substituted product **90**.<sup>89,133</sup> Application of the synthetic method afforded a mixture of the desired monoborylated pyrene **88** as well as diborylated pyrene **89** in fair yields of 22% and 36% respectively (Scheme 46). Although an interesting intermediate, disubstituted product **89** was superfluous for the formation of the desired substrates thus a strategy was necessary to hinder its formation.

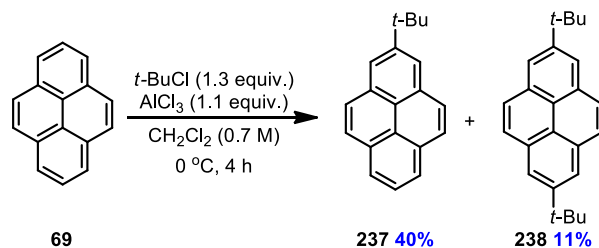
<sup>133</sup> Hartwig, J. F.; *Acc. Chem. Res.* **2012**, *45*, 864.





**Scheme 46:** Ir-catalyzed borylation of pyrene with bis(pinacolate)diboron.

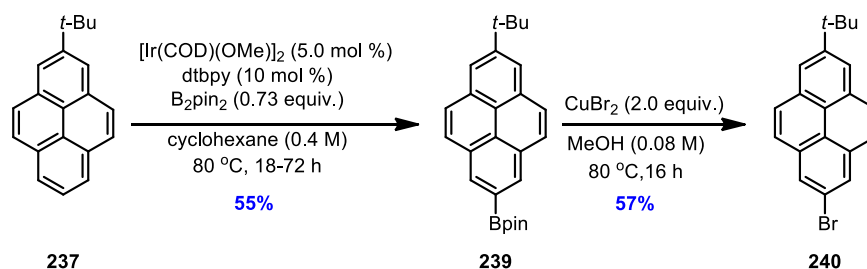
It was proposed that placing a sterically encumbering blocking group at one of the reactive 2-positions could resolve the oversubstitution problem. If the substituent was a bulky alkyl group, the overall solubility of the pyrene-derivative throughout the synthetic route would also be enhanced. A Friedel-Crafts alkylation was performed and a mixture of mono- and di-*t*-Bu products, separable by re-crystallization, was obtained in yields of 40% and 11% respectively after 4 h (Scheme 47).<sup>134</sup>



**Scheme 47:** Friedel-Crafts alkylation of pyrene.

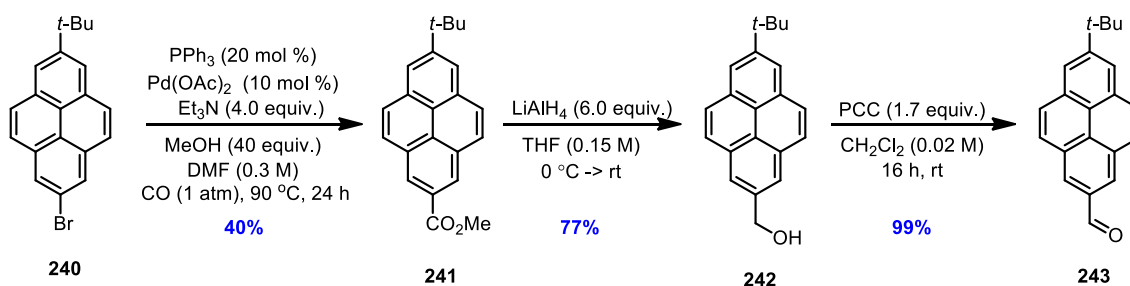
Subsequent Ir-catalyzed borylation provided the pinacol borane **239** in 55%. Although efforts were made to reduce the quantity of the costly Ir-catalyst used and the long reaction time, a minimal loading of 5 mol % was required as well as at least an 18 hour reaction time in order to obtain an acceptable yield. Fortunately, the reaction conditions were scalable and provided gram quantities of borylated product **239**. Pinacol borane substituted pyrene **239** was then converted to its bromine derivative **240** in 57% yield using superstoichiometric quantities of  $CuBr_2$  in methanol (Scheme 48).<sup>89, 133</sup>

<sup>134</sup> Miura, Y.; Yamano, E.; Tanaka, A. *J. Org. Chem.* **1994**, *59*, 3294.

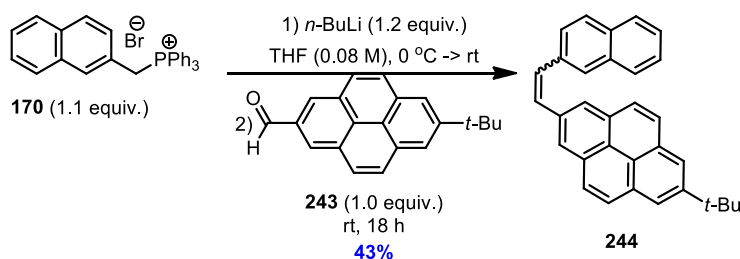


**Scheme 48:** Ir-catalyzed borylation followed by bromination of the 2-*t*-Bu-pyrene.

Brominated pyrene derivative **240** underwent a Pd-catalyzed carboxymethylation to afford desired methyl ester **241** in 40% yield after a 24 hour reaction time. Ester **241** was then reduced with lithium aluminium hydride to its corresponding alcohol **242** in good yield of 77%. It is important to note that over-reduction of the alcohol to its alkane counterpart has been previously observed, thus the reduction had to be conducted at room temperature. Alcohol **242** was further oxidized with pyridinium chlorochromate to aldehyde **243** in quantitative yield (Scheme 49). Aldehyde **243** underwent a Wittig olefination reaction with naphthyl triphenylphosphonium bromide **170** to provide stilbene-type precursor **244** in a moderate yield of 43% as a mixture of *cis* and *trans* isomers (Scheme 50).

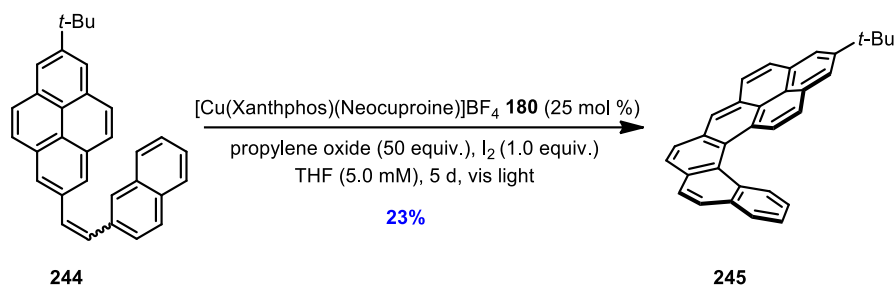


**Scheme 49:** Synthesis of aldehyde **243**.



**Scheme 50:** Wittig reaction for the formation of stilbene precursor **244**.

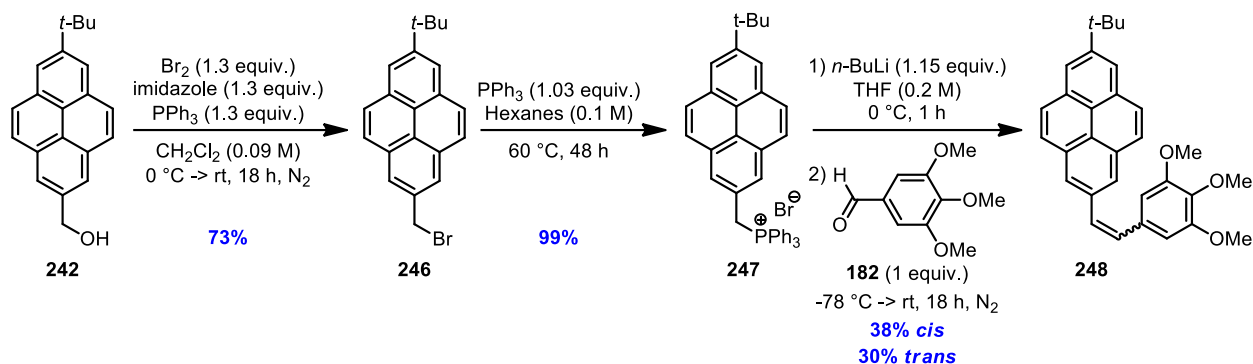
Stilbene precursor **244** was then subjected to the previously optimized visible-light-mediated photocyclization conditions.<sup>135</sup> The active Cu-based sensitizer<sup>123</sup> was prepared *in situ* with Xanthphos **176** and Neocuproine **177** added sequentially to Cu(MeCN)<sub>4</sub>BF<sub>4</sub> in THF and stirred at room temperature for 1 h after the addition of each ligand. The solution was then added to another flask containing the oxidant system, I<sub>2</sub> and propylene oxide, along with stilbene precursor **244**. The solution was irradiated with visible-light for 5 days and desired pyrene-[5]helicene **245** was isolated with a yield of 23% with recovered *cis* and *trans* isomers of the starting material (Scheme 51).



**Scheme 51:** Visible-light-mediated photocyclization of pyrene-[5]helicene **245**.

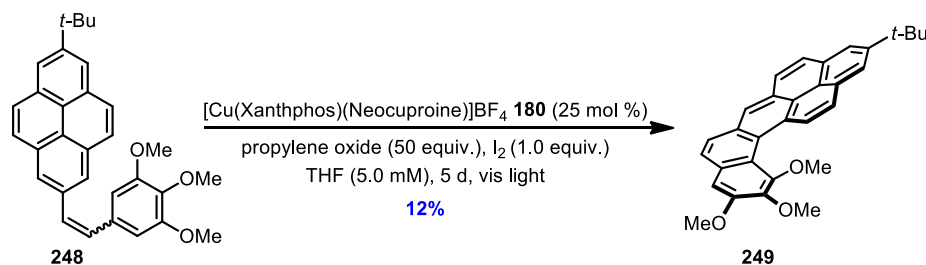
The next pyrene-helicene target was electronically enriched with three methoxy substituents at one extremity and possessed a [4]helicene motif. The formation of the trimethoxy pyrene[4]helicene **249** was done by Augusto Hernandez Perez. In order to achieve the synthesis of compound **249**, pyrene alcohol **242** was converted to its bromine derivative **246** with phosphorous tribromide in 73% yield. Following treatment with triphenylphosphine in toluene, phosphonium salt **247** was formed in quantitative yield. Salt **247** underwent a Wittig olefination with 3,4,5-trimethoxybenzaldehyde **182** to afford stilbene-type precursor **248** in 68% yield as a mixture of *cis* and *trans* isomers (Scheme 52).

<sup>135</sup> Hernandez-Perez, A. C.; Vlassova, A.; Collins, S. K. *Org. Lett.* **2012**, *14*, 2988.



**Scheme 52:** Formation of the stilbene-type precursor **248**.

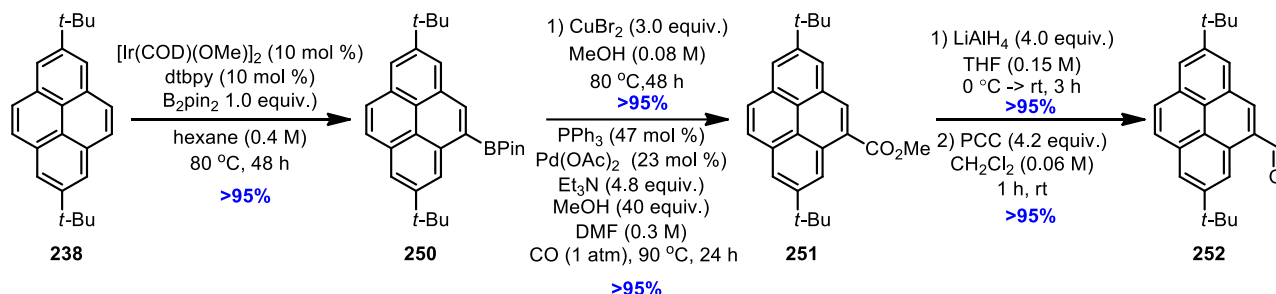
The stilbene-type precursor **248** underwent a photocyclization under the previously established conditions<sup>135</sup> with the *in situ* generated Cu-based catalyst. The desired trimethoxy pyrene-[4]helicene **249** was obtained with a yield of 12% along with recovered *cis* and *trans* isomers of the starting material (Scheme 53). The lower yield obtained for the formation of the pyrene-[4]helicene versus the pyrene-[5]helicene, may be due to the oxidative reaction mechanism. If the reaction pathway involves an electron abstraction from the aromatic moiety, it would be more difficult for the photoexcited Cu-based sensitizer to remove the initial electron from either the pyrene or the trimethoxy-benzene motif of the stilbene-type precursor **248** as they are less likely to break their aromaticity compared to a naphthalene moiety of stilbene compound **244**.



**Scheme 53:** Visible-light-mediated formation of trimethoxy pyrene-[4]helicene.

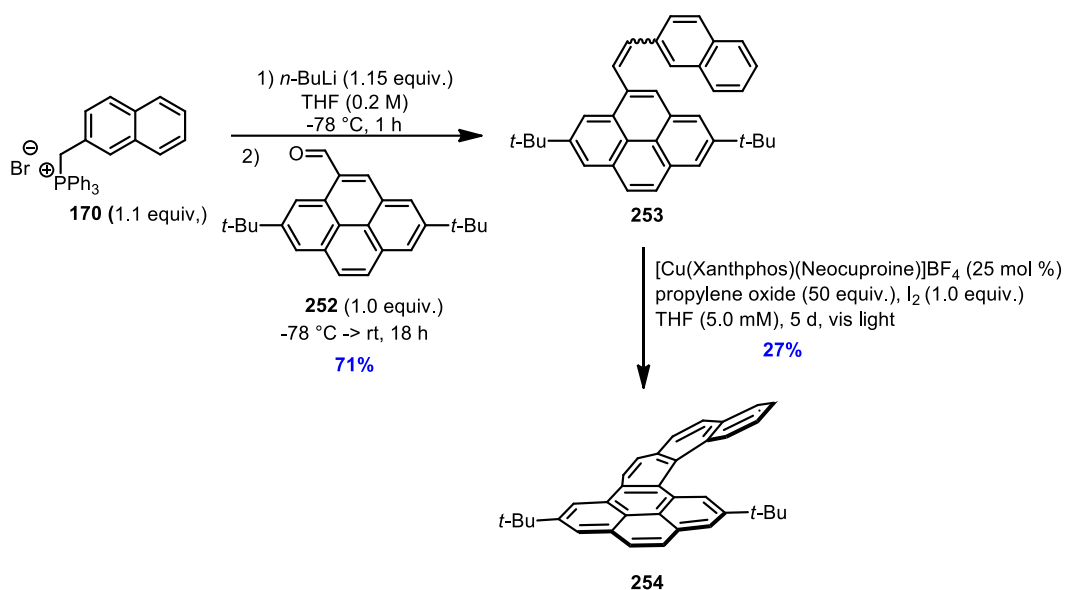
The synthesis of the last pyrene-helicene target **254** was completed in collaboration with Anne-Catherine Bédard and involved functionalization at the 5-position of pyrene. Selective functionalizations at the 5-position have been previously reported in the literature by several

groups.<sup>132</sup> The di-*t*-Bu pyrene product **238** from the Friedel-Crafts alkylation was employed as the substrate for functionalization since alkyl substituents were already present at positions 2 and 7 thus preventing oversubstitution and increasing the overall solubility of the compound throughout the synthesis. Because further functionalization was carried out with bulky boronate groups, no substitution would occur at positions ortho to the alkyl groups due to steric hindrance and only the desired 5-position would be affected. Disubstituted pyrene derivative **238** was subjected to Ir-catalyzed borylation and desired product **250** was obtained in 96% yield. Compound **250** underwent a bromination with superstoichiometric CuBr<sub>2</sub> in methanol which afforded the desired trisubstituted product in 99% yield. Pd-catalyzed carboxymethylation of the brominated compound provided methyl ester **251** in 97% yield which was subsequently reduced with lithium aluminium hydride to obtain the desired alcohol in 99% yield. Following an oxidation with pyridinium chlorochromate, desired trisubstituted aldehyde **252** was obtained in quantitative yield (Scheme 54).



**Scheme 54:** Formation of the 5-substituted aldehyde **252**.

Pyrene aldehyde **252** was coupled with naphthyl triphenylphosphonium bromide **170** via a Wittig olefination which afforded desired stilbene precursor **253** in 71% yield. Using the previously established conditions for visible-light-mediated photocyclization,<sup>135</sup> the final pyrene-helicene target **254** was obtained in 27% yield after 5 days of irradiation (Scheme 55).



**Scheme 55:** Synthesis of the stilbene-type precursor **253** and visible-light-mediated photocyclization of pyrene-helicene **254**.

Once the synthesis of structures **245**, **249** and **254** with increased  $\pi$ -surface using Cu-catalyzed visible-light-mediated photocyclization was complete, the analysis of the solid state structure of compound **245** was performed by Anne-Catherine Bédard and Augusto Hernandez-Perez. X-Ray quality crystals of pyrene[5]helicene were obtained from slow diffusion of hexanes into a DCM solution of **245** and the X-Ray crystallographic data was compared to that of parent [5]helicene **3** (Figure 29).<sup>136, 137</sup>

<sup>136</sup> Bédard, A.-C.; Vlassova, A.; Hernandez-Perez, A. C.; Bessette, A.; Hanan, G. S.; Heuft, M. A.; Collins, S. K. *Chem. Eur. J.* **2013**, *19*, 16295.

<sup>137</sup> CCDC-933555 ([5]helicene) and CCDC-933556 (pyrene[5]helicene) contain the supplementary crystallographic data which can be obtained from The Cambridge Crystallographic Data Centre via [www.ccdc.cam.ac.uk/data/data\\_request/cif](http://www.ccdc.cam.ac.uk/data/data_request/cif).

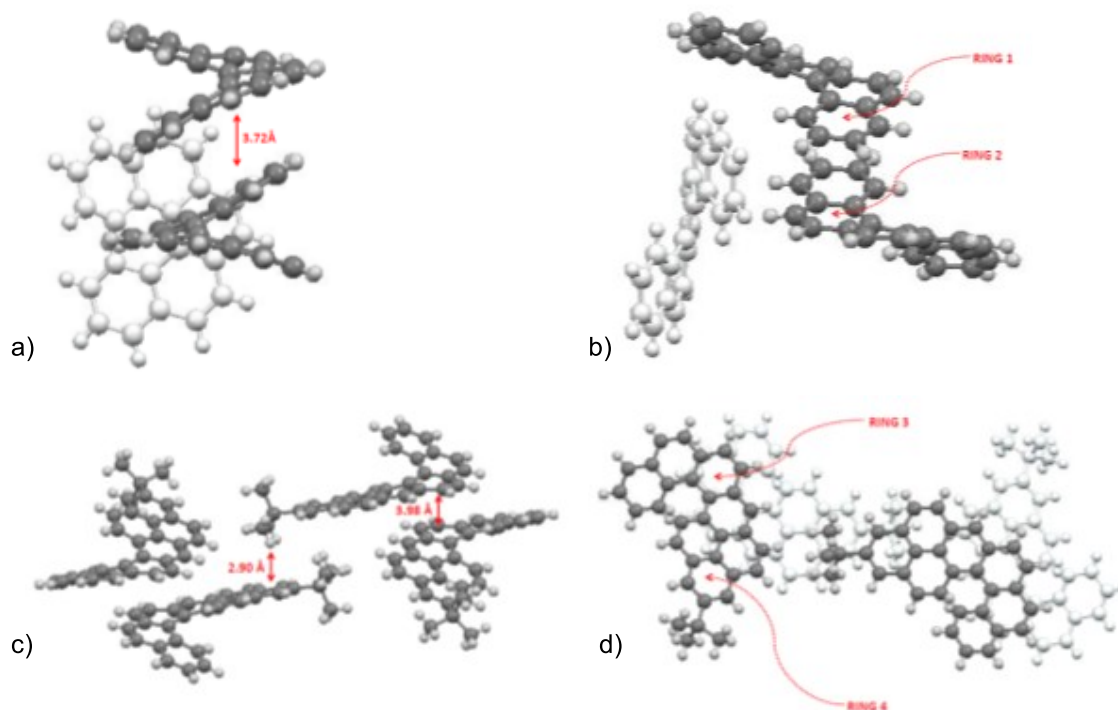


**Figure 29:** X-Ray crystallographic analysis of the molecular packing of [5]helicene **3** (a) side view, b) top view) and pyrene[5]helicene **245** (c) side view, b) top view).

The solid state structure of [5]helicene demonstrated a twisted helical structure with a distortion angle of  $51.2^\circ$  between the planes defined by the terminal aromatic rings. Every third molecule of the unit cell of [5]helicene was arranged perpendicular to two other molecules, however, the distances between the aryl C-H bonds and the centroids of the adjacent [5]helicene were too long to denote any significant interactions. Some  $\pi$ -overlap between the centroids of two aryl units (Rings 1 and 2, Figure 29b) was possible due to the intermolecular distance of 3.72 Å. The solid state structure of pyrene[5]helicene **245** also demonstrated a twisted helical conformation, but with a smaller distortion angle of  $43.3^\circ$ . The variation of  $7.9^\circ$  in helical pitch is fairly significant given that previous studies on [6]helicenes concluded that only  $3\text{--}4^\circ$  differences were observed following substitution of the terminal aromatic rings.<sup>138</sup> In addition, the packing structure of pyrene[5]helicene **245** was different than that of [5]helicene **3**. The solid state structure showed layers of the aromatic molecules with an intermolecular distance of 3.98 Å between the centroids of the two “central” benzene rings (Ring 3, Figure 29c and d) suggesting some  $\pi$ -overlap.

<sup>138</sup> Nakai, Y.; Mori, T.; Inoue, Y. *J. Phys. Chem. A* **2013**, *117*, 83.

Also, C-H--- $\pi$  interactions were observed in the solid state between the *t*-Bu group and the centroid of the terminal aromatic ring as the distance between them was 2.9 Å (Ring 4, Figure 29c and d). Finally, the layered structure of pyrene[5]helicene **245** demonstrated increased  $\pi$ -overlap in solid state when compared to [5]helicene **3** (Figure 29b and d). The co-planar and stacked-like arrangements shown in the solid state structure of pyrene[5]helicene are usually very important when developing organic electronic materials.<sup>139</sup>

---

<sup>139</sup> Anthony, J. E. *Chem. Rev.* **2006**, *106*, 5028.



## CHAPTER 3: DISCUSSION OF VISIBLE-LIGHT-MEDIATED SYNTHESIS OF HELICENES IN A CONTINUOUS FLOW PROCESS

### 3.1 Introduction to the Continuous Flow Processes

Continuous flow processes have been extensively used in industrial chemical and biotechnological production.<sup>140</sup> Over the past decade, the flow apparatus has evolved to a more compact, bench-size model and is now widely used in the academic setting providing an excellent alternative to the traditional batch synthesis.<sup>140</sup> The basic continuous flow system requires a syringe or HPLC-type pump that is connected to a reactor, either a coil made from various types of materials or a micro or meso-fluidic reactor chip.<sup>141</sup> Although some flow systems can be custom-made in the lab to fit the specific reaction requirements, a wide variety of instruments is now commercially available to fit a large spectrum of synthetic needs (Figure 30).



**Figure 30:** Various examples of commercially available continuous flow systems.

<sup>140</sup> Wegner, J.; Ceylan, S.; Kirschning, A. *Adv. Synth. Catal.* **2012**, *354*, 17.

<sup>141</sup> Pastre, J. C.; Browne, D. L.; Ley, S. V. *Chem. Soc. Rev.* **2013**, *42*, 8849.

There are many advantages to using continuous flow reactors over batch syntheses. The flow reactor allows for controlled heat transfer, controlled mixing (fast or slow), increased photon-flux (important for photochemical reactions), increased electrode surface-to-reactor volume ratio (important for electrochemical reactions) and controlled use of highly reactive or toxic materials. Reaction parameters such as temperature, time, quantity of reagents and solvents as well as their residence time are easily maintained and reproduced in the continuous flow system. Scale-up of any given reaction can be easily achieved with minimal process development work since the basis of the flow reactor, whether in an academic or industrial setting, remain the same. The conversion of a reaction from small (academic) to large (industrial) scale is done by simply increasing the reactor volume or running several reaction cycles and recalculating the flow rate in order to maintain the same residence time.<sup>142</sup>

Another important advantage of continuous flow processes is the possibility of running multistep reaction sequences in a continuous fashion. By aligning several bench-sized flow reactors in a linear arrangement, the necessary reagents can be introduced into the reaction sequence at any point in the system at the appropriate time. The multistep continuous flow system allows for the use of liquid as well as solid-phase reagents and further developments are underway to include various purification strategies such as liquid-liquid extraction and column chromatography throughout the multistep reaction sequence.<sup>140, 143</sup>

A wide array of chemical reactions have been established using continuous flow systems.<sup>144</sup> Alkylations, acylations, cycloadditions, olefinations, transition-metal-mediated cross-coupling reactions as well as electrochemical and photochemical reactions have been performed and have often showed increased reactivity under flow conditions. Several natural products such

---

<sup>142</sup> Tucker, J. W.; Zhang, Y.; Jamison, T. F.; Stephenson, C. R. J. *Angew. Chem., Int. Ed.* **2012**, *51*, 4144.

<sup>143</sup> Hartman, R. L.; McMullen, J. P.; Jensen, K. F. *Angew. Chem., Int. Ed.* **2011**, *50*, 7502.

<sup>144</sup> a) Wegner, J.; Ceylan, S.; Kirschning, A. *Chem. Commun.* **2011**, *47*, 4583. b) Watts, P.; Haswell, S. J. *Chem. Soc. Rev.* **2005**, *34*, 235. c) Ahmed-Omer, B.; Brandt, J. C.; Wirth, T. *Org. Biomol. Chem.* **2007**, *5*, 733. d) Ehrfeld, W.; Hessel, V.; Lowe, H. *Micoreactors: New Technology for Modern Chemistry*; Wiley: 2000. e) Malet-Sanz, L.; Susanne, F. *J. Med. Chem.* **2012**, *55*, 4062. f) Ley, S. V.; Baxendale, I. R. *Nat. Rev. Drug. Discov.* **2002**, 573. g) Ley, S. V.; Baxendale, I. R.; Bream, R. N.; Jackson, P. S.; Leach, A. G.; Longbottom, D. A.; Nesi, M.; Scott, J. S.; Storer, R. I.; Taylor, S. J. *J. Chem. Soc., Perkin Trans. 1* **2000**, 3815. h) Hartman, R. L.; Jensen, K. F. *Lab Chip* **2009**, *9*, 2495.

as neolignin grossamide,<sup>145</sup> ( $\pm$ )-oxomaritidine,<sup>146</sup> pristane,<sup>147</sup> asparagine-linked oligosaccharides<sup>148</sup> and the anti-Malaria drug Artemisinin<sup>149</sup> have been synthesized using flow chemistry.<sup>141</sup> The synthetic strategy has even made its way to materials synthesis and Seeberger *et al.* predicts that the ability to run multistep reactions in flow will enable novel block copolymer synthesis as well as the production of composite capsules and fibers.<sup>150</sup>

It was reported that many reactions showed faster conversions and improved yields, particularly in the case of photochemical processes. Any photochemical transformation involves specific wavelengths of light. One of the main challenges in photoredox chemistry is maintaining an efficient photon flux in the reaction system to efficiently activate the sensitizers and thus have the desired substrate transformation. As the reaction is scaled up in a batch process, the vessel and the reaction volume increase in size. It becomes difficult to achieve an efficient light penetration throughout the system because of the Beer-Lambert law which states that the penetration of visible-light through a reaction medium decreases exponentially with increasing path length.<sup>142</sup> Certain photochemical processes have been realized on an industrial scale, however a special reaction vessel had to be constructed with the light source embedded in the centre in order to achieve a maximum photon flux. Such setups generated a large amount of heat and thus required additional cooling systems. Because batch scale-up of photochemical reactions is costly and possess a multitude of problems, such as reaction setup and overheating, other methods had to be explored to achieve the desired light-mediated transformations.

Using a continuous flow system can be an excellent alternative to the traditional batch reaction because the flow setup provides a high surface area to volume ratio due to the small depth

---

<sup>145</sup> a) Yoshihara, T.; Yamaguchi, K.; Takamatsu, S.; Sakamura, S. *Agric. Biol. Chem.* **1981**, *45*, 2593. b) Baxendale, I. R.; Griffiths-Jones, C. M.; Ley, S. V.; Tranmer, G. K. *Synlett.* **2006**, 427.

<sup>146</sup> a) Herrera, M. R.; Machocho, A. K.; Brun, R.; Viladomat, F.; Codina, C.; Bastida, J. *Planta. Med.* **2001**, *67*, 191. b) Baxendale, I. R.; Deeley, J.; Griffiths-Jones, C. M.; Ley, S. V.; Saaby, S.; Tranmer, G. *Chem. Commun.* **2006**, 2566. c) Ley, S. V.; Schucht, O.; Thomas, A. W.; Murray, P. J. *J. Chem. Soc., Perkin Trans. 1* **1999**, 1251. d) Hinzen, B.; Ley, S. V. *J. Chem. Soc., Perkin Trans 1* **1997**, 1907.

<sup>147</sup> a) Bigelow, H. B.; Schroeder, W. C. *I. Sharks Mem. Sears Found. Mar. Res.* **1948**, 189. b) Tanaka, K.; Motomatsu, S.; Koyama, K.; Tanaka, S.-I.; Fukase, K. *Org. Lett.* **2007**, *9*, 299.

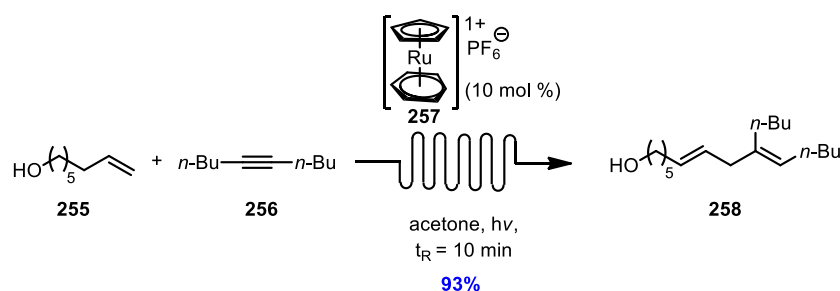
<sup>148</sup> a) Kamerling, J. P.; Boons, G.-J.; Lee, Y. C.; Suzuki, A.; Taniguchi, N.; Voragen, A. G. J. *Comprehensive Glycoscience, From Chemistry to Systems Biology*; Elsevier: Oxford, 2007, vol. 2 and 3. b) Tanaka, K.; Fukase, K. *Org. Process Res. Dev.* **2009**, *13*, 983. c) Tanaka, K.; Miyagawa, T.; Fukase, K. *Synlett*, **2009**, 1571. d) Tanaka, K.; Fujii, Y.; Tokimoto, H.; Mori, Y.; Tanaka, S.-I.; Bao, G.-M.; Siwu, E. R. O.; Nakayaba, A.; Fukase, K. *Chem. -Asian J.* **2009**, *4*, 574. e) Uchinashi, Y.; Nagasaki, M.; Zhou, J.; Tanaka, K.; Fukase, K. *Org. Biomol. Chem.* **2011**, *9*, 7243.

<sup>149</sup> Lévesque, F.; Seeberger, P. H. *Angew. Chem., Int. Ed.* **2012**, *51*, 1706.

<sup>150</sup> McQuade, D. T.; Seeberger, P. H. *J. Org. Chem.* **2013**, *78*, 6384.

of the microreactor. The setup allows for efficient and uniform irradiation of the entire system and an overall increased photon flux that can accelerate the reaction rate.<sup>146a, 151</sup> In order to adjust the reaction time of the photochemical process, the residence time of the solution must be increased by either lining up a series of microreactors or looping the system and running multiple cycles. Microstructured reactors also possess high heat transfer coefficients, thus cooling can be easily achieved. Various light sources can be used for irradiation, from standard household light-bulbs to miniature light emitting diodes (LEDs).<sup>140, 146a</sup>

Jamison and co-workers recently reported the development of continuous flow photochemistry for the UV-mediated formation of catalytically active  $[\text{CpRu}]^+$ -complexes from  $\text{CpRu}(\eta^6\text{-C}_6\text{H}_6)\text{PF}_6$ , which catalyzed ene-yne coupling reactions (Scheme 56) with recoverable Ru-sensitizer **257** in quantitative yield post reaction.<sup>152</sup>



**Scheme 56:** Jamison's UV-mediated ene-yne coupling in a continuous flow process.

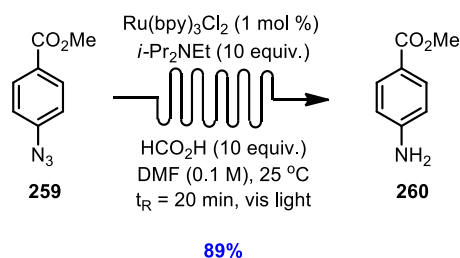
Other advances soon followed with Seeberger *et al.* who reported the application of visible-light-mediated synthetic photochemistry using a  $\text{Ru}(\text{bpy})_3\text{Cl}_2$  photocatalyst in continuous flow.<sup>153</sup> The group explored a reduction of methyl-4-azidobenzoate to the corresponding amine and observed an increase in reactivity when compared with the batch reaction (Scheme 57). The group then tested three other previously reported and synthetically useful photocatalytic transformations:

<sup>151</sup> a) Andrews, R. S.; Becker, J. J.; Gagné, M. R. *Angew. Chem., Int. Ed.* **2012**, *51*, 4140. b) Pimparkar, K.; Yen, B.; Goodell, J. R.; Martin, V. I.; Lee, W. H.; Porco, J. A.; Beeler, A. B.; Jensen, K. F. *J. Flow. Chem.* **2011**, *2*, 53. c) Elvira, K. S.; Wootton, R. C. R.; Reis, N. M.; Mackley, M. R.; deMello, A. J. *ACS Sustainable Chem. Eng.* **2013**, *1*, 209. d) Zhang, Y.; Blackman, M. L.; Leduc, A. B.; Jamison, T. F. *Angew. Chem., Int. Ed.* **2013**, *52*, 4251.

<sup>152</sup> Gutierrez, A. C.; Jamison, T. F. *Org. Lett.* **2011**, *13*, 6414.

<sup>153</sup> Bou-Hamdan, F. R.; Seeberger, P. H. *Chem. Sci.* **2012**, *3*, 1612.

tin-free reduction of activated C-Br and C-Cl bonds,<sup>154</sup> reductive opening of epoxides<sup>155</sup> and phosphine free halogenation of alcohols.<sup>156</sup> All of the reactions showed rate enhancement in flow when compared with batch reactions likely due to the increased photon flux which the flow setup provides.<sup>150, 153</sup>



**Scheme 57:** Visible-light-mediated reduction of aromatic azides.

Stephenson *et al.* reported a variety of photoredox-mediated transformations such as intermolecular radical reactions, intramolecular radical cyclizations, intramolecular heterocycle functionalization, hexenyl radical cyclization and tandem radical cyclization/Cope re-arrangement sequences. Again, accelerated reaction rates were continuously observed when compared with the batch method.<sup>157</sup>

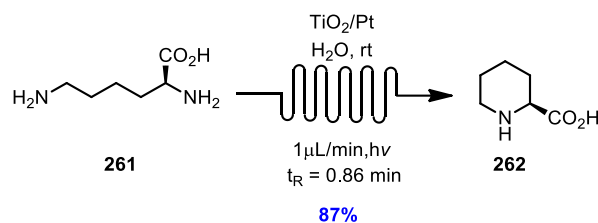
Flow photochemistry has also been used in total synthesis sequences for the formation of an important key intermediate for the divergent synthesis of *C*-glycoconjugate mimics<sup>151a</sup> as well as the synthesis of L-pipecolic acid **262** from photocatalytic degradative cyclization of L-lysine **261** (Scheme 58). In the latter example, the reaction rate in flow was 70 times higher than in the batch process and enantiomeric excess was maintained.<sup>146a</sup> In general, continuous flow chemistry makes visible-light-mediated routes an attractive means of synthesis as it lessens the environmental impact while increasing the reaction rate.<sup>151a</sup>

<sup>154</sup> Stephenson, C. R. J.; Narayanam, J. M. R.; Tucker, J. W. *J. Am. Chem. Soc.* **2009**, *131*, 8756.

<sup>155</sup> Fensterbank, L.; Larraufie, M. H.; Pellet, R.; Goddard, J. P.; Lacote, E.; Malacria, M.; Ollivier, C. *Angew. Chem., Int. Ed.* **2011**, *50*, 4463.

<sup>156</sup> Dai, C. H.; Narayanam, J. M. R.; Stephenson, C. R. J. *Nat. Chem.* **2011**, *3*, 140.

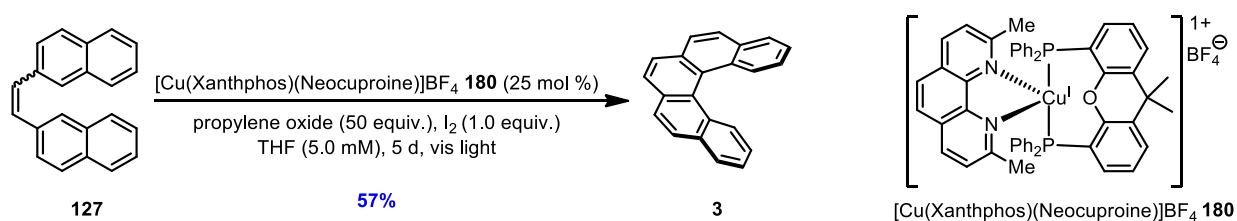
<sup>157</sup> Tucker, J. W.; Zhang, Y.; Jamison, T. F.; Stephenson, C. R. J. *Angew. Chem., Int. Ed.* **2012**, *51*, 4144.



**Scheme 58:** UV-mediated photocatalytic synthesis of L-pipecolinic acid using the continuous flow system.

### 3.2 Development of Visible-Light-Mediated Photocyclization Conditions in a Continuous Flow Process

In an effort to improve the previously established photoredox formation of helicenes and reduce the reaction time while maintaining or improving the reaction yield, the visible-light-mediated synthesis was explored in a continuous flow process. The investigation began with the model system for the formation of [5]helicene under the optimized conditions (Scheme 59).



**Scheme 59:** Optimized conditions for the batch visible-light-mediated synthesis of [5]helicenes.

The Uniqsis FlowSyn continuous flow system was employed in the development and optimization of the flow process visible-light-mediated synthesis of [5]helicene (Figure 31a). The first reactions were run using a chemically inert transparent borosilicate glass mixing block (Figure 31b).

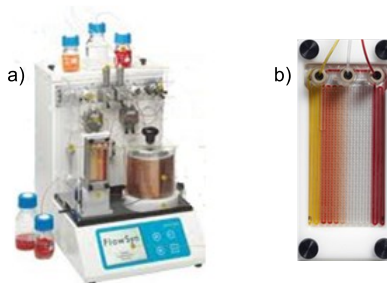


**Figure 31:** a) The Uniqsis FlowSyn Multi-X continuous flow system and b) borosilicate glass mixing block.

The initial reaction conditions were the optimized conditions for the batch process, except the concentration varied to accommodate the residence time in the continuous flow system. Table 5 shows the various reaction parameters that were explored. The residence time was calculated based on the total volume of the system multiplied by the flow rate in order to approximate the time of irradiation of a given volume travelling through the flow tubing (Figure 32).

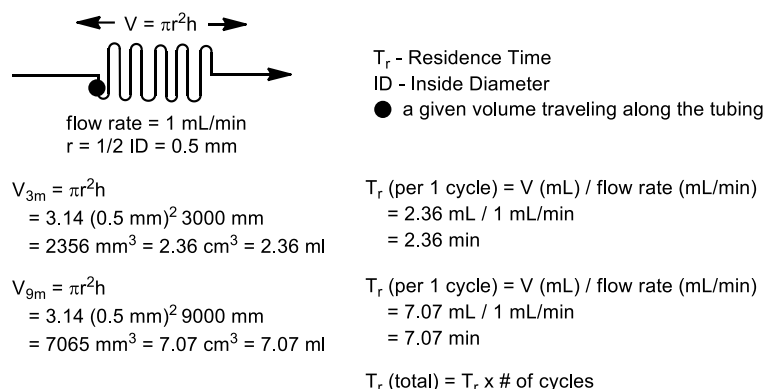
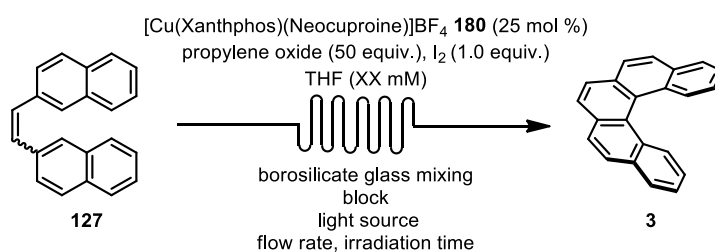


**Figure 32:** Calculation examples for volume and residence time.

Different reaction setups were tested in order to achieve optimal irradiation. Firstly, two two-pin compact fluorescent light bulbs (30 W) were attached to a regular desk lamp and the borosilicate glass mixing block was placed in-between the pins to ensure a maximal irradiation (Entries 1 and 2). The reaction solution was pumped through the mixing block at a flow rate of 1 mL/min. The reaction was performed for several cycles of 6 h each and after 4 and 5 cycles, 9.4 min and 11.8 min residence time respectively, yields of 20% to 24% were obtained with recovery

of *cis* and *trans* isomers of the starting material (Entries 1 and 2). The formation of the desired product was followed by NMR and a reactivity plateau, with no further conversion of starting material to product, was seen after the 3<sup>rd</sup> cycle of 6 h, 7.1 min residence time. Overall, it was very encouraging to see the conversion of starting material to the desired product after only 7.1 minutes of residence time or 18 h overall reaction time at a concentration of 0.4 mM, a significant improvement from the 120 h reaction time required for the batch process. Unfortunately, the yield of 20% could not be surpassed under the given conditions, therefore alternative light sources were explored in an effort to improve the reactivity.

**Table 5:** Optimization of reaction parameters for the formation of [5]helicene using a borosilicate glass mixing block and various sources of light in a continuous flow process.



Entry	Light Source	Concentration (mM)	Flow Rate	Reaction Time (cycles)	Residence Time (t <sub>R</sub> ) (min)	Yield
1	Lamp	0.4	1 mL/min	24 h (4 x 6 h)	9.4	20% <sup>a</sup>
2	Lamp	0.4	1 mL/min	30 h (5 x 6 h)	11.8	24% <sup>a</sup>
3	Blue LED	0.4	1 mL/min	18 h (3 x 6 h)	7.1	0% <sup>a</sup>
4	White LED	0.4	1 mL/min	18 h (3 x 6 h)	7.1	3% <sup>b</sup>
5	UV	0.1	2 mL/min	15 h (1 x 15h)	1.2	0% <sup>b</sup>

<sup>a</sup>*Cis* and *trans* starting material recovered. <sup>b</sup> *Cis* starting material recovered.

In an effort to investigate various light sources, blue and white light-emitting diodes (LEDs) were used (Entries 3 and 4). The reaction solution at a concentration of 0.4 mM was passed through the mixing block in 3 cycles of irradiation of 6 h each, a 7.1 min residence time. No desired product was observed with the blue LED and *cis* and *trans* isomers of the starting material were recovered (Entry 3). Only traces of the desired product were observed using the white LED with



recovered *cis* starting material (Entry 4). A UV lamp ( $\lambda = 190 - 400$  nm) was also used as a light source, unfortunately after 15 h of reaction time, 1.2 min residence time, no desired product was observed and only the *cis* starting material was recovered (Entry 6). Unfortunately, changing the light source led to much lower reaction yields.



**Figure 33:** Fluorinated ethylene propylene tubing.

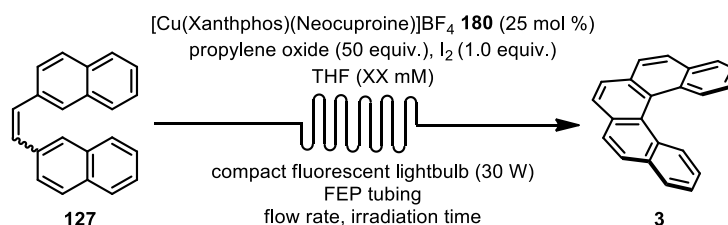
Varying the light source led to a significant decrease in reactivity when compared with the compact fluorescent light (30 W) which led to a yield of 24%. It was suspected that perhaps the problem lay within the reaction medium as the borosilicate glass mixing block could be hindering maximal photon flux. The fluorinated ethylene propylene (FEP) tubing (Figure 33) purchased from IDEX Health & Science (#1673) of natural colour with an outside diameter (OD) of 2 mm and inside diameter (ID) of 1 mm was proposed as an alternative reaction medium. The material was low friction and non-reactive as well as heat resistant and highly transparent, characteristics important for photochemical reactions.<sup>158</sup> It was also successfully used by Seeberger *et al.* in various photochemical reactions.<sup>153</sup>

---

<sup>158</sup> IDEX Health & Science.

<http://www.idexhs.com/products/870/FEPTubing.aspx?ProductTypeID=1&ProductFamilyID=5> (accessed May 25, 2014).

**Table 6:** Optimization of the reaction parameters for the formation of [5]helicene using FEP-Teflon tubing and a compact fluorescent energy-saving light bulb (30 W).



Entry	Concentration (mM)	Flow Rate	Reaction Time (cycles)	Residence Time (t <sub>R</sub> ) (min)	Yield
1	0.4	1 mL/min	18 h (3 x 6 h)	7.1	40% <sup>a, c</sup>
2	5	1 mL/min	1.5 h (3 x 30 min)	7.1	8% <sup>a, c</sup>
3	5	1 mL/min	18 h (36 x 30 min)	85	39% <sup>a, c</sup>
4	5	1 mL/min	19.5 h (39 x 30 min)	92	23% <sup>a, d</sup>
5	5	1 mL/min	18 h (12 x 90 min)	85	32% <sup>a, e</sup>
6	5	1 mL/min	18 h (36 x 30 min)	85	31% <sup>a, f</sup>

<sup>a</sup> *Cis* and *trans* starting material recovered. <sup>b</sup> *Cis* starting material recovered. <sup>c</sup> Tubing wrapped between two metal poles with light sources in the middle, some heating observed. <sup>d</sup> 3 m of tubing wrapped around a glass test-tube and irradiated by light bulbs, minimal heating observed. <sup>e</sup> 9 m of tubing wrapped around 3 glass test-tubes and irradiated by light bulbs, minimal heating observed. <sup>f</sup> 3 m of tubing wrapped around the light bulb, significant heating observed.

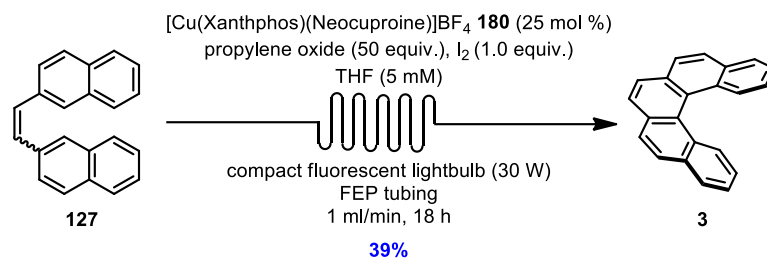
The investigation of the visible-light-mediated synthesis of [5]helicene in a continuous flow process using FEP tubing involved various reaction setups (Table 6). Initially, 3 meters of tubing was wrapped between two metal rods and three compact fluorescent energy-saving light bulbs (30 W) were placed in the center. The inlet tube and the outlet tubes were put in the same round bottom flask with the reaction solution in complete darkness. Such a “closed” reaction cycle allowed for the solution to run continuously for a given amount of time. The first reaction was run at the more dilute concentration of 0.4 mM, when compared with the batch synthesis concentration of 5 mM, and after 18 h, 7.1 min residence time, a yield of 40% was observed (Entry 1) with recovery of *cis* and *trans* isomers of the starting material. Mild heating of the tubing was noted where it was closest to the light source. The yield obtained, 40%, after only 18 h reaction time was getting closer to the 57% optimal yield, obtained after 120 h of irradiation, of the batch process. The FEP reaction medium was also better suited for photochemical reactions than the borosilicate

glass mixing tube as it provided almost double the yield observed with the mixing block, 24% versus 40%.

The reaction concentration was increased to 5 mM, which significantly decreased the reaction volume which in turn diminished the reaction time from 18 h to 1.5 h in order to maintain the same residence time and flow rate. After 1.5 h of reaction time, 7.1 min residence time, a yield of only 8% was observed with recovered *cis* and *trans* isomers of the starting material (Entry 2). Increasing the reaction time from 1.5 h to 18 h, a residence time increase from 7.1 to 85 min, afforded a yield of 39% which nearly matched the 40% obtained at the lower reaction concentration of 0.4 mM (Entry 3).

Another reaction setup was explored where 3 m of the FEP tubing was wrapped around a glass test tube, which allowed for a larger amount of tubing to be irradiated by the light source with minimal heating observed. After 19.5 h of reaction time, 92 min residence time, a yield of 23% was observed (Entry 4). Another setup was tried, where the length of the tubing was increased from 3 to 9 m, thus increasing the length of each cycle. The setup yielded 32% of the desired product, with recovered starting material after 18 h of reaction time, 85 min residence time (Entry 5). Unfortunately, increasing the length of the tubing from 3 to 9 m did not provide a significant increase in the reaction yield.

In an effort to further improve the yield and achieve maximum irradiation, 3 m of FEP tubing was wrapped directly around an energy-saving compact fluorescent light bulb (30 W). After 18 h of reaction time, 85 min residence time, a yield of 31% was observed along with recovered starting material (Entry 6). Significant heating of the tubing was also noted, however when a control batch reaction was run and heated to a temperature of 45 °C, no increase of the yield was seen, therefore it was concluded that heating had no significant effect on the reactivity of the process.



**Scheme 60:** Optimized conditions for the formation of [5]helicene in a continuous flow system.

After numerous optimization efforts, the best conditions for the first generation visible-light-mediated formation of [5]helicene using FEP tubing in a continuous flow process were 25 mol % of the Cu-based photosensitizer, formed *in situ*, 1 equivalent of iodine, 50 equivalents of propylene oxide and a concentration of 5 mM with THF as solvent. The optimal flow rate was 1 mL/min and the reaction time was 18 h, 85 min residence time. Under these conditions, a yield of 39% was obtained (Scheme 60). Although the yield is slightly lower than that of the batch reaction, 39% versus 57%, the significant reduction in the reaction time makes the flow synthesis a very attractive alternative to the batch formation of [5]helicenes. A scale-up of [5]helicene was also attempted in flow, where 3 g of the stilbene-type precursor was converted to the desired [5]helicene in 25% yield after a 70 h reaction time. Although, it is a 17% decrease from the yield of 42% obtained in the batch synthesis, the reaction is run in about half the time and the starting material could be recycled and re-run to obtain more of the desired [5]helicene.

### 3.3 Application of the Optimized Visible-Light-Mediated Conditions in Flow to the Synthesis of Pyrene-Helicene Derivatives

As a significant improvement in the overall reactivity for the synthesis of [5]helicene in a continuous flow process was observed, the synthetic strategy was also applied to the photocyclization of the three pyrene-helicene derivatives which demonstrated low to moderate yields under batch conditions.

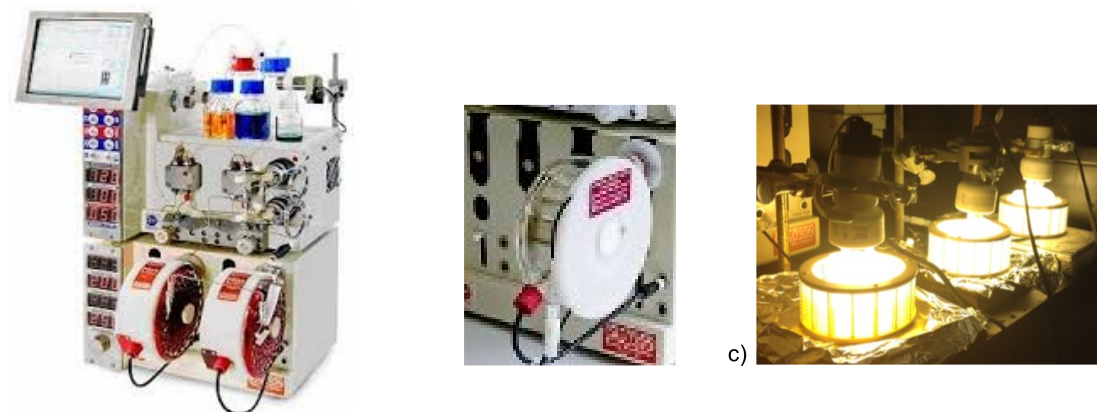


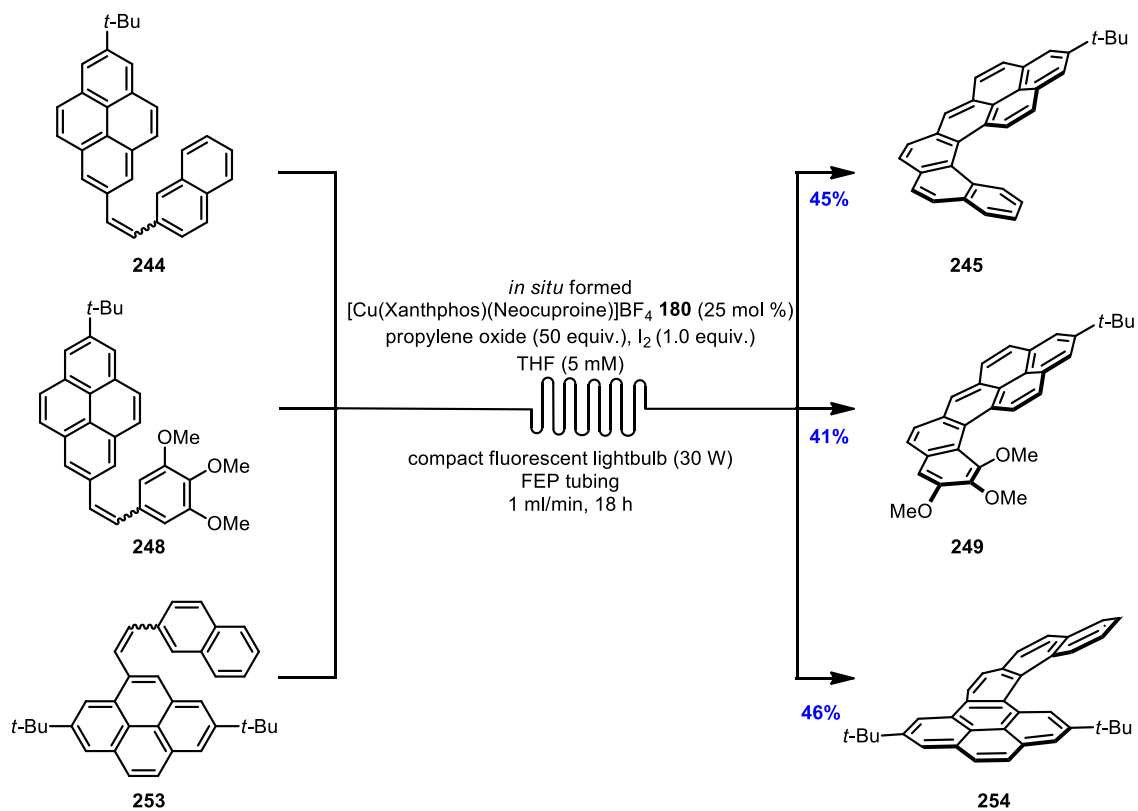
**Figure 34:** a) Vapourtec R-Series continuous flow system, b) standard PFA coiled tube reactor and c) the irradiation setup.

The first substrate tested in collaboration with Anne-Catherine Bédard was the pyrene-naphthyl stilbene precursor **244**. Using the *in situ* procedure for the formation of the Cu-based sensitizer, the reaction system was submitted to the optimized continuous flow setup which provided the desired product **245** in 45% yield after only 18 h of reaction time, 85 min residence time. Therefore, in about one tenth of the reaction time, the batch yield of 23% was almost doubled under the flow conditions (Scheme 61).

A novel continuous flow system was used – the Vapourtec R4 reactor with an R2+ pumping module<sup>159</sup> for the synthesis of the trimethoxy-substituted pyrene-[4]helicene derivative **249**, done by Augusto Hernandez-Perez. The flow reactor contained two pumping channels along with two continuously monitored HPLC pumps (Figure 34). The FEP tubing was looped around the plastic reactor ring and a compact fluorescent light bulb (30 W) was placed in the center of each ring (Figure 34b and c). The system was a significant improvement from the 1<sup>st</sup> generation Uniqsis FlowSyn reactor used in the optimization of [5]helicene and the formation of pyrene[5]helicene **245**. The synthesis of the Cu-based sensitizer was performed using the *in situ* protocol for the formation of pyrene-helicene substrate **249**. After 18 h of reaction time, 85 min residence time, the desired product was obtained in 41% yield, a fourfold increase from the batch yield of 12% (Scheme 61). Finally, the pyrene-helicene stilbene-type substrate **253**, synthesized by Anne-

<sup>159</sup> Vapourtec – The R-Series Integrated Flow Chemistry System. <http://www.vapourtec.co.uk/products/rseriessystem> (accessed June 24, 2014).

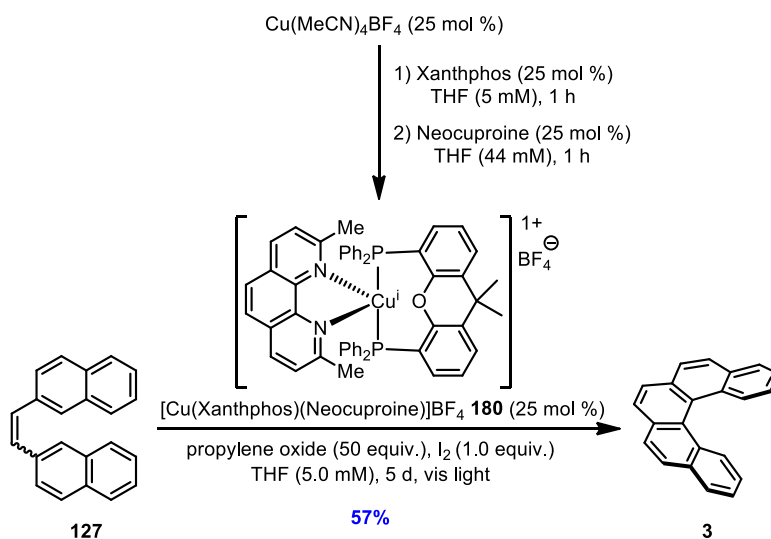
Catherine Bédard, also showed improved reactivity under continuous flow conditions with *in situ* generated Cu-sensitizer. After 18 h of reaction time, 85 min of residence time, a yield of 46% was obtained, which is about a twofold improvement from the batch yield of 27% (Scheme 61).



**Scheme 61:** Formation of various pyrene-helicenes in a continuous flow process.

## CHAPTER 4: CONCLUSION AND FUTURE WORK

A visible-light-mediated photoredox-based synthesis of various helical molecules was developed. The formation of [5]helicene was used as a model system and after a rigorous screening, the sensitizer, solvent, oxidant system and reaction time were optimized. An *in situ* protocol for the formation of Cu-based sensitizers was also developed, where the sequential addition of the phosphine and the diamine ligand to a solution of  $\text{Cu}(\text{MeCN})_4\text{BF}_4$  in THF led to the formation of the desired sensitizer complex which was used directly in the photocyclization reaction without isolation or purification. The optimal catalyst system for the visible-light-mediated synthesis of helicenes was  $[\text{Cu}(\text{Xanthphos})(\text{Neocuproine})]\text{BF}_4$  with THF as solvent and an oxidant system of stoichiometric iodine and an excess of propylene oxide. The conditions afforded [5]helicene **3** in 57% yield with recovered *cis* and *trans* isomers of the starting material (Scheme 62). No overoxidation of [5]helicene to benzo[*ghi*]perylene **13**, the main product in UV-light-mediated photocyclization towards [5]helicene, was observed. Also, no product resulting from [2+2] intermolecular cycloaddition of **127** was detected. The reaction concentration was 5 mM, an increase over the traditional UV reaction concentration of 0.2 mM. A scale-up synthesis of [5]helicene, previously a challenge due to the high dilution required under UV conditions, was performed using the visible-light-mediated method and desired product **3** was obtained in 42% yield with recovered *cis* and *trans* isomers of the starting material.



**Scheme 62:** Visible-light-mediated synthesis of [5]helicenes in a batch process with *in situ* formation of the Cu-based sensitizer.

Preliminary mechanistic studies were carried out to elucidate the reaction mechanism, where an electron-poor and an electron-rich stilbene-type precursor were submitted to the photocyclization conditions. Only the electron-rich substrate cyclized which supported the theory that the reaction followed an oxidative pathway, where upon excitation with visible-light the Cu(I)\* species reduces I<sub>2</sub> via an SET process. The generated Cu(II) complex could oxidize stilbene precursor **127** which in turn undergoes a cyclization and a series of oxidations to afford desired [5]helicene **3** (Figure 35).

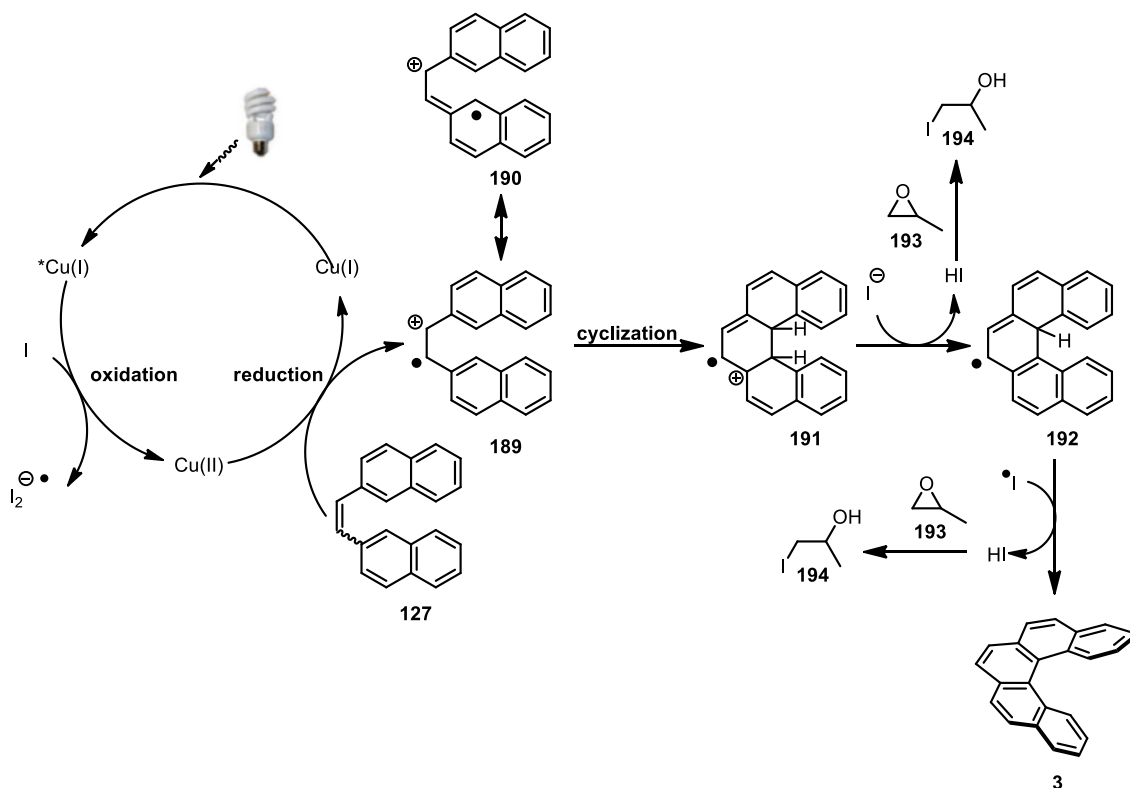
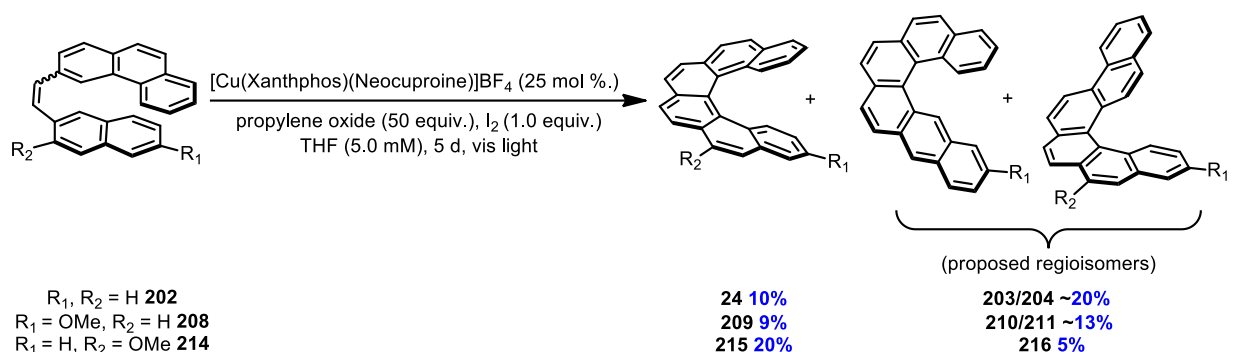


**Figure 35:** The proposed oxidative mechanism for the formation of [5]helicene.

The novel conditions for the visible-light-mediated synthesis of [5]helicene were applied to the synthesis of [6]helicenes. The photocyclization of unsubstituted and 6-methoxy stilbene-type precursors **202** and **208** provided a mixture of several regioisomers, including desired [6]helicene products **24** and **209**, inseparable by flash chromatography, in an overall yield of 30% and 22% respectively with recovered *cis* and *trans* isomers of the starting material (Scheme 63). To prevent the formation of multiple regioisomers, one of the potential cyclization sites was blocked with a methoxy substituent. The strategy provided desired substituted [6]helicene **215** in



a yield of 20% with traces of another regioisomer (5%) and recovered *cis* and *trans* isomers of the starting material (Scheme 63).



**Scheme 63:** Visible-light-mediated synthesis of [6]helicene and its methoxy derivatives.

The newly developed visible-light-mediated photocyclization conditions were also applied to the synthesis of thioheterohelicenes. The initial exploration began with attempts to cyclize dithiophene and styrylthiophene compounds **225**, **226** and **227**, unreactive substrates under the traditional UV-light-mediated cyclization conditions. Unfortunately, the novel visible-light-mediated method also failed to provide the desired products. Expanding the helical backbone to phenanthro[3,4-b]thiophene proved successful and desired product **229** was obtained in 26% yield with recovered *cis* and *trans* isomers of the starting material (Figure 36).

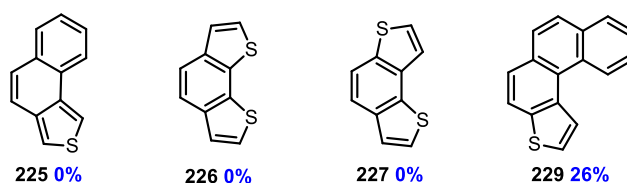


**Figure 36:** Visible-light-mediated formation of thiohelicenes.

The expansion of the  $\pi$  surface of the helical backbone was explored by fusing a pyrene moiety with a [4]- and [5]helicene skeleton. The main synthetic challenge of the multistep synthesis of the pyrene-containing stilbene-type precursors **244**, **248** and **254** was installing a carbon substituent at positions 2, 7 and 5 of the pyrene moiety. The goal was achieved through the use of sterically bulky alkyl groups, which improved the overall solubility of the product, or boronate groups, which were further transformed to the desired substituent. Desired cyclization

precursors **244**, **248** and **254** were obtained in seven to eight synthetic steps and were cyclized under the optimized visible-light-mediated conditions to provide desired pyrene-helicene products **245**, **249**, and **254** in 23%, 12% and 27% respectively with recovered *cis* and *trans* isomers of the starting material (Figure 37).

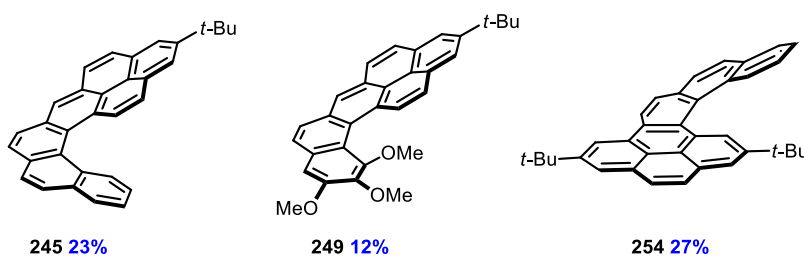
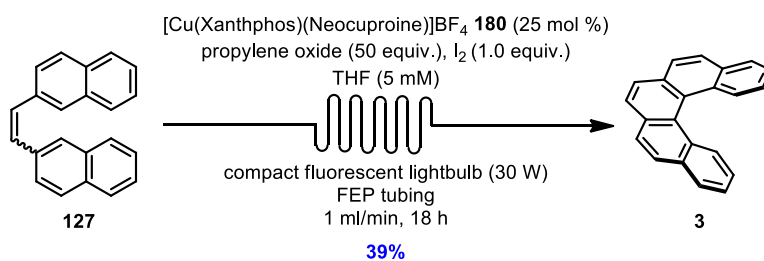


**Figure 37:** Visible-light-mediated formation of pyrene-helicenes.

In a continued effort to further develop the visible-light-mediated photocyclization of helicenes, a continuous flow process was explored as an alternative to the traditional batch method. The optimized batch conditions were applied to the flow process and after screening various light sources, reaction media and flow rate, the best setup was established (Scheme 64). A compact fluorescent light bulb (30 W) irradiating a reaction running through FEP tubing at a flow rate of 1 mL/min provided a yield of 39% which is close to the batch yield of 57%.



**Scheme 64:** Optimized conditions for the formation of [5]helicene in a continuous flow system.

The newly developed continuous flow process was applied to the photocyclization of the pyrene-helicene compounds **245**, **249** and **254**. In all cases the yields were doubled from about 20% in batch to approximately 40% in flow (Figure 38). Also, the reaction time was decreased from 120 h in the batch method to 18 h in flow. Overall the continuous flow process afforded a

more efficient photocyclization of helicenes in one tenth of the reaction time required for the batch method.

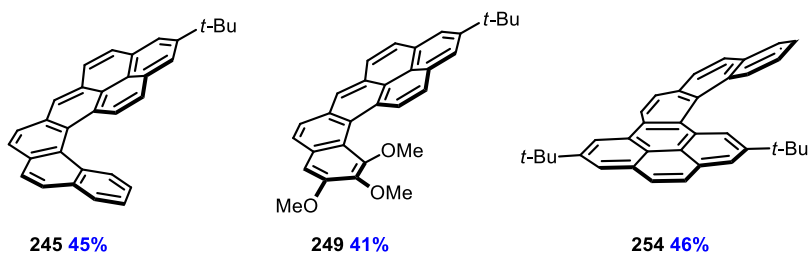


**Figure 38:** Photocyclization of pyrene-helicene derivatives under continuous flow conditions.

Future work will focus on more in-depth mechanistic studies to confirm the proposed oxidation mechanism. The effect of adding excess iodine will be explored as well as radical traps could be employed in an effort to isolate intermediate species. Molecules which displayed lower yields in the batch process such as [6]helicenes and thiohelicenes will be subjected to the optimized continuous flow conditions for the visible-light-mediated formation of helicenes in an effort to improve the reaction yields. Photocyclization of other classes of molecules, such as carbazoles, will be explored and other metal-based sensitizers, such as  $[\text{Fe}(\text{phen})_3](\text{NTf}_2)_2$ , will be investigated in an effort to replace the copper catalyst and iodine oxidant.

## CHAPTER 5: EXPERIMENTAL SECTION

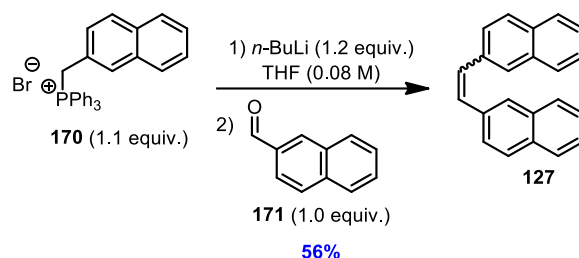
### General:

All reactions that were carried out under anhydrous conditions were performed under an inert nitrogen atmosphere in glassware that had previously been dried overnight at 120 °C or had been flame dried and cooled under a stream of nitrogen.<sup>160</sup> All chemical products were obtained from Sigma-Aldrich Chemical Company or Strem Chemicals and were reagent quality. Technical solvents were obtained from VWR International Co. Anhydrous solvents (DCM, Et<sub>2</sub>O, THF, DMF, Toluene, and *n*-hexane) were dried and deoxygenated using a GlassContour system (Irvine, CA). Isolated yields reflect the mass obtained following flash column silica gel chromatography. Organic compounds were purified using the method reported by W. C. Still<sup>161</sup> and using silica gel obtained from Silicycle Chemical division (40-63 nm; 230-240 mesh). Analytical thin-layer chromatography (TLC) was performed on glass-backed silica gel 60 coated with a fluorescence indicator (Silicycle Chemical division, 0.25 mm, F<sub>254</sub>). Visualization of TLC plate was performed by UV (254 nm), KMnO<sub>4</sub> or *p*-anisaldehyde stains. All mixed solvent eluents are reported as v/v solutions. Concentration refers to removal of volatiles at low pressure on a rotary evaporator. All reported compounds were homogeneous by thin layer chromatography (TLC) and by <sup>1</sup>H NMR. NMR spectra were taken in CDCl<sub>3</sub> using Bruker AV-300 and AV-400 instruments unless otherwise noted. Signals due to the solvent served as the internal standard (CHCl<sub>3</sub>: δ 7.26 for <sup>1</sup>H, δ 77.16 for <sup>13</sup>C). The acquisition parameters are shown on all spectra. The <sup>1</sup>H NMR chemical shifts and coupling constants were determined assuming first-order behaviour. Multiplicity is indicated by one or more of the following: s (singlet), d (doublet), t (triplet), q (quartet), m (multiplet), br (broad); the list of couplings constants (*J*) corresponds to the order of the multiplicity assignment. High resolution mass spectroscopy (HRMS) was done by the Centre Régional de Spectrométrie de Masse at the Département de Chimie, Université de Montréal from an Agilent LC-MSD TOF system using ESI mode of ionization unless otherwise noted.

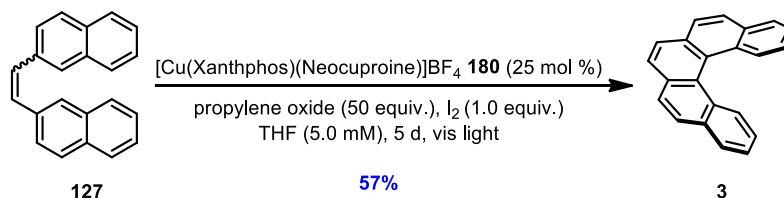
---

<sup>160</sup> Shriver, D. F.; Drezdon, M. A. in *The Manipulation of Air-Sensitive Compounds*; Wiley-VCH: New York, 1986.

<sup>161</sup> Still, W. C.; Kahn, M.; Mitra, A. *J. Org. Chem.* **1978**, *43*, 2923.



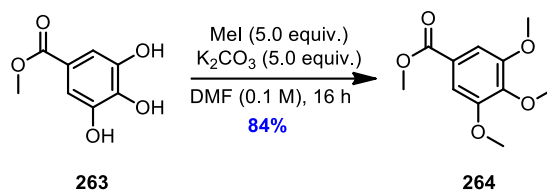
**1,2-Di(naphthalen-2-yl)ethene (127):** Freshly titrated *n*-BuLi (3.7 mL, 7.4 mmol, 1.2 equiv.) was added dropwise to a solution of (naphthalen-2-ylmethyl)triphenylphosphonium bromide (3.4 g, 7.0 mmol, 1.1 equiv.) in anhydrous THF (80 mL, 0.08 M) at 0 °C under N<sub>2</sub>. The resulting yellow mixture was stirred for 1 h at 0 °C and then 2-naphthaldehyde (1.0 g, 6.4 mmol, 1.0 equiv.), pre-dissolved in 1.0 ml of anhydrous THF, was added at 0 °C and the resulting red solution was warmed up to room temperature and stirred for 18 h. Brine was added to the reaction mixture and the aqueous and organic phases were separated. The aqueous phase was extracted with EtOAc (3 times) and the combined organic phases were washed with brine, dried over Na<sub>2</sub>SO<sub>4</sub>, filtered and concentrated. The crude mixture was purified by column chromatography (100% hexanes) to afford the desired product **127** as a white solid (1.0 g, 56%). <sup>1</sup>H NMR spectrum corresponds to the literature.<sup>162</sup>



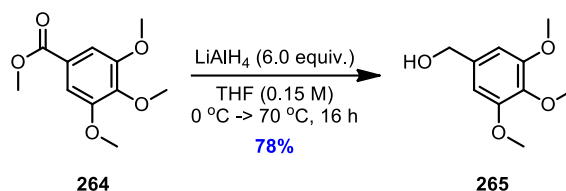
**[5]Helicene via Batch Reaction (3):** [Cu(NCCH<sub>3</sub>)<sub>4</sub>]BF<sub>4</sub><sup>163</sup> (9.3 mg, 0.04 mmol, 0.25 equiv.) and Xantphos (21 mg, 0.04 mmol, 0.25 equiv.) were dissolved in THF (7.4 mL, 5.0 mM) in a round bottom flask equipped with a stir bar. The solution was stirred at room temperature for 1 h and a solution of Neocuproine (7.7 mg, 0.04 mmol, 0.25 equiv.) in THF (10 mL, 4.0 mM) was added. The resulting mixture was stirred for 1 h, added to a round bottom flask containing 1,2-di(naphthalen-2-yl)ethane **127** (41 mg, 0.15 mmol, 1.0 equiv.) and diluted with THF to achieve a final concentration of 5.0 mM with respect to **127**. Iodine (39 mg, 0.15 mmol, 1.0 equiv.) and propylene oxide (0.54 mL, 7.3 mmol, 50 equiv.) were added and the reaction stirred in front of a compact fluorescent light bulb (30 W) for 5 days. The reaction was quenched with Na<sub>2</sub>S<sub>2</sub>O<sub>3</sub> (sat.) (30 mL) and diluted with EtOAc. The phases were separated and the aqueous layer was washed with EtOAc (3 times). The combined organic layers were washed with brine, dried over Na<sub>2</sub>SO<sub>4</sub>, filtered and concentrated. The crude product was purified by flash chromatography (2% to 8% toluene/hexanes) to give the desired product as a white solid (23 mg, 57%). <sup>1</sup>H NMR spectrum corresponds to the literature.<sup>135</sup>

<sup>162</sup> Maya, A. B. S.; Perez-Melero, C.; Mateo, C.; Alonso, D.; Fernandez, J. L.; Gajate, C.; Mollinedo, F.; Pelaez, R.; Caballero, E.; Medarde, M. *J. Med. Chem.* **2005**, *48*, 556.

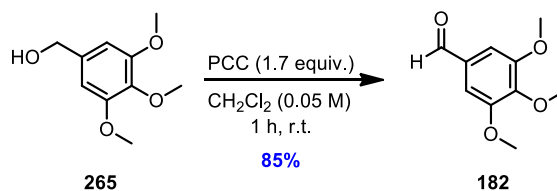
<sup>163</sup> Tang, X.; Woodward, S.; Krause, N. *Eur. J. Org. Chem.* **2009**, *17*, 2836.



**Methyl 3,4,5-Trimethoxybenzoate (264):** Methyl 3,4,5-trihydroxybenzoate (0.50 g, 2.7 mmol, 1.0 equiv.), methyl iodide (0.85 mL, 14 mmol, 5.0 equiv.) and potassium carbonate (1.9 g, 14 mmol, 5.0 equiv.) were added to a round bottom flask, dissolved in DMF (14 mL, 0.20 M) and left to stir overnight. Upon completion, the reaction was filtered through a Fisherbrand P8-creped coarse filter paper and the organic phase was extracted with EtOAc (3 times). The combined organic extracts were washed with brine, dried with Na<sub>2</sub>SO<sub>4</sub> and concentrated under reduced pressure. A flash chromatography purification (20% to 50% EtOAc/hexanes) afforded desired product **264** as a white solid (0.52 g, 85%). <sup>1</sup>H NMR spectrum corresponds to the literature.<sup>164</sup>



**(3,4,5-Trimethoxyphenyl)methanol (265):** Lithium aluminium hydride (0.40 mg, 11 mmol, 6.0 equiv.) was suspended in anhydrous THF (12 mL, 0.15 M) in a dry round bottom flask under N<sub>2</sub>. The reaction mixture was cooled to 0 °C and methyl 3,4,5-trimethoxybenzoate **264** (0.47 g, 2.1 mmol, 1.0 equiv.) was added. The reaction was left to stir at 0 °C for 30 min and then heated to 70 °C for 16 h. Upon complete consumption of ester **264**, the reaction was cooled to 0 °C and slowly quenched with 10% NaOH and H<sub>2</sub>O. An excess of Rochelle's salt was then added and the mixture was left to stir overnight. The reaction was diluted with EtOAc and the phases separated. The aqueous phase was washed with EtOAc (3 times) and the combined organic extracts were washed with brine and dried with Na<sub>2</sub>SO<sub>4</sub>. Following filtration, the organic phase was concentrated under reduced pressure and purified by flash column chromatography (100% hexanes to 30% EtOAc/hexanes) to afford **265** as a white solid. (0.32 g, 78%). <sup>1</sup>H NMR spectrum corresponds to the literature.<sup>165</sup>

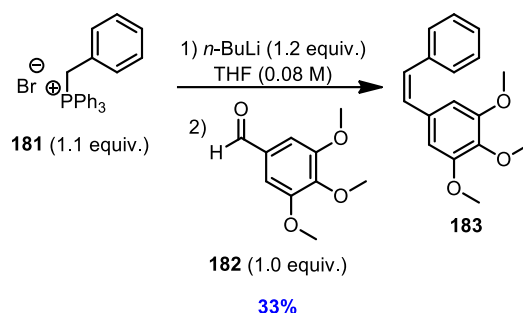


**3,4,5-Trimethoxybenzaldehyde (182):** (3,4,5-Trimethoxyphenyl)methanol (0.30 g, 1.5 mmol, 1.0 equiv.) was dissolved in DCM (30 mL, 0.05 M) in a round bottom flask. Pyridinium

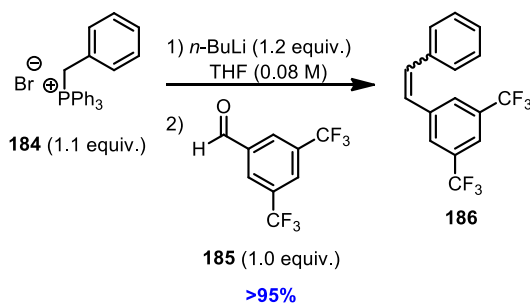
<sup>164</sup> Keck, G. E.; McLaws, M. D.; Wager, T. T. *Tetrahedron* **2000**, *56*, 9875.

<sup>165</sup> Odlo, K.; Fournier-Dit-Chabert, J.; Ducki, S.; Gani, O. A. B. S. Sylte, I.; Hansen, T. V. *Bioorg. & Med. Chem.* **2010**, *18*, 6874.

chlorochromate (0.56 g, 2.6 mmol, 1.7 equiv.) was added to the solution and the reaction mixture was left to stir for 1 h at room temperature. The reaction was diluted with Et<sub>2</sub>O and about 20 mg of silica gel were added. The mixture was filtered through a pad of silica gel and the pad was washed with Et<sub>2</sub>O. The filtrate was concentrated and the desired product **182** isolated as a beige solid. (0.25 g, 85%). <sup>1</sup>H NMR spectrum corresponds to the literature.<sup>166</sup>



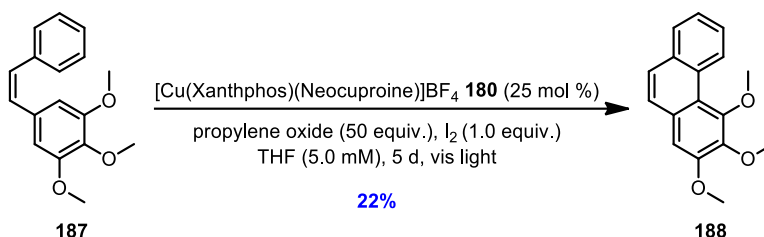
**1,2,3-Trimethoxy-5-styrylbenzene (183):** Freshly titrated *n*-BuLi (1.6 mL, 1.2 mmol, 1.2 equiv.) was added dropwise to a solution of benzyltriphenylphosphonium bromide (0.49 g, 1.1 mmol, 1.1 equiv.) in anhydrous THF (13 mL, 0.08 M) at 0 °C under N<sub>2</sub>. The resulting yellow mixture was stirred for 1 h at 0 °C and then 3,4,5-trimethoxybenzaldehyde **182** (0.20 g, 1.0 mmol, 1.0 equiv.), pre-dissolved in 1 ml of anhydrous THF, was added at 0 °C and the resulting red solution was slowly warmed up to room temperature and stirred for 18 h. Brine was added to the reaction mixture and the aqueous and organic phases were separated. The aqueous phase was extracted with EtOAc (3 times) and the combined organic phases were washed with brine, dried over Na<sub>2</sub>SO<sub>4</sub>, filtered and concentrated *in vacuo*. The crude mixture was purified by column chromatography (100% hexanes to 10% ethyl acetate/hexanes) to afford product **183** as a single isomer as an off-white solid (94 mg, 33%). <sup>1</sup>H NMR (300 MHz, CDCl<sub>3</sub>) δ ppm 7.52 (d, *J* = 7.2 Hz, 2 H), 7.37 (t, *J* = 7.8 Hz, 2 H), 7.27 (t, *J* = 7.4 Hz, 1 H), 7.03 (d, *J* = 2.8 Hz, 2 H), 6.75 (s, 2 H), 3.93 (s, 6 H), 3.88 (s, 3 H). <sup>13</sup>C NMR (75 MHz, CDCl<sub>3</sub>) δ ppm 153.4, 138.0, 137.2, 133.1, 128.7, 128.6, 128.2, 127.6, 126.4, 103.6, 60.9, 56.1. HRMS (ESI+) for C<sub>17</sub>H<sub>19</sub>O<sub>3</sub> [M + H]<sup>+</sup> calculated: 271.1329, found: 271.1333.



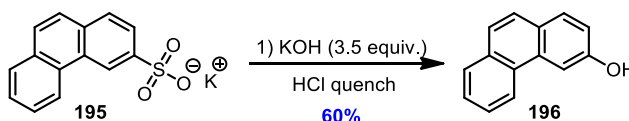
**1,3-bis(trifluoromethyl)-5-styrylbenzene (186):** Freshly titrated *n*-BuLi (1.8 mL, 2.38 mmol, 1.2 equiv.) was added dropwise to a solution of benzyltriphenylphosphonium bromide (0.99 g, 2.3 mmol, 1.1 equiv.) in anhydrous THF (26 mL, 0.08 M) at 0 °C under N<sub>2</sub>. The resulting yellow mixture was stirred for 1 h at 0 °C and then 3,5-bis(trifluoromethyl)benzaldehyde (0.34 mL, 2.1

<sup>166</sup> Wang, L.; Li, J.; Yang, H.; Lv Y.; Gao, S. *J. Org. Chem.* **2012**, *77*, 790.

mmol, 1.0 equiv.), pre-dissolved in 1 ml of anhydrous THF, was added at 0 °C and the resulting red solution was slowly warmed up to room temperature and stirred for 18 h. Brine was added to the reaction mixture and the aqueous and organic phases were separated. The aqueous phase was extracted with EtOAc (3 times) and the combined organic phases were washed with brine, dried over Na<sub>2</sub>SO<sub>4</sub>, filtered and concentrated *in vacuo*. The crude mixture was purified by column chromatography (100% hexanes to 10% ethyl acetate/hexanes) to afford product **186** as a mixture of *cis* and *trans* isomers as a clear solid (675.4 mg, > 99%). <sup>1</sup>H NMR (300 MHz, CDCl<sub>3</sub>) δ ppm 7.94 (s, 10H), 7.75 (d, *J* = 26.4 Hz, 2H), 7.68 (s, 2H), 7.57 (d, *J* = 7.2 Hz, 1H), 7.49 – 7.34 (m, 16H), 7.33 – 7.19 (m, 42H), 7.14 (d, *J* = 16.3 Hz, 1H), 6.87 (d, *J* = 12.1 Hz, 7H), 6.61 (d, *J* = 12.2 Hz, 7H). <sup>13</sup>C NMR (75 MHz, CDCl<sub>3</sub>) δ ppm 139.5, 139.2, 136.0, 135.7, 133.9, 132.5, 132.2, 131.9, 131.7, 131.3, 129.0, 129.0, 128.9, 128.8, 128.6, 128.6, 128.1, 127.8, 127.0, 126.9, 126.2, 126.1, 125.5, 124.8, 124.6, 122.0, 121.9, 120.8, 120.8, 120.6, 120.6, 120.6. <sup>19</sup>F NMR (376 MHz, CDCl<sub>3</sub>) δ ppm -63.1, -63.2.



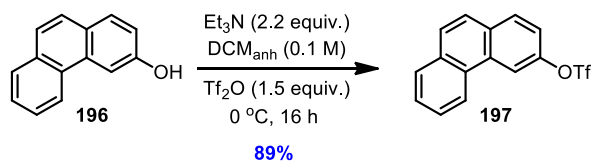
**2,3,4-Trimethoxyphenanthrene (188):** [Cu(NCCH<sub>3</sub>)<sub>4</sub>]BF<sub>4</sub><sup>163</sup> (12 mg, 0.04 mmol, 0.25 equiv.) and Xantphos (22 mg, 0.04 mmol, 0.25 equiv.) were dissolved in THF (8.0 mL, 5.0 mM) in a round bottom flask. The solution was allowed to stir at room temperature for 1 h and a solution of Neocuproine (8.1 mg, 0.04 mmol, 0.25 equiv.) in THF (10 mL, 4.0 mM) was added. The resulting mixture was stirred for 1 h, added to a round bottom flask containing 1,2,3-trimethoxy-5-styrylbenzene **187** (24 mg, 0.16 mmol, 1.0 equiv.) and diluted in THF to achieve a final concentration of 5.0 mM with respect to **187**. Iodine (39 mg, 0.16 mmol, 1.0 equiv.) and propylene oxide (0.54 mL, 7.8 mmol, 50 equiv.) were added and the reaction stirred in front of a compact fluorescent light bulb (30 W) for 5 days. The reaction was quenched with Na<sub>2</sub>S<sub>2</sub>O<sub>3</sub> (sat.) (30 mL) and diluted with EtOAc. The combined organic layers were washed with brine, dried over Na<sub>2</sub>SO<sub>4</sub>, filtered and concentrated. The crude product was purified by flash chromatography (100% hexanes) to afford product **188** as a white solid (9.1 mg, 22%). <sup>1</sup>H NMR (300 MHz, CDCl<sub>3</sub>) δ ppm 9.51 (d, *J* = 8.7 Hz, 1 H), 7.85 (d, *J* = 7.8 Hz, 1 H), 7.68 – 7.51 (m, 4 H), 7.11 (s, 1 H), 4.04 (s, 3 H), 4.035 (s, 3 H), 4.03 (s, 3 H). <sup>13</sup>C NMR (75 MHz, CDCl<sub>3</sub>) δ ppm 152.5, 152.5, 142.8, 131.8, 130.2, 129.9, 128.4, 127.2, 126.7, 126.5, 125.5, 118.9, 105.2, 61.3, 60.3, 55.9. HRMS (ESI+) for C<sub>17</sub>H<sub>17</sub>O<sub>3</sub> [M + H]<sup>+</sup> calculated: 269.1172, found: 269.1174.



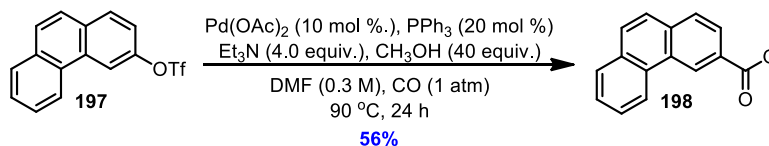
**Phenanthren-3-ol (196):** Potassium phenanthrene-3-sulfonate (50 g, 180 mmol, 1.0 equiv.) was added in 5.0 g portions to molten potassium hydroxide (3-4 g) in a porcelain crucible and heated with a propane torch while stirring. Once all sulphur dioxide was released (the mixture ceased to



bubble), the contents of the crucible were poured into a 2 L Erlenmeyer flask filled with ice water and concentrated HCl. The same procedure was repeated until all of the starting material was consumed. The aqueous mixture was extracted with DCM, dried with Na<sub>2</sub>SO<sub>4</sub> and concentrated to afford the desired product as a beige solid (~20 g, 60%). <sup>1</sup>H NMR spectrum corresponds to the literature.<sup>167</sup>



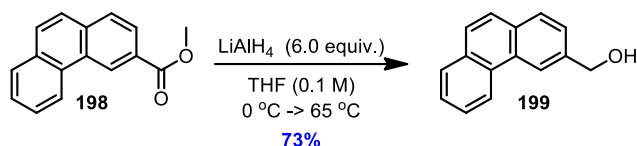
**Phenanthren-3-yl Trifluoromethanesulfonate (197):** Phenanthren-3-ol (4.6 g, 24 mmol, 1.0 equiv.) and Et<sub>3</sub>N (3.0 mL, 52 mmol, 2.2 equiv.) were dissolved in DCM (0.25 L, 0.1 M) in a dry round bottom flask. The reaction mixture was cooled to 0 °C, trifluoromethanesulfonic anhydride (5.9 ml, 35 mmol, 1.5 equiv.) was added and the reaction left to stir for 16 h at ambient temperature. Once complete by TLC, the reaction was quenched with NH<sub>4</sub>Cl<sub>(aq)</sub>, Et<sub>2</sub>O was added and the phases separated. The aqueous phase was extracted with Et<sub>2</sub>O (3 times) and combined organic extracts were washed with brine, dried with Na<sub>2</sub>SO<sub>4</sub> and concentrated. Purification with flash chromatography (5% - 20% EtOAc/ hexanes) afforded the desired product as a yellow oil (6.9 g, 89%). <sup>1</sup>H NMR (400 MHz, CDCl<sub>3</sub>) δ ppm 8.58 (d, *J* = 8.0 Hz, 1 H), 8.54 (d, *J* = 4.0 Hz, 1 H) 7.97 (d, *J* = 8.8 Hz, 1 H), 7.93 (dd, *J* = 7.8, 1.4 Hz, 1 H), 7.82 (d, *J* = 9.2 Hz, 1 H), 7.75 (d, *J* = 8.0 Hz, 1 H), 7.72 – 7.66 (m, 2 H), 7.50 (dd, *J* = 8.8, 2.4 Hz, 1 H). <sup>13</sup>C NMR (101 MHz, CDCl<sub>3</sub>) δ ppm 148.1, 132.3, 131.5, 131.4, 130.8, 129.6, 128.9, 128.5, 127.8, 127.3, 125.9, 122.8, 119.8, 115.2. HRMS (ESI+) for C<sub>15</sub>H<sub>9</sub>F<sub>3</sub>O<sub>3</sub>S [M + H]<sup>+</sup> calculated: 326.0219, found: 326.0232.



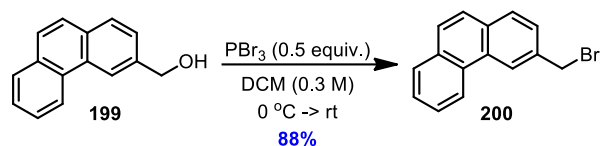
**Methyl Phenanthrene-3-carboxylate (198):** Phenanthren-3-yl trifluoromethanesulfonate (5.0 g, 15 mmol, 1.0 equiv.) and triphenylphosphine (0.80 g, 3.1 mmol, 20 mol %) were dissolved in anhydrous DMF (51 mL, 0.3 M) in a dry round bottom flask under N<sub>2</sub>. Anhydrous MeOH (25 mL, 610 mmol, 40 equiv.), Pd(OAc)<sub>2</sub> (0.34 g, 1.5 mmol, 10 mol %) and anhydrous triethylamine (8.5 mL, 61 mmol, 4.0 equiv.) were added. Carbon monoxide was bubbled into the reaction *via* balloon for 30 minutes and the reaction mixture was left to stir at room temperature for 5 h. Carbon monoxide was bubbled into the solution *via* balloon for 30 more minutes and the reaction mixture was warmed to 90 °C for 16 h. The reaction mixture was quenched with NH<sub>4</sub>Cl<sub>(aq)</sub>, diluted with EtOAc and H<sub>2</sub>O and the phases separated. The aqueous phase was extracted with EtOAc (3 times)

<sup>167</sup> Wu, A.; Duan, Y.; Xu, D.; Harvey, R. G.; Penning, T. M. *Tetrahedron*, **2010**, *66*, 2111. (supporting information in acetone-d<sub>6</sub>)

and the combined organic extracts were washed with saturated  $\text{CuSO}_{4(\text{aq})}$ , brine and dried over  $\text{Na}_2\text{SO}_4$ . Following filtration through a Fisherbrand P8-creped coarse filter paper, the organic phase was concentrated under reduced pressure and purified by flash column chromatography (100% hexanes to 10% EtOAc/hexanes) to afford the desired product as a yellow solid (2.0 g, 56%).  $^1\text{H}$  NMR spectrum corresponds to the literature.<sup>168</sup>



**Phenanthren-3-ylmethanol (199):** Lithium aluminium hydride (1.3 g, 34 mmol, 6.0 equiv.) was suspended in anhydrous THF (28 mL, 0.15 M) in a round bottom flask under  $\text{N}_2$  and the reaction mixture was cooled to  $0\text{ }^\circ\text{C}$ . Methyl phenanthrene-3-carboxylate **198** (1.0 g, 4.2 mmol, 1.0 equiv.) was added and the reaction was left to stir at  $0\text{ }^\circ\text{C}$  for 30 min and then heated to  $70\text{ }^\circ\text{C}$  and left to stir for 16 h. Upon complete consumption of the ester **198**, the reaction was cooled to  $0\text{ }^\circ\text{C}$  and slowly quenched with 10% NaOH and  $\text{H}_2\text{O}$ . An excess of Rochelle's salt was then added and the mixture was left to stir overnight. The reaction was diluted with EtOAc and the phases separated. The aqueous phase was washed with EtOAc (3 times) and the combined organic extracts were washed with brine and dried with  $\text{Na}_2\text{SO}_4$ . Following filtration, the organic phase was concentrated under reduced pressure and purified by flash column chromatography (100% hexanes to 50% EtOAc/hexanes) to afford **199** as a white solid. (0.64 g, 73%).  $^1\text{H}$  NMR spectrum corresponds to the literature.<sup>169</sup>

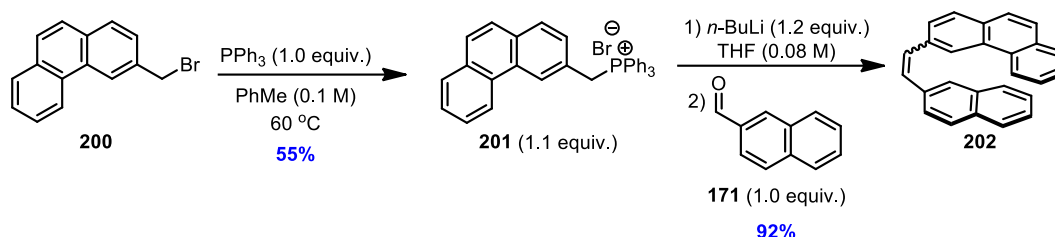


**3-(Bromomethyl)phenanthrene (200):** Phenanthren-3-ylmethanol (0.76 g, 3.6 mmol, 1.0 equiv.) was dissolved in DCM (12 mL, 0.3 M) in a round bottom flask. The reaction mixture was set to  $0\text{ }^\circ\text{C}$  and phosphorous tribromide (0.17 mL, 1.8 mmol, 0.5 equiv.) was added dropwise. The reaction was left to stir for 16 h at ambient temperature. Once complete by TLC, the reaction was quenched with  $\text{H}_2\text{O}$  and diluted with DCM. The two phases were separated and the aqueous phase was extracted with DCM. The combined organic extracts were washed with brine and dried with  $\text{Na}_2\text{SO}_4$ . Following filtration, the organic phase was passed through a thin pad of basic alumina and concentrated to afford product **200** as a beige solid (0.85 g, 87%).  $^1\text{H}$  NMR spectrum corresponds to the literature.<sup>170</sup>

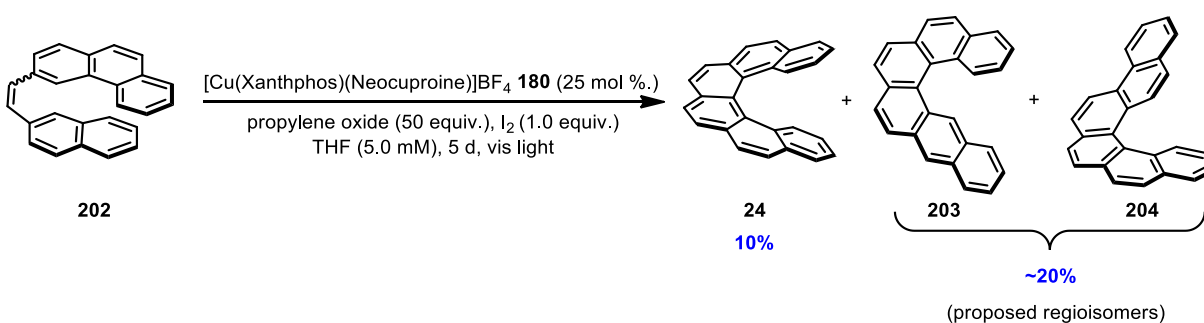
<sup>168</sup> Smith, J. G.; Fogg, D. E.; Munday, I. J.; Sandborn, R. E.; Dibble, P. W. *J. Org. Chem.* **1988**, *53*, 2942.

<sup>169</sup> Ouellette, R. J.; Vanleuwen, B. G. *Tetrahedron* **1969**, *25*, 819.

<sup>170</sup> Puls, C.; Stolle, A.; de Meijere, A. *Chem. Ber.* **1993**, *126*, 1635.



**(E/Z)-3-(2-(Naphthalen-2-yl)vinyl)phenanthrene (202):** 3-(Bromomethyl) phenanthrene (0.5 g, 1.8 mmol, 1.0 equiv.) and triphenylphosphine (0.48 g, 1.8 mmol, 1.0 equiv.) were dissolved in toluene (6.1 mL, 0.3 M) in a round bottom flask. The reaction mixture was left to stir overnight at  $60\text{ }^\circ\text{C}$ . Upon completion, the reaction was filtered and the filtrate washed with  $\text{Et}_2\text{O}$  and dried under vacuum for 24 h to provide (phenanthren-3-ylmethyl)triphenylphosphonium bromide **201** as a white solid (0.53 g, 55%). The product was used directly in the next step.<sup>171</sup>  $^1\text{H NMR}$  (400 MHz,  $\text{CDCl}_3$ )  $\delta$  ppm 8.42 (s, 1H), 8.21 – 8.16 (m, 1H), 7.86 – 7.78 (m, 7H), 7.74 (dd,  $J = 8.3, 6.7$  Hz, 3H), 7.67 – 7.52 (m, 11H), 7.39 – 7.35 (m, 1H), 5.75 (d,  $J = 14.5$  Hz, 2H). Freshly titrated  $n\text{-BuLi}$  (0.58 mL, 1.2 mmol, 1.2 equiv.) was added dropwise to a solution of (phenanthren-3-ylmethyl)triphenylphosphonium bromide **201** (0.59 g, 1.1 mmol, 1.1 equiv.) in anhydrous THF (13 mL, 0.08 M) under  $\text{N}_2$  at  $0\text{ }^\circ\text{C}$ . The resulting yellow mixture was stirred for 1 h at  $0\text{ }^\circ\text{C}$  and then 2-naphthaldehyde **171** (0.16 g, 1.0 mmol, 1.0 equiv.), pre-dissolved in 1.0 mL of anhydrous THF, was added at  $0\text{ }^\circ\text{C}$  and the resulting red solution was slowly warmed up to room temperature and stirred for 18 h. Brine was added to the reaction mixture and the aqueous and organic phases were separated. The aqueous phase was extracted with  $\text{EtOAc}$  (3 times) and the combined organic phases were washed with brine, dried over  $\text{Na}_2\text{SO}_4$ , filtered and concentrated *in vacuo*. The crude mixture was purified by column chromatography (100% hexanes) to afford the desired product **202** as a white solid, mixture of *cis* and *trans* isomers (0.30 g, 92%).  $^1\text{H NMR}$  spectrum corresponds to the literature.<sup>172</sup>

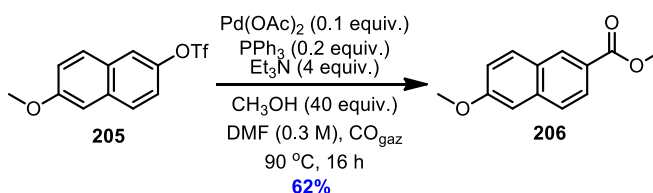


**[6]Helicene (24):**  $[\text{Cu}(\text{NCCH}_3)_4]\text{BF}_4$ <sup>163</sup> (12 mg, 0.04 mmol, 0.25 equiv.) and Xantphos (23 mg, 0.04 mmol, 0.25 equiv.) were dissolved in THF (8.0 mL, 5.0 mM) in a round bottom flask. The

<sup>171</sup> Abbate, S.; Bazzini, C.; Caronna, T.; Fontana, F.; Gambarotti, C.; Gangemi, F.; Longhi, G.; Mele, A.; Sora, I.N.; Panzeri, W. *Tetrahedron* **2005**, 62, 139.

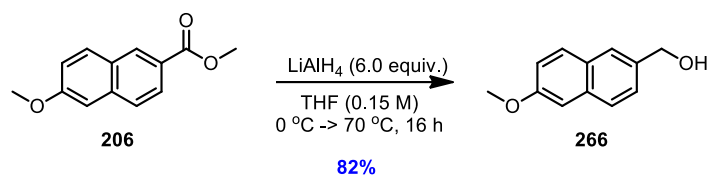
<sup>172</sup> de Jong, M. H.; Laarhoven, W. H. *Recueil des Travaux de Chimie des Pays-Bas* **1973**, 92, 673.

solution was stirred at room temperature for 1 h and a solution of Neocuproine (8.1 mg, 0.04 mmol, 0.25 equiv.) in THF (10 mL, 4.0 mM) was added in one portion. The resulting mixture was stirred for an additional hour, added to a round bottom flask containing 3-(2-(naphthalen-2-yl)vinyl)phenanthrene **202** (51 mg, 0.16 mmol, 1.0 equiv.) and THF was added to achieve a final concentration of 5.0 mM with respect to **202**. Iodine (39 mg, 0.16 mmol, 1.0 equiv.) and propylene oxide (0.54 mL, 7.8 mmol, 50 equiv.) were then added and the reaction stirred in front of a compact fluorescent light bulb (30 W) for 5 days. The reaction was quenched with Na<sub>2</sub>S<sub>2</sub>O<sub>3</sub> (sat.) (30 mL) and diluted with EtOAc. The phases were separated and the aqueous layer was washed with EtOAc (3 times). The combined organic layers were washed with brine, dried over Na<sub>2</sub>SO<sub>4</sub>, filtered and concentrated. The crude product was purified by flash chromatography (100% hexanes) to give the desired product as a white solid, a mix of several regioisomers along with *cis* and *trans* isomers of the starting material (15 mg, 30%). <sup>1</sup>H NMR (400MHz, CDCl<sub>3</sub>) a mixture of several products δ ppm 9.65 (s, 0.67 H), 9.34 (d, *J* = 8.0 Hz, 0.7 H), 9.27 (s, 0.7 H), 8.92 (d, *J* = 8.0 Hz, 0.7 H), 8.78 (d, *J* = 8.0 Hz, 2 H), 8.65 (s, 0.9 H), 8.37 (d, *J* = 8.0 Hz, 0.9 H), 8.14 (d, *J* = 8.0 Hz, 0.7 H), 8.08 (d, *J* = 8.0 Hz, 0.7 H), 8.00 – 7.42 (m, 43 H), 7.24 – 7.20 (m, 0.6 H), 6.97 – 6.89 (m, 2 H), 6.70 – 6.66 (m, 0.4 H). <sup>1</sup>H NMR spectrum for desired [6]helicene **24** corresponds to the literature.<sup>26</sup>

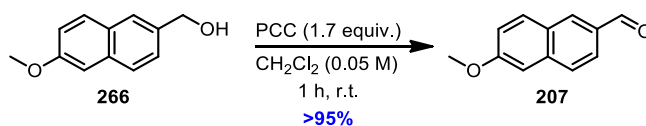


**Methyl 6-Methoxy-2-naphthoate (206):** 6-Methoxynaphthalen-2-yl trifluoromethanesulfonate **205** (0.90 g, 2.9 mmol, 1.0 equiv.), triphenylphosphine (0.15 g, 0.6 mmol, 20 mol %) and anhydrous DMF (10 mL, 0.3 M) were added to a dry round bottom flask under N<sub>2</sub>. Anhydrous methanol (4.7 mL, 120 mmol, 40 equiv.), Pd(OAc)<sub>2</sub> (65 mg, 0.3 mmol, 10 mol %) and anhydrous triethylamine (1.6 mL, 12 mmol, 4.0 equiv.) were then added. Carbon monoxide was bubbled through the reaction *via* balloon for 30 minutes and the reaction mixture was left to stir at room temperature for 5 h. Carbon monoxide was again bubbled through the solution *via* balloon for 30 minutes and the reaction mixture was heated to 90 °C for 16 h. The reaction mixture was quenched with NH<sub>4</sub>Cl<sub>(aq)</sub>, diluted with EtOAc and H<sub>2</sub>O and the phases separated. The aqueous phase was extracted with EtOAc (3 times) and the combined organic extracts were washed with saturated CuSO<sub>4(aq)</sub> and brine and dried over Na<sub>2</sub>SO<sub>4</sub>. Following filtration through a Fisherbrand P8-creped coarse filter paper, the organic phase was concentrated under reduced pressure and purified by flash column chromatography (100% hexanes to 10% EtOAc/hexanes) to afford the desired product as a yellow solid (0.39 g, 62%). <sup>1</sup>H NMR spectrum corresponds to the literature.<sup>173</sup>

<sup>173</sup> Watanabe, N.; Kobayashi, H.; Azami, M.; Matsumoto, M. *Tetrahedron* **1999**, *55*, 6831.



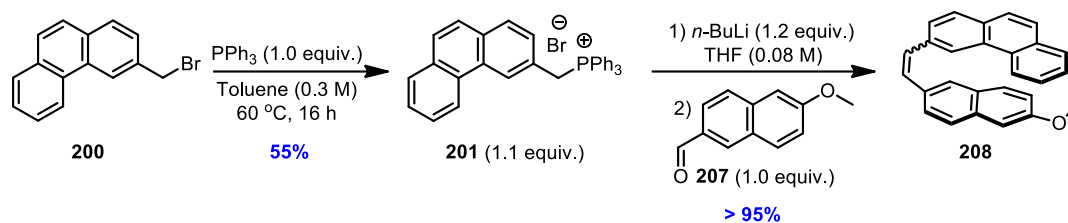
**(6-Methoxynaphthalen-2-yl)methanol (266):** Lithium aluminium hydride (0.37 g, 9.7 mmol, 6.0 equiv.) was suspended in anhydrous THF (16 mL, 0.1 M) in a round bottom flask under N<sub>2</sub> and the reaction mixture was cooled to 0 °C. The methyl 6-methoxy-2-naphthoate (0.35 g, 1.6 mmol, 1.0 equiv.) was added and the reaction was left to stir at 0 °C for 30 min and then heated to 70 °C for 16 h. Upon complete consumption of the ester **206**, the reaction was cooled to 0 °C and slowly quenched with 10% NaOH and H<sub>2</sub>O. An excess of Rochelle's salt was then added and the mixture was left to stir overnight. The reaction was then diluted with EtOAc and the phases separated. The aqueous phase was washed with EtOAc (3 times) and the combined organic extracts were washed with brine and dried with Na<sub>2</sub>SO<sub>4</sub>. Following filtration, the organic phase was concentrated under reduced pressure and purified by flash column chromatography (100% hexanes to 50% EtOAc/hexanes) to afford **266** as a white solid. (0.25 g, 82%). <sup>1</sup>H NMR spectrum corresponds to the literature.<sup>174</sup>



**6-Methoxy-2-naphthaldehyde (207):** (6-Methoxynaphthalen-2-yl)methanol (0.23 g, 1.2 mmol, 1.0 equiv.) was dissolved in DCM (24 mL, 0.05 M) in a round bottom flask. Pyridinium chlorochromate (0.45 g, 2.1 mmol, 1.7 equiv.) was added and the reaction mixture was left to stir overnight at ambient temperature. The reaction was diluted with Et<sub>2</sub>O and 20 mg of silica gel was added. The mixture was filtered through a pad of silica gel and the pad was washed with Et<sub>2</sub>O. The filtrate was concentrated under reduced pressure to provide the product **207** as a beige solid (0.24 g, 99%). <sup>1</sup>H NMR spectrum corresponds to the literature.<sup>175</sup>

<sup>174</sup> MacCarthy, J. R. *J. Org. Chem.* **1984**, *49*, 4995.

<sup>175</sup> Vilches-Herrera, M.; Miranda-Sepulveda, J.; Rebolledo-Fuentes, M.; Fierro, A.; Luhr, S.; Iturriaga-Vasquez, P.; Cassels, B. K.; Reyes-Parada, M. *Bioorg. Med. Chem.* **2009**, *17*, 2452.

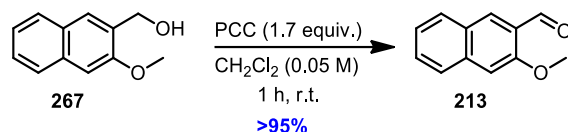


**(E/Z)-3-(2-(6-Methoxynaphthalen-2-yl)vinyl)phenanthrene (208):** 3-(Bromomethyl)phenanthrene (0.5 g, 1.8 mmol, 1.0 equiv.) and triphenylphosphine (0.48 g, 1.8 mmol, 1.0 equiv.) were dissolved in toluene (6.1 mL, 0.3 M) in a round bottom flask. The reaction mixture was left to stir overnight at  $60^\circ\text{C}$ . Upon completion, the reaction was filtered and the filtrate washed with  $\text{Et}_2\text{O}$  and dried under vacuum for 24 h to provide (phenanthren-3-ylmethyl)triphenylphosphonium bromide **201** as a white solid (0.53 g, 55%). The product was used directly in the next step.<sup>171</sup>  **$^1\text{H}$  NMR (400MHz,  $\text{CDCl}_3$ )**  $\delta$  ppm 8.42 (s, 1H), 8.21 – 8.16 (m, 1H), 7.86 – 7.78 (m, 7H), 7.74 (dd,  $J = 8.3, 6.7$  Hz, 3H), 7.67 – 7.52 (m, 11H), 7.39 – 7.35 (m, 1H), 5.75 (d,  $J = 14.5$  Hz, 2H). Freshly titrated  $n\text{-BuLi}$  (0.31 mL, 0.62 mmol, 1.2 equiv.) was added dropwise to a solution of (phenanthren-3-ylmethyl)triphenylphosphonium bromide (0.32 g, 0.59 mmol, 1.1 equiv.) in anhydrous THF (6.8 mL, 0.08 M) under  $\text{N}_2$  at  $0^\circ\text{C}$ . The resulting yellow mixture was stirred for 1 h at  $0^\circ\text{C}$  and then 6-methoxy-2-naphthaldehyde (0.10 g, 0.54 mmol, 1.0 equiv.), pre-dissolved in 1.0 mL of anhydrous THF, was added at  $0^\circ\text{C}$  and the resulting red solution was slowly warmed up to room temperature and stirred for 18 h. Brine was added to the reaction mixture and the aqueous and organic phases were separated. The aqueous phase was extracted with  $\text{EtOAc}$  (3 times) and the combined organic phases were washed with brine, dried over  $\text{Na}_2\text{SO}_4$ , filtered and concentrated *in vacuo*. The crude mixture was purified by column chromatography (100% hexanes) to afford the desired product **208** as a white solid, mixture of *cis* and *trans* isomers (0.19 g, > 95%).  **$^1\text{H}$  NMR (400MHz,  $\text{CDCl}_3$ )**  $\delta$  ppm 8.67 (s, 1 H), 8.40 (d,  $J = 8.0$  Hz, 1 H), 7.88 – 7.86 (m, 1 H), 7.77 (s, 1 H) 7.72 – 7.67 (m, 3 H), 7.63 (d,  $J = 12$  Hz, 1 H), 7.56 – 7.51 (m, 4 H), 7.42 – 7.40 (m, 1 H), 7.13 – 7.09 (m, 1 H), 6.90 (d,  $J = 4.0$  Hz, 2 H), 3.91 (s, 3 H).  **$^{13}\text{C}$  NMR (101 MHz,  $\text{CDCl}_3$ )**  $\delta$  ppm 158.0, 135.8, 134.4, 134.0, 132.9, 132.8, 132.5, 132.3, 131.3, 130.9, 130.4, 130.2, 129.7, 129.65, 129.51, 129.3, 129.1, 128.8, 128.7, 128.5, 128.4, 128.2, 127.7, 127.5, 127.4, 127.1, 127.0, 126.8, 126.7, 126.7, 126.6, 124.3, 123.3, 122.8, 122.7, 121.6, 119.2, 119.0, 106.1, 105.9, 55.5, 55.5. **HRMS (ESI+)** for  $\text{C}_{27}\text{H}_{20}\text{OAg}$  [ $\text{M} + \text{Ag}$ ]<sup>+</sup> calculated: 467.0560, found: 467.0580.

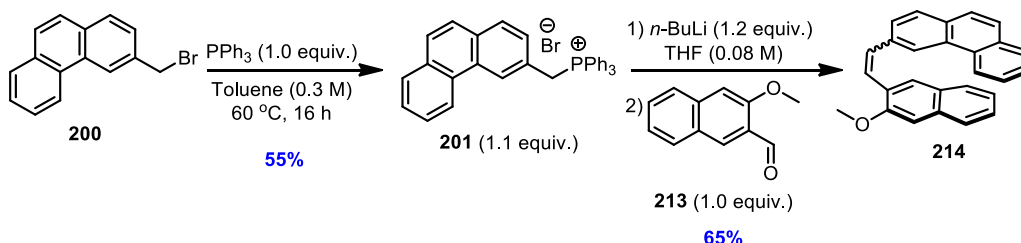




aqueous phase was washed with EtOAc (3 times) and the combined organic extracts were washed with brine and dried with Na<sub>2</sub>SO<sub>4</sub>. Following filtration, the organic phase was concentrated under reduced pressure and purified by flash column chromatography (100% hexanes to 50% EtOAc/hexanes) to afford **267** as a white solid. (0.30 g, 68%). <sup>1</sup>H NMR spectrum corresponds to the literature.<sup>177</sup>



**3-Methoxy-2-naphthaldehyde (213):** (3-Methoxynaphthalen-2-yl)methanol (0.28 g, 1.5 mmol, 1.0 equiv.) was dissolved in DCM (30 mL, 0.05 M) in a round bottom flask. Pyridinium chlorochromate (0.55 g, 2.5 mmol, 1.7 equiv.) was added and the reaction mixture was left to stir overnight at ambient temperature. The reaction was diluted with Et<sub>2</sub>O and 20 mg of silica gel was added. The mixture was filtered through a pad of silica gel and the pad was washed with Et<sub>2</sub>O. The filtrate was concentrated under reduced pressure and product **213** was isolated as a beige solid (0.27 g, > 95%). <sup>1</sup>H NMR spectrum corresponds to the literature.<sup>178</sup>



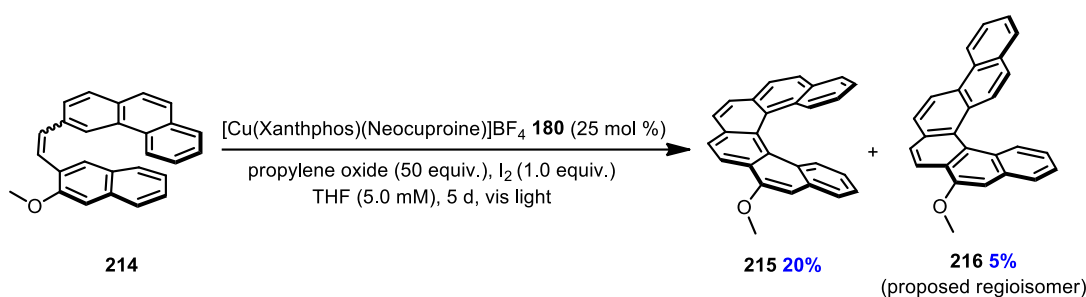
**(E/Z)-3-(2-(3-Methoxynaphthalen-2-yl)vinyl)phenanthrene (214):** 3-(Bromomethyl)phenanthrene (0.50 g, 1.8 mmol, 1.0 equiv.) and triphenylphosphine (0.48 g, 1.8 mmol, 1.0 equiv.) were dissolved in toluene (6.1 mL, 0.3 M) in a round bottom flask. The reaction mixture was left to stir overnight at 60 °C. Upon completion, the reaction was filtered and the filtrate washed with Et<sub>2</sub>O and dried under vacuum for 24 h to provide (phenanthren-3-ylmethyl)triphenylphosphonium bromide **201** as a white solid (0.53 g, 55%). The product was used directly in the next step.<sup>171</sup> <sup>1</sup>H NMR (400MHz, CDCl<sub>3</sub>) δ ppm 8.42 (s, 1H), 8.21 – 8.16 (m, 1H), 7.86 – 7.78 (m, 7H), 7.74 (dd, *J* = 8.3, 6.7 Hz, 3H), 7.67 – 7.52 (m, 11H), 7.39 – 7.35 (m, 1H), 5.75 (d, *J* = 14.5 Hz, 2H). Freshly titrated *n*-BuLi (0.31 mL, 0.61 mmol, 1.2 equiv.) was added dropwise to a solution of (phenanthren-3-ylmethyl)triphenylphosphonium bromide **201** (0.31 g, 0.58 mmol, 1.1 equiv.) in anhydrous THF (6.6 mL, 0.08 M) under N<sub>2</sub> at 0 °C. The resulting yellow mixture was stirred for 1 h at 0 °C and then 3-methoxy-2-naphthaldehyde **213** (0.10 g, 0.53 mmol, 1.0 equiv.), pre-dissolved in 1.0 ml of anhydrous THF, was added at 0 °C and the resulting red solution was slowly warmed

<sup>177</sup> Wu, K.-C.; Lin, Y.-S.; Yeh, Y.-S.; Chen, C.-Y.; Ahmed, M. O.; Chou, P.-T.; Hon, Y.-S. *Tetrahedron*, **2004**, *60*, 11861.

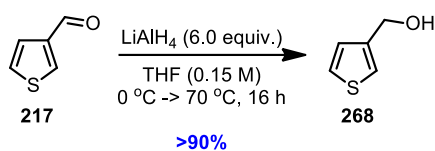
<sup>178</sup> Oslund, R. C.; Cermak, N.; Gelb, M. H. *J. Med. Chem.* **2008**, *51*, 4708. (supporting information)



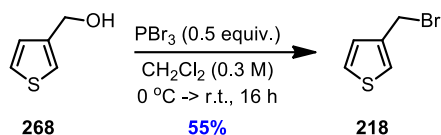
up to room temperature and stirred for a total of 18 h. Brine was added to the reaction mixture and the aqueous and organic phases were separated. The aqueous phase was extracted with EtOAc (3 times) and the combined organic phases were washed with brine, dried over Na<sub>2</sub>SO<sub>4</sub>, filtered and concentrated *in vacuo*. The crude mixture was purified by column chromatography (100% hexanes) to afford the desired product **214** as a white solid and a mixture of *cis* and *trans* isomers (0.12 g, 65%). <sup>1</sup>H NMR (400 MHz, CDCl<sub>3</sub>) δ ppm 8.78 (d, *J* = 8.0 Hz, 1 H), 8.63 (s, 1 H), 8.36 (d, *J* = 8.0 Hz, 1 H), 8.13 – 7.82 (m, 3 H), 7.77 – 7.35 (m, 16 H), 7.24 – 7.18 (m, 2 H), 7.00 (d, *J* = 12 Hz, 1 H), 6.94 (d, *J* = 12 Hz, 1 H), 4.06 (s, 1.5 H), 3.93 (s, 3 H). <sup>13</sup>C NMR (101 MHz, CDCl<sub>3</sub>) δ ppm 155.8, 136.2, 134.3, 132.5, 131.8, 131.5, 130.9, 129.4, 129.1, 128.8, 128.4, 128.2, 127.9, 127.4, 127.0, 126.8, 126.8, 126.7, 126.6, 126.6, 126.4, 125.9, 124.6, 124.4, 124.1, 123.9, 122.8, 121.9, 105.5, 55.7. HRMS (ESI+) for C<sub>27</sub>H<sub>20</sub>OAg [M + Ag]<sup>+</sup> calculated: 467.0560, found: 467.0576.



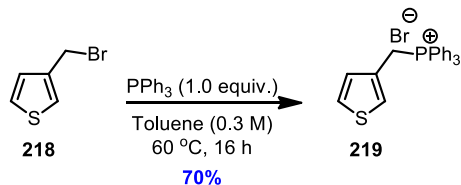
**6-Methoxy-[6]-Helicene (215):** [Cu(NCCH<sub>3</sub>)<sub>4</sub>]BF<sub>4</sub><sup>163</sup> (12 mg, 0.04 mmol, 0.25 equiv.) and Xantphos (23 mg, 0.04 mmol, 0.25 equiv.) were dissolved in THF (8.0 mL, 5.0 mM) in a round bottom flask equipped with a stir bar. The solution was stirred at room temperature for 1 h and a solution of Neocuproine (8.1 mg, 0.04 mmol, 0.25 equiv.) in THF (10 mL, 4.0 mM) was added. The resulting mixture was stirred for an additional hour, added to a round bottom flask containing 3-(2-(3-Methoxynaphthalen-2-yl)vinyl)phenanthrene **214** (56 mg, 0.16 mmol, 1 equiv.) and THF was added to achieve a final concentration of 5.0 mM with respect to **214**. Iodine (39 mg, 0.16 mmol, 1.0 equiv.) and propylene oxide (0.54 mL, 7.8 mmol, 50 equiv.) were added and the reaction stirred in front of a compact fluorescent light bulb (30 W) for 5 days. The reaction was quenched with Na<sub>2</sub>S<sub>2</sub>O<sub>3</sub> (sat.) (30 mL) and diluted with EtOAc. The phases were separated and the aqueous layer was washed with EtOAc (3 times). The combined organic layers were washed with brine, dried over Na<sub>2</sub>SO<sub>4</sub>, filtered and concentrated. The crude product was purified by flash chromatography (100% hexanes) to give a mix of several products, as *cis* and *trans* isomers of the starting material, as a white solid (33.6 mg, 20% one regioisomer, 5% another regioisomer and 37% *cis* and *trans* starting materials). <sup>1</sup>H NMR (400 MHz, CDCl<sub>3</sub>) a mixture of the *cis* and *trans* starting material and one major product δ ppm 9.62 (s, 0.9 H), 9.27 (s, 0.9 H), 9.21 – 9.19 (m, 1 H), 8.91 (d, *J* = 8.0 Hz, 1.0 H), 8.79 – 8.77 (m, 2.0 H), 8.62 (s, 0.50 H), 8.41 (d, *J* = 8.0 Hz, 1.0 H), 8.36 (d, *J* = 8.0 Hz, 0.6 H), 8.17 (d, *J* = 12 Hz, 1.0 H), 8.12 (s, 1.0 H), 7.97 – 7.35 (m, 30.9 H), 7.23 – 7.18 (m, 2.4 H), 7.02 – 6.91 (m, 2.4 H), 4.21 (s, 0.4 H), 4.16 (s, 2.7 H), 4.06 (s, 3.0 H), 3.93 (s, 1.5 H). <sup>13</sup>C NMR (101 MHz, CDCl<sub>3</sub>) δ ppm 155.83, 153.7, 136.2, 134.4, 134.3, 132.5, 132.3, 131.8, 130.9, 130.7, 130.5, 129.0, 128.8, 128.8, 128.4, 128.2, 127.9, 127.8, 127.6, 127.3, 127.0, 127.0, 126.8, 126.8, 126.7, 126.5, 126.4, 126.4, 125.9, 124.6, 124.4, 124.2, 124.1, 123.3, 122.8, 122.0, 121.9, 120.4, 105.5, 104.0, 55.9, 55.7, 29.9. HRMS (ESI+) for C<sub>27</sub>H<sub>19</sub>O [M + H]<sup>+</sup> calculated: 359.1430, found: 359.1441.



**Thiophen-3-ylmethanol (268):** Lithium aluminium hydride (2.6 g, 69 mmol, 6.0 equiv.) was suspended in anhydrous THF (76 mL, 0.10 M) in a round bottom flask under N<sub>2</sub> and the reaction mixture was cooled to 0 °C. Thiophene-3-carbaldehyde (1.3 g, 11 mmol, 1.0 equiv.) was added and the reaction was left to stir at 0 °C for 30 min, then allowed to warm up to room temperature and then heated to 70 °C and left to stir for 16 h. Upon complete consumption of the ester **217**, the reaction was cooled to 0 °C and slowly quenched with 10% NaOH and H<sub>2</sub>O. An excess of Rochelle's salt was then added and the mixture was left to stir overnight. The reaction was diluted with EtOAc and the phases separated. The aqueous phase was washed with EtOAc (3 times) and the combined organic extracts were washed with brine and dried with Na<sub>2</sub>SO<sub>4</sub>. Following filtration, the organic phase was concentrated under reduced pressure and purified by flash column chromatography (100% hexanes to 50% EtOAc/hexanes) to afford **271** as a white solid. (1.2 g, > 90%). <sup>1</sup>H NMR spectrum corresponds to the literature.<sup>179</sup>



**3-(Bromomethyl)thiophene (218):** Thiophene-3-ylmethanol (0.50 g, 4.4 mmol, 1.0 equiv.) was dissolved in DCM (15 mL, 0.30 M) in a round bottom flask. The reaction mixture was set to 0 °C and phosphorous tribromide (0.21 mL, 2.2 mmol, 0.50 equiv.) was added dropwise. The reaction was left to stir for 16 h at ambient temperature. Once complete by TLC, the reaction was quenched with H<sub>2</sub>O and diluted with DCM. The two phases were separated and the aqueous phase was extracted with DCM. The combined organic extracts were washed with brine and dried with Na<sub>2</sub>SO<sub>4</sub>. Following filtration, the organic phase was passed through a thin pad of basic alumina and concentrated to afford the desired product as a beige solid (0.42 g, 55%). <sup>1</sup>H NMR spectrum corresponds to the literature.<sup>180</sup>

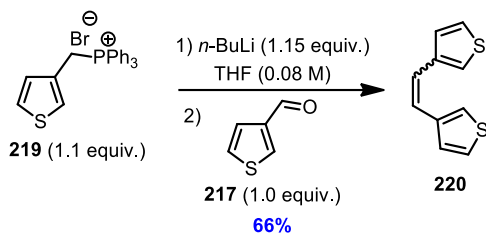


**3-(Methyltriphenylphosphine)thiophene Bromide (219):** 3-(Bromomethyl)thiophene (0.34 g, 1.9 mmol, 1.0 equiv.) and triphenylphosphine (0.59 g, 2.3 mmol, 1.0 equiv.) were dissolved in toluene (23 mL, 0.30 M) in a round bottom flask. The reaction mixture was left to stir overnight at 60 °C. Upon completion, the reaction was filtered and the filtrate washed with Et<sub>2</sub>O and left to

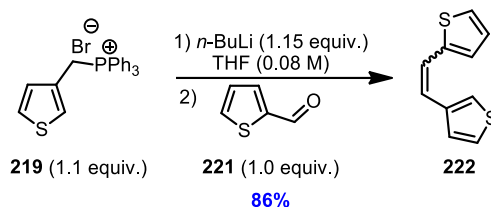
<sup>179</sup> University of Washington Patent: WO2004/65384 A1, 2004.

<sup>180</sup> Ngwendson, J. N.; Atemnkeng, W. N.; Schultze, C. M.; Banerjee, A. *Org. Lett.* **2006**, 8, 4085.

dry under vacuum for 24 h. The desired product was obtained as a white solid (0.60 g, 70%).  $^1\text{H}$  NMR spectrum corresponds to the literature.<sup>180</sup>



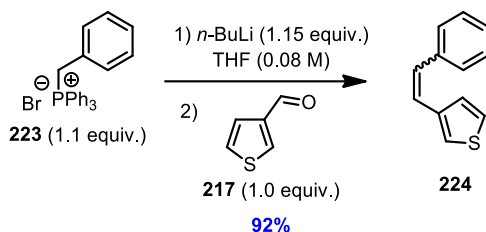
**(E/Z)-1,2-Di(thiophen-3-yl)ethane (220):** Freshly titrated *n*-BuLi (0.50 mL, 0.60 mmol, 1.2 equiv.) was added dropwise to a solution of 3-(methyltriphenylphosphine)thiophene bromide **219** (0.25 g, 0.60 mmol, 1.1 equiv.) in anhydrous THF (6.5 mL, 0.08 M) under  $\text{N}_2$  at 0 °C. The resulting yellow mixture was stirred for 1 h at 0 °C and commercially available thiophene-3-carbaldehyde **217** (45  $\mu\text{L}$ , 0.52 mmol, 1.0 equiv.) was added at 0 °C. The resulting red solution was slowly warmed up to room temperature and stirred for a total of 18 h. Brine was added to the reaction mixture and the aqueous and organic phases were separated. The aqueous phase was extracted with EtOAc (3 times) and the combined organic phases were washed with brine, dried over  $\text{Na}_2\text{SO}_4$ , filtered and concentrated *in vacuo*. The crude mixture was purified by column chromatography (100% hexanes) to afford desired product **220** as a white solid (65 mg, 66%).  $^1\text{H}$  NMR spectrum corresponds to the literature.<sup>181</sup>



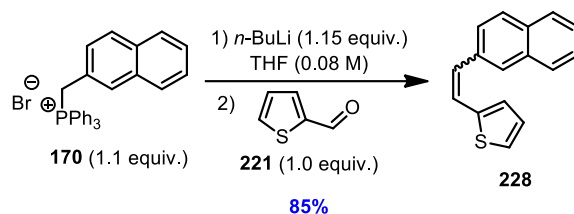
**(E/Z)-2-(2-(Thiophen-3-yl)vinyl)thiophene (222):** Freshly titrated *n*-BuLi (0.50 mL, 0.60 mmol, 1.2 equiv.) was added dropwise to a solution of 3-(methyltriphenylphosphine)thiophene bromide **219** (0.25 g, 0.57 mmol, 1.1 equiv.) in anhydrous THF (6.5 mL, 0.08 M) under  $\text{N}_2$  at 0 °C. The resulting yellow mixture was stirred for 1 h at 0 °C and commercially available thiophene-2-carbaldehyde **221** (48.3  $\mu\text{L}$ , 0.52 mmol, 1.0 equiv.) was added at 0 °C. The resulting red solution was slowly warmed up to room temperature and stirred for a total of 18 h. Brine was added to the reaction mixture and the aqueous and organic phases were separated. The aqueous phase was extracted with EtOAc (3 times) and the combined organic phases were washed with brine, dried over  $\text{Na}_2\text{SO}_4$ , filtered and concentrated *in vacuo*. The crude mixture was purified by column chromatography (100% hexanes) to afford the desired product **222** as a white solid and mixture of *cis* and *trans* isomers (86 mg, 86%).  $^1\text{H}$  NMR (400 MHz,  $\text{CDCl}_3$ )  $\delta$  ppm 7.29 – 7.28 (m, 2 H), 7.17 (d,  $J = 4$  Hz, 1 H), 7.05 – 7.01 (m, 2 H), 6.95 – 6.92 (m, 1 H), 6.65 (d,  $J = 12$  Hz, 1 H), 6.48 (d,  $J = 12$  Hz, 1 H).  $^{13}\text{C}$  NMR (101 MHz,  $\text{CDCl}_3$ )  $\delta$  ppm 143.0, 139.8, 127.7, 126.4, 125.9, 124.9,

<sup>181</sup> Castedo, L.; Cid, M. M.; Dominguez, R.; Seijas, J. A.; Villaverde, M. C. *Heterocycles*, **1990**, *31*, 1271.

124.2, 122.8, 122.3, 122.0. **HRMS (ESI+)** for  $C_{10}H_9S_2[M + H]^+$  calculated: 193.0140, found: 193.0141.



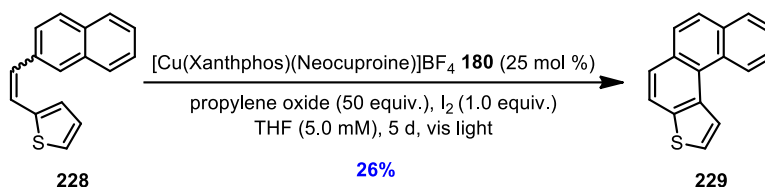
**(E/Z)-3-Styrylthiophene (224):** Freshly titrated *n*-BuLi (1.0 mL, 1.2 mmol, 1.2 equiv.) was added dropwise to a solution of commercially available benzyltriphenylphosphonium bromide **223** (0.50 g, 1.2 mmol, 1.1 equiv.) in anhydrous THF (13 mL, 0.08 M) under  $N_2$  at 0 °C. The resulting yellow mixture was stirred for 1 h at 0 °C and commercially available thiophene-3-carbaldehyde **217** (92  $\mu$ L, 1.1 mmol, 1.0 equiv.) was added at 0 °C and the solution was slowly warmed up to room temperature and stirred for a total of 18 h. Brine was added to the reaction mixture and the aqueous and organic phases were separated. The aqueous phase was extracted with EtOAc (3 times) and the combined organic phases were washed with brine, dried over  $Na_2SO_4$ , filtered and concentrated *in vacuo*. The crude mixture was purified by column chromatography (100% hexanes) to afford the desired product **224** as a white solid (0.18 g, 92%).  $^1H$  NMR spectrum corresponds to the literature.<sup>182</sup>



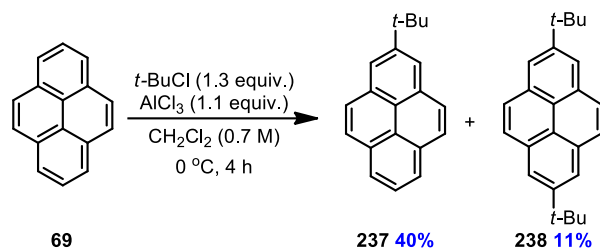
**(E/Z)-2-(2-(Naphthalen-2-yl) vinyl) thiophene (228):** Freshly titrated *n*-BuLi (0.90 mL, 1.1 mmol, 1.2 equiv.) was added dropwise to a solution of (naphthalen-2-ylmethyl)triphenylphosphonium bromide **170** (0.50 g, 1.0 mmol, 1.1 equiv.) in anhydrous THF (12 mL, 0.08 M) under  $N_2$  at 0 °C. The resulting yellow mixture was stirred for 1 h at 0 °C and commercially available thiophene-2-carbaldehyde **221** (90  $\mu$ L, 0.94 mmol, 1.0 equiv.) was added at 0 °C. The resulting red solution was slowly warmed up to room temperature and stirred for a total of 18 h. Brine was added to the reaction mixture and the aqueous and organic phases were separated. The aqueous phase was extracted with EtOAc (3 times) and the combined organic phases were washed with brine, dried over  $Na_2SO_4$ , filtered and concentrated *in vacuo*. The crude mixture was purified by column chromatography (100% hexanes) to afford the desired product **228** as a white solid (0.19 g, 85%).  $^1H$  NMR (400 MHz,  $CDCl_3$ )  $\delta$  ppm 7.87 (s, 1 H), 7.85 – 7.78 (m, 3 H), 7.49 – 7.45 (m, 3 H), 7.06 (d,  $J = 4.0$  Hz, 1 H) 7.01 (d,  $J = 4.0$  Hz, 1 H) 6.89 – 6.87 (m, 1 H), 6.79 (d,  $J = 12$

<sup>182</sup> Molander, G. A.; Bernardi, C. R. *J. Org. Chem.* **2002**, *67*, 8424. (spectra for the product (6d) found in the supporting information)

Hz, 1 H), 6.72 (d,  $J = 12$  Hz, 1 H).  $^{13}\text{C}$  NMR (101 MHz,  $\text{CDCl}_3$ )  $\delta$  ppm 143.1, 134.6, 133.9, 133.1, 128.6, 128.5, 128.1, 127.8, 127.8, 126.6, 126.5, 126.3, 126.1, 124.6, 123.4, 122.3. HRMS (ESI+) for  $\text{C}_{16}\text{H}_{13}\text{S}$   $[\text{M} + \text{H}]^+$  calculated: 237.0733, found: 237.0734.



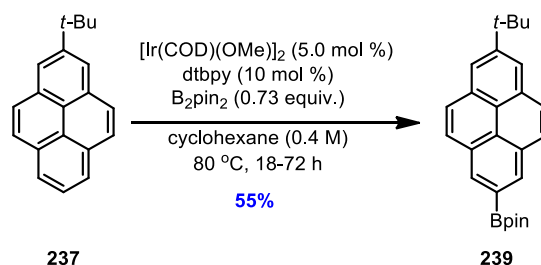
**Phenanthro[3,4-*b*]thiophene (229):**  $[\text{Cu}(\text{NCCH}_3)_4]\text{BF}_4$ <sup>163</sup> (12 mg, 0.04 mmol, 0.25 equiv.) and Xantphos (23 mg, 0.04 mmol, 0.25 equiv.) were dissolved in THF (8.0 mL, 5.0 mM) in a round bottom flask equipped with a stir bar. The solution was stirred at room temperature for 1 h and a solution of Neocuproine (8.1 mg, 0.04 mmol, 0.25 equiv.) in THF (10 mL, 4.0 mM) was added. The resulting mixture was stirred for an additional hour, added to the round bottom flask containing 2-(2-(Naphthalen-2-yl)vinyl)thiophene **228** (37 mg, 0.16 mmol, 1.0 equiv.) and THF was added to achieve a final concentration of 5.0 mM with respect to **228**. Iodine (39 mg, 0.16 mmol, 1.0 equiv.) and propylene oxide (0.54 mL, 7.8 mmol, 50 equiv.) were then added and the reaction stirred in front of a compact fluorescent light bulb (30 W) for 5 days. The reaction was quenched with  $\text{Na}_2\text{S}_2\text{O}_3$  (sat.) (30 mL) and diluted with EtOAc. The phases were separated and the aqueous phase extracted with EtOAc (3 times). The combined organic layers were washed with brine, dried over  $\text{Na}_2\text{SO}_4$ , filtered and concentrated. The crude product was purified by flash chromatography (100% hexanes) to give the desired product mixed with the *trans*-isomer of the starting material as a white solid (9.4 mg, 26%).  $^1\text{H}$  NMR (400 MHz,  $\text{CDCl}_3$ ) *mix of the trans isomer of starting material and the desired product.*  $\delta$  ppm 9.16 (d,  $J = 8.0$  Hz, 1 H), 8.66 (d,  $J = 4.0$  Hz, 1 H), 8.09 (d,  $J = 8.0$  Hz, 1 H), 8.01 (d,  $J = 8.0$  Hz, 1 H), 7.90 – 7.64 (m, 11.5 H), 7.49 – 7.47 (m, 3 H), 7.37 (d,  $J = 16$  Hz, 0.4 H), 7.23 (d,  $J = 4.0$  Hz, 2 H), 7.13 – 7.01 (m, 2.7 H), 6.90 – 6.88 (m, 0.9 H), 6.80 (d,  $J = 12$  Hz, 0.4 H), 6.73 (d,  $J = 12$  Hz, 1 H).  $^1\text{H}$  NMR spectrum for compound **229** corresponds to the literature.<sup>183</sup>



**2-*t*-Bu-pyrene (237):**<sup>134</sup> Pyrene (5.0 g, 25 mmol, 1.0 equiv.) was dissolved in DCM (35 mL, 0.70 M) in a round bottom flask equipped with a stir bar. *t*-BuCl (3.5 mL, 31 mmol, 1.3 equiv.) was added to the solution and the reaction mixture was cooled to 0 °C.  $\text{AlCl}_3$  (3.6 g, 27 mmol, 1.1 equiv.) was then added in several portions and the dark brown slurry was allowed to stir for 3 h, while gradually warming to room temperature. The reaction was quenched by pouring the mixture

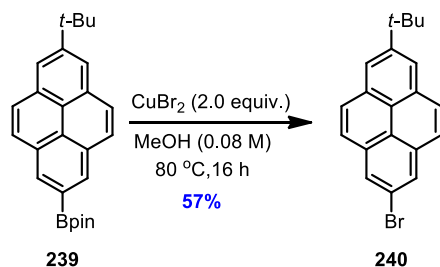
<sup>183</sup> Kumar, S.; Saravanan, S.; Reuben, P.; Kumar, A. *J. Heterocyclic Chem.* **2005**, *42*, 1345.

into an Erlenmeyer flask filled with ice water, DCM was added and the phases separated. The aqueous phase was washed with DCM (3 times) and the combined organic extracts were washed with brine and dried over Na<sub>2</sub>SO<sub>4</sub>. Following filtration through a Fisherbrand P8-creped coarse filter paper, the filtrate was concentrated and then dissolved in a minimal amount of boiling MeOH (~500 mL). The solution was cooled to room temperature and then put in the freezer overnight. The precipitate was filtered off and the 2,7-di-*t*-Bu-pyrene was obtained as a light brown solid (0.85 g, 11%). The mother liquor was concentrated under reduced pressure and dissolved in a minimal amount of boiling hexanes (~20 mL). The mixture was left to re-crystallize overnight in the freezer. Filtration offered the desired product **237** as a white solid (2.5 g, 40% yield). Additional re-crystallizations may be done on the mother liquor to obtain more of **237**. 2,7-di-*t*-Bu-pyrene (**238**): <sup>1</sup>H NMR (400 MHz, CDCl<sub>3</sub>) δ ppm 8.19 (s, 4 H), 8.03 (s, 4 H), 1.59 (s, 18 H). <sup>13</sup>C NMR (75 MHz, CDCl<sub>3</sub>) δ ppm 148.7, 130.9, 127.6, 123.0, 122.1, 35.4, 32.1. HRMS (ESI+) for C<sub>24</sub>H<sub>27</sub> [M+H]<sup>+</sup> calculated: 314.2029 found: 314.2028. 2-*t*-Bu-pyrene (**237**): <sup>1</sup>H NMR (400 MHz, CDCl<sub>3</sub>) δ ppm 8.22 (s, 2 H) 8.15 (d, *J* = 8.0 Hz, 2 H), 8.06 (s, 4 H), 7.97 (t, *J* = 8.0 Hz, 1 H), 1.59 (s, 9 H), 1.54 (s, H<sub>2</sub>O). <sup>13</sup>C NMR (75 MHz, CDCl<sub>3</sub>) δ ppm 149.2, 131.1, 127.7, 127.4, 125.6, 124.9, 123.1, 122.4, 35.4, 32.1. HRMS (ESI+) for C<sub>20</sub>H<sub>19</sub> [M + H]<sup>+</sup> calculated: 258.1403 found: 258.1398.

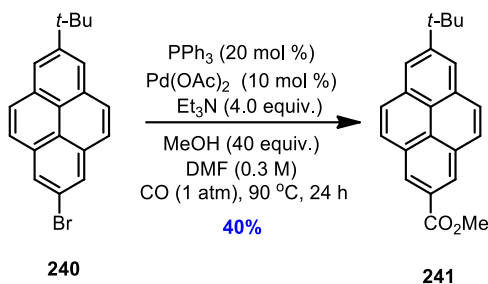


**2-(7-(*t*-Bu)pyren-2-yl)-4,4,5,5-tetramethyl-1,3,2-dioxaborolane (239):**<sup>89</sup> 2-*t*-Bu-pyrene (0.75 g, 2.9 mmol, 1 equiv.), B<sub>2</sub>Pin<sub>2</sub> (0.81 g, 3.2 mmol, 1.1 equiv.), 4,4-di-*t*-Bu-2,2-bipyridine (dtbpy) (78 mg, 0.29 mmol, 10 mol%) and dry cyclohexane (7.3 mL, 0.40 M) were added to a dry round bottom flask under N<sub>2</sub>. The catalyst [Ir(COD)(OMe)<sub>2</sub>] (96 mg, 0.15 mmol, 5.0 mol %) was then added and the reaction set to 70–80 °C for 18–72 h (slightly better yields were observed with longer reaction times). The reaction mixture was concentrated under reduced pressure and purified by flash column chromatography (100% hexanes to 75% DCM/hexanes) to afford **239** as a yellow solid (0.61 g, 55% yield). <sup>1</sup>H NMR (400 MHz, CDCl<sub>3</sub>) δ ppm 8.60 (s, 2 H), 8.20 (s, 2 H), 8.08 (d, *J* = 12 Hz, 2 H), 8.03 (d, *J* = 8.0 Hz, 2 H) 1.58 (s, 9 H), 1.46 (s, 12 H). <sup>13</sup>C NMR (75 MHz, CDCl<sub>3</sub>) δ ppm 149.7, 131.6, 131.3, 130.4, 127.8, 127.6, 126.5, 123.0, 122.2, 84.2, 35.4, 32.1, 25.2. HRMS (ESI+) for C<sub>26</sub>H<sub>30</sub>BO<sub>2</sub> [M + H]<sup>+</sup> calculated: 385.2333 found: 385.2340.





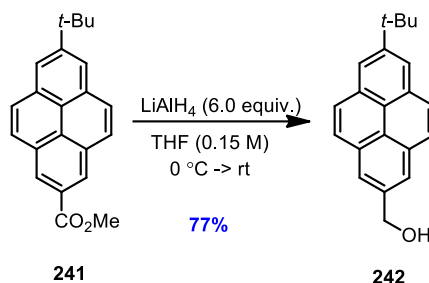
**2-Bromo-7-*t*-Bu-pyrene (240):**<sup>184</sup> 2-(7-(*t*-Bu)pyren-2-yl)-4,4,5,5-tetramethyl-1,3,2-dioxaborolane (1.0 g, 2.6 mmol, 1.0 equiv.) and dry MeOH (33 mL, 0.08 M) were added to a dry round bottom flask. The reaction mixture was heated to 80 °C to fully dissolve **239** and then CuBr<sub>2</sub> (1.7 g, 7.8 mmol, 3.0 equiv.) was added. The reaction was left to stir for 24–72 h (better yields were observed with longer reaction times). Upon completion, the reaction mixture was concentrated under reduced pressure and purified by flash column chromatography (100% hexanes) to afford the desired product as a yellow solid (0.50 g, 57%). Un-reacted **239** could be recovered by flushing the column with 50% DCM/hexanes and re-submitted to the reaction conditions to obtain a complete conversion. <sup>1</sup>H NMR (400 MHz, CDCl<sub>3</sub>) δ ppm 8.23 (s, 2 H), 8.16 (s, 2 H), 7.99 (d, *J* = 8.0 Hz, 2 H), 7.82 (d, *J* = 8.0 Hz, 2 H) 1.64 (s, 9 H). <sup>13</sup>C NMR (101 MHz, CDCl<sub>3</sub>) δ ppm 149.0, 132.1, 130.3, 128.4, 126.4, 125.7, 122.6, 122.6, 122.1, 119.1, 35.0, 31.6. HRMS (ESI+) for C<sub>20</sub>H<sub>18</sub>Br [M + H]<sup>+</sup> calculated: 337.0586 found: 337.0588.



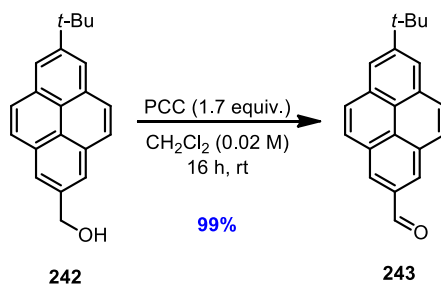
**Methyl 7-(*t*-Bu)pyrene-2-carboxylate (241):** 2-bromo-7-(*t*-Bu)pyrene (0.50 g, 1.5 mmol, 1.0 equiv.) and PPh<sub>3</sub> (0.16 g, 0.60 mmol, 40 mol %) were dissolved in anhydrous DMF (5.0 mL, 0.30 M) in a dry round bottom flask under N<sub>2</sub>. Anhydrous MeOH (2.4 mL, 59 mmol, 40 equiv.), Pd(OAc)<sub>2</sub> (67 mg, 0.30 mmol, 20 mol %) and anhydrous Et<sub>3</sub>N (0.83 mL, 5.9 mmol, 4.0 equiv.) were then added to the reaction mixture. CO was bubbled through the reaction *via* balloon for 30 minutes and the reaction mixture was left to stir at room temperature for 5 h. CO was again bubbled through the solution *via* balloon for 30 minutes and the reaction mixture was warmed up to 90 °C for 16 h. Upon completion, the reaction was diluted with EtOAc and water and the phases separated. The aqueous phase was extracted with EtOAc (3 times) and the combined organic extracts were washed with saturated CuSO<sub>4(aq)</sub> and brine and dried over Na<sub>2</sub>SO<sub>4</sub>. Following filtration through a Fisherbrand P8-creped coarse filter paper, the organic phase was concentrated under reduced pressure and purified by flash column chromatography (100% hexanes to 10% EtOAc/hexanes) to afford the desired product as a yellow solid (0.19 g, 40%). <sup>1</sup>H NMR (300

<sup>184</sup> Murphy, J. M.; Liao, X.; Hartwig, J. F. *J. Am. Chem. Soc.* **2007**, *129*, 15434.

**MHz, CDCl<sub>3</sub>**)  $\delta$  ppm 8.82 (s, 2 H), 8.25 (s, 2 H), 8.12 (d,  $J = 8.0$  Hz, 2 H), 8.09 (d,  $J = 8.0$  Hz, 2 H), 4.08 (s, 3 H), 1.59 (s, 9 H). **<sup>13</sup>C NMR (75 MHz, CDCl<sub>3</sub>)**  $\delta$  ppm 168.0, 150.6, 131.8, 130.8, 128.5, 127.8, 127.0, 127.0, 125.7, 122.8, 122.7, 52.5, 35.5, 32.0. **HRMS (ESI+)** for C<sub>22</sub>H<sub>21</sub>O<sub>2</sub> [M + H]<sup>+</sup> calculated: 317.1536 found: 317.1535.



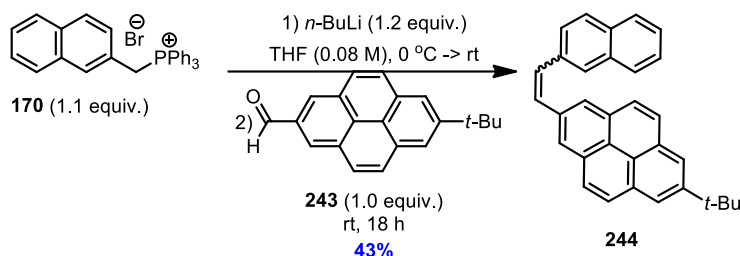
**(7-(*t*-Bu)pyren-2-yl)methanol (242):** Lithium aluminium hydride (0.250 g, 6.6 mmol, 6.0 equiv.) was suspended in anhydrous THF (7.3 mL, 0.15 M) in a dry round bottom flask under N<sub>2</sub> and the reaction mixture was cooled to 0 °C. Methyl 7-(*t*-Bu)pyrene-2-carboxylate (0.35 g, 1.1 mmol, 1.0 equiv.) was added and the reaction was left to stir at 0 °C for 30 min and then allowed to warm up to room temperature and left to stir for 6–12 h. Careful monitoring of the reduction by TLC was required to prevent over-reduction. Upon complete consumption of ester **241**, the reaction was cooled to 0 °C and slowly quenched with 10% NaOH and H<sub>2</sub>O. An excess of Rochelle's salt was then added and the mixture was left to stir overnight. The reaction was diluted with EtOAc and the phases separated. The aqueous phase was extracted with EtOAc (3 times) and the combined organic extracts were washed with brine and dried over Na<sub>2</sub>SO<sub>4</sub>. Following filtration, the organic phase was concentrated under reduced pressure and purified by flash column chromatography (100% hexanes to 30% EtOAc/hexanes) to afford **242** as a white solid. (0.25 g, 77% yield). **<sup>1</sup>H NMR (400 MHz, CDCl<sub>3</sub>)**  $\delta$  ppm 8.22 (s, 2 H), 8.16 (s, 2 H), 8.07 (d,  $J = 8.0$  Hz, 2 H), 8.04 (d,  $J = 8.0$  Hz, 2 H), 5.15 (d,  $J = 4.0$  Hz, 2 H), 1.59 (s, 9 H). **<sup>13</sup>C NMR (101 MHz, CDCl<sub>3</sub>)**  $\delta$  ppm 149.1, 138.1, 131.2, 130.9, 127.9, 127.1, 124.1, 123.2, 122.7, 122.4, 65.9, 35.2, 31.9. **HRMS (ESI+)** for C<sub>21</sub>H<sub>21</sub>O [M + H]<sup>+</sup> calculated: 289.1587 found: 289.1585.



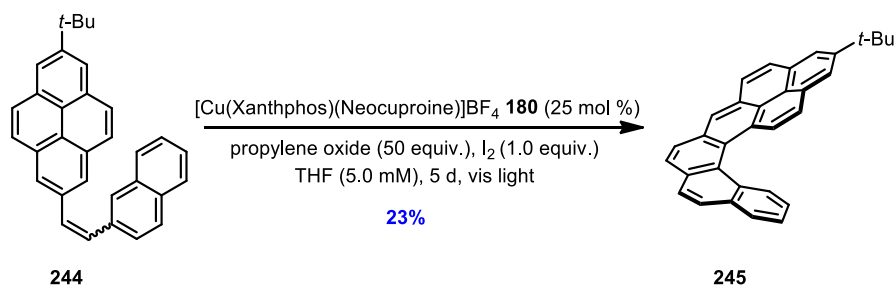
**7-(*t*-Bu)pyrene-2-carbaldehyde (243):** 7-(*t*-Bu)pyren-2-yl)methanol (41 mg, 0.14 mmol, 1.0 equiv.) was dissolved in DCM (7.0 mL, 0.02 M) in a round bottom flask. Pyridinium chlorochromate (0.13 g, 0.59 mmol, 1.7 equiv.) was added to the solution and the reaction mixture was left to stir overnight at ambient temperature. The reaction was diluted with Et<sub>2</sub>O and silica gel (~20 mg) was added. The mixture was filtered through a thin pad of silica gel, washed with Et<sub>2</sub>O and the filtrate concentrated under reduced pressure to afford the desired product **243** as a beige



solid (40 mg, 99%).  $^1\text{H NMR}$  (300 MHz,  $\text{CDCl}_3$ )  $\delta$  ppm 10.42 (s, 1 H), 8.60 (s, 2 H), 8.27 (s, 2 H), 8.12 (s, 4 H), 1.60 (s, 9 H).  $^{13}\text{C NMR}$  (101 MHz,  $\text{CDCl}_3$ )  $\delta$  ppm 193.0, 150.8, 133.0, 131.7, 131.0, 128.8, 127.8, 127.6, 125.4, 123.0, 122.5, 35.4, 31.8. **HRMS (ESI+)** for  $\text{C}_{21}\text{H}_{19}\text{O}$   $[\text{M} + \text{H}]^+$  calculated: 287.1430 found: 287.1425.

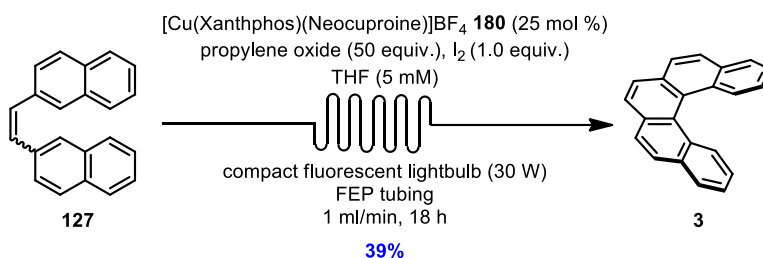


**2-(*t*-Bu)-7-(2-(naphthalen-2-yl)vinyl)pyrene (244)**: Freshly titrated *n*-BuLi (0.39 mL, 0.72 mmol, 1.15 equiv.) was added dropwise to a solution of (naphthalene-2-ylmethyl)triphenylphosphonium bromide **170** (307 mg, 0.63 mmol, 1.1 equiv.) in anhydrous THF (3 mL, 0.2 M) under  $\text{N}_2$  at 0 °C. The resulting yellow mixture was stirred for 1 h and a solution of 7-(*t*-Bu)pyrene-2-carbaldehyde **243** (165 mg, 0.57 mmol, 1 equiv.) in anhydrous THF (4 mL, 0.14 M) was added and the resulting red solution was stirred for 18 h. Water was added to the reaction mixture and the aqueous and organic phases separated. The aqueous layer was extracted with EtOAc (3 times) and the combined organic phases were washed with brine, dried over  $\text{Na}_2\text{SO}_4$ , filtered and concentrated *in vacuo*. The crude mixture was purified by column chromatography (100% hexanes) to afford product **244**, a mixture of *cis* and *trans* isomers, as a yellow solid (42 mg, 43%).  $^1\text{H NMR}$  (300 MHz,  $\text{CDCl}_3$ )  $\delta$  ppm = 8.33 (s, 2H), 8.22 (s, 2H), 8.11 - 8.02 (m, 4H), 7.98 (s, 1H), 7.93 - 7.82 (m, 5H), 7.63 (d,  $J = 2.1$  Hz, 2H), 7.59 - 7.43 (m, 2H), 1.61 (s, 9H).  $^{13}\text{C NMR}$  (75 MHz,  $\text{CDCl}_3$ )  $\delta$  ppm = 149.1, 134.9, 134.6, 133.8, 133.1, 131.3 (2C), 130.9 (2C), 129.6, 129.5, 128.4, 128.1, 128.0 (2C), 127.7, 127.3 (2C), 126.8, 126.4 (2C), 125.9, 124.3, 123.6, 122.9 (2C), 122.4 (2C), 35.2, 31.9 (3C). **HRMS (ESI+)**  $m/z$  calculated for  $\text{C}_{32}\text{H}_{26}\text{Ag}$   $[\text{M} + \text{Ag}]^+$ , 517.1080; found: 517.1077.



**Pyrene-[5]helicene (245)**:  $[\text{Cu}(\text{MeCN})_4]\text{BF}_4$  (6.7 mg, 0.02 mmol, 25 mol%) and Xantphos (12 mg, 0.02 mmol, 25 mol%) were dissolved in anhydrous THF (4.2 mL, 5 mM) in a round bottom flask. The mixture was stirred for 1 h at room temperature and Neocuproine (4.4 mg, 0.02 mmol, 25 mol%) was added as a solution in THF (5.3 mL, 4.0 mM). The resulting yellow solution was stirred for 1 h at ambient temperature. 2-(*t*-Bu)-7-(2-(naphthalen-2-yl)vinyl)pyrene **245** (35 mg, 0.09 mmol, 1.0 equiv.) was added followed by  $\text{I}_2$  (22 mg, 0.09 mmol, 1.0 equiv.), propylene oxide

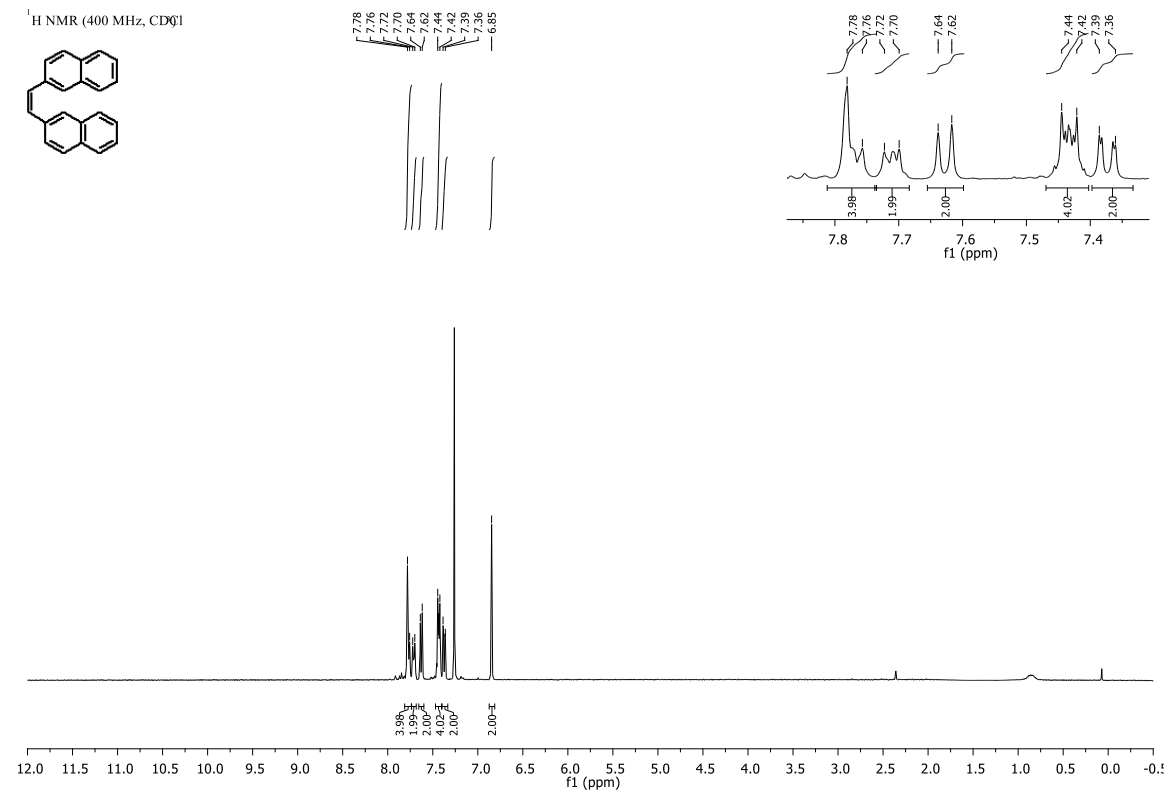
(0.30 mL, 4.3 mmol, 50 equiv.) and THF (8.0 mL) to achieve a final concentration of 5.0 mM with respect to **245**. The reaction was stirred in front of a compact fluorescent light bulb (30 W) for 120 h. The reaction was quenched with Na<sub>2</sub>S<sub>2</sub>O<sub>3</sub> (sat.) and diluted with EtOAc. The aqueous and organic phases were separated and the aqueous layer was extracted with EtOAc (3 times) and the combined organic extracts were washed with brine, dried over Na<sub>2</sub>SO<sub>4</sub>, filtered and concentrated. The crude mixture was purified by flash column chromatography (hexanes/toluene/diethyl ether, 70:20:10) to afford the desired product **XX** as a pale yellow solid (8.6 mg, 23%). <sup>1</sup>H NMR (400 MHz, CDCl<sub>3</sub>) δ ppm = 8.63-8.56 (d, *J* = 8.6 Hz, 1H and s, 1H), 8.43 (d, *J* = 8.6 Hz, 1H), 8.24 (s, 2H), 8.17 (m, 2H), 8.11 - 7.91 (m, 6H), 7.57 (t, *J* = 7.4 Hz, 1H), 7.33 (t, *J* = 7.4 Hz, 1H), 1.63 (s, 9H). <sup>13</sup>C NMR (75 MHz, CDCl<sub>3</sub>) δ ppm = 149.3, 132.5, 131.7, 131.5, 131.13, 131.05, 131.03, 130.0, 129.0, 129.1, 128.4, 128.2, 127.8, 127.6, 127.5, 126.9, 126.4, 126.2, 126.0, 125.2, 124.8, 124.0, 123.8, 123.6, 123.1, 122.8, 122.1, 35.2, 31.9 (3C). HRMS (ESI+) *m/z* calculated for C<sub>32</sub>H<sub>24</sub> [M]<sup>+</sup>, 408.1873; found: 408.1872.4.

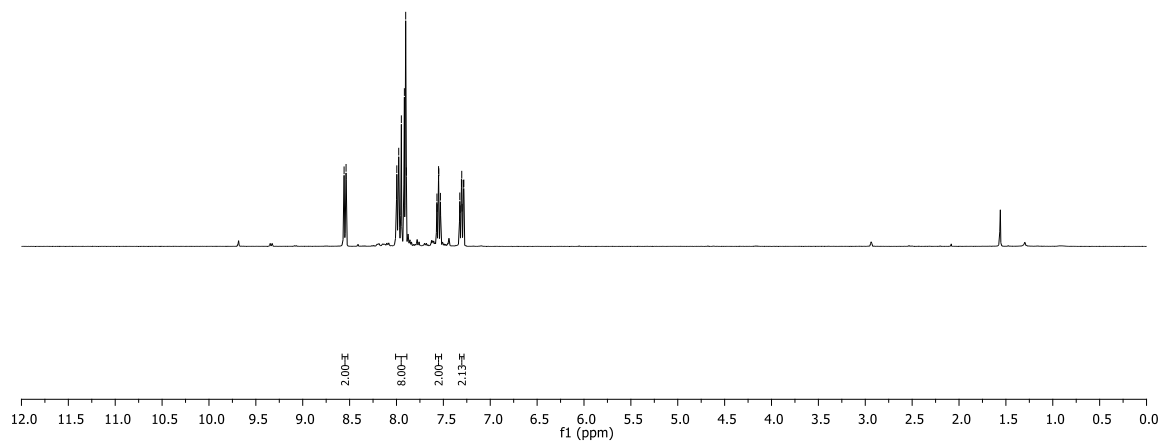
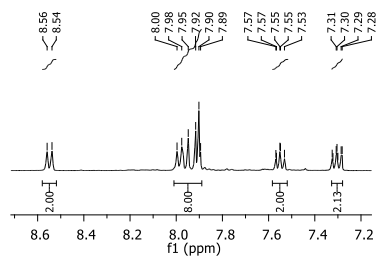
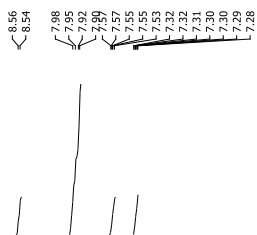
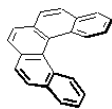


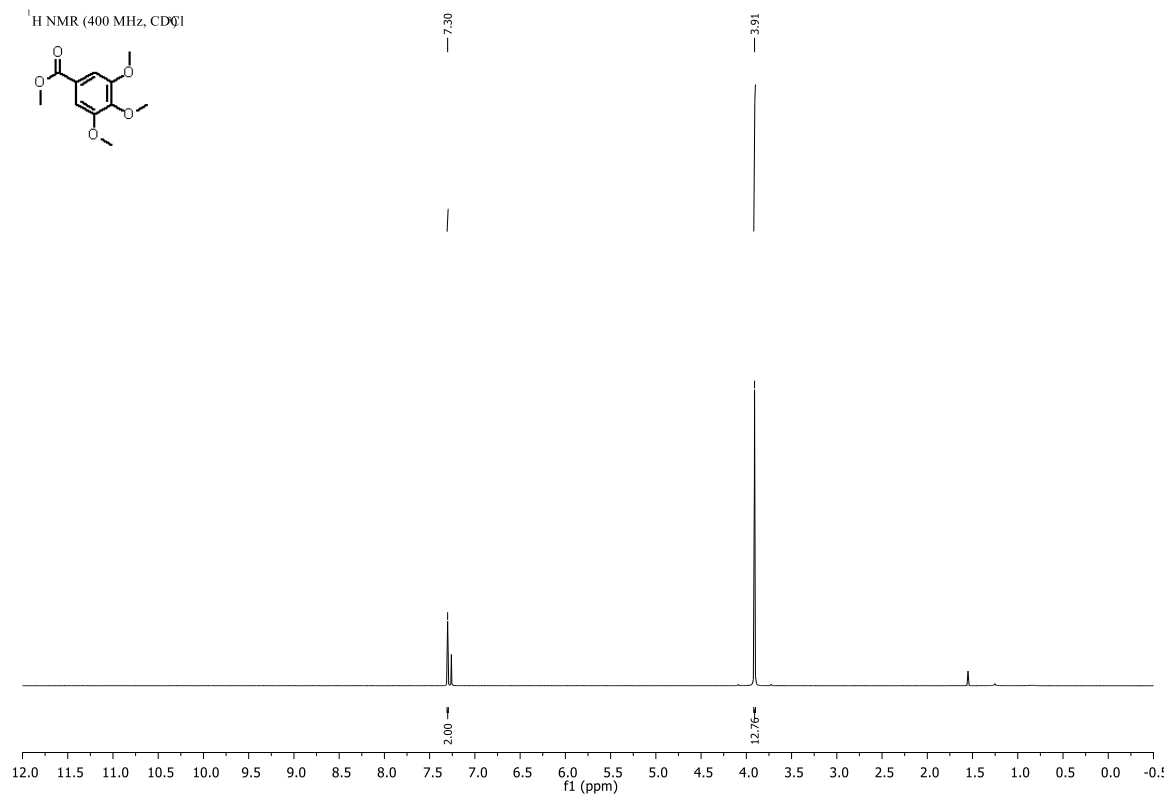
**[5]Helicene (3) using the Flow Reactor:** [Cu(MeCN)<sub>4</sub>]BF<sub>4</sub> (12 mg, 0.04 mmol, 25 mol %) and Xantphos (23 mg, 0.04 mmol, 25 mol %) were dissolved in THF (8.0 mL, 5.0 mM) in a round bottom flask. The mixture was stirred for 1 h at room temperature, Neocuproine (8.1 mg, 0.04 mmol, 25 mol%) was added as a solution in THF (10 mL, 4.0 mM) and the resulting yellow solution was stirred for 1 h.<sup>185</sup> 1,2-Di(naphthalen-2-yl)ethane **127** (44 mg, 0.16 mmol, 1.0 equiv.) was added to the mixture as a solution in THF (0.29 L, overall 0.5 mM), followed by I<sub>2</sub> (39 mg, 0.16 mmol, 1 equiv.) and propylene oxide (0.54 mL, 32 mmol, 50 equiv.). The reaction mixture was injected and cycled through the flow reactor for 18 h at a flow rate of 1 mL/min. The flow reaction was conducted in a FlowSyn Multi-X reactor purchased from Uniqsis and equipped with a modified HPLC pump. The reactor was connected to FEP tubing (fluorinated ethylene polymer tubing purchased from IDEX Health & Science, #1673) of natural colour with an outside diameter (OD) of 2 mm and an internal diameter (ID) of 1 mm. 9 m of FEP tubing was wrapped around four compact fluorescent light bulbs (30 W). FEP tubing was chosen due to its high transmittance, high chemical resistance and flexibility. Mild heating of the tubing during the reaction was observed. Following elution through the flow reactor, the reaction mixture was collected and quenched with a saturated sodium thiosulfate solution. The aqueous and organic phases were separated and the aqueous layer was extracted with EtOAc (3 times) and the combined organic layers were washed with brine, dried over Na<sub>2</sub>SO<sub>4</sub>, filtered and concentrated *in vacuo*. The crude mixture was purified by column chromatography (100% hexanes) to afford the desired product **3** as a pale yellow solid (17 mg, 39%). <sup>1</sup>H NMR spectrum corresponds to the literature.<sup>135</sup>

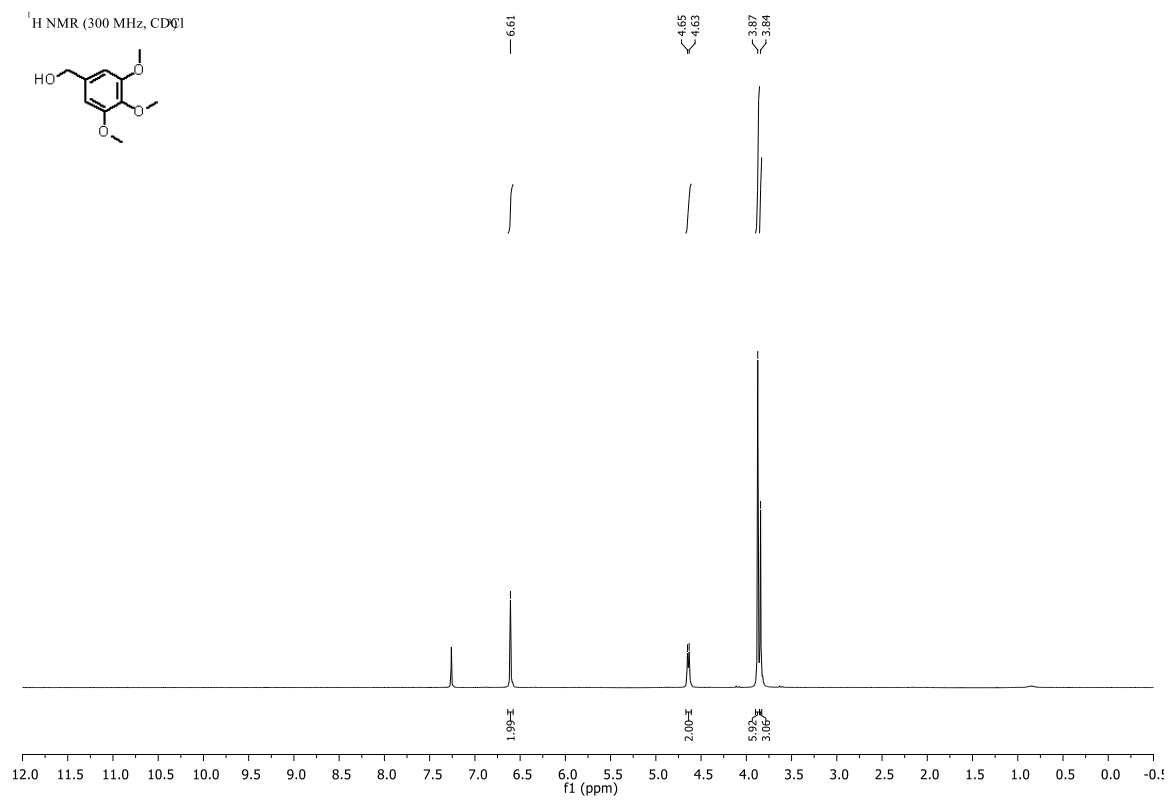
<sup>185</sup> For a procedure to form the discreet Cu catalyst see: Smith, C. S.; Branham, C. W.; Marquardt, B. J.; Mann, K. *R. J. Am. Chem. Soc.* **2010**, *132*, 14079-14085.

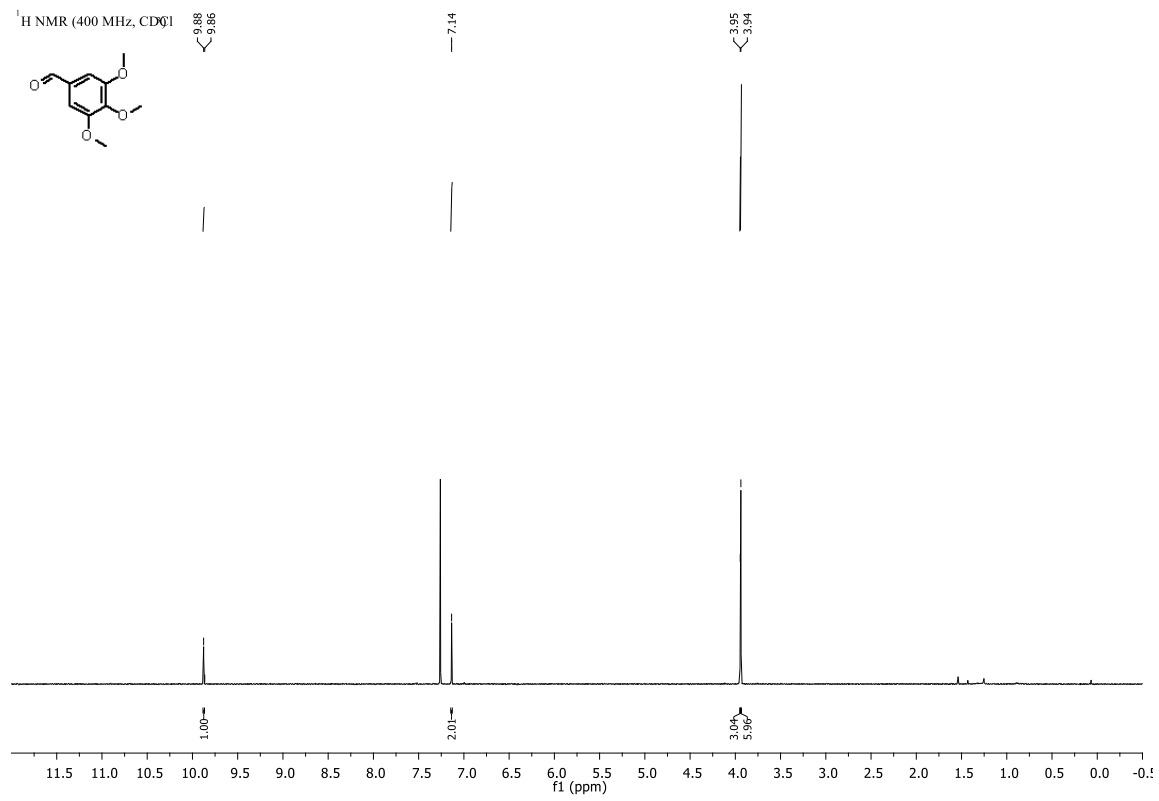
## ANNEX 1 - SPECTRAL DATA

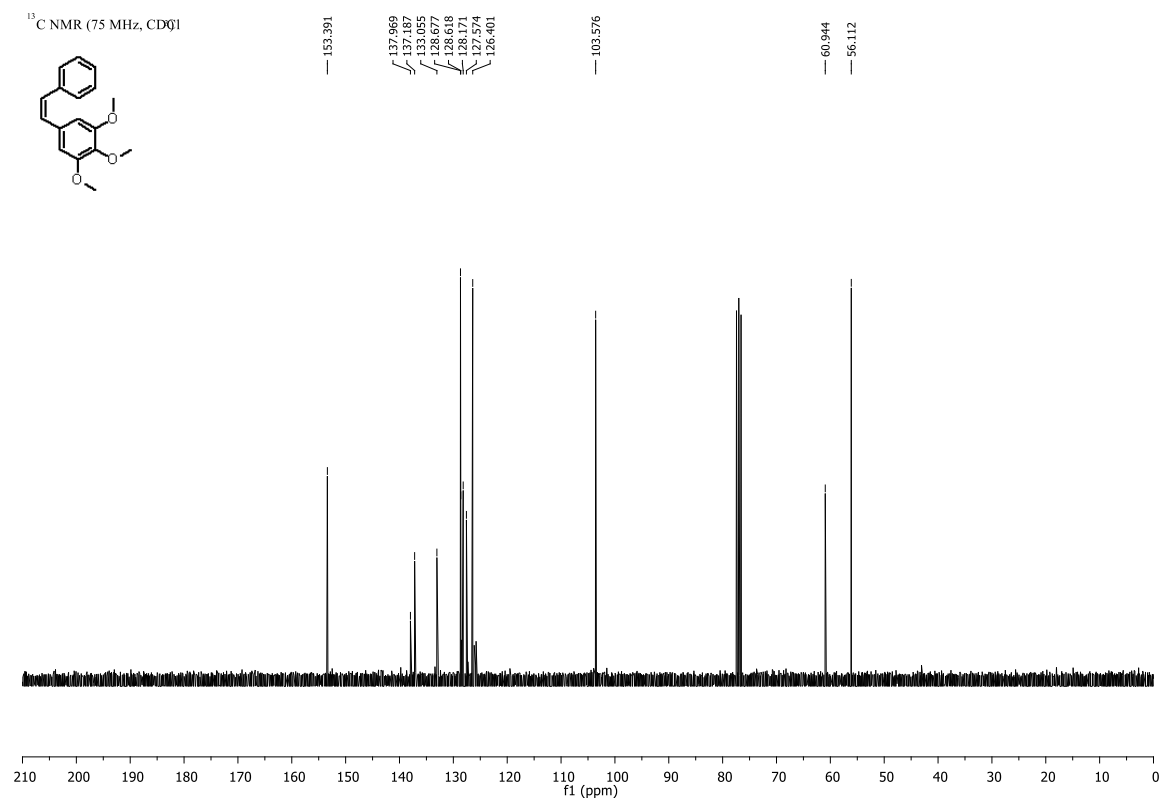
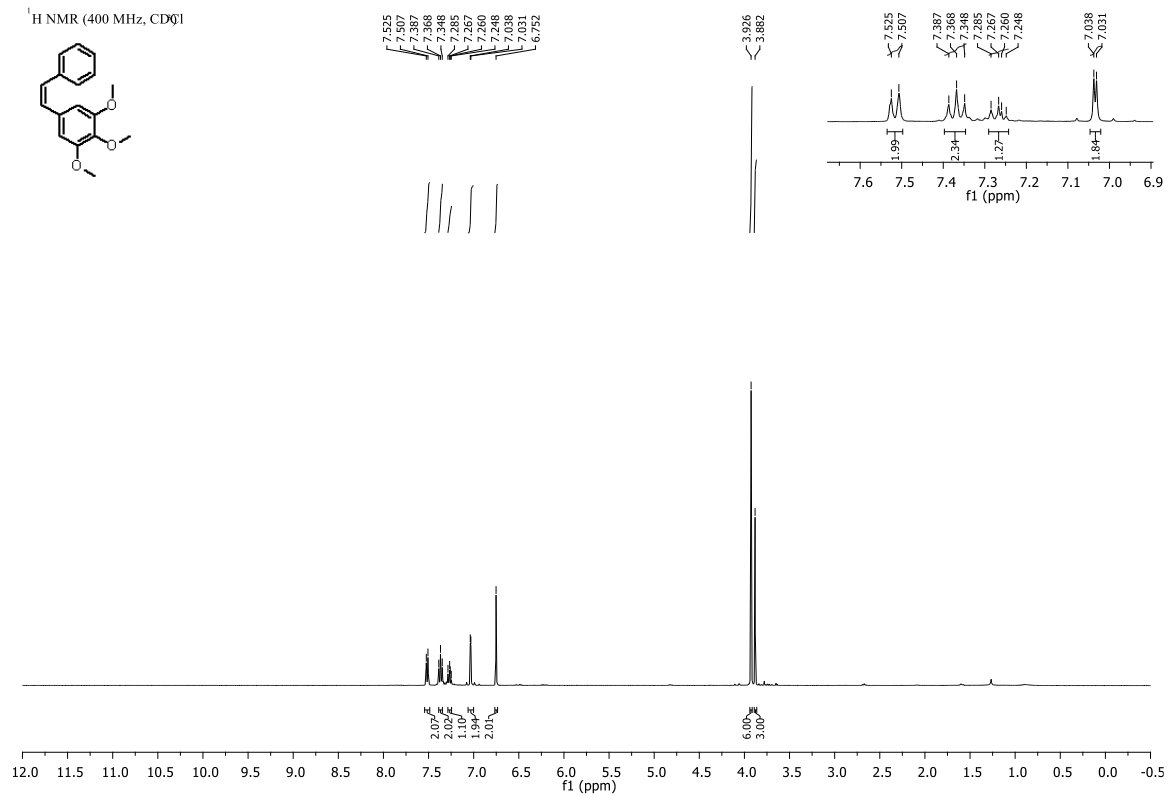


NMR (400 MHz, CDCl<sub>3</sub>)

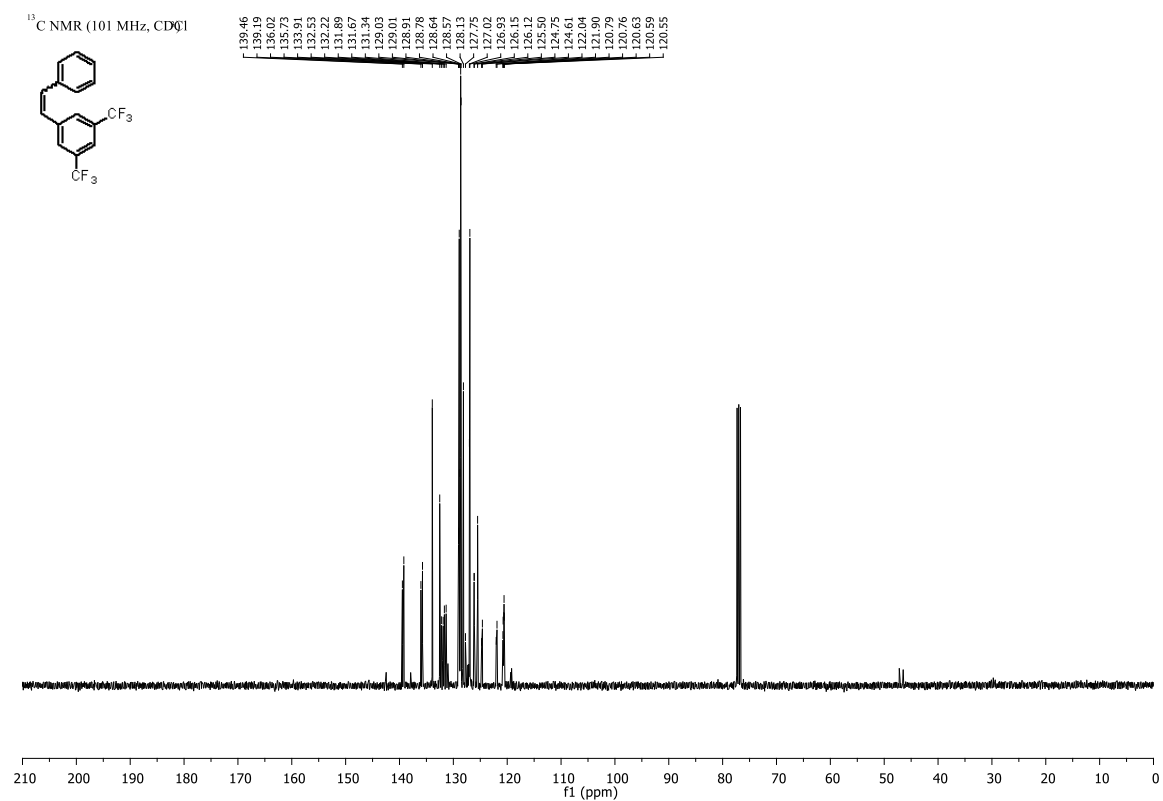
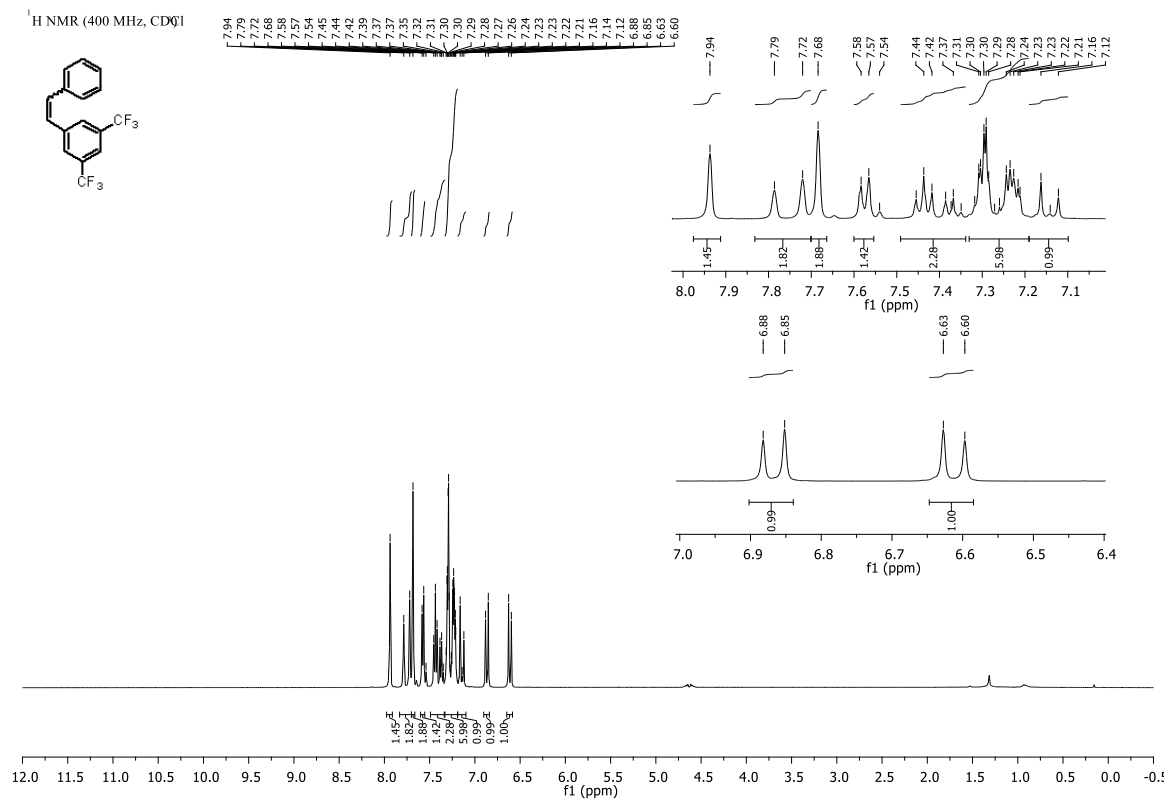




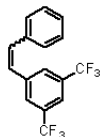




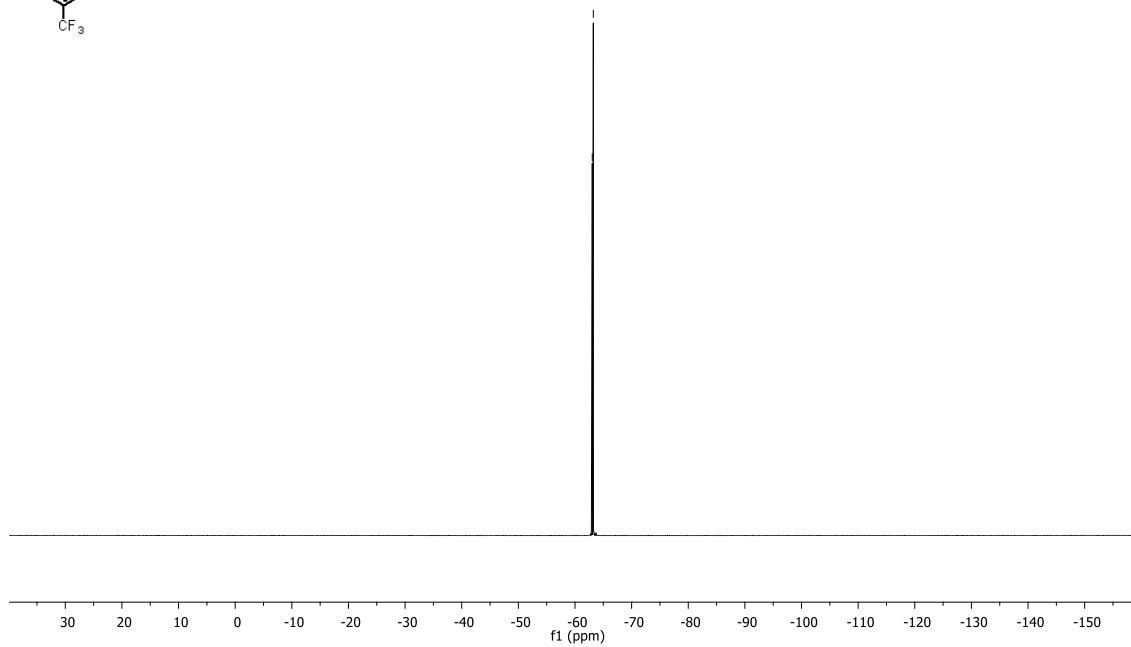


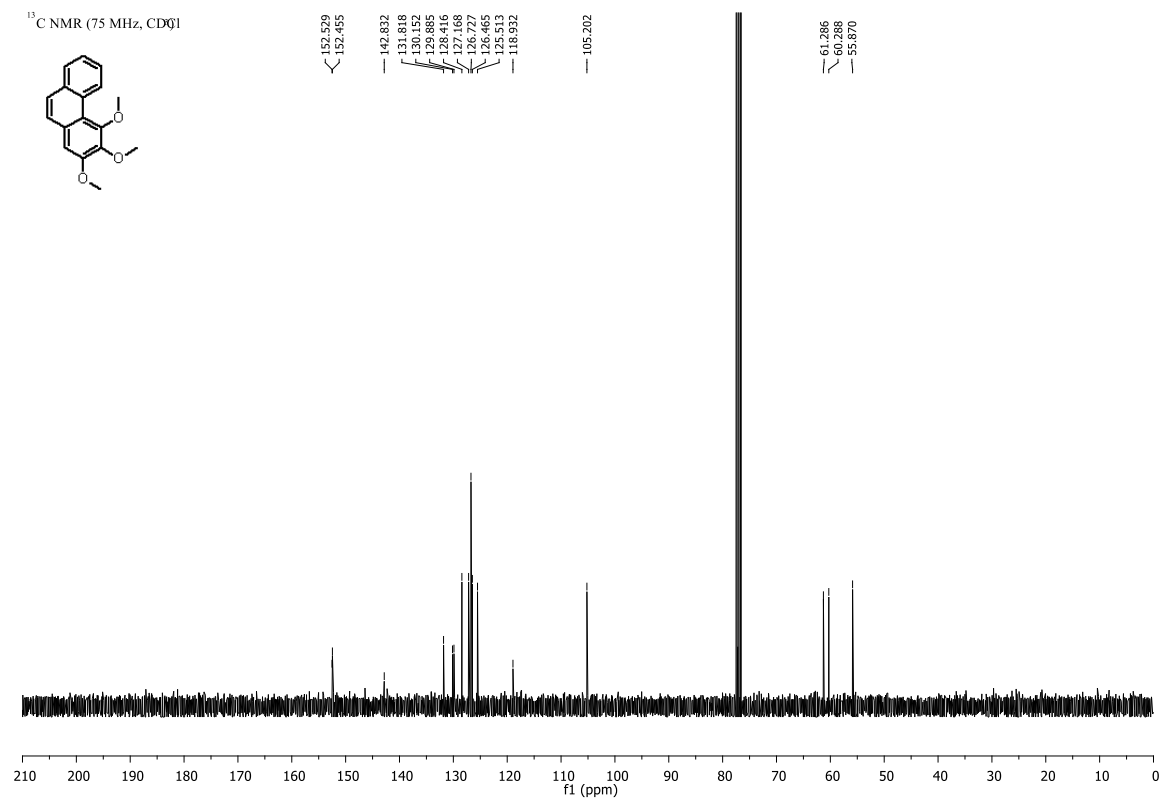
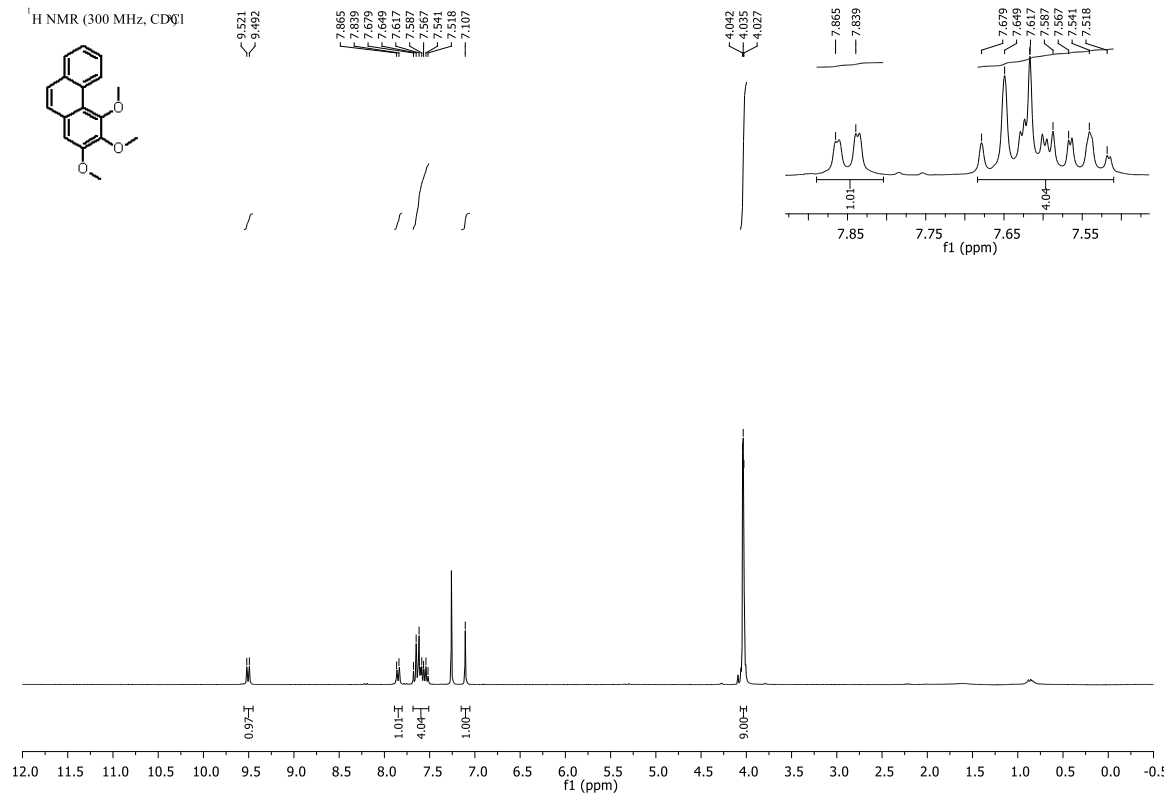


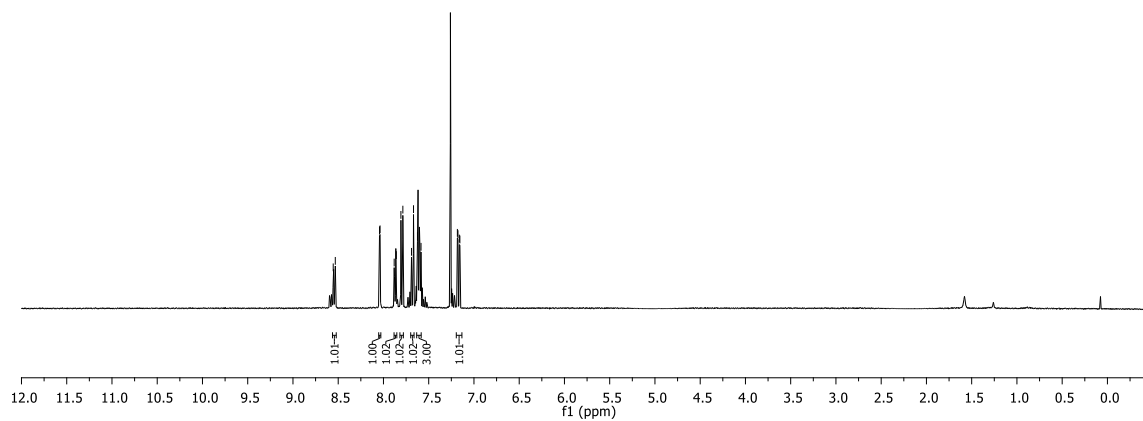
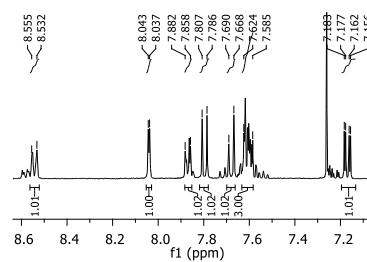
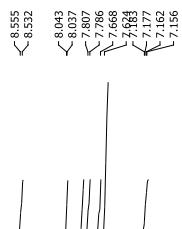
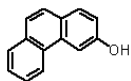
<sup>19</sup>F NMR (376 MHz, CDCl<sub>3</sub>)

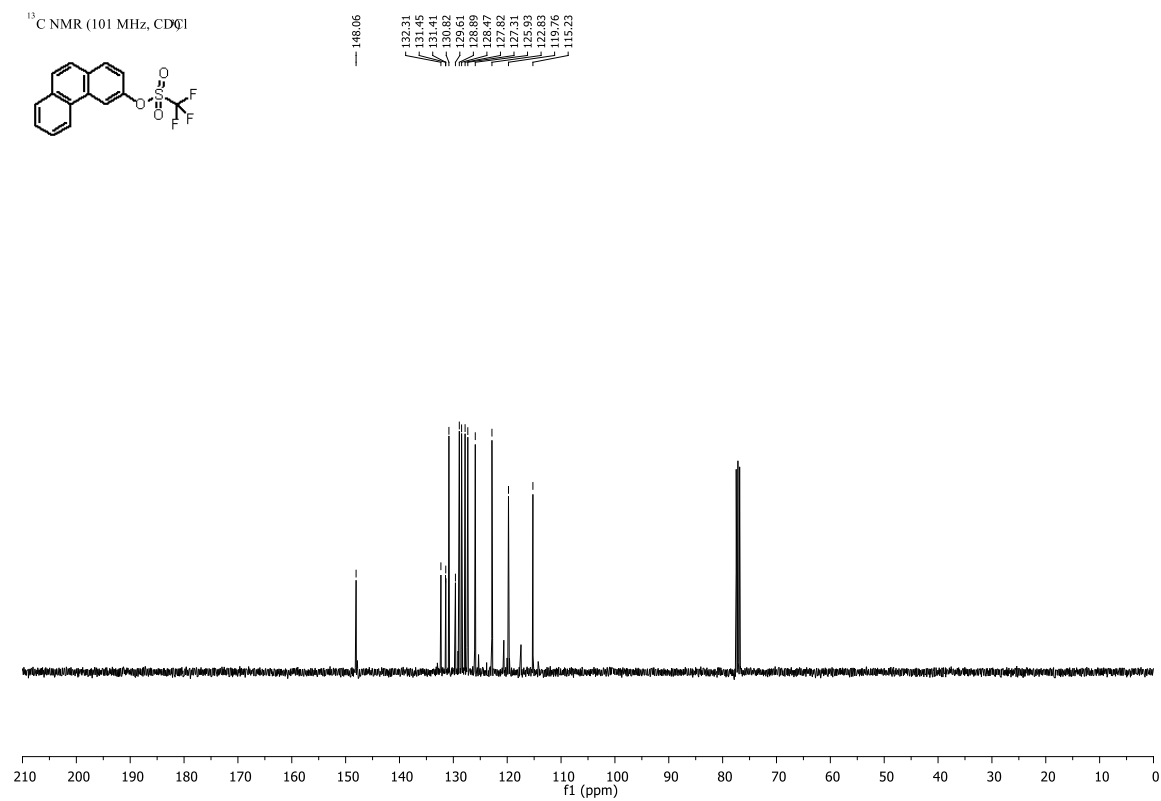
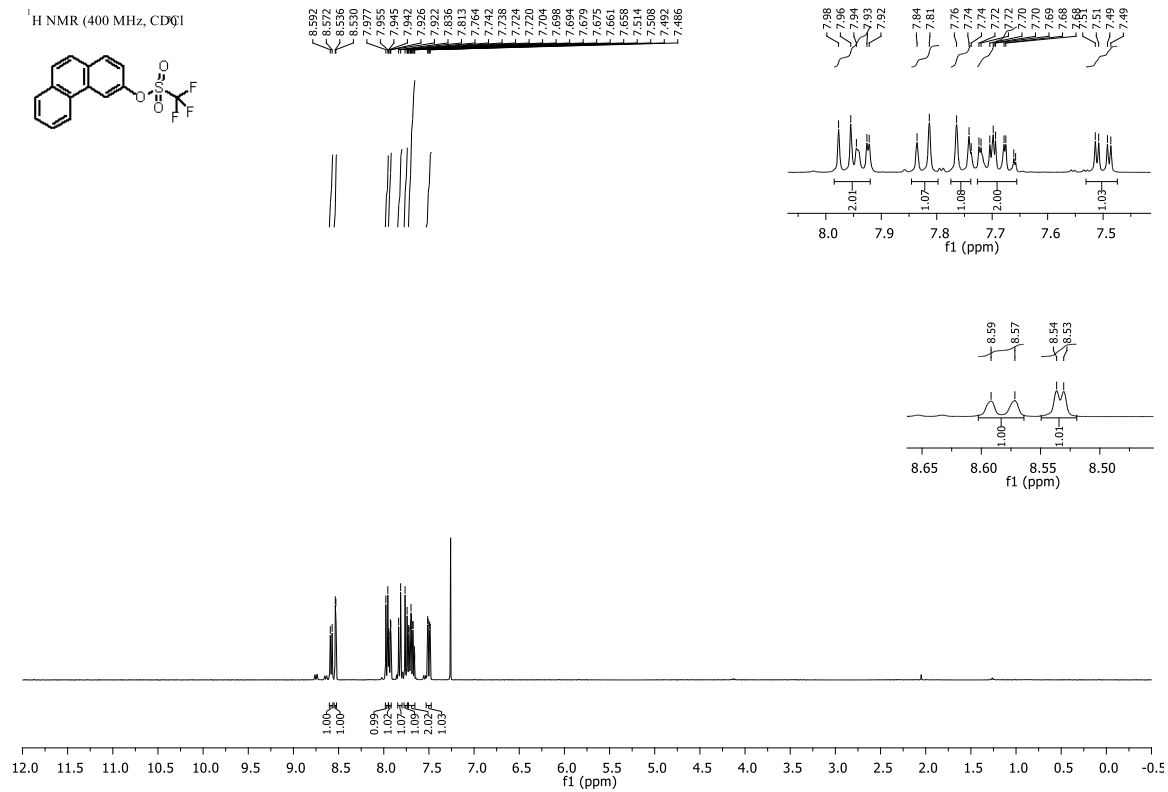


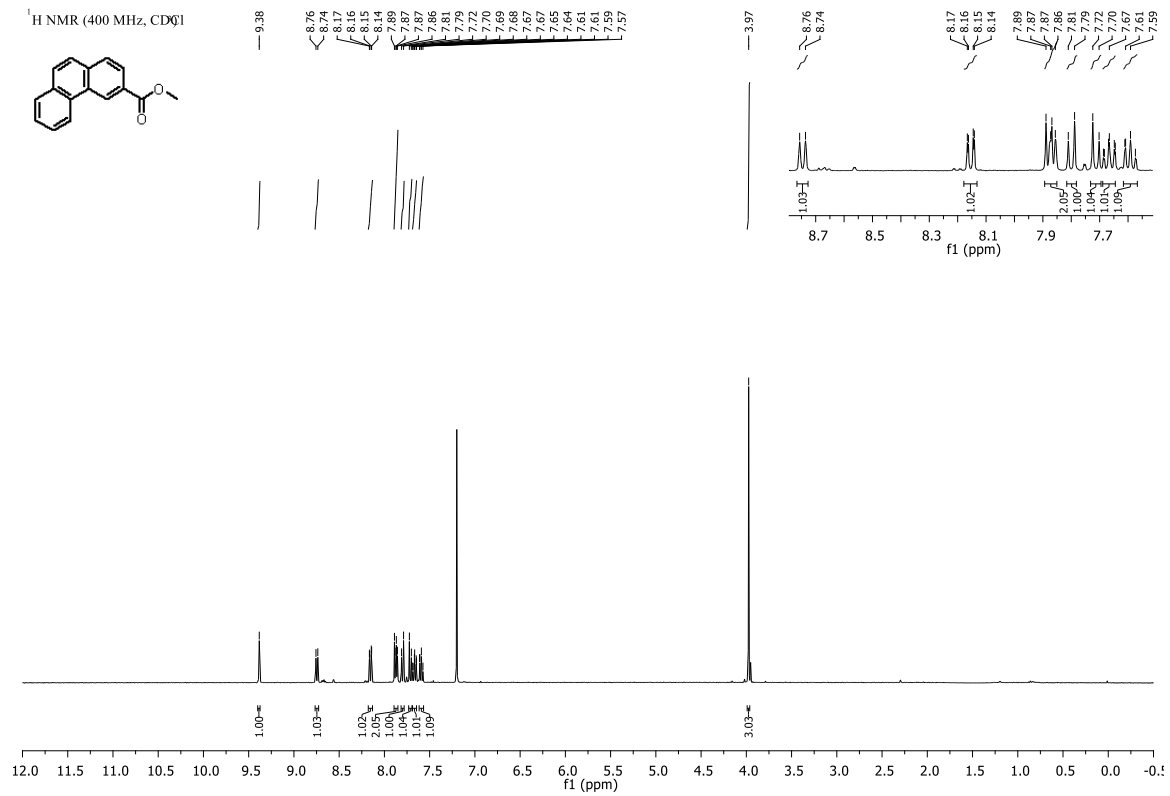
δ -63.05  
δ -63.23



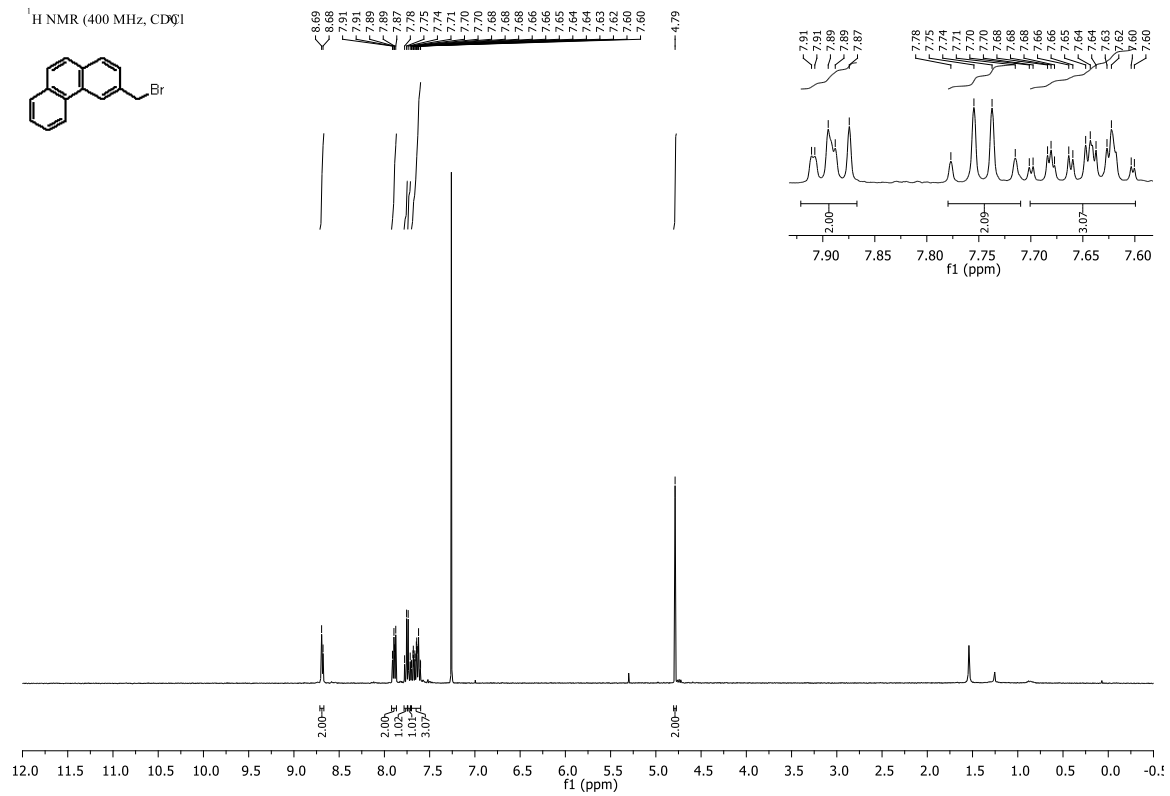


<sup>1</sup>H NMR (400 MHz, CDCl<sub>3</sub>)

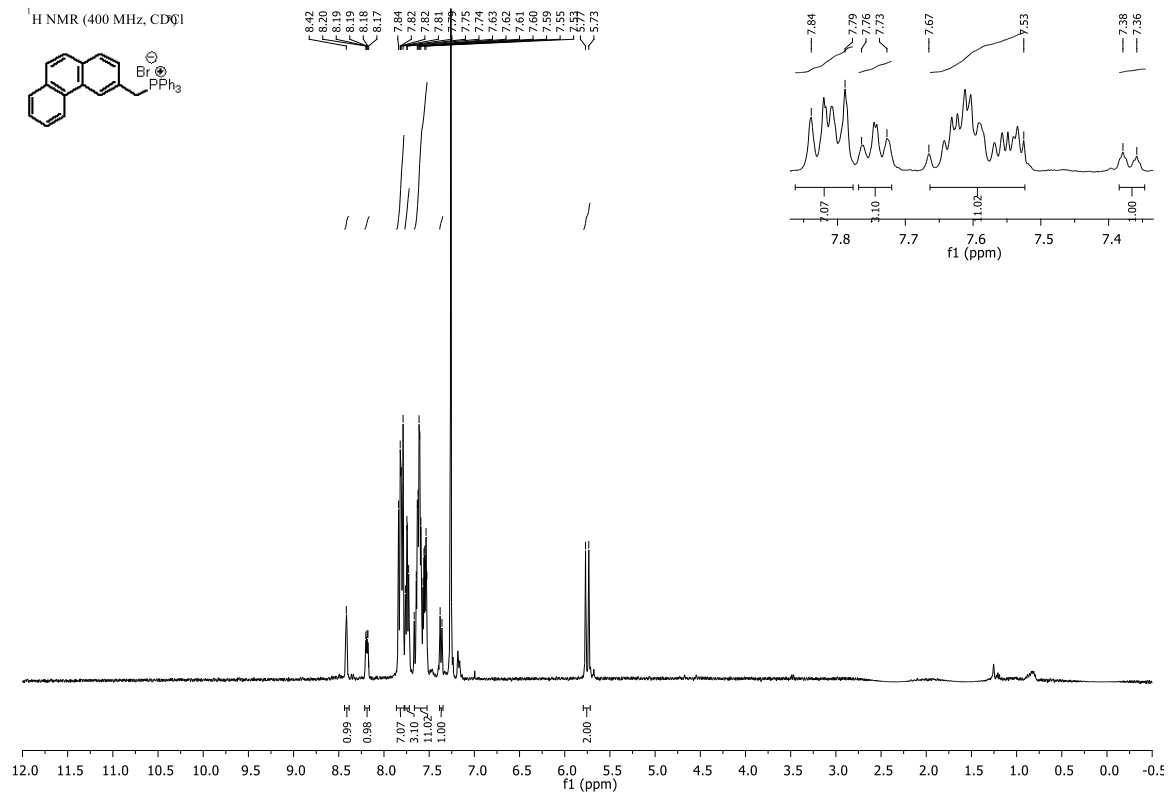


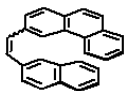




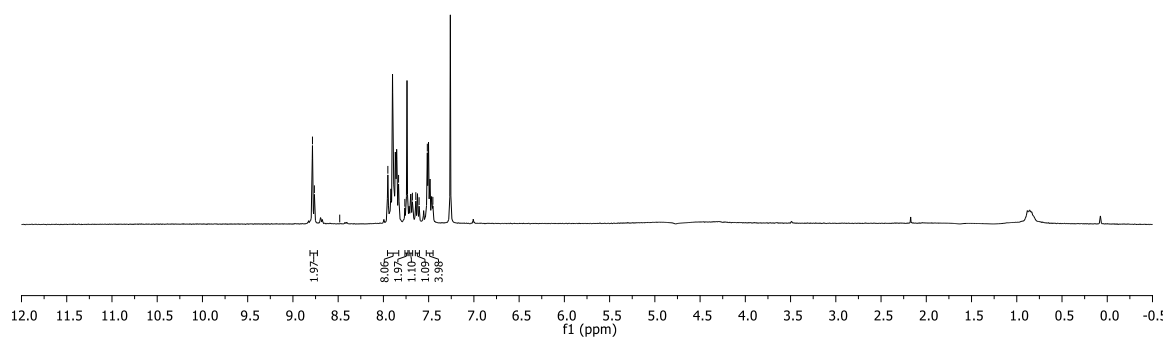
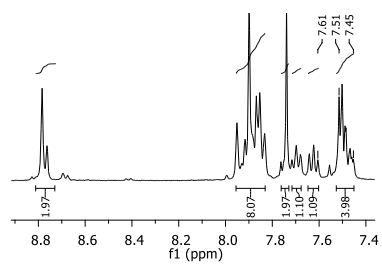


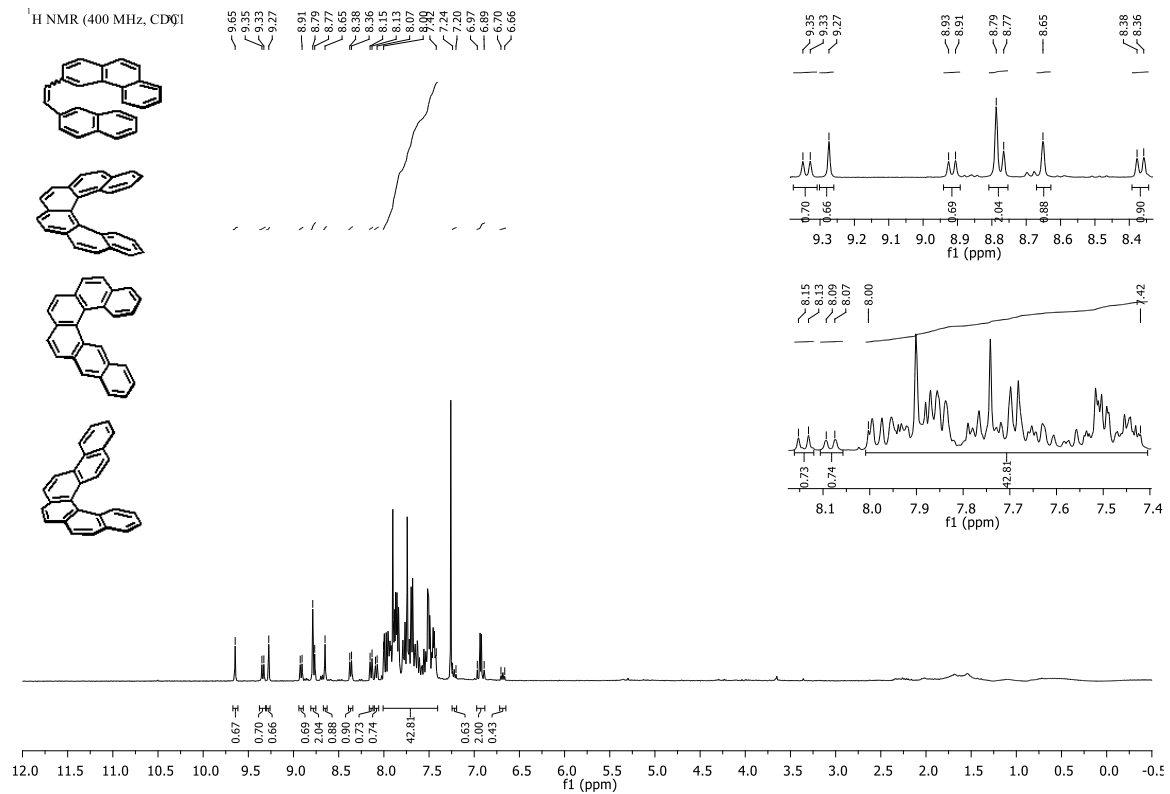


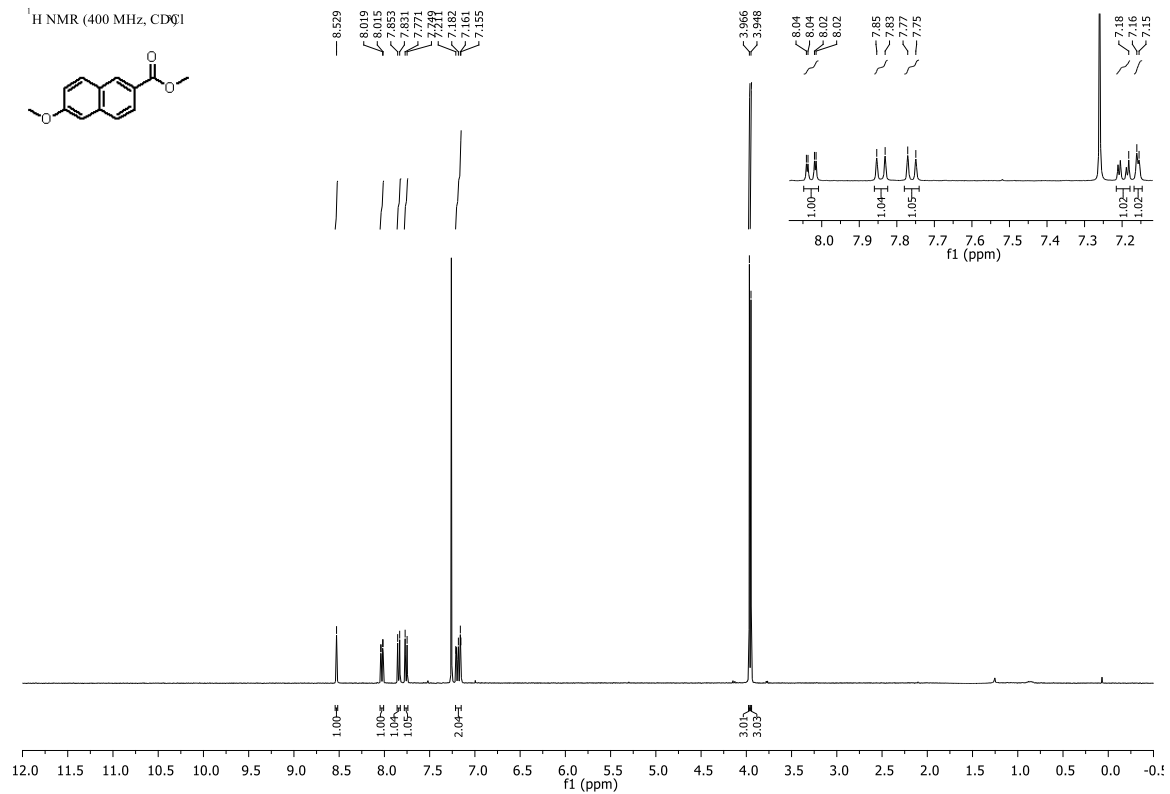


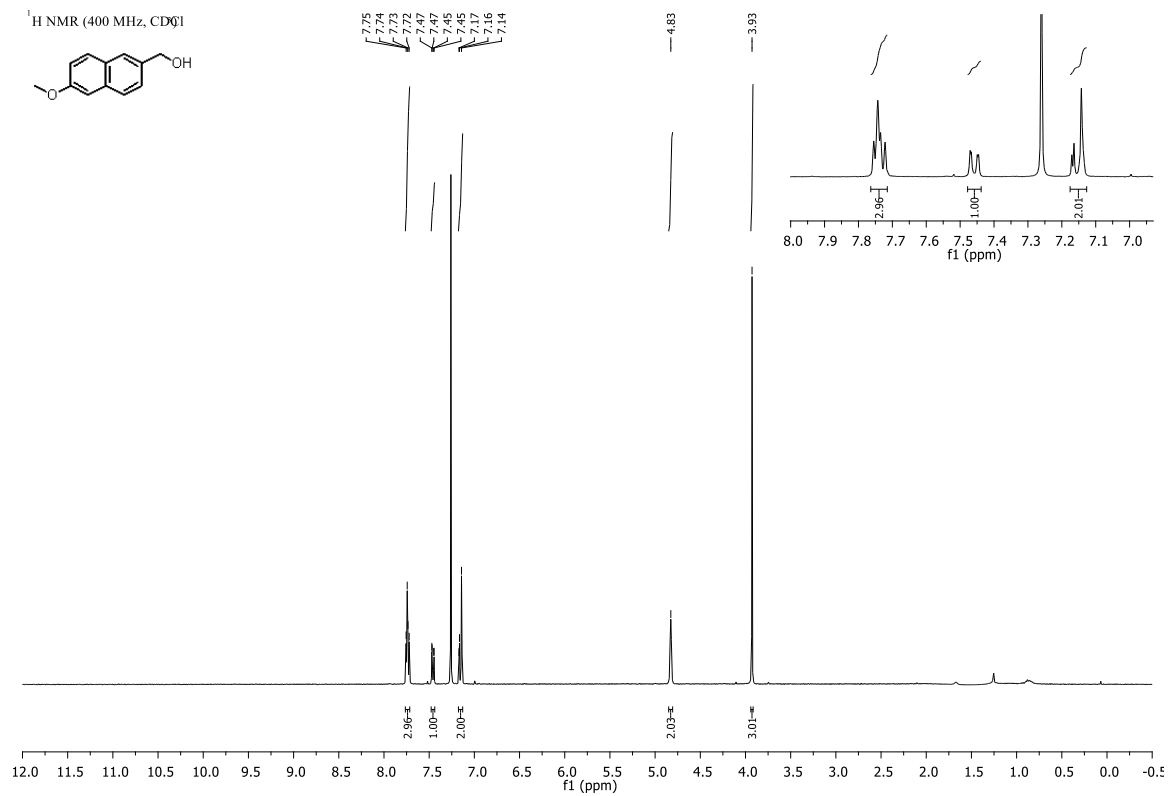
<sup>1</sup>H NMR (400 MHz, CDCl<sub>3</sub>)

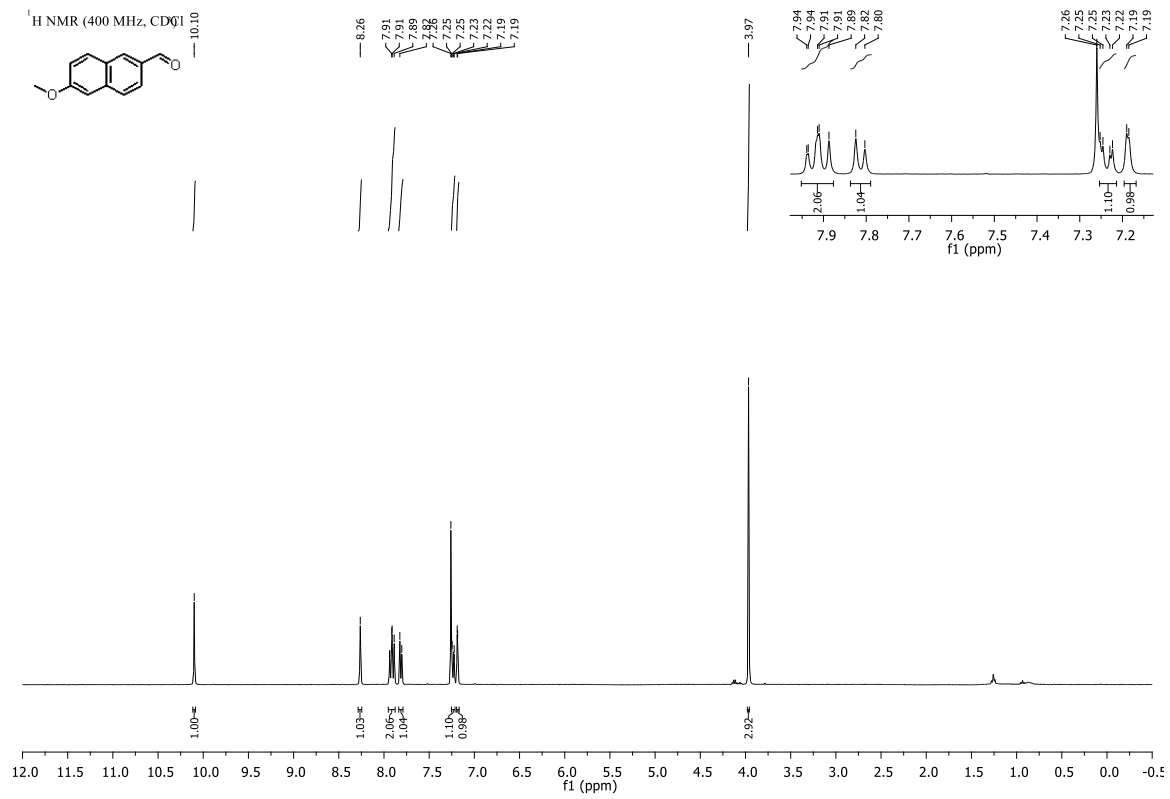
8.78  
8.76  
8.48  
7.95  
7.83  
7.76  
7.68  
7.64  
7.61  
7.51  
7.45

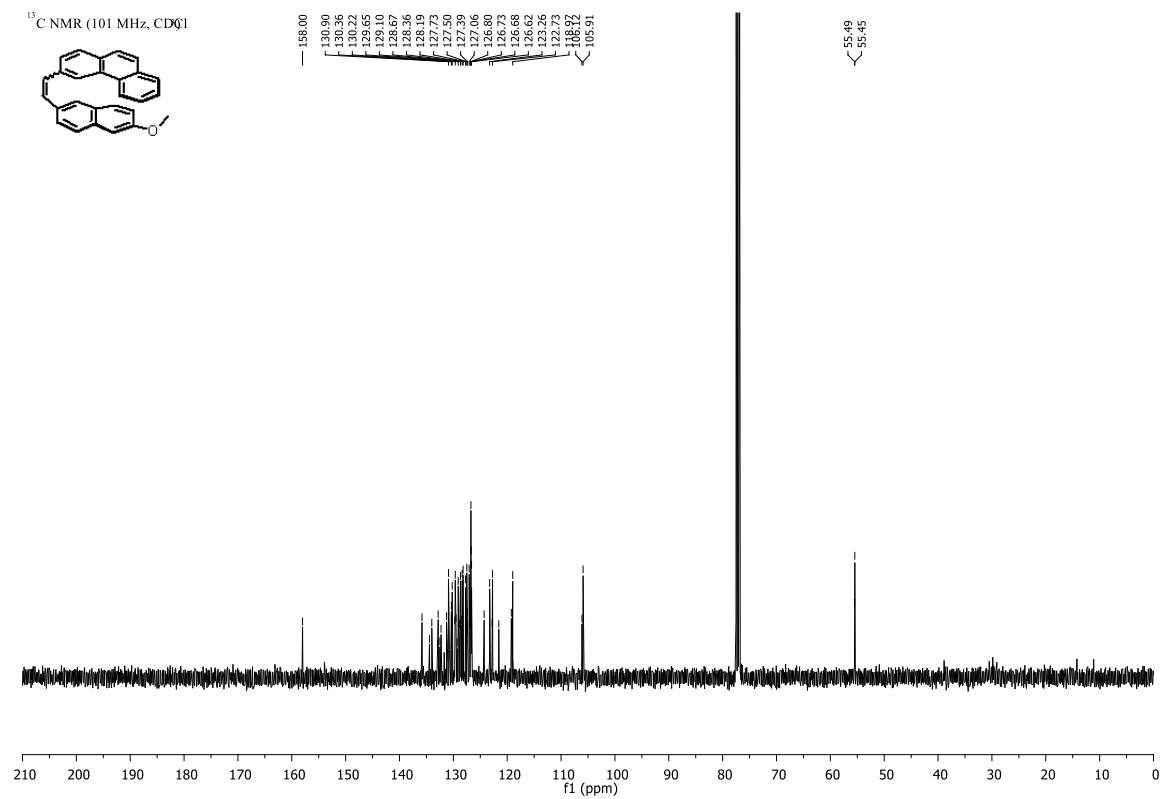
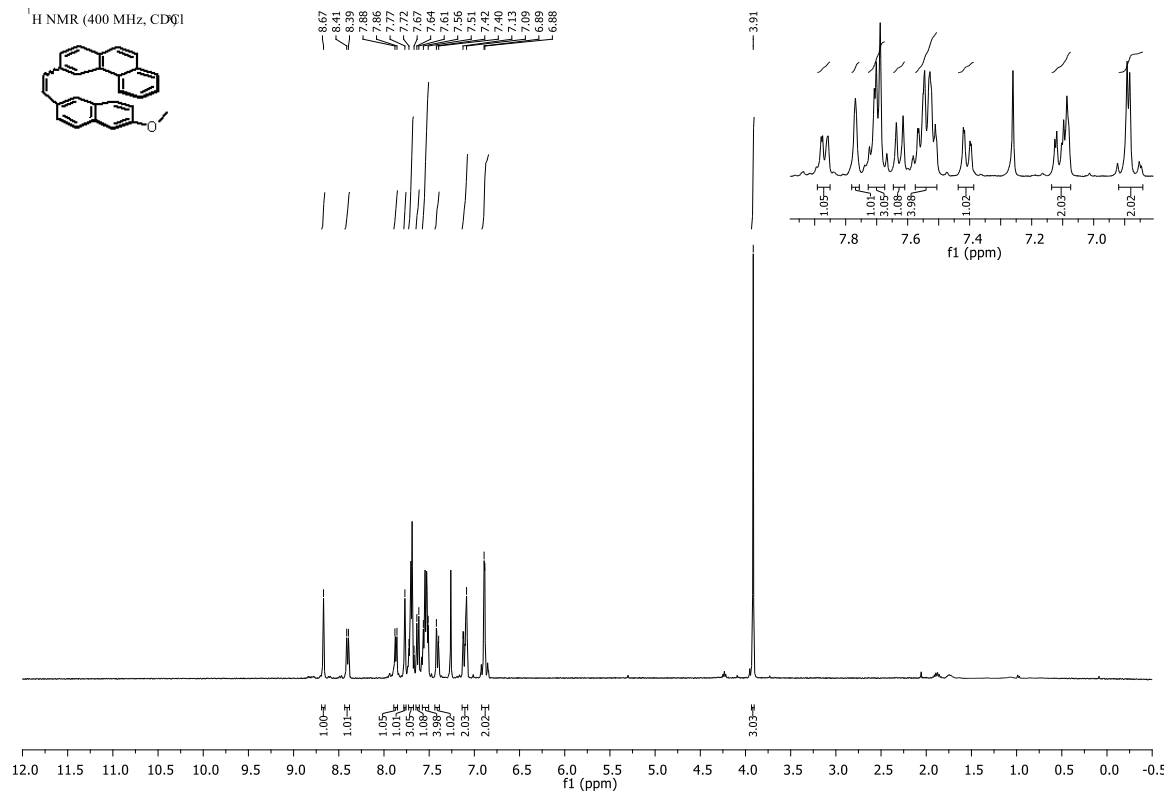


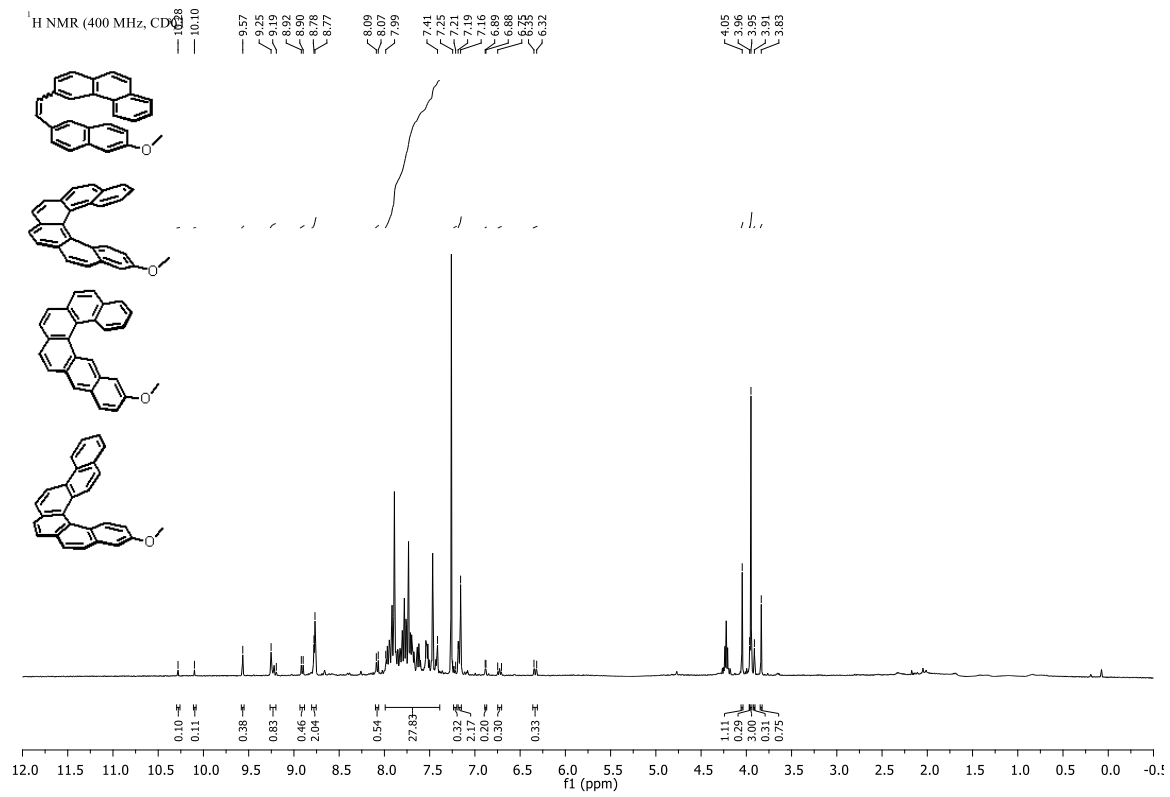




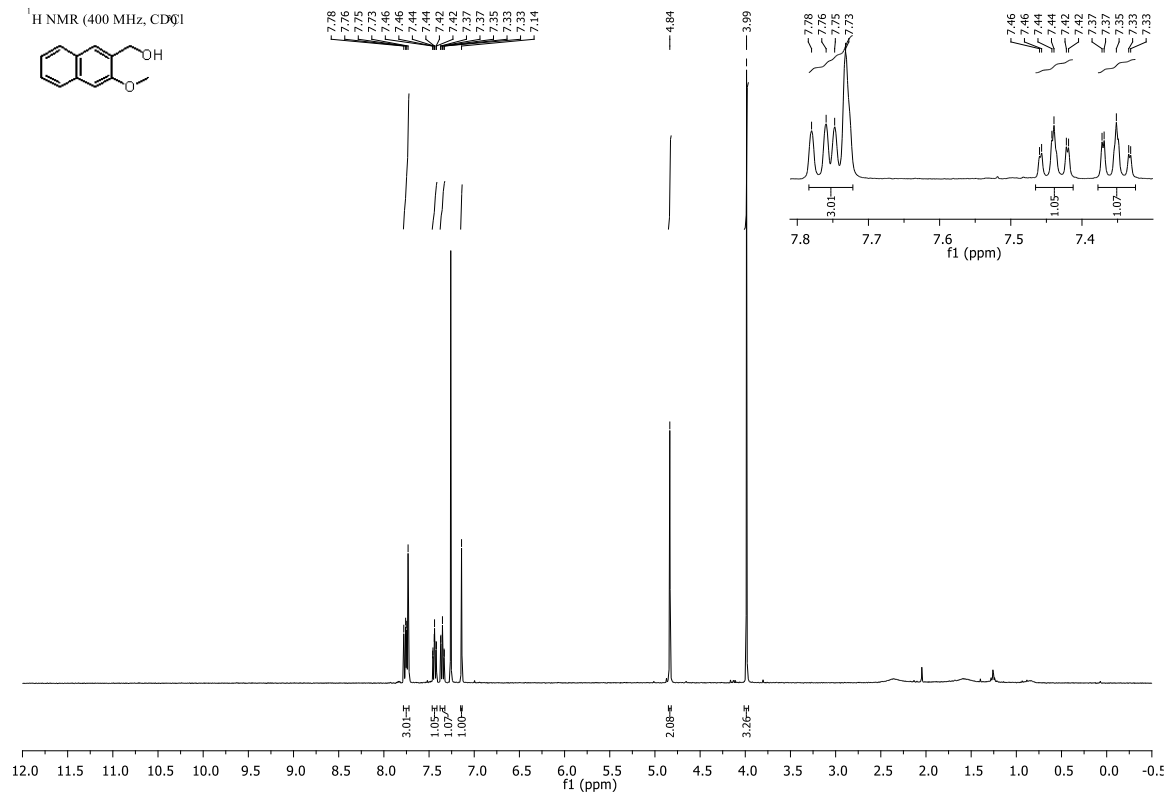


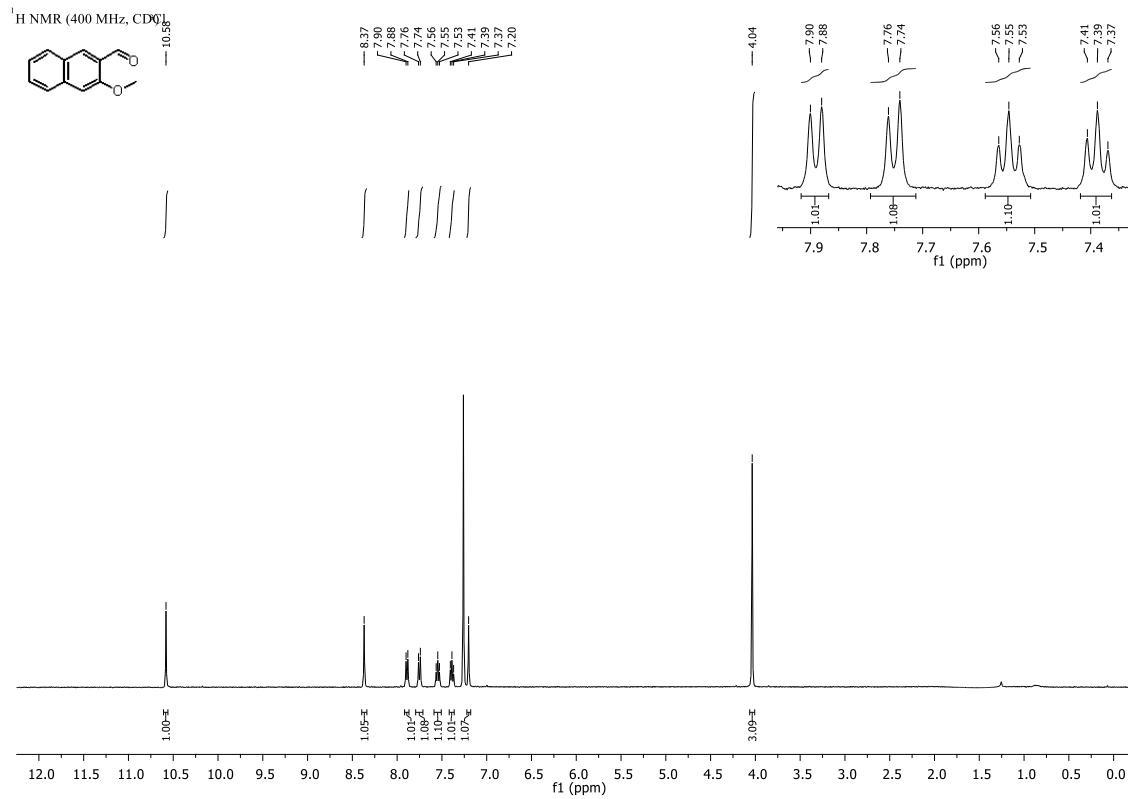


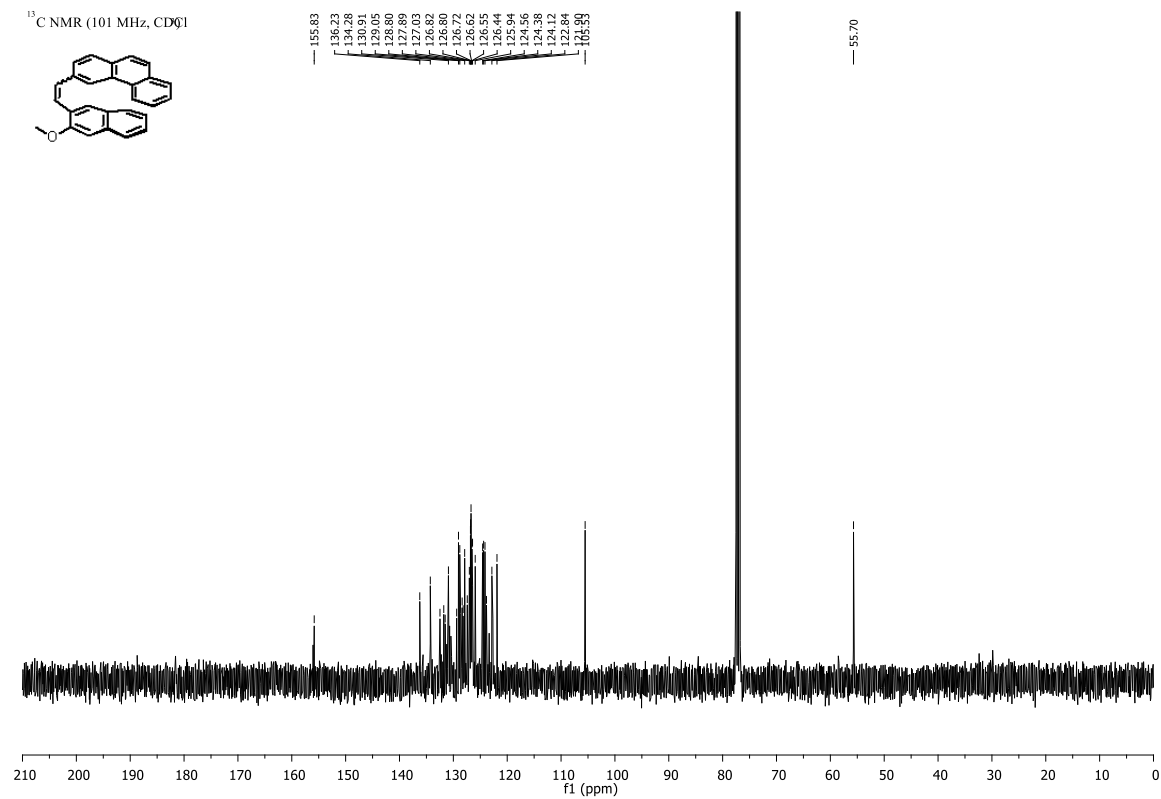
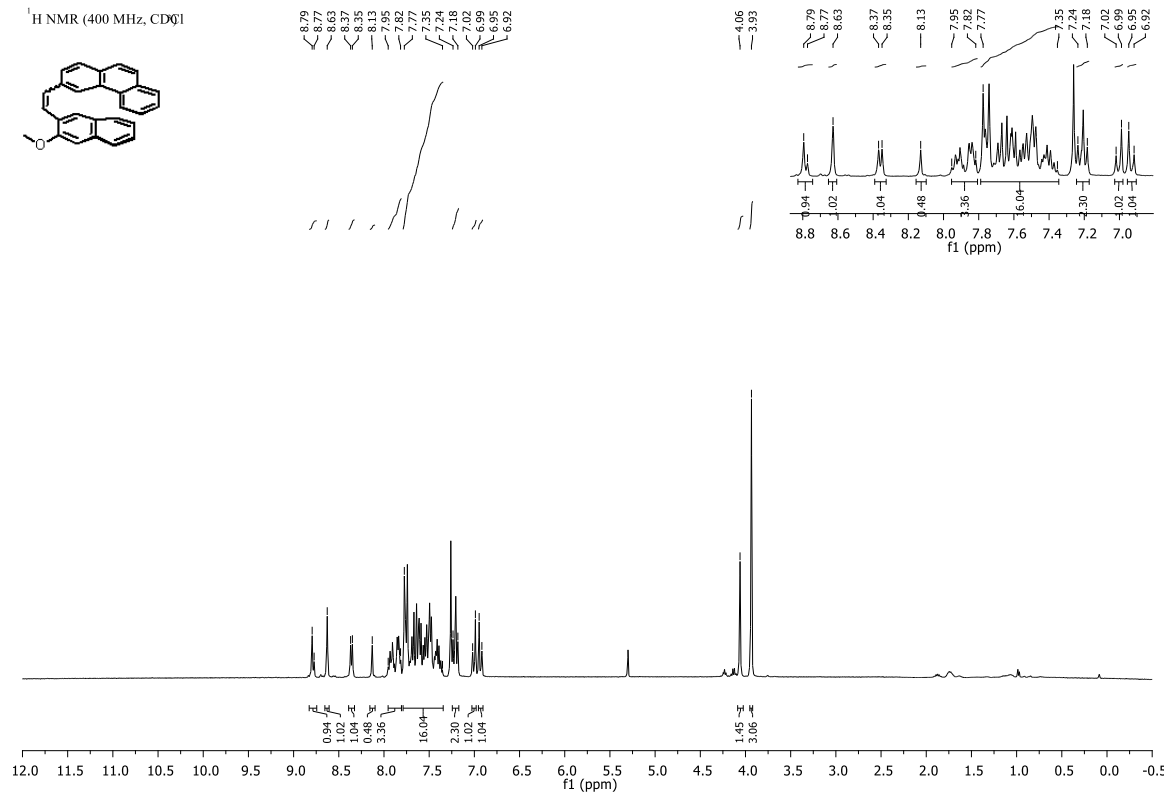


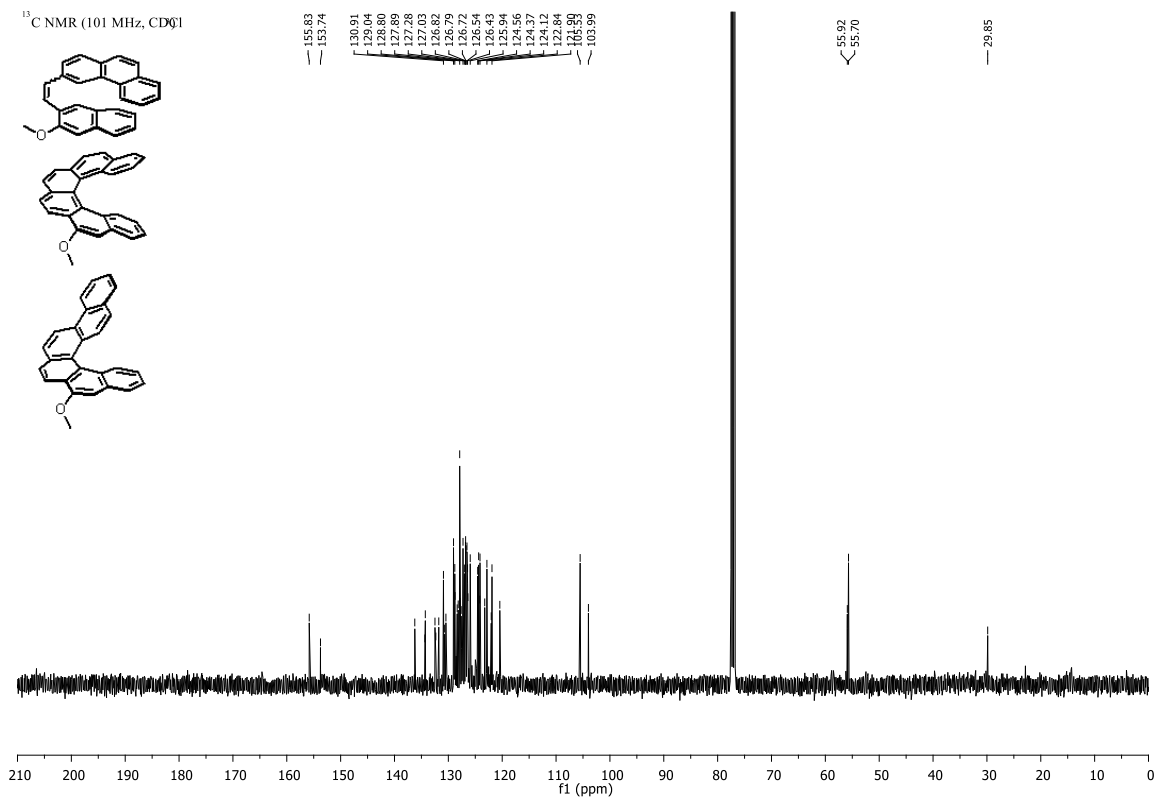
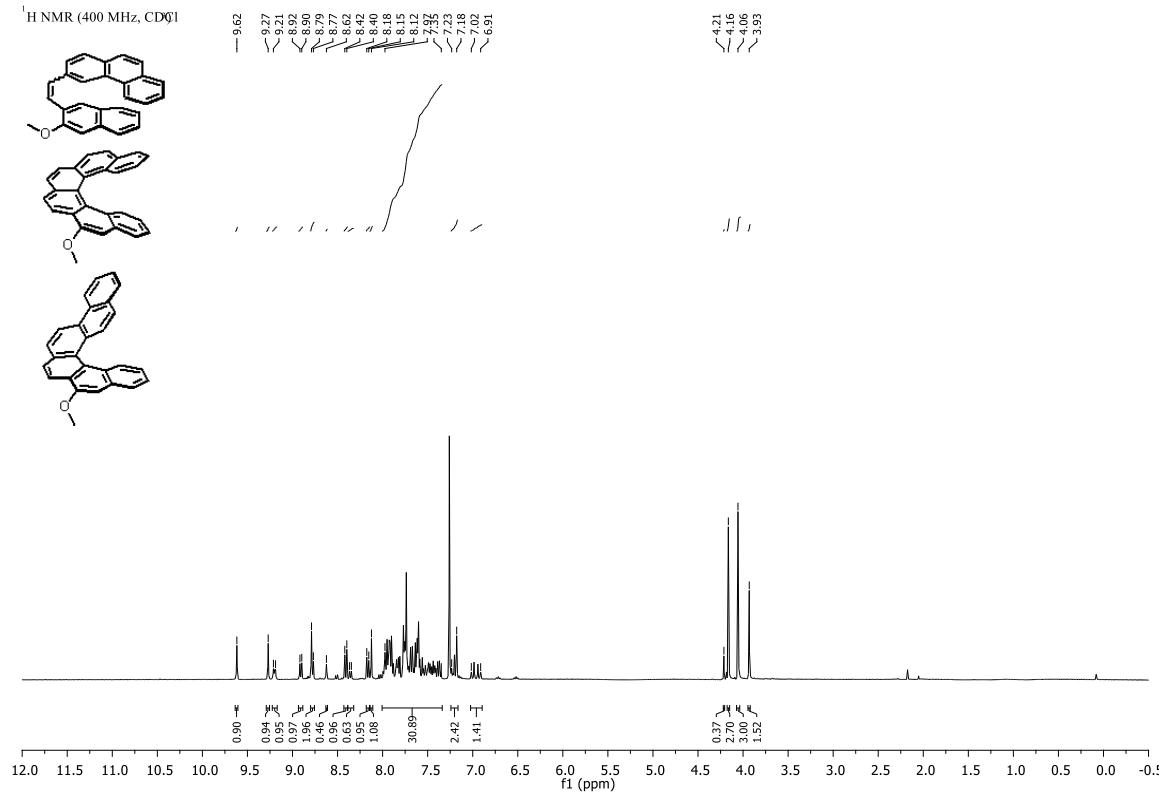


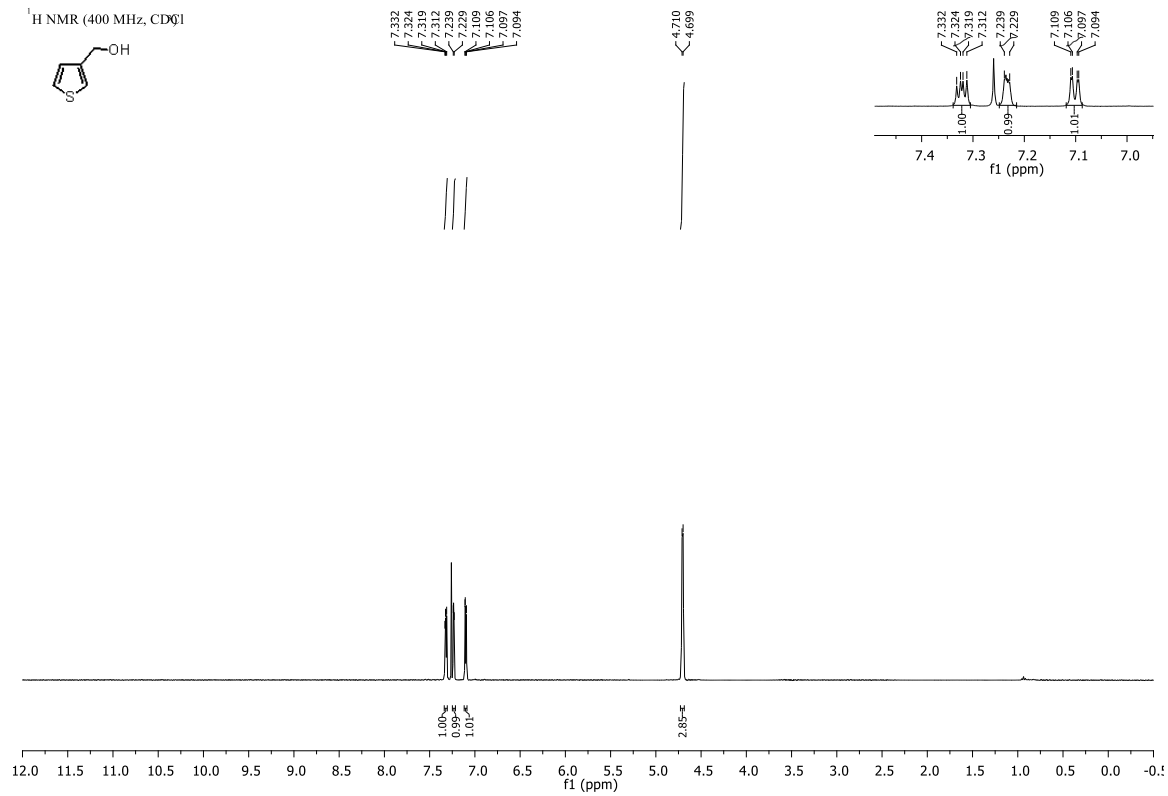










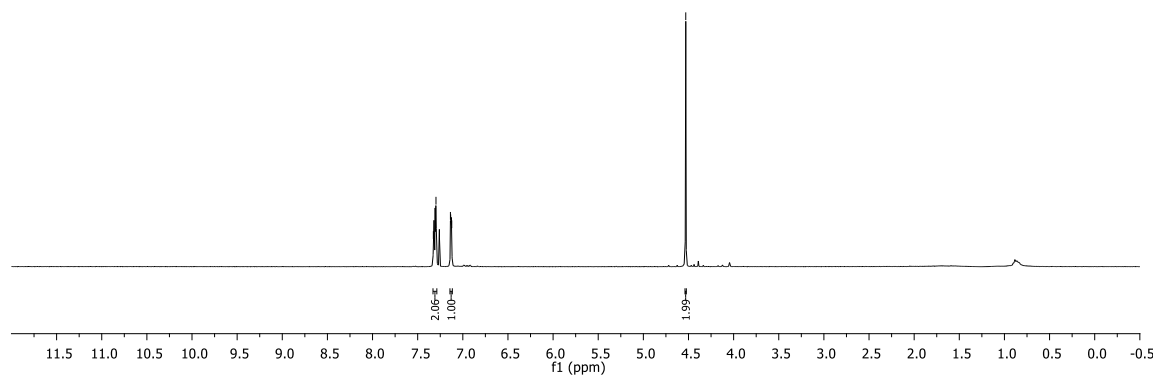
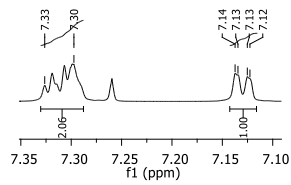


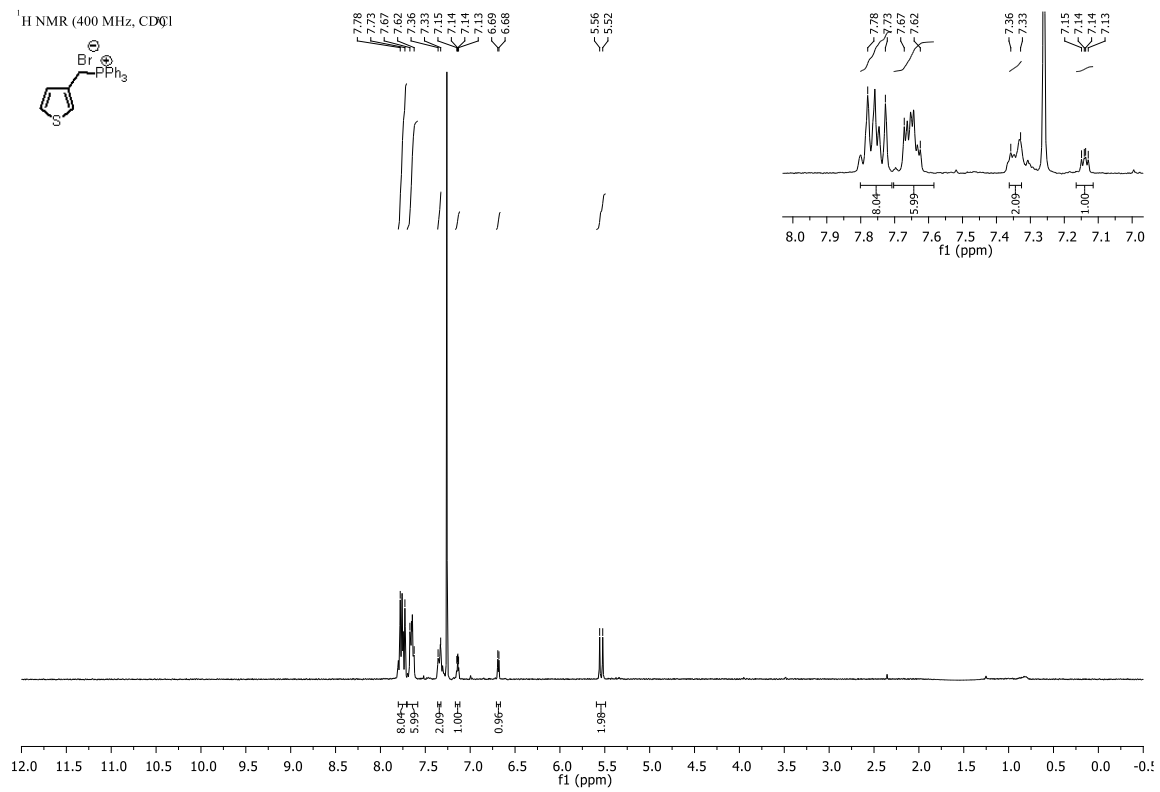
<sup>1</sup>H NMR (400 MHz, CDCl<sub>3</sub>)



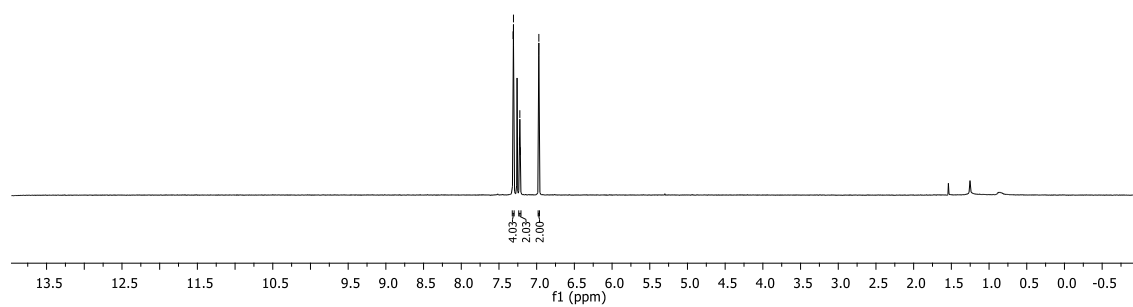
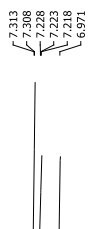
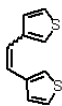
7.33  
7.30  
7.14  
7.13  
7.12

4.53

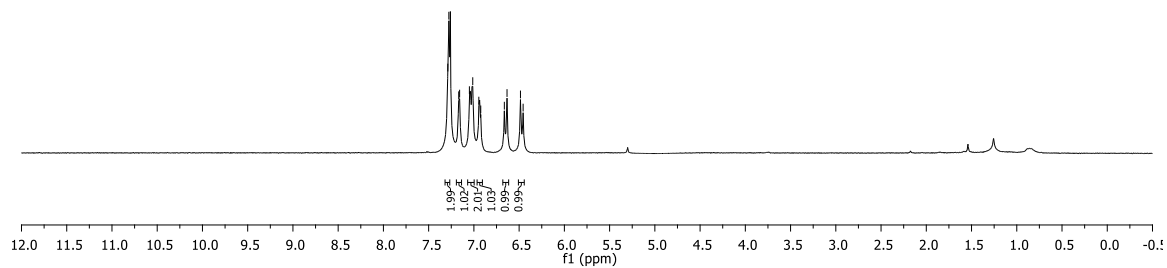
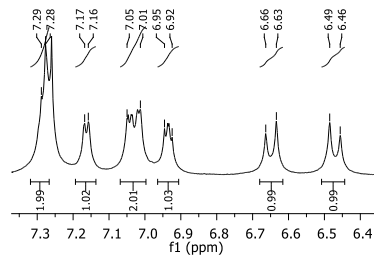
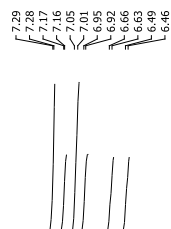
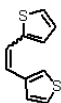
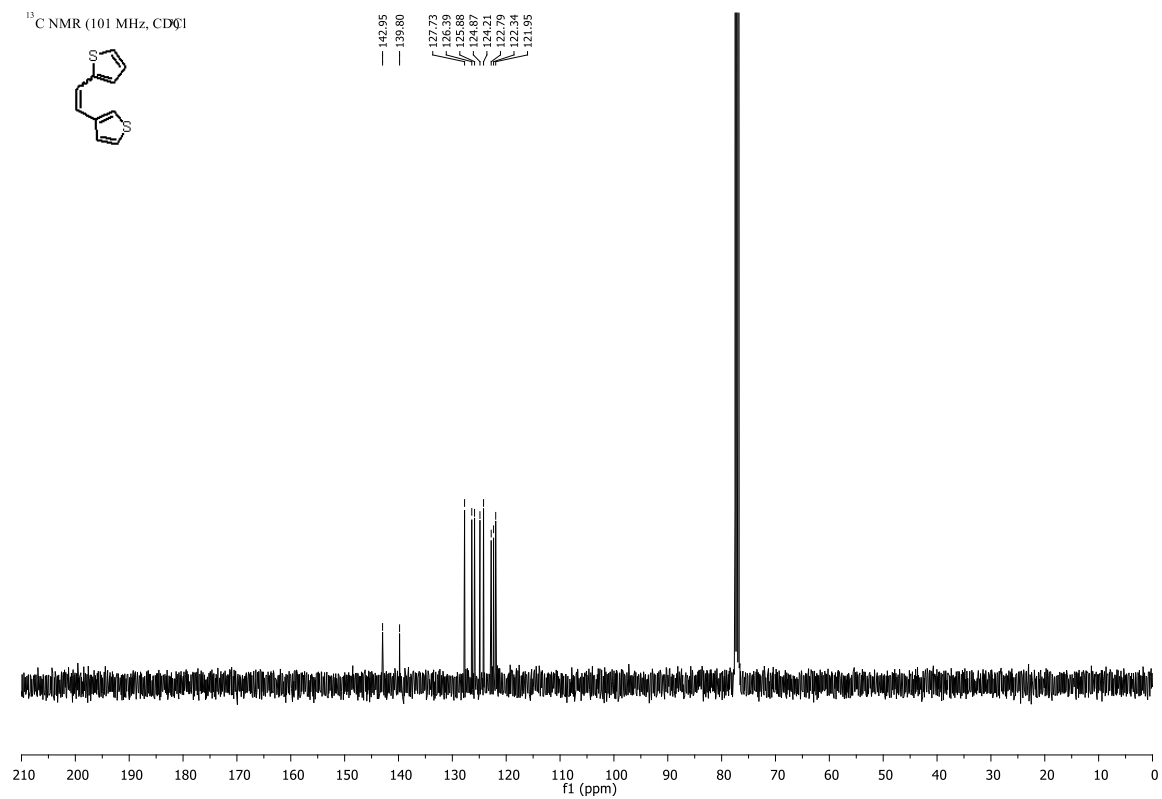
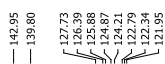
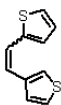




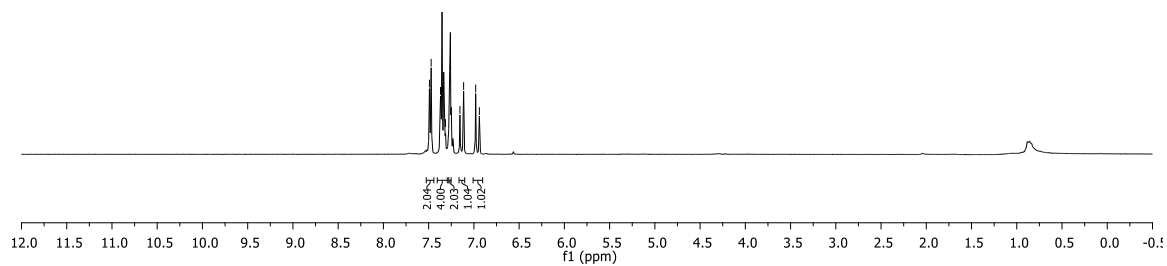
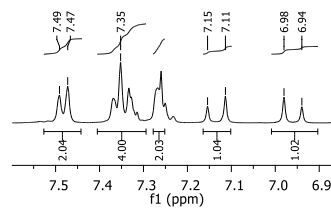
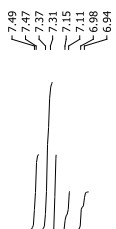
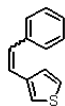
<sup>1</sup>H NMR (400 MHz, CDCl<sub>3</sub>)

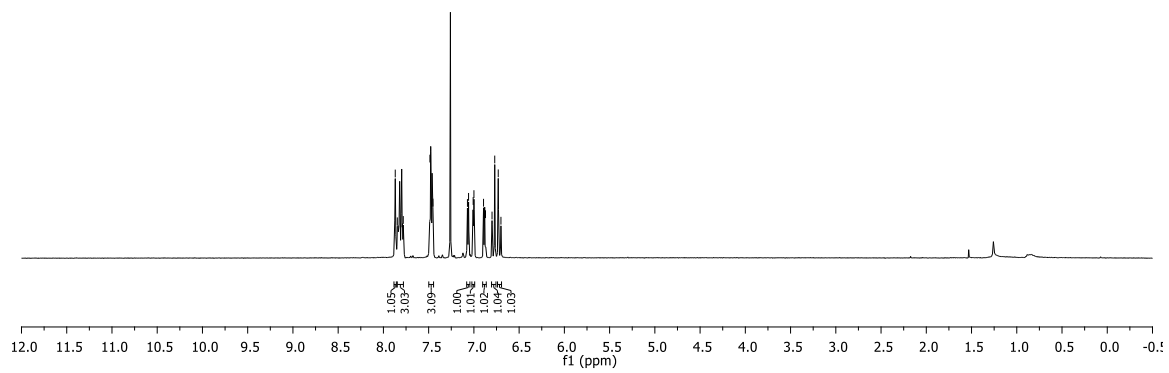
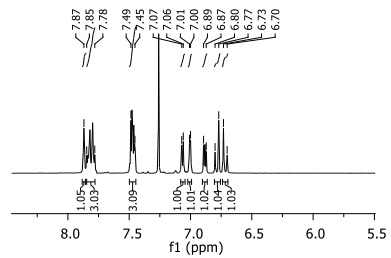
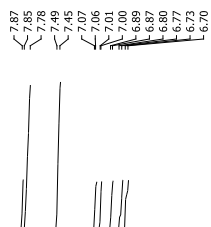
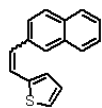
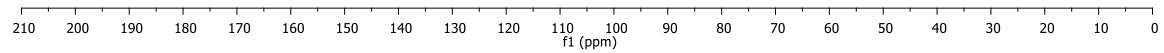
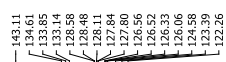
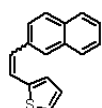




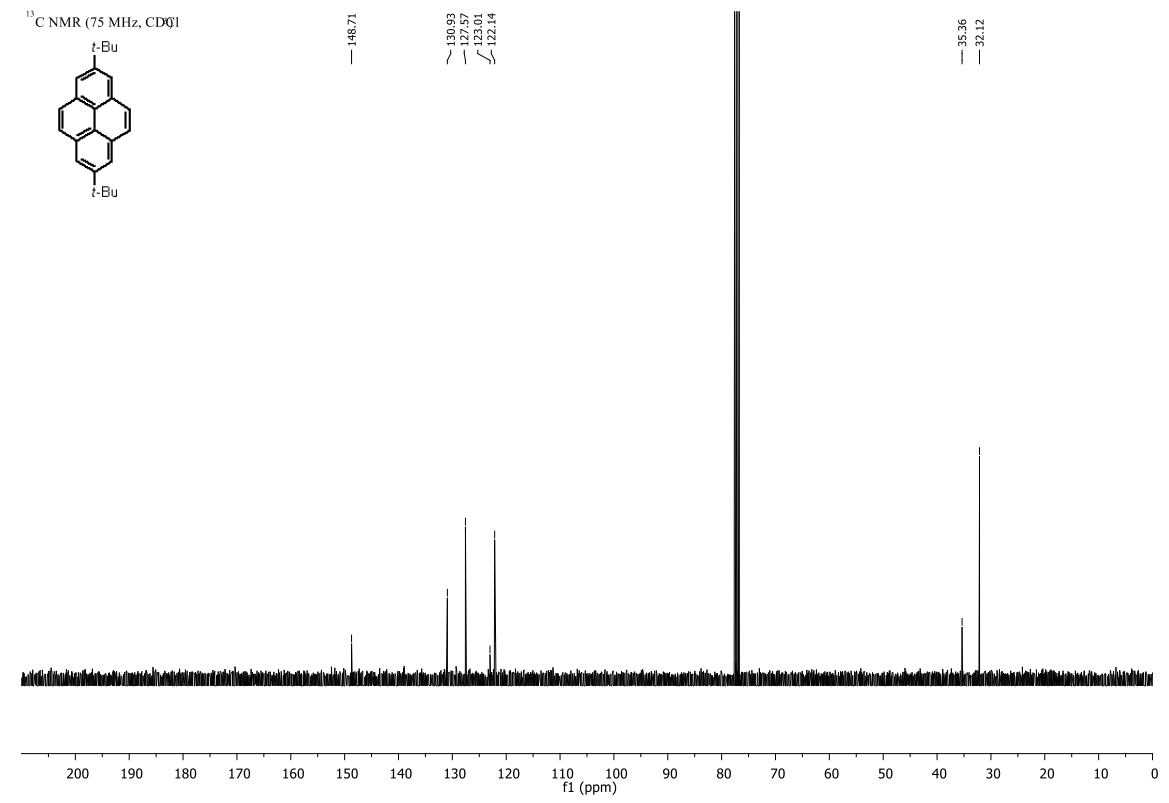
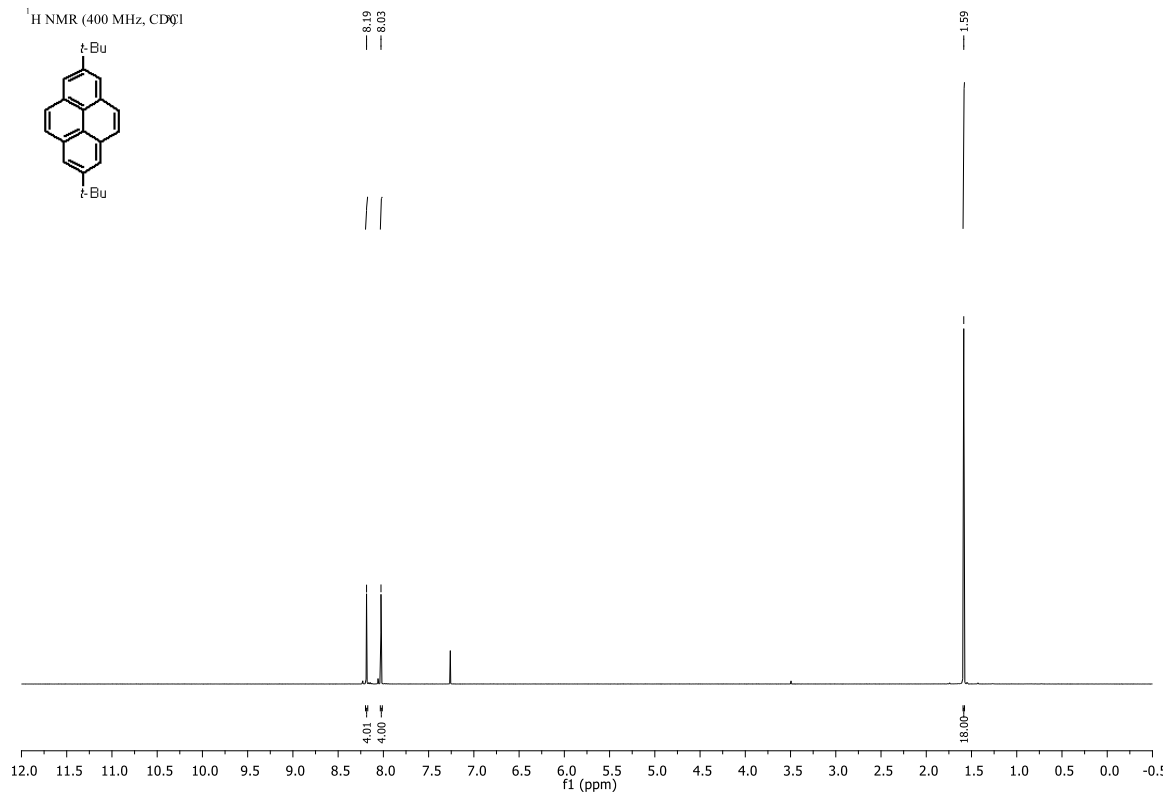
<sup>1</sup>H NMR (400 MHz, CDCl<sub>3</sub>)<sup>13</sup>C NMR (101 MHz, CDCl<sub>3</sub>)

<sup>1</sup>H NMR (400 MHz, CDCl<sub>3</sub>)

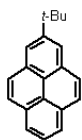


<sup>1</sup>H NMR (400 MHz, CDCl<sub>3</sub>)<sup>13</sup>C NMR (101 MHz, CDCl<sub>3</sub>)

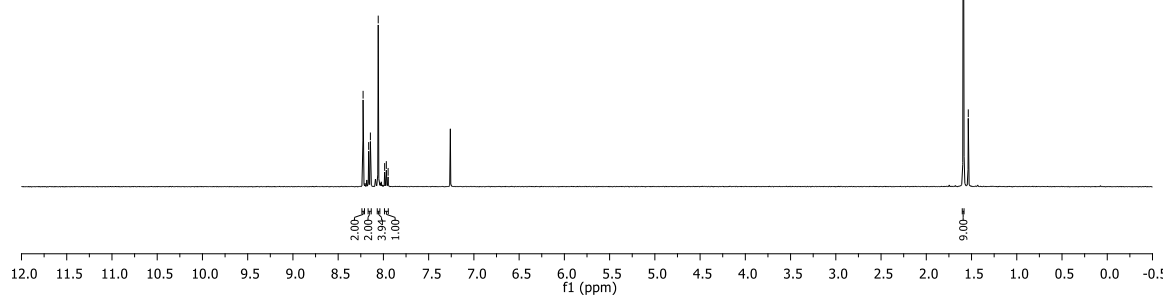
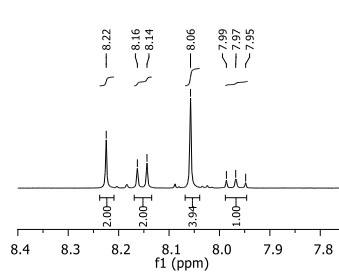




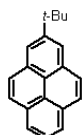
<sup>1</sup>H NMR (400 MHz, CDCl<sub>3</sub>)



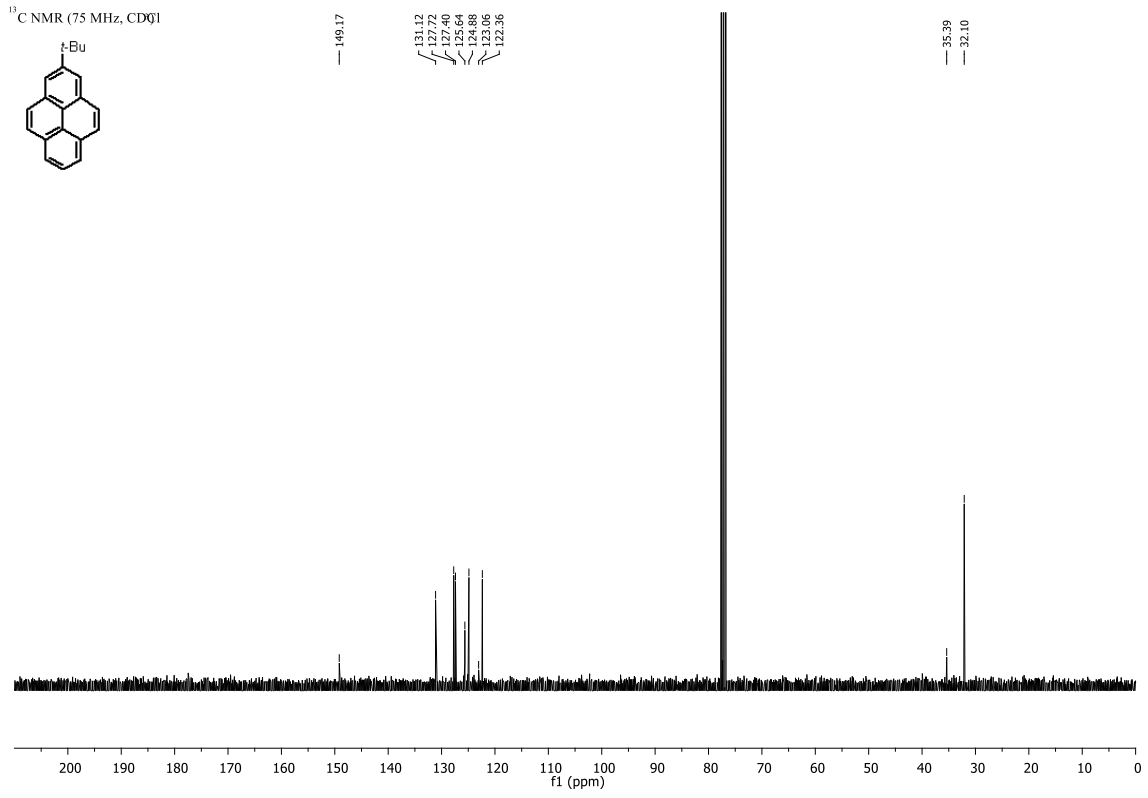
8.22  
8.16  
8.06  
7.99  
7.97  
7.95

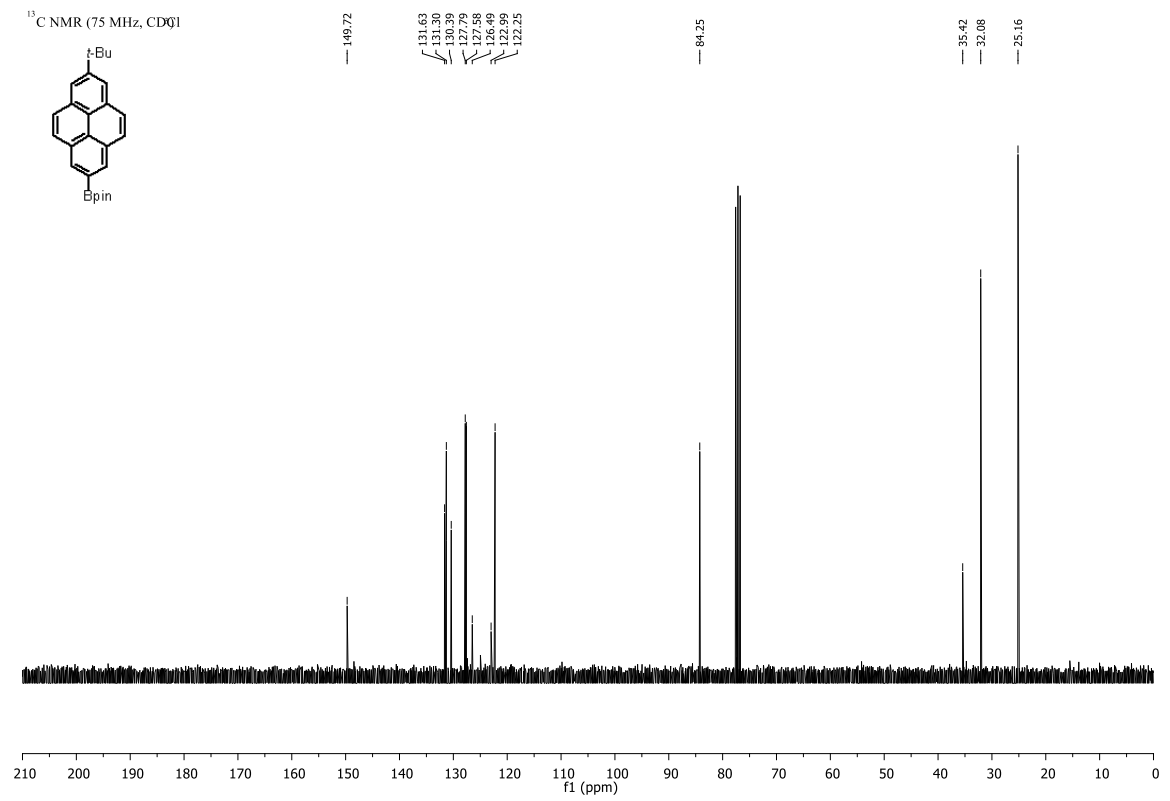
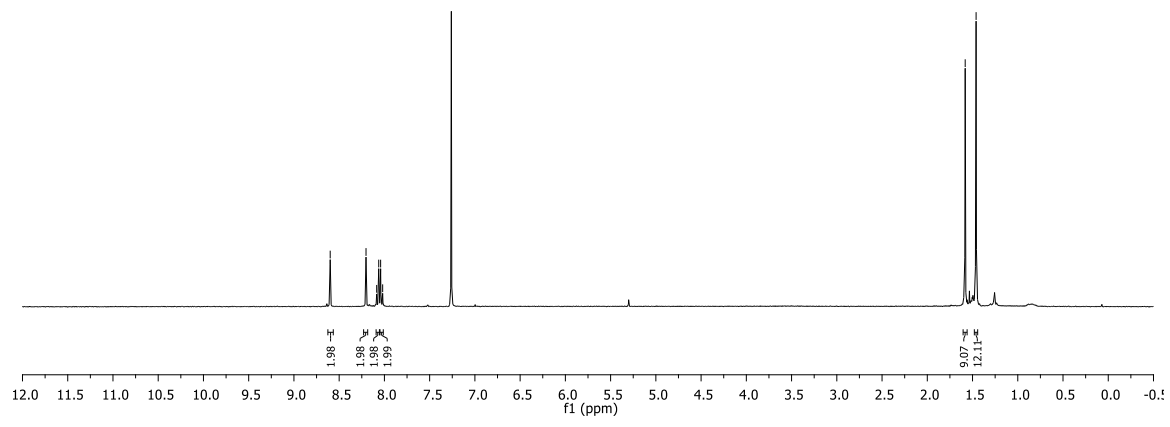
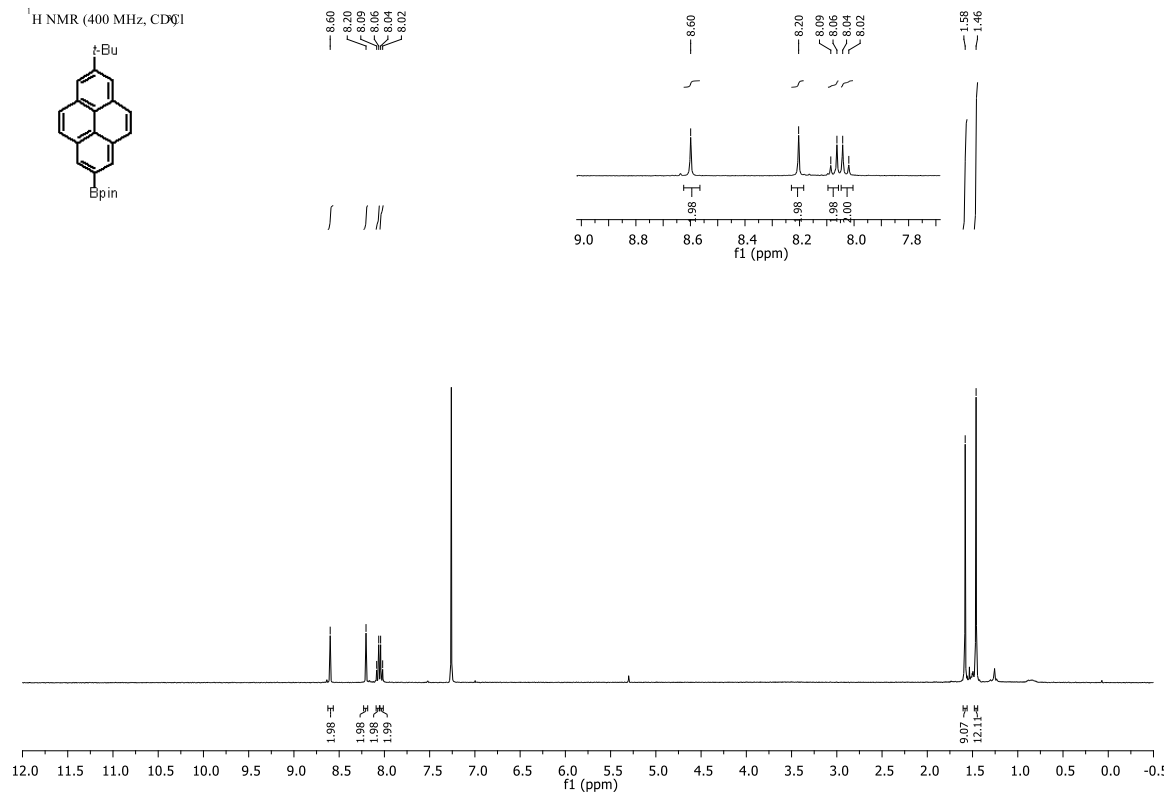


<sup>13</sup>C NMR (75 MHz, CDCl<sub>3</sub>)

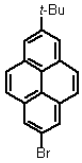


149.17  
131.12  
127.72  
127.40  
124.86  
124.88  
123.06  
122.36

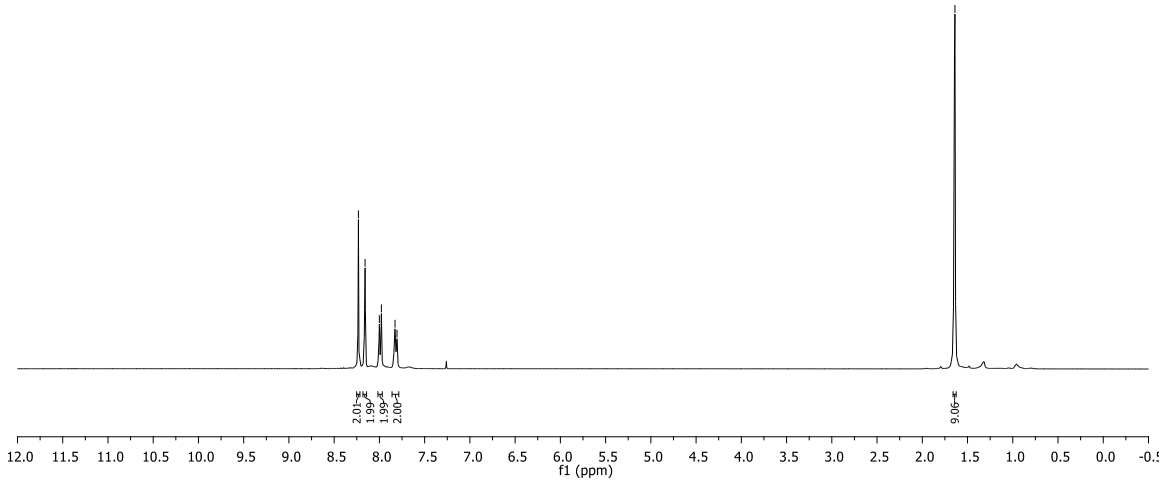
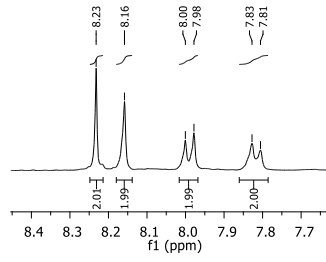




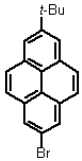
<sup>1</sup>H NMR (400 MHz, CDCl<sub>3</sub>)



8.23  
8.16  
8.00  
7.98  
7.83  
7.81



<sup>13</sup>C NMR (101 MHz, CDCl<sub>3</sub>)



149.03

132.07  
130.27  
128.37  
126.44  
125.70  
122.65  
122.10  
119.14

34.95  
31.60

